SYNTHESIS, THERMAL AND SPECTRAL STUDIES OF SOME TRANSITION METAL COMPLEXES OF HETERO CYCLIC SCHIFF BASES

Thesis submitted to the University of Calicut
in partial fulfilment of the requirements
for the award of the degree of
Doctor of Philosophy
in Chemistry

B. SLEEMA, *M.Sc., M.Phil*

DEPARTMENT OF CHEMISTRY
UNIVERSITY OF CALICUT
KERALA - 673 635
SEPTEMBER
1999

DEPARTMENT OF CHEMISTRY
UNIVERSITY OF CALICUT

Telex 0804-243
Grams : UNICAL
Phone : 0494-400245

Calicut University (P.O.)
Pin: 673 635, Kerala
India

CERTIFICATE

This is to certify that the thesis entitled **'Synthesis, Thermal and Spectral Studies of some Transition metal Complexes of Heterocyclic Schiff Bases'**, is an authentic record of the research work carried out by **Ms. B. Sleema**, under my supervision in partial fulfilment of the requirements for the degree of Doctor of Philosophy in Chemistry of the University of Calicut, and further that no part thereof has been presented before for any other degree.

Geetha

Dr. GEETHA PARAMESWARAN
Professor of Chemistry
(Supervising Teacher)

C.U. Campus,
September 24, 1999

DECLARATION

I hereby declare that this thesis entitled **'Synthesis, Thermal and Spectral Studies of some Transition metal Complexes of Heterocyclic Schiff Bases'** submitted to the University of Calicut in partial fulfilment of the requirements for the Doctoral degree in Chemistry is a bonafide research work done by me under the supervision and guidance of Dr. Geetha Parameswaran, Professor, Department of Chemistry, University of Calicut.

I further declare that this thesis has not previously formed the basis for the award of any degree, diploma or other similar title.

Department of Chemistry
University of Calicut
September 24, 1999

Sleema B
B. Sleema

Preface

Interest in the study of Schiff base complexes in the field of inorgan chemistry was originated from Schiff's time (1869). This field of study h claimed increasingly greater attention due to the discovery of the application in analytical chemistry - both in qualitative and quantitati analysis - industry and medicinal field such as drug against virus, bacteri fungi, protozoa and certain kinds of tumour. Nowadays the research this field of chemistry has increased to a considerable proportion. Sch base complexes coordinate through nitrogen atom of azomethine group metal ion. The presence of functional group with replaceable hydrog atom near enough to >C=N renders extra stability to metal complex through chelation.

In the present investigation the complexation of five new Schiff bas formed by the condensation of vanillin and o-vanillin with aminopyridine, 2-aminothiazole and L-histidine have been studi extensively. 50 Metal complexes have been synthesized and characterize based on physicochemical studies. Manganese, iron, cobalt, nickel, copp zinc, cadmium, mercury, zirconium and uranium are the metals used f complexation.

Most of the metal complexes were studied for their behaviour duri nonisothermal heating. The kinetics and mechanism have been investigat using Coats and Redfern and nine mechanistic equations. Based on X r

power diffraction pattern the crystal lattice and dimensions of Fe(II),Ni(II) and Cu(II) complexes have been reported in part III.

The application of the some selected metal complexes as antibacterial drugs have been explored. Different types of bacteria isolated from soil and prawn were used for the study and the results are given in Part IV. Part IV ends with summary .For the sake of brevity , symbols and formulae, instead of names have been used in this thesis which is given by the Abbreviations at the starting of the thesis.

ACKNOWLEDGMENTS

It is my privilege and pleasure to express my sincere gratitude to Dr. Geetha Parameswaran, Professor, Department of Chemistry, University of Calicut, who as my teacher and guide, gave constant encouragement and whole-hearted co-operation at all stages of this research work. Only with a deep sense of gratitude and indebtedness I could remember her for her expert and inspiring guidance, supervision unfailing interest, pertinent criticism apt suggestions, timely exhortations, maternal affection and the excellent hospitality extended to me, which transformed my dream of a thesis into reality.

I owe a deep sense of gratitude to Dr. M.P. Kannan, Professor and Head of the Department of Chemistry and Dr. T.D. Radhakrishnan Nair, Professor and former Head of the Department of Chemistry, University of Calicut, for having provided me with all the facilities to carry out this research work.

The investigator records her obligation and profound gratitude to Dr. P.K. Surendran and Dr. Nirmala Thampuran, Central Institute of Fisheries Technology, Kochi, without whose valuable suggestions and cooperation the Part IV, antibacterial studies of some selected complexes would not have been possible.

I am indebted to the authorities of IIT Bombay, IIT Madras, RSIC Chandigarh, CLRI Madras, RRL Trivandrun, RSIC Nagpur, Central University Hyderabad, CMET Trissur, Cochin University of Science and Technology, Kochi, CIFT Kochi for providing necessary instrumental facilities and microanalyses of samples.

In completing this thesis, I have received valuable assistance from teachers, friends and non-teaching staff of Department of Chemistry, University of Calicut. I remember them with gratitude.

With heartfelt gratitude I record my obligation to Sri. V.R. Ajithkumar, Principal; Prof. C.G. Dharman, former Principal; the Management, S.N.M. College, Maliankara for having given me permission, co-operation and words of encouragement to undertake this research.

I wish to thank all my colleagues in the Department of Chemistry, S.N.M. College Maliankara for their help at different levels and words of encouragement.

I would like to acknowledge warmly the generous help I have received from Mr. V.B. Sajeev, for his expertise and artistic talents shown and Dr. M. V. Nandakumar, RRL Trivandrum for his timely help.

Let me express my depth of gratitude to Dr. N.L. Mary and Miss P.S. Sheeba for their valuable help. I take this opportunity to thank Mr. Balu, Beena Commercial Institute for patiently typing this thesis amidst his busy engagements.

Special mention has to be made about my family members especially my husband, Dr. M.G. Ramesh Babu, Senior Grade Lecturer, S.N.M College Maliankara, whose inspiration and whole-hearted co-operation helped me to achieve this goal. But for his abiding interest and constant encouragement it would not have been possible for me to complete this research work in its present form.

Above all, I submit my thoughts and actions to the Almighty, who always guides me in the path of righteousness to help me to achieve my goal.

B. Sleema

LIST OF PUBLICATIONS

1. Kinetics and Mechanism of thermal decomposition of Mn(II), Co(II), Ni(II), Cu(II) and Zn(II) complexes of vanillin-2-aminopyridine by TG, communicated to Thermochimica Acta.

2. Physicochemical studies and thermal decomposition kinetics of Mn(II), Co(II), Ni(II), Cu(II) and Zn(II) complexes of vanillin-2-aminothiazole, communicated to Croatica Chemica Acta.

3. X-ray studies of Fe(II), Ni(II) and Cu(II) complexes of o-vanillin-L-histidine (To be communicated).

4. Studies on antibacterial activities of Fe(II), Co(II), Ni(II) and Cu(II) complexes (To be communicated).

5. Kinetics and mechanism of thermal decomposition of Mn(II), Co(II), Zn(II), Cd(II) and ZrO(II) complexes of o-vanillin-L-histidine, communicated to Journal of Thermal Analysis.

6. Spectral and thermal studies on o-vanillin-2-aminopyridine complexes of Mn(II), Co(II), Ni(II), Cu(II), Zn(II) and UO_2(II), communicated to Synth. and Rec. Inorg. and Met. Org. Chem.

7. Preparation and characterization of five solid complexes of mercury with schiff base ligands, communicated to Asian Journal of Chemistry.

8. Physicochemical studies and thermal decomposition kinetics of Mn(II), Co(II), Ni(II), Cu(II) and Zn(II) complexes of *o*-vanillin-2-aminothiazole (To be communicated).

9. Thermal and spectral studies of some copper complexes (To be communicated).

10. Kinetics and mechanism of the thermal decomposition of orthorhombic crystalline complexes of Ni(II) and Cu(II) complexes of *o*-vanillin-L-histidine (To be communicated).

11. Preparation and characterization of Zn(II), Cd(II) and Hg(II) complexes of vanillin and *o*-vanillin Schiff bases (To be communicated).

12. Physicochemical investigations on the complexes of Mn(II), Fe(II), Co(II), Ni(II), Cu(II) and Zn(II) with cinnamaldehyde Schiff bases. B. Sleema and Geetha Parameswaran, Proceedings of the Eighth Kerala Science Congress, (1996) 416. M.Phil.

ABBREVIATIONS

For convenience, certain abbreviations have been used freely in this thesis.

VAAP	:	Vanillin-2-aminopyridine
VAAT	:	Vanillin-2-aminothiazole
o-VAAP	:	*o*-Vanillin-2-aminopyridine
o-VAAT	:	*o*-Vanillin-2-aminothiazole
o-VALH	:	*o*-Vanillin-L-histidine
M	:	Central metal atom in a complex
L	:	Ligand moiety in a complex
OAc	:	Acetate

While describing ir spectral bands, s, m, w and br have been used for strong, medium, weak and broad respectively.

CONTENTS

PART I

SYNTHESIS AND CHARACTERIZATION

PART II

THERMOANALYTICAL STUDIES

PART I

SYNTHESIS AND CHARACTERIZATION

CHAPTER I

INTRODUCTION

Coordination chemistry is currently one of the most important a rewarding fields of research in inorganic chemistry and it promises ma contributions to science as well as to the mankind. About sever percent of the papers appearing in inorganic chemistry journals recent years deal with various aspects of coordination compounds wh play important roles in applied science and industry. The involvement metal ions in biological processes and the role of metal complexes biological systems have culminated in the emergence of a new branch vi Bioinorganic chemistry. Metal chemotherapy and chelation therapy ha now drawn attention as additional outlets for coordination chemistry.

The modern study of metal complexes begins with the work of t men, Alfred Werner and Sorphus Mads Jorgensen. Coordination chemist has grown from a readily defined and limited topic into what is now most active research area in inorganic chemistry encompassing a gre variety of subjects and phenomena. Reason for this advancement can attributed to the formulation of excellent theories of electronic structure metal ions in coordination compounds such as ligand field and molecul orbital theories and the availability of modern sophisticated instrumer which are powerful tools for structure determination.

Complexation reactions are used in qualitative as well as quantitative analysis. There are some extremely sensitive and selecti organic reagents for the determination of metal ions. For examp

dimethylglyoxime is a good precipitating reagent for the gravimetric analysis of nickel and palladium; while EDTA is a good reagent for the volumetric analysis of calcium, magnesium, zinc etc. The role of coordination compounds in colorimetric, spectrophotometric and polarographic analysis is also significant.

Transition metal complexes act as catalysts in many industrial processes like Wacker process, Oxoprocess, Monsanto process etc. Many enzymes contain a small prosthetic group which is usually a complexed metal ion. Haemoglobin, myoglobin, chlorophyll and cytochromes are some of the most important complex compounds in living systems.

Coordination compounds find use in analytical chemistry for the identification and extraction of metal ions in cation exchange resins and in solvent extraction for the seperation of radioactive metals.

Schiff base ligands

Schiff bases constitute an important class of nitrogen donor ligands and occupy a prominent position amongst the recent achievements in the field of coordination chemistry. Schiff bases contain the azomethine group and are usually formed by the condensation of a primary amine with an active carbonyl compound. They have the general structure RN=CR' where R and R' are aryl, alkyl, cycloalkyl or hetrocyclic groups, which may be variously substituted. The synthesis and properties of Schiff bases are widely reviewed[1,2]. Works on bidentate ligands have been reviewed exclusively by Holm *et al.*[3]. A number of other reviews have also appeared on the chemistry of Schiff bases and their metal complexes[4-12].

The bonding ability of ligands depends on the nature of atoms which act as coordination sites, their electronegativity and steric factors. The possibility of having a lone pair of electrons in either a π or sp^2 hybridised orbital or trigonally hybridised nitrogen in the >C=N group is of the fundamental chemical and biological importance. If the coordinating ligand bears a functional group usualy -OH or -COOH sufficiently near to the site of condensation, then a very stable five or six membered chelate ring can be formed. Tridentate Schiff base ligands forming two annulated rings form comparatively stable complexes[13-18].

Schiff base ligands and their complexes are known to possess tuberculostic[19-20], bactericidal[6], fungicidal[21], antimicrobial[22,23] and anticancer activities[24,25]. The possibility of using them in chemical analysis[26] selective separation and enrichment of certain metals[27,28] catalysis and gas chromatography[29,30] and also in stabilizing polyolefins against oxidation and ultraviolet light deterioration[31] is being explored.

Among the numerous selective and specific complexing agents, the Schiff base ligands derived from *o*- and *p*-vanillin and heterocyclic amines like aminopyridine, aminothiazole and histidine, deserve special mention due to many outstanding features of the complexing system that they provide.

Metal chelates of Schiff bases derived from amino acid, vanillin and related compounds

In the vast and enchanting world of Schiff base complexes, the work on those of vanillin Schiff bases, especially of *o*-vanillin is limited.

A series of Ti(IV), Zr(IV), Fe(III), Co(II), Ni(II), Cu(II), Zn(II), Th(IV), UO_2(II) and La(III) complexes of vanillidine anthranilic acid and its bromoderivative were synthesised and characterised by Geetha and Jessy[32-34]. All these complexes were found to be dimeric in nature except those of Th(IV), UO_2(II) and La(III) which were monomeric. It supports the view that in some cases these ligands act as monobasic bidentate and in other cases as dibasic tridentate. Purushotham Chakraworthi *et al.* have studied the transition metal complexes of vanillin anthranilic acid. Complexes of Mn(II), Co(II), Ni(II) and Cu(II) were prepared and characterized by analytical, spectral and magnetic data[35]. The Schiff base coordinates through carboxylate oxygen and azomethine nitrogen atoms. The dimeric nature of Co(II), Ni(II) and Mn(II) complexes has been explained by the abnormal magnetic moments obtained at room temperature.

Mn(II) complexes of Schiff bases derived from glycine, β-alanine and L-leucine with salicylaldehyde and its derivatives have been isolated and characterised by Dutta and Ray[36]. Synthesis, spectral and thermal studies of Co(II), Ni(II), Zn(II) and Cd(II) complexes with aminoacid Schiff bases have been reported by Sharma, Sen and Dubey[37]. Some work has also been reported on the complexation abilities of N-salicylidene amino acids with 3d-transition metals[38].

Cu(II) complexes of Schiff bases derived from 2-hydroxy-1-naphthaldehyde and substituted aromatic amines have been prepared and characterized by spectral studies and magnetic measurements[39]. Recently, V0 (II) complexes of Schiff bases of salicylaldehyde, 5-bromosalicylaldehyde and 2-hydroxy-1-naphthaldehyde with anthranilic acid have been isolated and characterized by Mohanty *et al.*[40]. Complexes

of Mn(II), Fe(II), Co(II), Cu(II) and Cd(II) with N-(5-bromosalicylidene) -5-bromoanthranilic acid have been prepared and characterized[41].

Cinnamaldehyde complexes of Mn(II), Fe(II), Co(II), Ni(II), Cu(II), Zn(II), La(III), Ce(IV), Pr(III) and UO_2(II) with anthranilic acid and 5-bromoanthranilic acid were synthesised and analysed[42,43]. All these complexes were found to possess 1:1 stoichiometry. Cu(II) complexes were found to be square planar and Zn(II) complexes tetrahedral. Octahedral geometry was exhibited by all the other complexes.

Construction of a table of vanillin and *o*-vanillin Schiff bases of various amino compounds makes the study of literature of the particular ligand an easier one (Tables 1.1.1 - 1.1.2).

New dioxouranium(VI) complexes were synthesised using N-(salicylidene)-L-histidine (H_2Sal-L-his) and N-*O* vanillidine -L-Histidine (H_2van-L-his) and the corresponding D-Histidines. They are characterised by elemental analysis and physicochemical studies[76].

Sharma, Sen and Dubey synthesized seven complexes of Co(II), Ni(II), Zn(II) and Cd(II) by the metal ion template condition of amino acids (L-phenylalanine, L-leucine, L-histidine, L-tryptophan) and aldehyde/ ketone (salicylaldehyde, *o*-hydroxynaphthaldehyde, pyruvic acid, *o*-vanillin, Isatin). The elemental analysis, conductance and magnetic susceptibility measurements, IR, H^1 NMR and electronic spectral data indicate that the ligands function as dibasic terdentate with O, N, O donor set. The thermal degradation of the complexes was studied in air by DTA and dynamic TG from ambient temperature to 900°. Kinetic parameters were evaluated[77].

Solid-state complexes of poly(L-histidine) with metal chlorides from the first row of the d-block was separated and studied by MP Mc Curdie and LA Belfiore[78].

Metal Chelates of Schiff bases derived from heterocyclic amines

The systematic investigation and a considerable amount of work have been reported on the complex compounds of various Schiff bases by Pfeiffer and Coworkers. Complexes of Schiff bases derived from mixed heterocyclic amines as yet remained largely neglected. The first study of the complex of a Schiff base derivative of 2-aminothiazole was reported only in 1975. Thus there is a vast scope of synthetic work in this field and has current interest due to biochemical significance. We have, therefore, taken up a brief study on the Schiff base complexes derived from heterocyclic amines, namely aminopyridine and aminothiazole.

The condensation between carbonyl compounds and heterocyclic primary amines yield an interesting type of schiff base ligands which are really good enough for chelation with transition and inner transition metal ions. Ligands of this kind and their metal complexes are widely being used as analytical reagents[79] and medicinal compounds[80, 81].

Ayad and coworkers have isolated and characterized Cu(II) chelates of Schiff bases of 2-aminopyridine with salicylaldehyde and 2-hydroxy-1-naphthaldehyde[82]. They have also reported the thermal behaviour of these complexes using TG studies. Complexes of Zn(II) and Cd(II) with anionic forms of Schiff bases obtained from the condensation of Salicyaldehyde

with 2-aminopyridines were also synthesized by electrochemical oxidation[83].

Infrared and Raman spectral studies of 2-aminopyridine complexes of Zn(II), Cd(II) and Hg(II) halides have been reported[84]. Mixed complexes of Cu(II) with Schiff bases derived from Salicylaldehyde and 2-aminopyridines have also been synthesized and characterized[85].

Bhaskara has synthesized the complexes of Schiff bases derived from 4-*p*-methoxyphenyl-2-aminothiazole with Cu(II) and Zn(II)[86]. Bhatnagar and Kiran have prepared 1:1 adducts of antimony with Schiff bases of 2-aminothiazole and 2-aminobenzothiazole[87]. The ligands coordinate to the metal atom through their azomethine nitrogen. Metal chelates of Schiff bases derived from 2-amino pyridine and their derivatives have been widely analysed by numerous scientists[85,88,89].

2-, 3- and 4-Aminopyridines (L) yield Cu $(O_2CR)_2$ L and Cu$(O_2CR)_2$ L_2 on interaction with Cu(O_2CR) (R=Me, Et, Pr, $CHMe_2$). The complexes are solid, stable and are green or blue-violet in colour. Conductance, magnetic moments, electronic andIR specta reveal that they are neutral 6-coordinate species[90].

A study on Schiff base derived from 2-aminothiazole and their metal complexes were carried out by Manju, Sangeeta and Sinha[91]. Octahedral ML_3 M = Co, Ni; HL = 5-R-Salicylidene-4-(4-ethoxyphenyl)-2-aminothiazole (R = Me, Cl, Br) and 2-hydroxy-1-naphthyl methylene-4-(4-ethoxyphenyl)-2-amino thiazole were prepared from $M(OAc)_2$ and HL. The complexes were characterized by electronic and IR Spectra and

magnetic susceptibility measurements. The Schiff bases are coordinated through the phenolic O and azomethine N atoms. Crystal field parameters were determined[92].

Ahmad and Mohammad synthesized and characterized complexes of some transition metal chlorosulphates with thiazoles and thiocarbamate[93].

At room temperature, dibenzoyl peroxide undergoes oxidative addition on metallic Cu powder and 2-aminopyridine in a mixed solvent (acetone and THF), which affords the product as binuclear Cu(II) complex. The Cu(II) ion is coordinated by four bridging bidentate benzoate and two 2-aminopyridine to form dimeric mols[94]. $CuL_2F_2.nH_2O$ (L = 2-, 3- and 4-aminopyridine, 2-, 3- and 4-acetamidopyridine) were prepared and characterized by elemental analytical, IR, electronic spectra, magnetic and conductance measurements[95].

Tetrabenzoatobis (2-aminothiazole) dicopper(II) was synthesised and its crystal structure was studied. X-Ray analysis revealed that each Cu ion is coordinated by four bridging bidentate benzoate ligands and one 2-aminothiazole to form a binuclear mol[96]. Lanthanide complexes of 2-aminothiazole were prepared from ethanol solutions of lanthanide chlorides and 2-aminothiazole and their physico chemical properties were studied[97].

Platinum group metal Schiff-base complexes were derived from salicylaldehyde and 2-aminopyridine[98]. Schiff bases (HL) salicylidine-*o*-aminopyridine, its 5-bromo analogue, salicylidine-*o*-aminothiazole, its 5-bromo analogue, and 2-hydroxynaphthalidene-*o*-aminopyridine were

prepared and characterized by Rosmma, Joby and Geetha[99]. UO_2L_2 were also prepared and kinetics of their thermal decomposition are reported.

The synthesis of several mono and bimetallic Pt and Pd complexes of 2-aminothiazole are reported[100]. Thermodynamic characterization of 2-amino-thiazole and 2-amino-4-phenyl thiazole was performed[101]. ΔG, ΔH and ΔS was calculated with the help of stability constants of the complexes at different temperatures. By conductometric and photometric titrations as well as IR spectra, the structure of the complexes could be confirmed.

Spectral study of Pd(II) complexes with 2-aminopyridine were carried out by some authors[102]. Mechanism of 2-aminopyridine complexation with Pd(II) was studied by Dinkov and Annaudov[103]. An IR-spectral study of sulphato- and chloro complexes of Pd(II) with 2-aminopyridine and aniline respectively, is reported[104]. The results obtained confirm the bidentate co-ordination of both 2-aminopyridine and SO_4 group in the case of sulphato-2-aminopyridine-palladium(II) leading to polynuclear structure of the complex in solution.

Scope of present investigation

The literature survey revealed that the systematic investigation on the coordinating behaviour of aromatic Schiff bases derived from *o*- / *p*-vanillin and 2-aminopyridine/2-amino thiazole/histidine is very scanty. The observation that many such ligands, especially their metal complexes, have ample biological activities, viz., antifungal, antibacterial, antiviral, antimicrobial, antitumour etc., demands the detailed investigation of the donor characteristics of these chelating agents. The nature of metal ligand bonding and stereochemistry of such complexes also, therefore, merit detailed exploration.

In the present investigation, aromatic Schiff base ligands such as vanillin-2-aminopyridine, vanillin-2-aminothiazole, *o*-vanillin-2-aminopyridine, *o*-vanillin-2-aminothiazole and *o*-vanillin-L histidine have been synthesized and characterized. Their complexes with several transition and one innertransition metal ions have also been isolated. Generally employed metal ions, during the current course of studies are Mn(II), Fe(II), Co(II), Ni(II), Cu(II), Zn(II), Cd(II), Hg(II), ZrO(II) and UO_2(II).

The solid complexes were characterized by various physicochemical methods. Their room temperature magnetic moments have been determined and interpreted in structural contexts. Tentative assignments of the molecular formulae of both the ligands and chelates were made based on their microanalytical data. Correlation between structure and spectral data have been evaluated in a critical manner. Electrolytic behaviour of the complexes were analysed on the basis of conductivity

experiments. The thermal decomposition character of certain representative complexes in air have been studied by TGA technique so as to understand their general thermal stabilities and decomposition pattern. Crystalline state of few of the complexes Fe(II), Ni(II) and Cu(II) complex of *o*-vanillin L-histidine was established empirically by indexing it's X ray powder diffraction pattern.

TABLE 1.1.1 **Metal Chelates of Schiff bases derived from Vanillin**

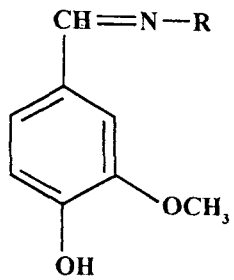

R	Metals	Reference Number
$-C_6H_4COOH$	Ti(IV), Zr(IV), Fe(III), Co(II), Ni(II), Cu(II), Zn(II), Th(IV), UO_2(II), La(III)	44, 45, 46
$-NH-\overset{\overset{O}{\|}}{C}-NH_2$	Mn(II), Fe(II), Co(II), Ni(II), Cu(II), Zn(II), Cd(II), Hg(II)	47
$-NH_2$	Mn(II), Fe(II), Co(II), Ni(II), Cu(II)	48
$-NH-\overset{\overset{S}{\|}}{C}-NH_2$	Mn(II), Fe(II), Co(II), Ni(II), Cu(II), Zn(II), Cd(II), Hg(II)	49
$-NH-\overset{\overset{S}{\|}}{C}-NH_2$	Mo(III)	50
$-C_5H_3NNH_2$	Th(IV), UO_2(II)	51
$-NH-\overset{\overset{S}{\|}}{C}-NH_2$	Ti(IV), Zr(IV), Hf(IV)	52
$-C_6H_4-COOH$	La(III), Ce(III), Pr(III), Nd(III), Sm(III)	53
$-C_6H_4-C_6H_4-NH_2$	ZrO(II)	54
$-NH-\overset{\overset{O}{\|}}{C}-NH_2$	UO_2(II)	55
$-NH_2$	Co(II), Ni(II), Cu(II), Zn(II), Cd(II)	56
$-NH-\overset{\overset{S}{\|}}{C}-NHC_6H_5$	Co(II), Ni(II), Cu(II), Zn(II), Cd(II), UO_2(II)	57
$-C_6H_4-CH_3$	Ce(III), Pr(III), Nd(III), Sm(III), Eu(III), Gd(III), Dy(III)	58
$-CH_2-CH_2-NH_2$	Mn(II), Fe(II), Co(II), Ni(II), Cu(II)	59

TABLE 1.1.2**Metal Chelates of Schiff bases derived from o-vanillin**

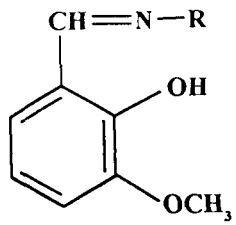

R	Metals	Reference Number
-OH	Cr(III), Mn(II), Fe(II), Co(II), Ni(II), Cu(II)	60
HOOC CH3 -CH-CH-CH3	UO_2(II)	61
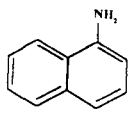	Th(IV)	62
$-C_5H_4NNH_2$	Sn(IV)	63
$-C_5H_3NNH_2CH_3$	Sn(IV)	63
-OH	La(III), Ce(II), Pr(III), Nd(III), Sm(III), Gd(III), Tb(III), Dy(III), Ho(III), Yb(III)	64
HOOC CH3 -CH-CH -CH3	La(III), Pr(III), Nd(III), Sm(III)	65
COOH -CH-CH_2-C_6H_4-OH	La(III), Pr(III), Nd(III), Sm(III)	65
-OH	Fe(III), Fe(II), Co(II), Co(III), Ni(II), Cu(II)	66
S -NH-C-NH_2	Pd(II), Pt(II)	67
S -NH-C-NHC_6H_5	Pd(II), Pt(II)	67

R	Metals	Reference number
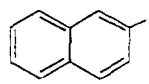	La(III), Ce(III), Pr(III), Nd(III), Sm(III), Eu(III), Tb(III), Dy(III), Ho(III), Er(III), Tm(III), Yb(III), Lu(III)	68
$-C_6H_4-CH_3$	La(III), Ce(III), Pr(III), Nd(III), Sm(III), Eu(III), Tb(III), Dy(III), Ho(III), Er(III), Tm(III), Yb(III), Lu(III)	69
$-CH_2-CH_2NH_2$	Lanthanides(III)	70, 71
$C_6H_4-NH_2$ (ortho)	Lanthanides(III)	70, 71
$-C_6H_4-NH_2$ (para)	Lanthanides(III)	70, 71
$-C_6H_4-C_6H_4-NH_2$	Lanthanides(III)	71
$-C_6H_4-CH_3$	Ho(III), Er(III), Tm(III), Yb(III), Lu(III)	72
$-NH-\overset{\overset{O}{\|}}{C}-NH_2$	Co(II), Ni(II), Cu(II), Zn(II), Pd(II)	73
$-CH_2-COOH$, $-\underset{\underset{CH_3}{\|}}{CH}-COOH$, $-\underset{\underset{CH(CH_3)_2}{\|}}{CH}-COOH$, $-\underset{\underset{CH_2-CH_2-S-CH_3}{\|}}{CH}-COOH$, $-\underset{\underset{CH_2-CH(CH_3)_2}{\|}}{CH}-COOH$, $-\underset{\underset{CH_2-C_6H_5}{\|}}{CH}-COOH$	Cu(II), Zn(II)	74
$-\underset{\underset{CH_3}{\|}}{CH}-COOH$, $-\underset{\underset{CH_2-CH(CH_3)_2}{\|}}{CH}-COOH$, $-\underset{\underset{CH_2-C_6H_5}{\|}}{CH}-COOH$	Ni(II), Cu(II), Zn(II)	75

CHAPTER II

MATERIALS, METHODS AND INSTRUMENTS

In this chapter, a brief description of the general reagents employed for the present study are described. It also gives the theory and techniques of the analytical and physical methods used for the characterization of the ligands and complexes synthesized.

Materials

Analar grade samples of *o*- and *p*-vanillin, 2-aminopyridine, 2-aminothiazole and histidine supplied by E. Merck, BDH (India) or Sigma Company (USA) were used for the preparation of ligands.

During the preparation of complexes AR grade samples of metal salts were used. Solvents like chloroform, carbontetrachloride, dimethylformamide and dimethyl sulphoxide were used as such. But the LR grade methanol, ethanol and acetone were purified by standard procedures[105]. Spectroscopic grade samples of the solvents were employed for the spectral measurements. Nitrobenzene used for the conductivity measurements was purified by repeated distillation over P_4O_{10}. All the other reagents such as $HClO_4$, HNO_3, HCl, H_2SO_4, CH_3COONa etc. used in the present investigation were of AR grade.

Methods

The following methods were employed to test the purity of ligands and characterization of complexes.

CHN analysis

Carbon, hydrogen and nitrogen content of the ligands and their metal complexes were determined by microanalysis on a Heraous-CHN-O-rapid analyser.

Estimation of metals

Standard methods[106,107] like volumetric, gravimetric or pyrolytic techniques, were adopted for the estimation of metal content in the complexes.

For the volumetric and gravimetric estimations, a common method was used for decomposing the metal complexes. About 0.2 g of the complex was digested with concentrated nitric acid–perchloric acid mixture followed by con. HCl. The resultant solution was then quantitatively made upto 100 ml. Using a definite volume of this solution, the metal content in the complex was estimated.

Amount of copper was determined iodometrically by the addition of KI and subsequent titration of liberated iodine by standard sodium thiosulphate. Cobalt and cadmium were estimated volumetrically by complexometric titration using standard EDTA solution and xylenol orange indicator. Gravimetrically, nickel was estimated by precipitating as dimethylglyoximate. By complexometric titration, using standard EDTA and eriochrome black-T indicator, zinc and mangansese were estimated. Gravimetric method was adopted for the estimation of iron, mercury and zirconium. Mercury was precipitated as mercuric sulphide by hydrogensulphide in hydrochloric acid solution and zirconium as

zirconium mandalate which was ignited to and weighed as the dioxide. Uranium was determined gravimetrically by precipitating as $UO_2(C_9H_6ON)_2C_9H_7ON$ using 4% oxine solution.

Almost all these metals were estimated by pyrolysis method. About 0.2 g of each complex was weighed out in a silica crucible and heated strongly. During the heating, all the organic particles in the chelate was burnt off and the metallic oxide left behind was weighed. From the weight of oxide, metal percentage was calculated.

Estimation of sulphur and halogen

Sulphur content in the complexes was estimated after oxidising it with nitric acid to sulphate. The sulphate was then determined as $BaSO_4$ gravimetrically[106]. Volhard's method was adopted for the determination of halogen in the complexes[106].

Electrical conductance

Molar conductance measurements of the complexes were carried out in methanol, ethanol, nitrobenzene or double distilled water at 28 $\pm$ 2°C using solution of 10^{-4}M concentration. The conductance measured can be used to find the electrolytic or nonelectrolytic nature of complexes.

Magnetic moment

The magnetic susceptibility measurements were made using a Gouy balance at room temperature[108]. The Gouy tube was standardised using $Hg[Co(NCS)_4]$ as calibrant[109]. Diamagnetic corrections were applied using Pascals constants taking into consideration of the magnetic contribution of

various atoms and structural units[110,111]. The effective magnetic moment, μ_{eff} was calculated using the equation

$$\mu_{eff} = 2.84 \sqrt{\chi'_M \times T}$$

χ'_M = molar suscpetibility corrected for diamagnetism and T = absolute temperature.

The theoretical magnetic moments were calculated using the formula

$$\mu_{eff} = g \sqrt{S\,(S+1)}$$

Electronic spectra

The uv-visible spectra of the present ligands and complexes were recorded by using methanol, ethanol or distilled water as the solvent. Electronic spectral studies were carried out mainly in a structural diagnostic perspective so as to supplement any information obtained from magnetic studies.

Infrared spectra

The importance of ir spectroscopy lies in the fact that the characteristic infrared absorption bands of a group occurs at about the same frequency irrespective of the molecule in which the group is present. This makes ir spectroscopy, a finger print for identification and a powerful tool for studying molecular structures.

The infrared spectra of the ligands and metal chelates were recorded in the range 4000-400 cm^{-1} on a Shimadzu-FT-8101 or Perkin-Elmer 397 infrared spectrometer, by KBr disc technique.

^1H Nuclear magnetic resonance studies

Nuclear magnetic resonance spectra of ligands and selected complexes were charted from RSIC, Bombay, using the solvent $CDCl_3$ or d_6-DMSO on a Hitachi R-600 spectrometer.

Electron spin resonance spectra

ESR spectra of copper(II) complexes were recorded using varian E-4 band spectrometer at room temperature with a modulation frequency of 100 KHz. The metal donor atom band in metal complexes can be determined by this study.

X-ray diffraction - Powder method

The X-ray diffraction pattern of Fe(II), Ni(II), Cu(II), Cd(II) and UO_2(II) complexes were recorded with the powdered sample for 2θ values from 5° to 60° at a chart speed of 20 mm min^{-1} and scan speed 2°min^{-1} with Cuk_α radiation of wavelength 1.5418°A. The unit cell determination and calculation of cell dimensions from the crystallographic pattern can be used to confirm the structure of complexes assigned based on the above studies.

Thermal Studies

The thermograms of complexes were recorded nonisothermally using a sample weight of 5 mg in static air atmosphere at a heating rate of 10 or 15°C min^{-1}. Each mass loss consideration from the TG plot can be assigned to the decomposition or volatilisation of a particular group. The close examination of such steps during the nonisothermal heating of each complex can be found to be in agreement with the proposed structure.

CHAPTER III

TRANSITION METAL COMPLEXES OF VANILLIN-2-AMINOPYRIDINE

The Schiff bases derived from vanillin are very interesting due to their ability to form various types of metallic complexes. Many biologically important transition metal complexes of vanillin were prepared and studied. Along with these transition metal complexes uranyl(II) complex has also been characterised just to have an insight into the bonding of inner transition metal complexes also.

Schiff, bases obtained from heterocyclic amines have been little explored. These type of Schiff bases exhibit abnormal reactions and ligating behaviour[112-114]. Also they are of great biological significance and some important enzymatic reactions involve Schiff base formation[115]. In this chapter, therefore, we have described the results of the brief study of the coordination compounds of the Schiff base derived from 2-aminopyridine and vanillin.

Preparation of the ligand

The ligand vanillin-2-aminopyridine was prepared in ethanol medium from vanillin and 2-aminopyridine. An ethanolic solution of vanillin (1.5 g; 0.01 mol) was mixed with 2-aminopyridine (0.94 g; 0.01 mol) and was refluxed for 20 h. The resulting solution was concentrated, cooled and added dropwise to distilled water taken in a beaker with constant stirring. The yellow product separated was filtered, washed and dried over anhydrous calcium chloride. The melting point was found to be 80°C.

Characterization of the ligand

The ligand vanillin-2-aminopyridine was characterized on the basis of elemental analysis and spectral data.

Analytical data found	:	C, 68.15%; H, 5.12%, N, 12.21%
Calculated for $C_{13}H_{12}N_2O_2$	:	C, 68.34%; H, 5.26%; N, 12.27%

The uv, ir and nmr spectra of the ligand showed the characteristic bands. Based on the above results, the structure of the ligand was confirmed as

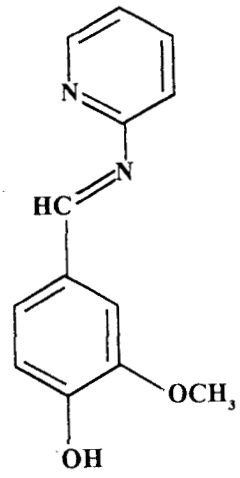

Studies on Mn(II), Fe(II), Co(II), Ni(II), Cu(II), Zn(II), Cd(II), Hg(II),ZrO(II) and $U0_2$(II) complexes of vanillin-2-aminopyridine

In this section the preparation and characterization of Mn(II), Fe(II), Co(II), N1(II), Cu(II), Zn(II), Cd(II), Hg(II), ZrO(II) and $U0_2$(II) complexes of vaniIlin-2-aminopyridine are described.

Preparation of complexes

Mn(II) complex was prepared by mixing a methanolic solution of the metal chloride with a solution of the ligand in methanoI. The mixture was refluxed for 3 h and the separated complex was filtered, washed with methanol and dried in a vacuum desiccator over anhydrous CaC12 (yield: 88%).

Fe(II) complex was prepared from ammonium ferrous sulphate. To the boiling ethanolic solution of ligand, an aqueous solution of the salt was added and boiled for ten minutes. The brown product formed was collected, washed with ethanol and dried over anhydrous $CaCl_2$ (yield : 80%)

A solution of cobalt(II) acetate in methanol was added dropwise to a refluxing solution of ligand in methanol until the metal to ligand ratio reached 1:2. Refluxing continued for 8 h. The resulting solution was added dropwise to distilled water taken in a beaker with constant stirring. Coffee brown product separated was filtered, washed with 50% methanol and dried over anhydrous calcium chloride (yield: 80%).

Ni(II), Cu(II), Zn(II) and Cd(II) complexes of vanillin-2 aminopyridine were prepared from their acetates by adopting the same procedure (yield: 80-85%).

Zirconyl nitrate was used for the preparation of ZrO(II) complex. Ethanolic solution of zirconyl nitrate was added drop by drop to a hot ethanolic solution of the ligand. Pale yellow product separated was filtered, washed and dried in vacuum (yield: 90%).

Hg(II) and UO_2(II) complexes were prepared from mercury(II) chloride and uranyl nitrate, by following the same synthetic procedure employed for ZrO(II) complex (yield: 90-95%).

Characterization of the complexes

The complexes were characterized on the basis of elemental analysis, magnetic measurements,electronic and infrared spectral data, conductance measurements and thermal data.

RESULTS AND DISCUSSION

The complexes are stable and coloured. They are insoluble in water and nonpolar solvents while slightly soluble in highly polar solvents.

Elemental analysis

The complexes were analysed for metal, sulphur and halogen by standard methods[106,107]. Percentage of carbon, hydrogen and nitrogen were determined by microanalytical methods. Vanillin-2-aminopyridine acts as a neutral monodentate ligand in reaction with common transition metal

ions. Complexes of Mn(II), Fe(II), Co(II), Ni(II), Cu(II), Zn(II), Cd(II), Hg(II), ZrO(II) and UO_2(II) possess 1:1 metal to ligand ratio based on molecular weight determined by Rast's method[116]. The analytical data and physical appearance are summarised in Table 1.3.1.

Molar conductance

The molar conductance measurements in ethanol were carried out at a concentration of 10^{-4}M at 28±2°C. For Mn(II), Fe(II) and UO_2(II) complexes the values obtained in the range 40-45 $ohm^{-1}cm^2mol^{-1}$ are agreeable for their 1:1 electrolytic nature. Molar conductance of the Co(II), Ni(II), Cu(II), Zn(II), Cd(II), Hg(II) and ZrO(II) complexes were found to be in the range 3-10 $ohm^{-1}cm^2mol^{-1}$ indicating their non electrolytic nature in ethanol.

Magnetic measurements

The values of magnetic moments are tabulated in Table 1.3.1. A magnetic moment of 6.29 B.M. for Mn(II) complex is suggestive of an octahedral geometry[117]. The room temperature magnetic moment of iron(II) complex is 5.2 B.M.[118] This indicates an octahedral geometry around the metal ion[117]. Co(II) complex possesses a magnetic moment of 4.88 B.M. The observed magnetic moment for the spin-free octahedral Co(II) ($^4T_{1g}$) has excess of spin only value and it may be due to the orbital contribution of both the ground state ($t_{2g}^5e_g^2$) and the first excited state ($t_{2g}^4e_g^3$). It is reported that octahedral high-spin geometry can be assigned to Co(II) complexes, if the measured μ_{eff} value is in the range of 4.7-5.2 B.M.[117] Ni(II) complex has a magnetic moment value of 3.52 B.M., which is

very close to the spin only value of octahedral Ni(II) complexes, indicating the presence of two unpaired electrons, with the electronic configuration of $t_{2g}^6 e_g^2 (^3A_2)$. Therefore an octahedral geometry can be assigned to the Ni(II) complex[117]. Cu(II) complex gave a magnetic moment value of 2.05 B.M., a close value expected for one unpaired electron of the d^9 electronic configuration which indicates octahedral geometry[117,118]. The remaining complexes are diamagnetic, as expected[117].

Infrared spectral studies

Infrared spectra of the ligand and the complexes were examined in detail. The characteristic ir bands are given in Table 1.3.2. A strong intense band due to νC=N stretch (azomethine) in ligand, appears around 1674 cm^{-1} which upon complexation shifts towards lower wave number region by 20-40 cm^{-1} indicating the participation of azomethine nitrogen in coordination with metal ions[119].

The presence of coordinated water molecule in all the present complexes is shown by the appearance of a broad and strong band at 3850-3250 cm^{-1} followed by a sharp peak at 840 cm^{-1} [120]. Since the pyridine ring deformation vibrations do not experience any positive or negative deviation, the non-involvement of pyridinyl-N in complexation is inferred.

The ligand ν(O-H) vibration appears as broad band between 2950-2870 cm^{-1} suggesting the coordination of a neutral ligand and not the anions of the ligand[121,122]. IR spectra of the chelates of Co(II), Ni(II), Cu(II), Zn(II) and Cd(II) suggest the presence of coordinated acetate group. The frequency difference value of about 200 cm^{-1} between the asymmetric and

symmetric modes of acetate group further indicates unidentate nature of this group[121,130].

Characteristic stretching frequency of C=N due to aminopyridine in a region of 1550 cm^{-1} is found to be present in all the complexes of aminopyridine Schiff bases.

In the case of zirconyl and uranyl complexes absence of absorption at 1380 cm^{-1} indicates the presence of non-ionic NO_3^-. The ν_1(1290), ν_2(1030) and ν_3(730) cm^{-1} modes in the ir spectra confirmed monodentate nitrate group in the complex[123,124,125].

Uranyl complex exhibited very strong band at 930 cm^{-1} due to O=U=O asymmetric stretching frequency of O=U=O group[126,127]. The force constant of U=O bond ($F_{U=O}$) in millidynes/A^o and the bond length in A^o were calculated by McGlynn method[128]. The values are found to be 7.19 and 1.73. Bands at 920 cm^{-1} and 910 cm^{-1} in ZrO(II) complex can be assigned to νZr=O.

The spectra of the chelates displayed two new bands in the range 550-420 and 470-430 cm^{-1} which were assigned to νM-N and νM-O respectively[131].

νM-Cl bands in Mn(II) and Hg(II) complexes can be identified only in the far IR region at about 360 cm^{-1} [121].

Electronic spectra

The electronic spectral data were found to be confirmative one tothe conclusions arrived at from magnetic susceptibility measurements. The

ligand exhibited bands around 40000 cm^{-1} and 28500 cm^{-1}. These bands have red shifted in complexes indicating the coordination of Schiff bases to metal ions[133].

The electronic spectrum of Mn(II) complex exhibited a band at 24800 cm^{-1} which was taken as an evidence to support the presence of Mn(II) in octahedral geometry[132]. The electronic spectrum of the Fe(II) complex is characterized by a weak band at 16140 cm^{-1} which may be attributed to $^5T_{2g} \rightarrow {}^5E_g$ transition, characteristic of octahedral stereochemistry around Fe(II)[133]. The electronic spectrum of Co(II) complex is characterized by two bands at 10530 cm^{-1} and 21830 cm^{-1} due to $^4T_{1g}(F) \rightarrow {}^4T_{2g}(F)$ and $^4T_{1g}(F) \rightarrow {}^4T_{1g}(P)$ transitions. Ni(II) complex also exhibit two d-d transitions inthe regions at about 10000 and 23500 cm^{-1} due to $^3A_{2g}(F) \rightarrow {}^3T_{1g}(F)$ and $^3A_{2g}(F) \rightarrow {}^3T_{1g}(P)$ transitions. The electronic spectrum of Cu(II) complex showed absorption maxima at about 15384 cm^{-1} which supports a distorted octahedral symmetry[133].

ZrO(II) complex exhibits 2 bands at 21186 cm^{-1} and 25000 cm^{-1}. This may be due to charge transfer transition from ligand to metal and vice versa.

The electronic spectrum of uranyl complex generally exhibit band systems characterised by a well defined vibronic structure between 29500-20000 cm^{-1}, which is essentially determined by the triatomic UO_2^{2+} entity[142,143]. Besides bands at 23200 cm^{-1} and 21700 cm^{-1} may be attributed to its very strong charge transfer band from ligand to metal and vice-versa.

Nuclear magnetic resonance spectroscopy

The ^1H nmr spectra of the ligand and a representative UO_2(II) chelate in DMSO-d_6 revealed important signals[145-147].

The nmr spectrum of vanillin-2-aminopyridine in $CDCl_3$ is characterised by 4 signals at δ 9.7, 8.1, 7.2 and 3.8 and they have been attributed to the various proton resonances due to -OH, HC=N, phenyl and methoxy groups respectively. In the spectrum of the UO_2(II) complex (in DMSO-d_6) the resonance due to -OH group does not disappear but the resonance due to the azomethine proton shifts to upfield due to shielding effect and merges with proton signal at 7.3δ. These observations suggest that the azomethine nitrogen coordinates with UO_2(II).

Signal observed at δ 3.5 arises due to water molecules. Signals of DMSO appear at about δ 2.5.

Electron spin resonance spectra

ESR spectrum of the Cu(II) complex of vanillin-2-aminopyridine was taken in solid form. DPPH was the reference. A two band spectrum exhibited was analysed and the spin Hamiltonian constants were evaluated ($g\perp$ = 2.1784; g_{11} = 2.3905). Strong interaction between the ligand and the Cu(II) ion was, therefore, established from the small g values (< 2.4)[144].

Thermal studies

Vanillin-2-aminopyridine complexes of Mn(II), Co(II), Ni(II), Cu(II) and Zn(II) were subjected to thermal analysis. Mass loss considerations of the decomposition indicate that the complexes have been converted into

corresponding metal oxides. The residues were found to be Mn_3O_4, Co_3O_4, NiO, CuO and ZnO respectively. Detailed kinetic analysis of the TG traces of these complexes are described in Part II.

From all the above studies it is clear that the ligand acts as neutral monodentate towards transition metal ions. The structure of complexes assigned are as shown below.

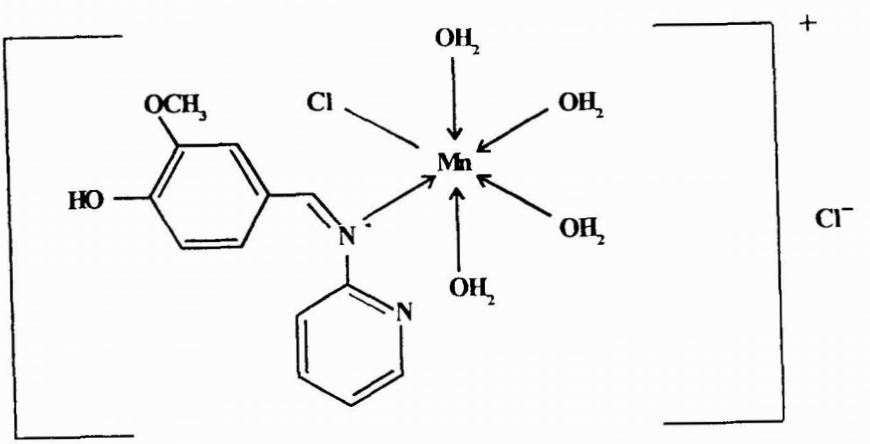

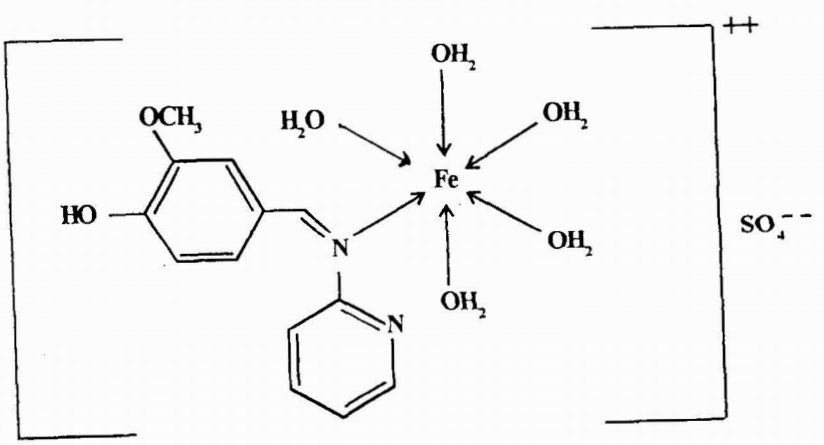

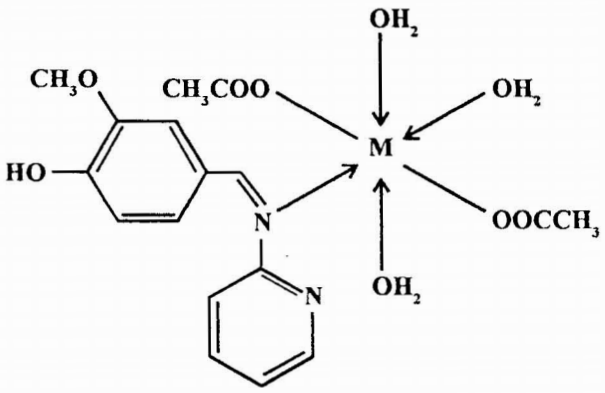

M = Co(II), Ni (II), Cu (II), or Zn (II)

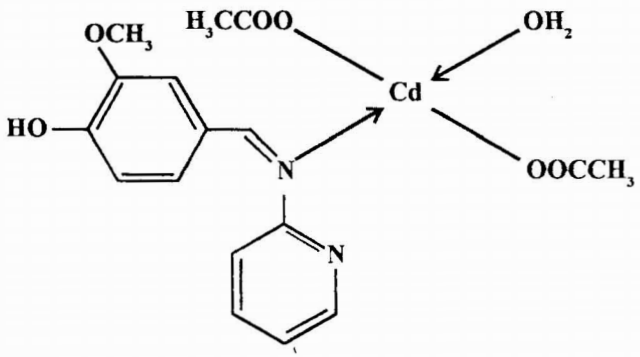

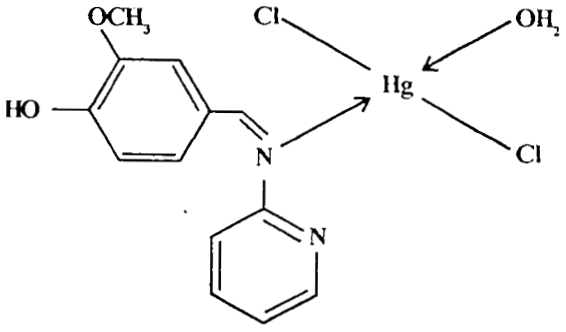
OCH3
Cl
OH2
HO
Hg
N
Cl
N

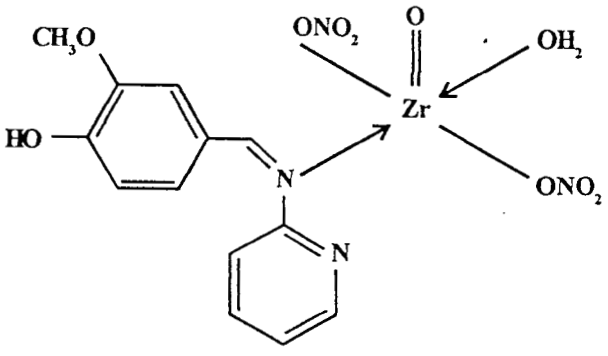
CH3O
ONO2
O
OH2
HO
Zr
N
ONO2
N

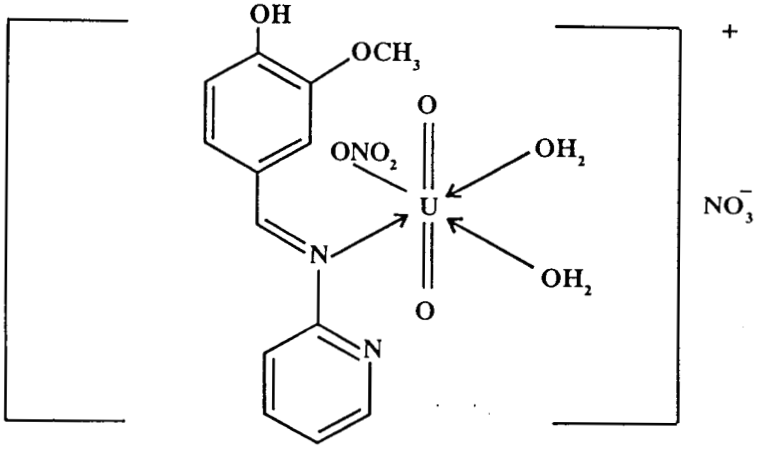
OH
OCH3
O
ONO2
OH2
U
N
OH2
O
N
+
NO3−

TABLE 1.3.1. **Microanalytical, magnetic and conductance data of transition metal chelates of vanillin-2-aminopyridine (L'H)**

Complex	Colour	M%	C%	H%	N%	S%	Cl%	μ_{eff} (B.M.)	Ω^{-1}
$[MnL'HCl(H_2O)_4]Cl$	Pale yellow	12.42 (12.90)	37.13 (36.64)	5.01 (4.70)	7.06 (6.58)	--	16.31 (16.65)	6.29	45.28
$[FeL'H(H_2O)_5]SO_4$	Brown	12.50 (11.89)	34.16 (33.20)	5.55 (4.68)	6.37 (5.96)	6.97 (6.81)	--	5.22	44.71
$[CoL'H(OAc)_2(H_2O)_3]$	Coffee brown	13.71 (12.84)	45.13 (44.45)	5.98 (5.23)	6.36 (6.10)	--	--	4.88	5.19
$[NiL'H(OAc)_2(H_2O)_3]$	Pale green	12.50 (12.80)	45.28 (44.47)	5.44 (5.23)	6.46 (6.10)	--	--	3.52	7.62
$[CuL'H(OAc)_2(H_2O)_3]$	Chocolate brown	13.29 (13.70)	44.98 (44.01)	6.02 (5.18)	6.58 (6.04)	--	--	2.05	9.67
$[ZnL'H(OAc)_2(H_2O)_3]$	Pale yellow	14.21 (14.05)	44.10 (43.84)	6.11 (5.16)	6.97 (6.02)	--	--	D	3.23
$[CdL'H(OAc)_2H_2O$	Lemon yellow	24.38 (23.59)	43.47 (42.82)	4.39 (4.20)	6.32 (5.88)	--	--	D	4.74
$[HgL'HCl_2(H_2O)]$	Lemonyellow	38.01 (38.76)	30.65 (30.14)	2.63 (2.70)	6.08 (5.41)	--	13.22 (13.70)	D	3.36
$[ZrOL'H(NO_3)_2H_2O]$	Pale yellow	19.39 (19.11)	33.71 (32.69)	3.12 (2.93)	12.55 (11.73)	--	--	D	9.83
$[UO_2L'H(NO_3)(H_2O)_2]NO_3$	Reddish brown	36.78 (36.17)	24.63 (23.71)	2.14 (2.43)	9.11 (8.51)	--	--	D	43.55

Calculated values are given in the parenthesis; D - diamagnetic; M - metal; Ω^{-1} - molar conductance in $ohm^{-1}cm^2mol^{-1}$

TABLE 1.3.2. **Characteristic infrared absorption frequencies (cm^{-1}) of transition metal chelates of vanillin-2-aminopyridine (L'H)**

Substance	νH2O	νC=N (azomethine)	νC=N (in ring)	νC-O (phenolic)	In plane deformation	Out of plane deformation	νM-N	νM-O
LH	--	1674s	1462m	1298s	821m	772, 733w	--	--
$[MnL'HCl(H_2O)_4]Cl$	3500-3100br	1651s	1458m	1309s	827m	781, 729w	557w	459w
$[FeL'H(H_2O)_5]SO_4$	3500-3100br	1649s	1456m	1308s	826m	771, 739w	550w	443w
$[CoL'H(OAc)_2(H_2O)_3]$	3500-3100br	1647s	1460m	1312s	820m	768,742w	532w	437w
$[NiL'H(OAc)_2(H_2O)_3]$	3500-3100br	1630s	1458m	1307s	828m	768,742w	526w	426w
$[CuL'H(OAc)_2(H_2O)_3]$	3500-3100br	1660s	1459m	1310s	824m	772,740w	592w	442w
$[ZnL'H(OAc)_2(H_2O)_3]$	3500-3100br	1657s	1461m	1310s	821m	771, 739w	520w	428w
$[CdL'H(OAc)_2H_2O$	3500-3100br	1654s	1460m	1300s	828m	779, 725w	527w	437w
$[HgL'HCl_2(H_2O)]$	3500-3100br	1654s	1458m	1306s	822m	779,748w	554w	449w
$[ZrOL'H(NO_3)_2H_2O]$	3500-3100br	1650s	1462m	1308s	828m	781,727w	542w	457w
$[UO_2L'H(NO_3)(H_2O)_2]NO_3$	3500-3100br	1640s	1457m	1308s	825m	774,742w	536w	450w
$[UO_2L'HNO_3(H_2O)_2]NO_3$								

br - broad; m - medium; s - strong; w - weak

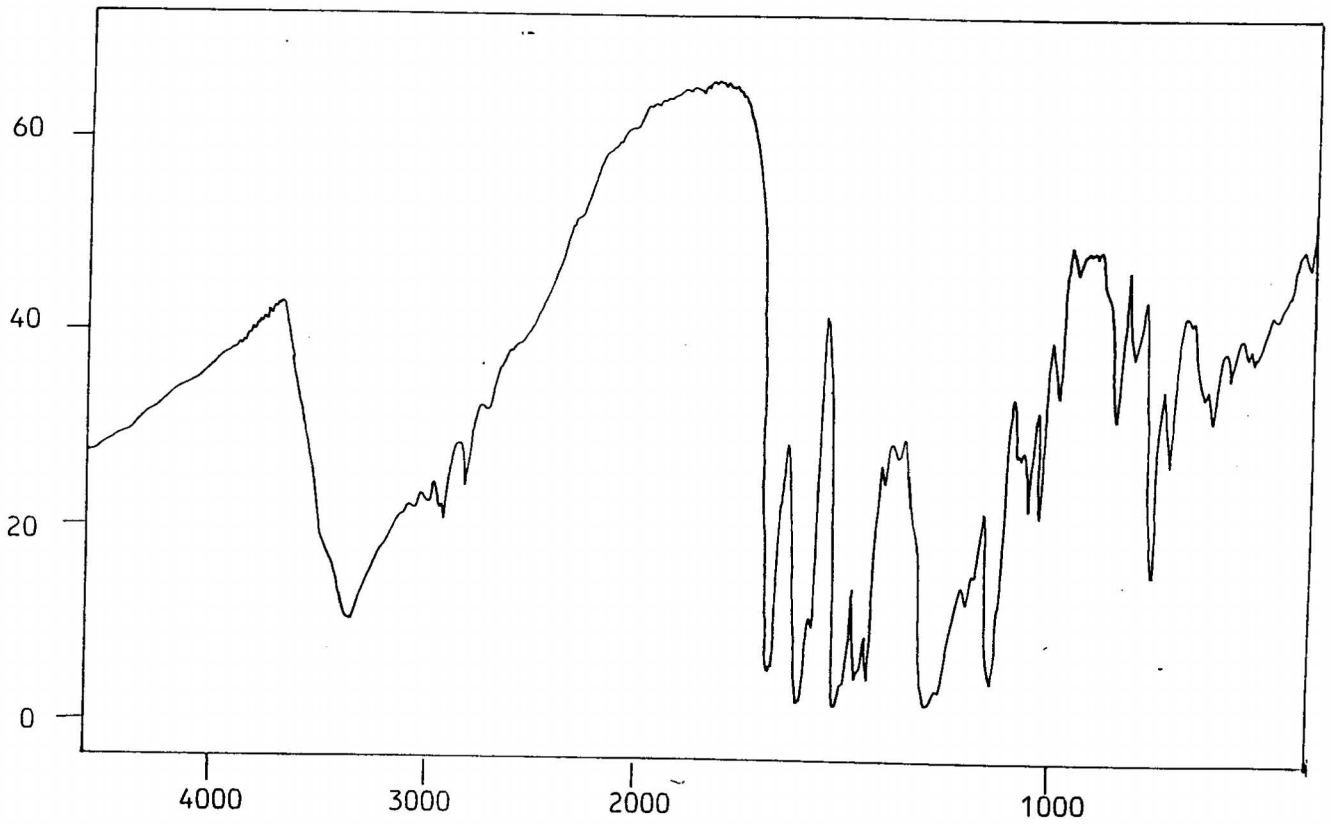

Figure I. 3.1 **IR Spectrum of vanillin-2-aminopyridine**

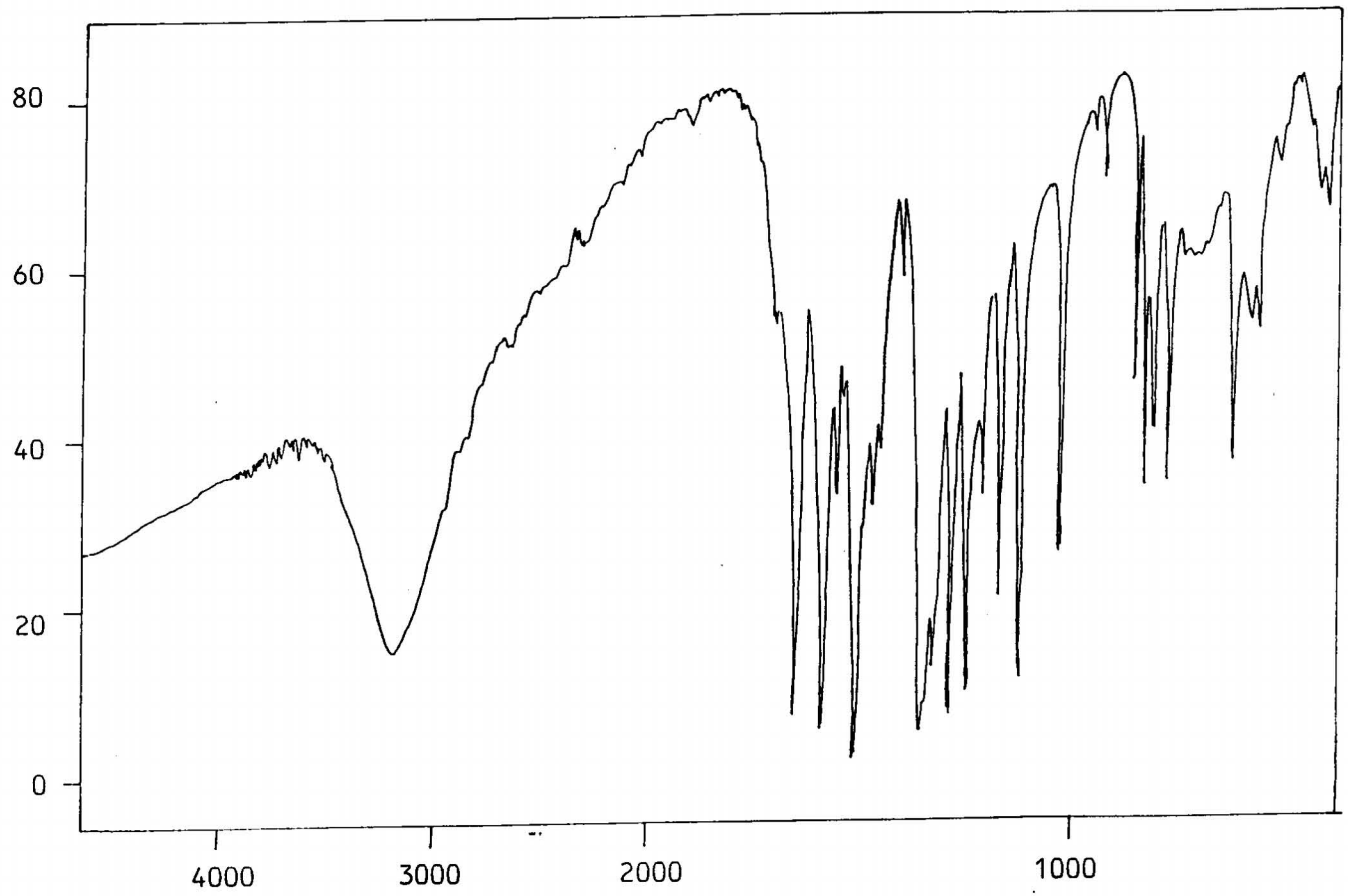

Figure I. 3.2 IR Spectrum of $[CoL^1H(OAc)_2(H_2O)_3]$

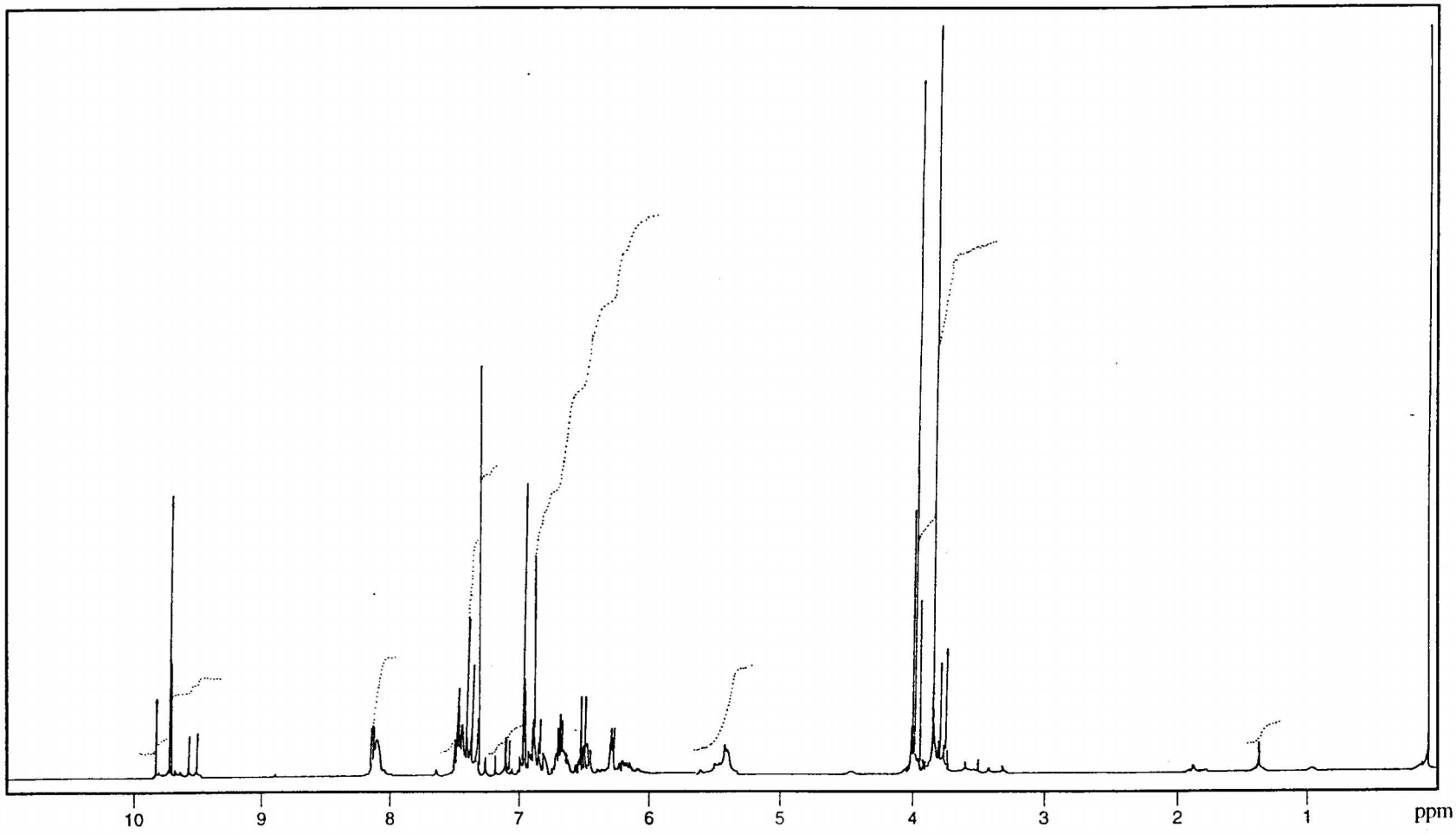

Figure I. 3.3 **NMR Spectrum of vanillin-2-aminopyridine**

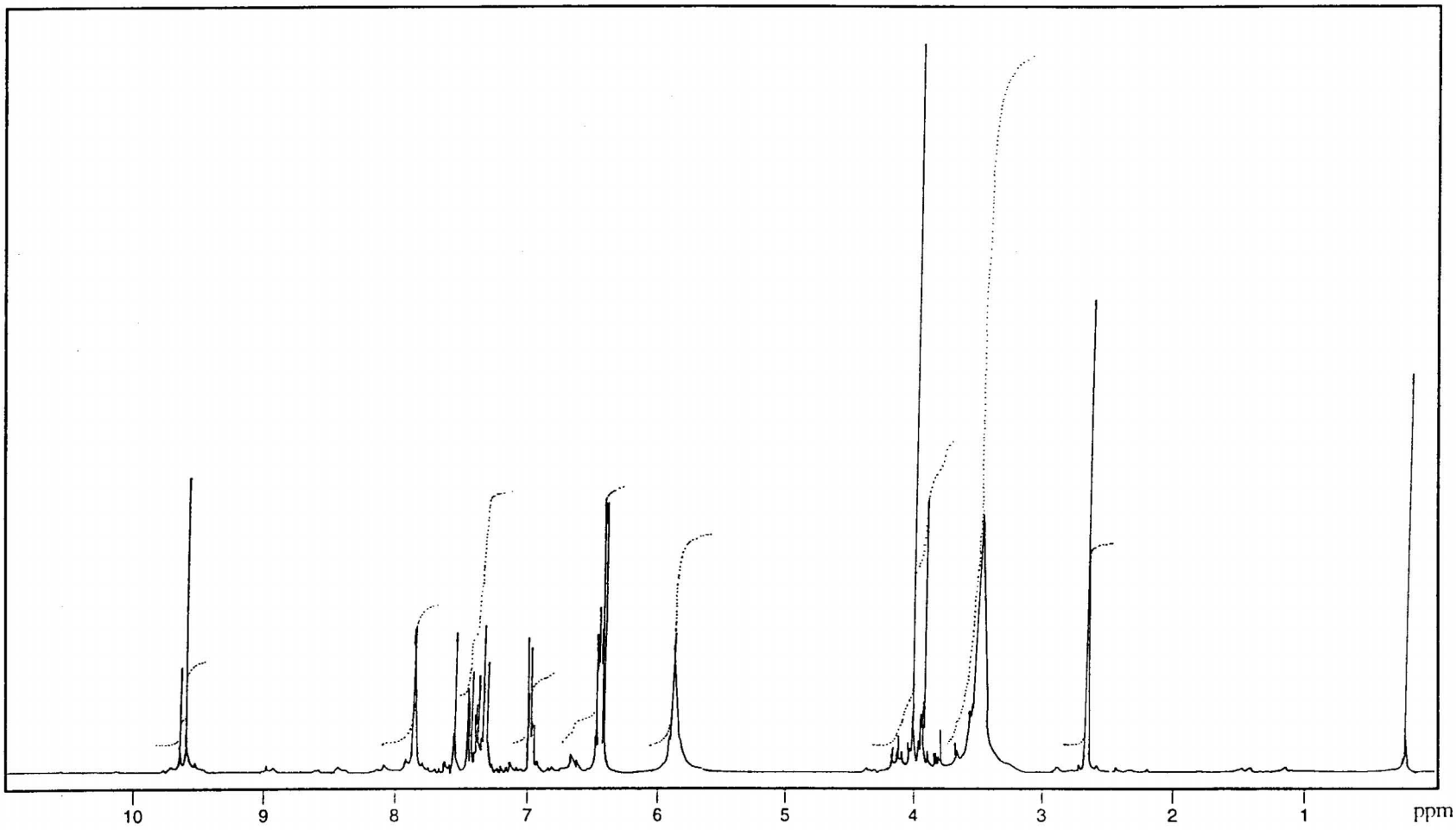

Figure I. 3.4 **NMR Spectrum of $[UO_2L^1HNO_3(H_2O)_2]NO_3$**

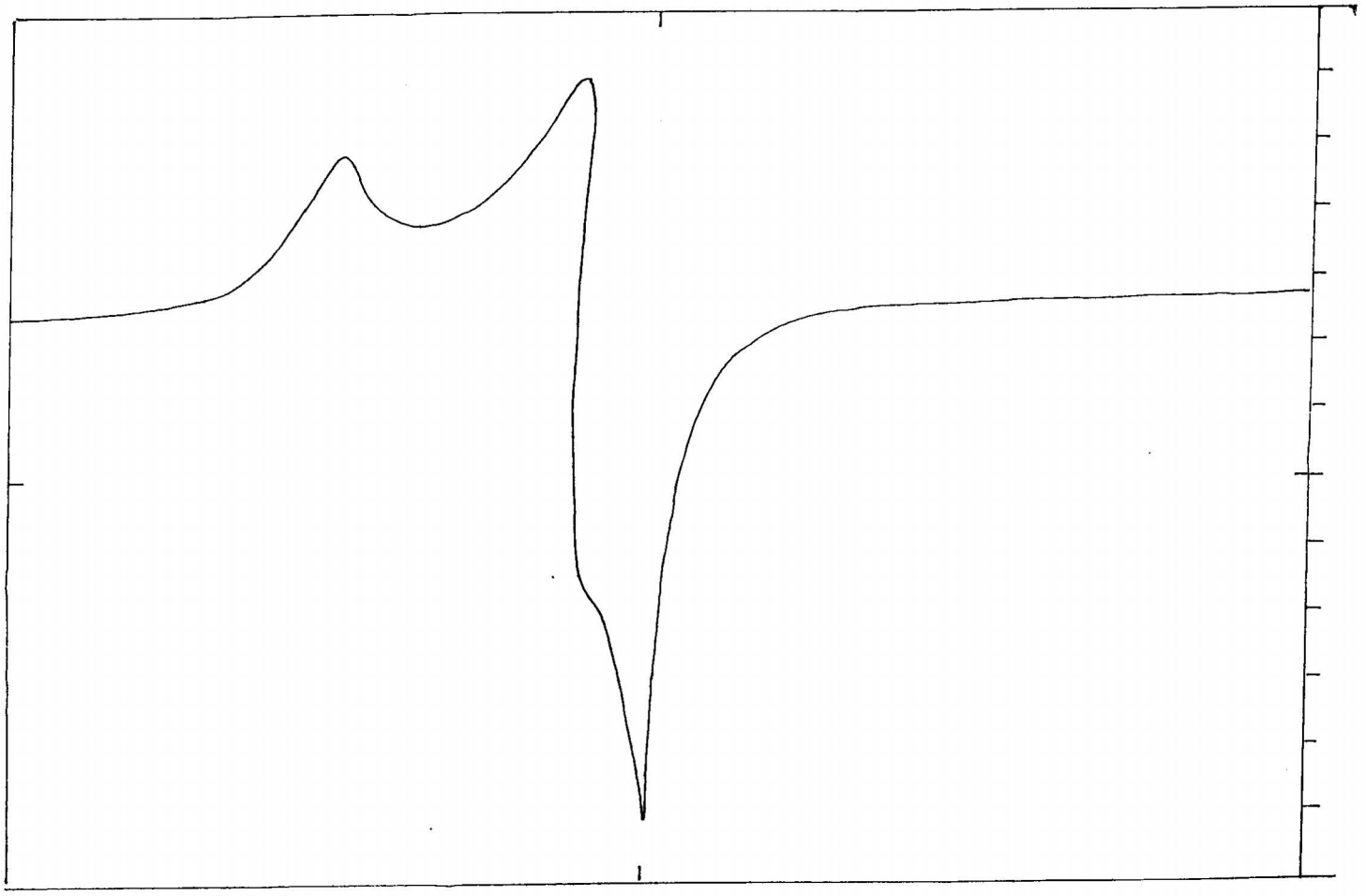

Figure 1.3.5. **ESR spectrum of $[CuL'H(OAc)_2(H_2O)_3]$**

CHAPTER IV

TRANSITION METAL COMPLEXES OF VANILLIN-2-AMINOTHIAZOLE

2-Aminothiazole derivatives are potential chelating agents because these form stable and coloured complexes with various metal ions. Schiff bases derived from 2-aminothiazole and their metal complexes have wide application in biological science. A recent review by Manju Bala,[134] on the metal complexes of Schiff bases derived from 2-aminothiazole points out the current interest of this type of complexes. Therefore, it was felt to be worthwhile to investigate the physicochemical aspects of some metal complexes of Schiff bases derived from 2-aminothiazole with vanillin.

Preparation of the ligand

Vanillin-2-aminothiazole (VAAT) was prepared by refluxing an ethanolic solution of vanillin (1.5 g; 0.01 mol) and 2-aminothiazole (1 g; 0.01 mol) for 16 h on a water bath. The resulting solution was added to distilled water dropwise with constant stirring. Brownish yellow crystals separated were filtered, washed and dried over anhydrous $CaCl_2$. m.p. 98°C.

Characterization of the ligand

The ligand vanillin-2-aminothiazole was characterized by elemental analysis and electronic and infrared spectral studies. The nmr spectrum of the ligand was also taken. Ligand is soluble in DMSO but is very sparingly soluble in methanol, ethanol, nitrobenzene etc.

Analyical data found	:	C, 56.39%; H, 4.21%; N, 11.92%.
Calculated for $C_{11}H_{10}N_2SO_2$	:	C, 56.41%; H, 4.27%; N, 11.97%.

The calculated and observed percentages of carbon, hydrogen and nitrogen were in good agreement. Based on the above results, the structure of the ligand was confirmed as

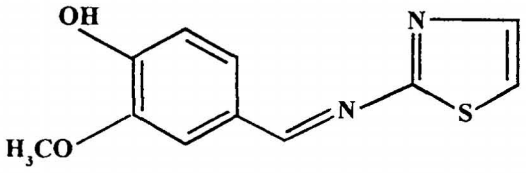

Studies on Mn(II), Fe(II), Co(II), Ni(II), Cu(II), Zn(II), Cd(II), Hg(II) ZrO(II) and UO_2(II) complexes of vanillin-2-aminothiazole

Vanillin-2-aminothiazole and its transition and uranium metal chelates have been synthesised, and examined in the context of the structural aspect of the ligand moiety in the metal chelates.

Preparation of complexes

Mn(II), Co(II), Ni(II), Cu(II), Zn(II), Cd(II) and UO_2(II) chelates were prepared by refluxing an ethanolic solution of the ligand with appropriate metal salts in methanol followed by the addition of the resulting solution in distilled water with constant stirring.

Complexes of Fe (II), ZrO (II) and Hg (II) were synthesised by adding their metal salt solutions to the boiling ethanolic solution of the ligand in 1:2 ratio. In all cases, the seperated complex was filtered, washed with ethanol-water (1:1) mixture and dried in a vacuum desiccator over unhydrous $CaCl_2$. Approximately 80% yield was obtained.

RESULTS AND DISCUSSION

Elemental analysis

The complexes were analysed for metal, sulphur and chlorine by standard methods. Percentage of carbon, hydrogen and nitrogen were determined by microanalytical methods. The results are summarised in

Table 1.4.1. All these complexes are stable, coloured and possess 1:1 stoichiometry except Mn(II) and Co(II) complexes which are 1:2 in nature.

Molar conductance

The molar conductance measurements in ethanol were carried out at a concentration of 10^{-4}M at 28 ± 2°C and the data are included in the Table 1.4.1. All these chelates except that of Fe(II) exhibited very low value of molar conductance (< 10 ohm^{-1} cm^2 mol^{-1}) which indicate their non-electrolytic nature. Fe(II) complex behaves as a 1:1 electrolyte.

Magnetic measurements

The observed magnetic moment values are summarised in the Table 1.4.1. An octahedral geometry is suggested for Mn(II) complex which shows a magnetic moment value of 5.91 B.M. which is nearer to the spin only value of 5.92 B.M.[117]. The observed value of 5.4 B.M. in the case of Fe(II) complex suggests an octahedral geometry[117,118]. Octahedral geometry of Co(II) was confirmed from the magnetic susceptibility value obtained, 5.2 B.M.[117]. Ni(II) complex which exhibited the spin only value of 2.44 B.M is assignable to octahedral geometry[117]. The magnetic moment value of copper(II) complex is suggestive of $t_{2g}^6eg^3$ electronic configuration in an octahedral ligand field (1.99 B.M.)[117,118]. As expected all the remaining complexes were found to be diamagnetic.

Infrared spectral studies

Characteristic ir absorption bands of the ligand and complexes are summarised in Table 1.4.2.

The presence of coordinated water molecules in the complexes of Mn(II), Fe(II), Co(II), Ni(II), Cu(II), Zn(II), Cd(II), Hg(II), ZrO(II) and UO_2(II) complexes is confirmed by the appearance of a double hump between 3300-3100 cm^{-1} followed by a rocking mode of vibration between 880-830cm^{-1}. The band appearing in the spectrum of ligand at 1620 cm^{-1} is due to νC=N, which undergo shift to lower frequency region in the complexes indicating coordination through azomethine nitrogen[121, 135].

In Co(II), Ni(II), Cu(II), Zn(II) and Cd(II) complexes, the asymmetric and symmetric stretching vibrations of the carboxylate groups occur at 1620 and ~1430 cm^{-1} showing a Δν of, about 190 cm^{-1}. Monodentate carboxylate group has a Δν value of 150-190 cm^{-1}, but a bidentate carboxylate has a much closer difference (< 120 cm^{-1}). Monodentate carboxylate groups are, therefore, indicated in the above chelates[121, 130].

The presence of Zr = 0 bond in ZrO(II) complex is confirmed by the presence of narrow bands at 980 cm^{-1} and 970 cm^{-1} [129,136]. The presence of ir absorption bands at 1450 cm^{-1}, 1340 cm^{-1} and 1160 cm^{-1} corresponds to $\nu_{asy}(NO_3)$, $\nu_{sy}(NO_3)$, and ν(N-O) vibrations respectively of coordinated unidentate nitrate group. Since the separation of highest frequency bands is 110 cm^{-1}, the nitrate group present in ZrO(II) and UO_2(II) complexes seems to be monodentate.

Uranyl complex is characterised with a band at 920 cm^{-1} which is a clear evidence of the O=U=O bond[127]. The force constant of U=O bond is found to be 7.21 millidynes A^o and bond length is 1.72A^o.

The conclusive evidence of bonding of the ligand to the central metal ion is provided by the appearance of bands at ~520 cm^{-1} and 410 cm^{-1}, which can be assigned to M-N and M-O bonds respectively[131].

Electronic spectra

Electronic spectrum of the ligand is characterized by two bands lying at 32258 and 27027 cm^{-1}. During complex formation a red shift is detected for these bands which indicate the involvement of Schiff base in coordination[133].

The octahedral environment of the ligand around the central Mn(II) ion is confirmed by the appearance of a broad band at 24875 cm^{-1} [132]. The expected $^5T_{2g} \rightarrow {}^5E_g$ electronic transition in the octahedral Fe(II) complex[133] has been recorded at about 16100 cm^{-1}. The $^4T_{1g}(F) \rightarrow {}_4T_{2g}(F)$ and $^4T_{1g}(F) \rightarrow {}^4T_{1g}(P)$ transitions expected for Co(II) complex with octahedral geometry was very clear in the spectrum at 9500-10530 cm^{-1} and 20000-22000 cm^{-1} respectively. The two electronic absorption bands at 10755 cm^{-1} and 23600 cm^{-1} present in Ni(II) complex is due to $^3A_{2g}(F) \rightarrow {}^3T_{1g}(F)$ and $^3A_{2g}(F) \rightarrow {}^3T_{1g}(P)$ transitions. Based on these observations the structure of Ni(II) complex can be confirmed to be octahedral. The distorted octahedral geometry of Cu(II) complex is clear from the absorption band at 16123 cm^{-1} [133].

A band at 18656 cm^{-1} can be seen in ZrO(II) complex. This may be due to charge transfer transition from ligand to metal. UO_2(II) chelate exhibited the characteristic band at 28600 cm^{-1} which indicate the presence of UO_2^{2+} in uranyl complex[142].

Electron spin resonance spectra

ESR spectrum of the Cu(II) complex of vanillin-2-aminothiazole was taken in the solid form using DPPH as the reference. The spectrum contained only one absorption line. Unusual spectra of this type have been noted for complexes which bear large organic molecules[149,150]. The g value is 2.1784 and this indicates strong interaction between the ligand and Cu(II) ion[144].

X-ray studies

Ni(II) and Cu(II) complexes of VAAT were subjected to X ray analysis, but it became very difficult to conduct a detailed study of crystal structure in the solid state. This may be due to the noncrystalline nature of these complexes.

Thermal studies

Mn(II), Co(II), Ni(II), Cu(II) and Zn(II) complexes of vanillin-2-aminothiazole were subjected to thermogravimetric analysis. There is no detectable change in the TG curves up to 100°C which indicates the absence of any hydrated water molecule. The mass loss around 150°C in the TG traces of Mn(II), Co(II) Ni(II), Cu(II) and Zn(II) complexes supports the presence of coordinated water. The residues were found to be the corresponding oxides of the metal in the complex. The kinetic analysis of thermogravimetric decomposition of these five complexes are described in Part II.

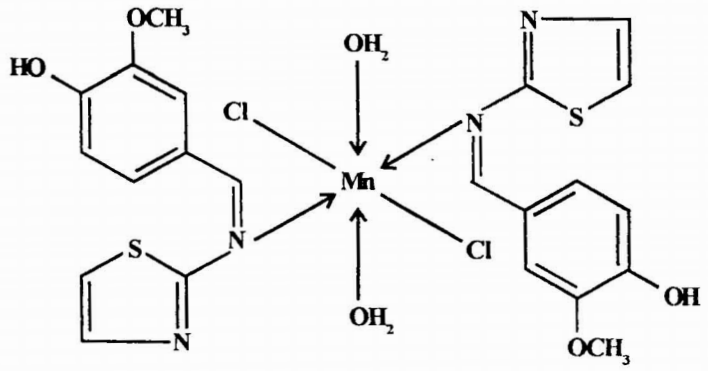
OCH3
HO
OH2
Cl
N
S
N
Mn
N
S
Cl
N
OH2
OH
OCH3

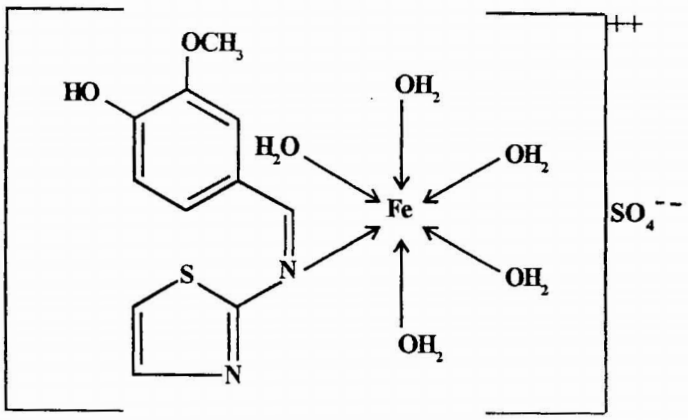
OCH3
HO
OH2
H2O
OH2
Fe
SO4--
++
S
N
N
OH2
OH2

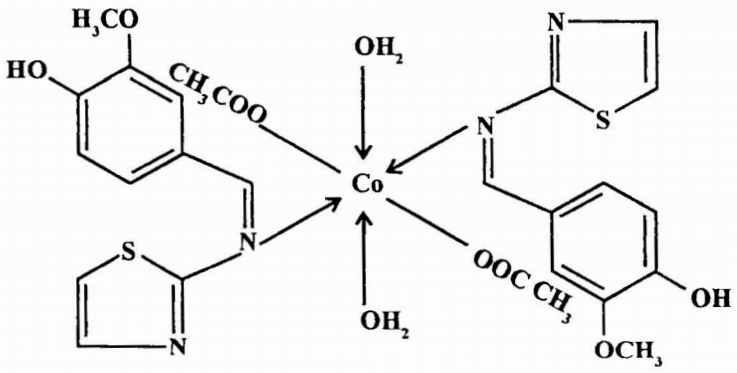
H3CO
HO
CH3COO
OH2
N
S
N
Co
N
S
N
OOC CH3
OH
OH2
OCH3

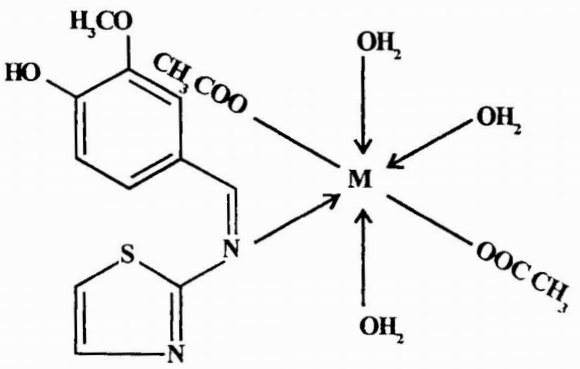

M = Ni (II), Cu (II) or Zn (II).

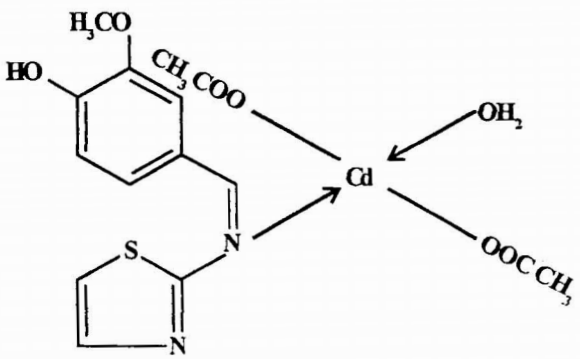

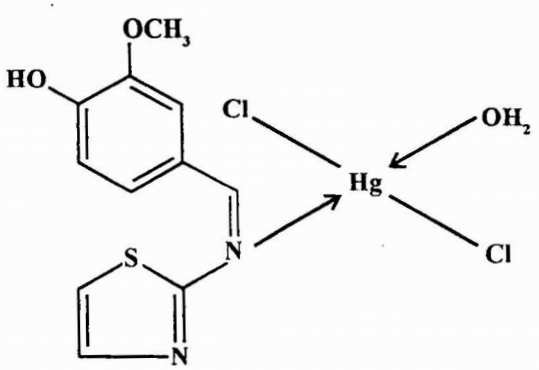

TABLE 1.4.1. **Microanalytical, magnetic and conductance data of transition metal chelates of vanillin-2-aminothiazole (L"H)**

Complex	Colour	M%	C%	H%	N%	S%	Cl%	μ_{eff} (B.M.)	Ω^{-1}
$[Mn(L"H)_2Cl_2(H_2O)_2]$	Brown	8.24 (8.72)	41.15 (41.92)	3.07 (3.81)	8.12 (8.89)	10.84 (10.16)	10.88 (11.26)	5.91	2.38
$[FeL"H(H_2O)_5]SO_4$	Brown	11.25 (11.74)	27.21 27.74)	3.88 (4.20)	6.02 (5.88)	13.61 (13.45)	--	5.42	43.71
$[Co(L"H)_2(OAc)_2(H_2O)_2]$	Brownish yellow	8.42 (8.66)	45.11 (45.82)	3.97 (4.40)	8.77 (8.22)	9.52 (9.40)	--	5.24	1.92
$[NiL"H(OAc)_2(H_2O)_3]$	Greenish yellow	12.54 (12.63)	38.46 (38.73)	5.01 (4.73)	6.33 (6.02)	6.57 (6.89)	--	2.43	8.63
$[CuL"H(OAc)_2(H_2O)_3]$	Coffee brown	13.31 (13.52)	37.84 (38.34)	4.84 (4.68)	5.66 (5.96)	6.21 (6.82)	--	2.08	1.25
$[ZnL"H(OAc)_2(H_2O)_3]$	Lemon yellow	13.36 (13.87)	38.54 (38.19)	4.21 (4.67)	5.81 (5.94)	5.99 (6.79)	--	D	1.87
$[CdL"H(OAc)_2H_2O$	Brownish yellow	23.85 (23.30)	37.88 (37.31)	3.79 (3.73)	5.92 (5.80)	6.09 (6.63)	--	D	1.65
$[HgL"HCl_2(H_2O)]$	Brownish yellow	37.94 (38.32)	25.34 (25.21)	2.11 (2.29)	5.39 (5.35)	6.50 (6.11)	13.19 (13.54)	D	4.48
$[ZrOL"H(NO_3)_2H_2O]$	Brownish yellow	18.21 (18.88)	27.13 (27.32)	2.52 (2.48)	12.02 (11.59)	6.00 (6.62)	--	D	4.29
$[UO_2L"H(NO_3)_2H_2O]$	Reddish brown	36.31 (36.84)	20.78 (20.43)	2.10 (1.86)	8.13 (8.67)	4.88 (4.95)	--	D	2.54

Calculated values are given in the parenthesis; D - diamagnetic; M - metal; Ω^{-1} - molar conductance in $ohm^{-1}cm^2mol^{-1}$.

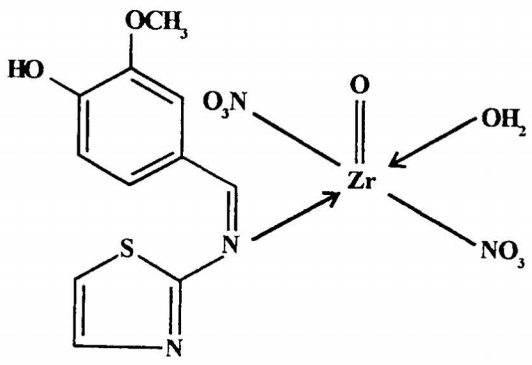
OCH3
HO
O3N
O
OH2
Zr
NO3
S
N
N

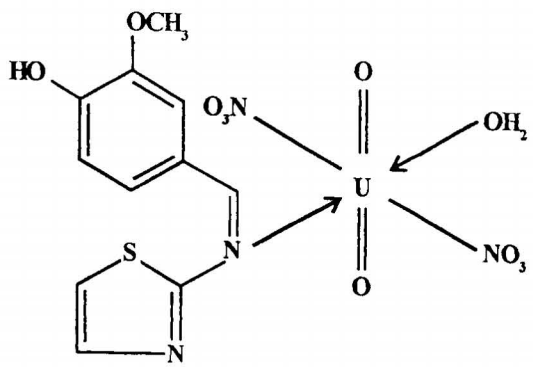
OCH3
HO
O3N
O
OH2
U
O
NO3
S
N
N

TABLE 1.4.2. **Characteristic infrared absorption frequencies (cm^{-1}) of transition metal chelates of vanillin-2-aminothiazole (L"H)**

Substance	νH_2O	$\nu C{=}N$ (azomethine)	$\nu C{=}N$ (in ring)	$\nu C{-}O$ (phenolic)	In plane deformation	Out of plane deformation	$\nu M{-}N$	$\nu M{-}O$
L"H	--	1620s	1458m	1308s	830m	740,710m	--	--
$[Mn(L"H)_2Cl_2(H_2O)_2]$	3300-3100br	1580s	1460m	1310s	820m	750,720 m	520w	420w
$[FeL"H(H_2O)_5]SO_4$	3300-3100br	1590s	1462m	1312s	820m	750,720m	510w	420w
$[Co(L"H)_2(OAc)_2(H_2O)_2]$	3300-3100br	1570s	1462m	1311s	830m	740,710m	530w	420w
$[NiL"H(OAc)_2(H_2O)_3]$	3300-3100br	1580s	1460m	1308s	825m	740,710m	520w	430w
$[CuL"H(OAc)_2(H_2O)_3]$	3300-3100br	1580s	1468m	1314s	828m	750,720m	520w	420w
$[ZnL"H(OAc)_2(H_2O)_3]$	3300-3100br	1590s	1458m	1312s	828m	750,720m	520w	420w
$[CdL"H(OAc)_2H_2O$	3300-3100br	1560s	1458m	1312s	820m	750,720m	535w	420w
$[HgL"HCl_2(H_2O)]$	3300-3100br	1580s	1465m	1316s	830m	750,710m	530w	430w
$[ZrOL"H(NO_3)_2H_2O]$	3300-3100br	1570s	1462m	1317s	826m	750,720m	520w	425w
$[UO_2L"H(NO_3)_2(H_2O)]$	3300-3100br	1590s	1466m	1310s	820m	740,710m	540w	420w

br - broad; m - medium; s - strong; w - weak

CHAPTER V

TRANSITION METAL COMPLEXES OF *o*-VANILLIN-2-AMINOPYRIDINE

A study of literature showed that there have been numerous studies on metal complexes of salicylaldehyde and vanillin. However, little information is available on metal complexes of Schiff bases derived from *o*-vanillin. Therefore, it is considered to be worthwhile and interesting to investigate the donor properties of *o*-vanillin (2-hydroxy-3-methoxy-benzaldehyde) ligands towards some metal ions such as Mn(II), Fe(II), Co(II), Ni(II), Cu(II), Zn(II), Cd(II), Hg(II), ZrO(II) and UO_2(II).

Synthesis of the ligand

o-Vanillin (1.52 g; 0.01 mol) was dissolved in methanol and mixed with a solution of 2-aminopyridine (0.94 g; 0.01 mol) in methanol. The solution was refluxed for 4 h in a water bath and the resulting solution was added to distilled water taken in a beaker with constant stirring. Orange red crystals formed were filtered and washed with dilute methanol (25%). Sample was recrystallised from methanol and dried over anhydrous $CaCl_2$. m.p. 60°C.

Characterization of the ligand

The ligand is soluble in organic solvents like methanol, ethanol, acetone, nitrobenzene etc. *o*VAAP was characterized on the basis of elemental analysis and spectral data. CHN analysis of the ligand is as follows:

Analytical data found : C, 67.98%; H, 5.12%; N, 11.67%

Calculated for $C_{13}H_{12}N_2O_2$: C, 68.34%; H, 5.26%; N, 12.27%

The electronic and infrared spectra of the ligand showed characteristic bands. Based on the above results, the structure of the ligand was confirmed as given below.

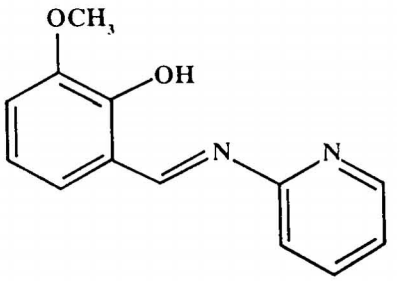

Studies on Mn(II), Fe(II), Co(II), Ni(II), Cu(II), Zn(II), Cd(II), Hg(II), ZrO(II) and UO_2(II) complexes of *o*-vanillin-2-aminopyridine

In this section, the preparation and characterization of ten new transition metal complexes of the Schiff base, *o*-Vanillin-2-aminopyridine are described.

Synthesis of complexes

Cu(II), Zn(II), Cd(II), Hg(II) and ZrO(II) complexes were prepared by refluxing the ethanolic solutions of ligand and metal(II) salt followed by the addition of the resulting solution to distilled water with constant stirring.

Complexes of Mn(II), Fe(II), Co(II) and Ni(II) were synthesised by refluxing the ethanolic solution of the ligand with methanolic or aqueous solution of metal acetate or sulphate.

UO_2(II) complex was formed with 100% yield on mixing uranyl nitrate dissolved in ethanol with ethanolic solution of the ligand.

In all cases the separated complexes were filtered, washed and dried over anhydrous $CaCl_2$. The yield was approximately found to be 80%.

Characterization of the complexes

The complexes were characterized on the basis of elemental analysis, uv and ir spectral data, magnetic studies, conductance measurements and thermal data.

RESULTS AND DISCUSSION

All these complexes are coloured, non-hygroscopic solids.

Elemental analysis

The complexes were analysed for metals and halogens by standard methods[106,107]. Carbon, hydrogen and nitrogen were estimated by microanalytical methods. The anlaytical data and physical appearance of the complexes under investigation are summarised in Table 1.5.1. *o*-VAAP acts as bidentate generally but in the Fe(II) complex it acts as monodentate.

Molar conductance

The conductivity of all the complexes at a concentration of 10^{-4}M at room temperature was measured in ethanol and the data are included in Table 1.5.1. Mn(II) complex possesses a molar conductance of 46.9 $ohm^{-1}\ cm^2mol^{-1}$ in agreement with the 1:1 electrolytic nature likewise UO_2(II) complex also behaves as a 1:1 electrolyte. Remaining chelates exhibited very low value of molar conductance (< 10 $ohm^{-1}cm^2mol^{-1}$) which indicate their non-electrolytic nature.

Magnetic measurements

The observed magnetic moment for Mn(II) complex is 6.03 B.M. This value is nearer to the spin only value of 5.92 B.M. which points out the presence of five unpaird electrons. The corresponding geometry, i.e., octahedral symmetry can therefore be assigned to the Mn(II) chelate[116].

The magnetic moment 5.6 B.M. exhibited by Fe(II) complex is in good agreement with the reported value for an octahedral geometry[118].

The μ_{eff} value for the Co(II) complex is 4.78 B.M. suggesting thereby a high-spin octahedral geometry for this complex, which is further supported by electronic spectral data[117]. The effective magnetic moment observed for Ni(II) complex (3.3 B.M.) is well within the range for spin-free complexes and also supports octahedral geometry[117].

The Cu(II) complex exhibited slightly higher magnetic moment (2.2 B.M.) than the normal value (1.7 B.M.) observed for d^9 system with one unpaired electron[117]. This accounts for a slight orbital contribution to the spin only value and absence of spin-spin interaction in the complex. Therefore an octahedral geometry is assigned to the Cu(II) complex. All other complexes were found to be diamagnetic.

Infrared spectral studies

Infrared spectral data of the free Schiff base ligand and the metal complexes studied are given in Table 1.5.2.

A strong intense band due to νC=N stretch (azomethine) in ligand, appears around 1605 cm^{-1} which upon complexation shifts towards higher wave number region by 10-30 cm^{-1} indicating the participation of azomethine nitrogen in coordination with metal ions[137]. The spectral band corresponding to the characteristic stretching mode of C=N group in the pyridine ring at 1450-1440 cm^{-1} remain almost unaltered in the spectra of the complexes suggesting the non-coordination of pyridine ring nitrogen[121].

The normal stretching mode of hydroxyl group, which is expected at 3600 cm^{-1} as a sharp and strong band, may be very much weakened and some times become insignificant, if the group undergoes strong hydrogen

bonding[138]. Absence of characteristic absorption bands of ν_{OH} in the ligands clearly explains the existence of a strong intramolecular hydrogen bonding as shown below.

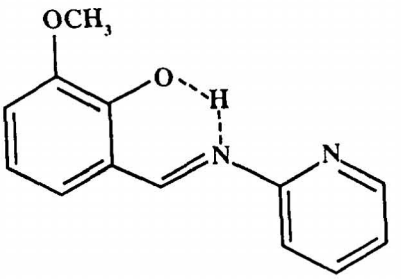

The disappearance of νO-H and the positive shift of the phenolic C-O stretching vibration by 40-70 cm^{-1} found in the spectra of the complexes indicate the coordination of phenolic oxygen after deprotonation.

The presence of coordinated water molecule in all the present complexes is shown by the appearance of a broad and strong band[120] at 3400-3100 cm^{-1} followed by a sharp peak at 835 cm^{-1}.

The appearance of two non-ligand bands at about 1560 and 1370 cm^{-1} in the ir spectra of the chelates of Co(II), Ni(II), Zn(II) and Cd(II) suggest the presence of coordinated acetate group. The frequency difference value of about 200 cm^{-1} between these asymmetric and symmetric modes of acetate group further indicates unidentate nature of this group[121].

The bands at ~ 1370, 1280, 1020 and 750 cm^{-1} in the spectrum of ZrO(II) complex can be ascribed to $\nu_{asy}(NO_3)$, $\nu_{sy}(NO_3)$ and νN-O vibrations of coordinated monodentate NO_3 group[139]. The bidentate nature of sulphate

present in Fe(II) complex is confirmed by the bands obtained at 1152, 1122, 1105, 1090, 1035, 638 and 605 cm^{-1} [121].

The bond strength and bond length of O=U=O bonds have been calculated from the characteristic stretching band present in the complex spectrum at 935 cm^{-1} and were found to be 7.27 millidynes/A^o and 1.76 A^o respectively[128].

ZrO(II) complex exhibited bands at 920 cm^{-1} and 910 cm^{-1} which can be assigned to νZr=O[129,130].

The spectra of the chelates displayed two new bands in the range 600-550 and 470-440 cm^{-1} which were assigned to νM-N and νM-O respectively[131].

Electronic spectra

Electronic spectra of the ligand exhibits three bands lying at 21881 cm^{-1}, 23041 cm^{-1} and 31645 cm^{-1} which can be assigned to $n \rightarrow \pi^*$, $\pi \rightarrow \pi^*$ and $n \rightarrow \sigma^*$ transitions respectively. These transitions are observed with high intensity. During complexation these bands are shifted to higher frequency region. Roughly about 2360 cm^{-1}, 2021 cm^{-1} and 1034 cm^{-1} upward shift was observed for $n \rightarrow \pi^*$, $\pi \rightarrow \pi^*$ and $n \rightarrow \sigma^*$ transition bands respectively. This clearly attributes the involvement of the ligand in coordination. In addition, a strong non-ligand band at 15698 cm^{-1} in the spectra of chelates can be assigned to charge transfer transition from ligand to metal[133].

The electronic spectrum of the Mn(II) complex contained a band at 24510 cm^{-1} which was taken as evidence to support the presence of Mn(II) in octahedral environment[132].

For the iron complex the bands observed at 29854 and 27000 cm^{-1} may be assigned to the charge transfer transitions. The low intensity bands observed at 20491 and 18900 cm^{-1} are due to the spin forbidden d-d transitions in the octahedral symmetry[140].

Expected octahedral transitions of cobalt $^4T_{1g}(F) \rightarrow {}^4T_{2g}(F)$ and $^4T_{1g}(F) \rightarrow {}^4T_{1g}(P)$ were observed at 9480 cm^{-1} and 21271 cm^{-1} in the spectrum of Co(II) complex[133]. Ni(II) complex exhibits three d-d transitions in the electronic spectrum. The observed bands can be assigned as follows:

$^3A_{2g}(F) \rightarrow {}^3T_{2g}(F)$; 9680 cm^{-1}

$^3A_{2g}(F) \rightarrow {}^3T_{1g}(F)$; 12135 cm^{-1}

$^3A_{2g}(F) \rightarrow {}^3T_{1g}(P)$; 22831 cm^{-1}

The charge transfer band observed at 37587 cm^{-1} might have obscured the d-d transitions in the electronic spectrum of Cu(II) complex.

ZrO(II) chelate exhibited a well defined band at 24814 cm^{-1} due to charge transfer transition.

The presence of UO_2^{2+} entity is established by the presence of a strong band at 27100 cm^{-1} in uranyl complex[142].

Nuclear Magnetic Resonance Spectroscopy

The ^1H nmr spectra of the ligand and a representative $UO_2(II)$ chelate were taken in DMSO-d_6. It is of particular interest whether or not the phenolic oxygen atom is coordinated to the metal ion along with the azomethine group. A sharp signal which appears at 13.4 δ in the free ligand can be assigned to the phenolic proton. The signal is absent in the complex which indicates that U-O bond is formed in the reaction[141].

Electron spin resonance spectra

The X-band esr spectrum of $[CuL'''_2(H_2O)_2]$ was recorded at microwave frequency 9.352 GHz and field strength 3200 g using DPPH as the reference. The complex exhibited only a weak absorption band. The small g value (2.1855) indicates strong interaction between the ligand and the Cu(II) ion which in turn reveals its covalent character[144].

Thermal studies

Mn(II), Co(II), Ni(II), Cu(II), Zn(II) and $UO_2(II)$ complexes of *o*-vanillin-2-aminopyridine were subjected to thermogravimetric analysis. The complexes were also subjected to direct pyrolytic studies to verify the results obtained from TG experiments. The observed mass loss in TG agreed fairly well with the values calculated from pyrolytic expriments. The mass loss data after the complete decomposition of the complexes showed that theresiduesleft behind were the corresponding metal oxides.

The complexes are proposed to have the following structures, based upon the above results.

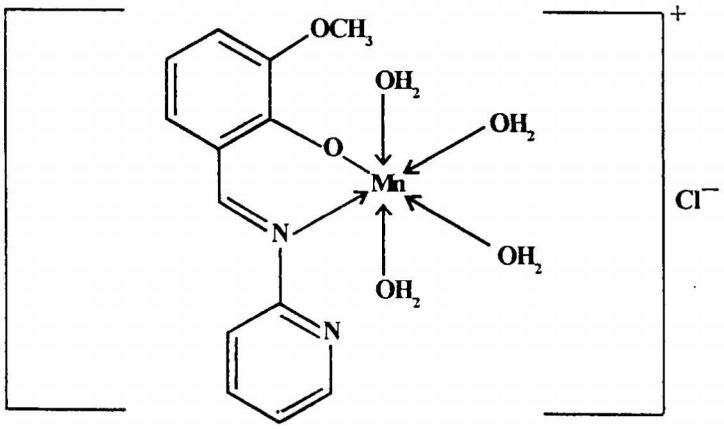
OCH3
OH2
OH2
O
Mn
N
OH2
OH2
N
Cl−
+

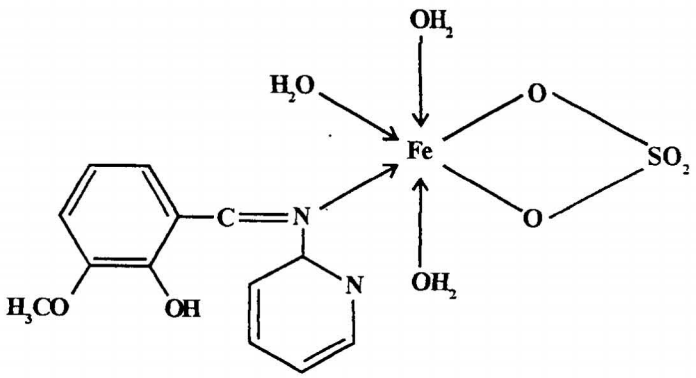
OH2
H2O
O
Fe
SO2
C
N
O
H3CO
OH
N
OH2

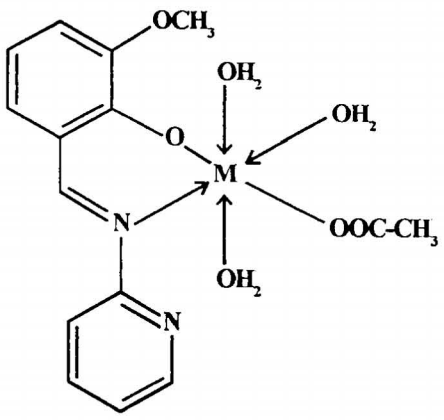
OCH3
OH2
OH2
O
M
N
OOC-CH3
OH2
N

M = Co, Ni or Zn

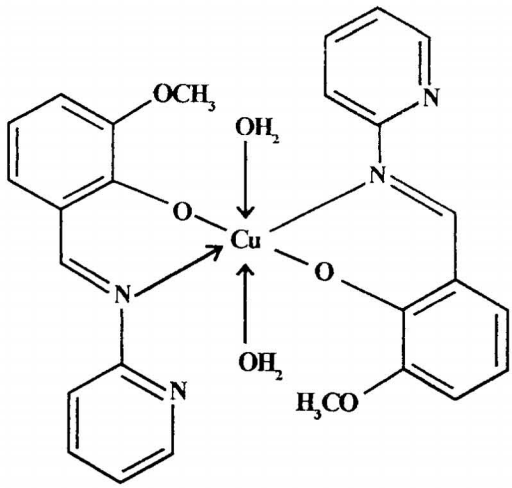
OCH3
OH2
N
O
Cu
N
O
N
OH2
N
H3CO

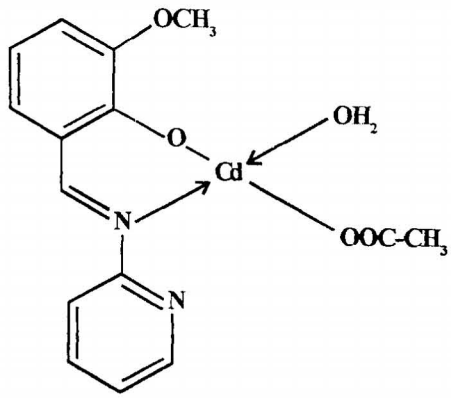
OCH3
O
OH2
Cd
N
OOC-CH3
N

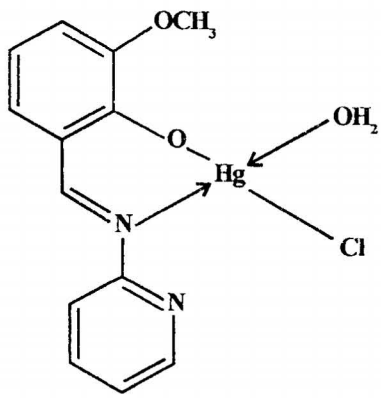
OCH3
O
OH2
Hg
N
Cl
N

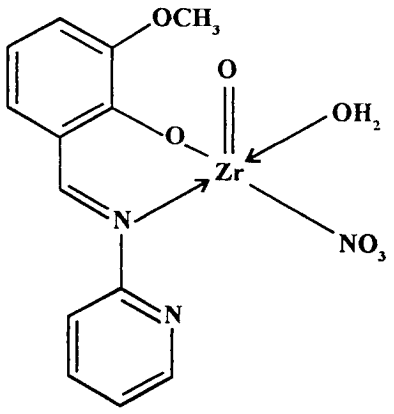
OCH3
O
OH2
O
Zr
N
NO3
N

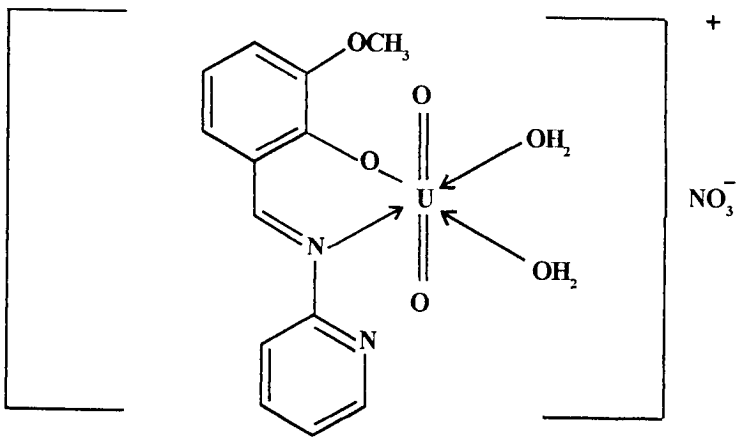
OCH3
O
OH2
O
U
N
OH2
O
N
+
NO3−

TABLE 1.5.1. **Microanalytical, magnetic and conductance data of transition metal chelates of o-vanillin-2-aminopyridine (L'''H)**

Complex	Colour	M%	C%	H%	N%	S%	Cl%	μ_{eff} (B.M.)	Ω^{-1}
$[MnL'''(H_2O)_4]Cl$	Yellow	14.52 (14.11)	40.91 (40.06)	4.20 (4.88)	7.37 (7.19)	--	9.02 (9.10)	6.03	46.92
$[FeL'''HSO_4(H_2O)_3]$	Black	12.70 (12.87)	36.13 (35.96)	4.63 (4.15)	6.51 (6.45)	7.10 (7.38)	--	5.12	3.67
$[CoL'''OAc(H_2O)_3]$	Coffee brown	14.83 (14.77)	45.63 (45.12)	5.21 (5.01)	7.68 (7.02)	--	--	4.78	3.16
$[NiL'''OAc(H_2O)_3]$	Parrot green	14.43 (14.72)	45.67 (45.15)	5.38 (5.02)	7.53 (7.02)	--	--	3.35	4.25
$[CuL_2'''(H_2O)_2]$	Greenish brown	11.98 (11.47)	56.93 (56.37)	4.62 (4.70)	5.01 (5.06)	--	--	2.24	4.81
$[ZnL''OAc(H_2O)_3]$	Lemon yellow	15.89 (16.13)	44.13 (44.40)	4.86 (4.93)	7.18 (6.91)	--	--	D	3.17
$[CdL'''OAcH_2O]$	Lemon yellow	27.13 (26.99)	43.81 (43.23)	3.63 (3.84)	6.75 (6.72)	--	--	D	5.32
$[HgL'''ClH_2O]$	Orange red	42.01 (41.70)	32.79 (32.43)	2.35 (2.70)	5.18 (5.82)	--	7.14 (7.37)	D	2.66
$[ZrOL''NO_3H_2O]$	Lemon yellow	22.96 (22.02)	37.62 (37.66)	3.76 (3.14)	10.27 (10.14)	--	--	D	1.85
$[UO_2L'''(H_2O)_2]NO_3$	Coffee brown	40.02 (40.00)	26.23 (26.22)	2.55 (2.52)	7.07 (7.06)	--	--	D	43.73

Calculated values are given in the parenthesis; D - diamagnetic; M - metal; Ω^{-1} - molar conductance in $ohm^{-1}cm^2mol^{-1}$

TABLE 1.5.2. **Characteristic infrared absorption frequencies (cm^{-1}) of transition metal chelates of *o*-vanillin-2-aminopyridine (L"'H)**

Substance	νH_2O	νC=N (azomethine)	νC=N (in ring)	νC-O (phenolic)	In plane deformation	Out of plane deformation	νM-N	νM-O
LH	--	1605s	1441m	1280s	870m	770,735w	--	--
$[MnL'''(H_2O)_4]Cl$	3400-3100br	1621s	1440m	1320s	860m	780,735w	560w	440w
$[FeL'''HSO_4(H_2O)_3]$	3400-3100br	1632s	1442m	1350s	880m	770,735w	580w	440w
$[CoL'''OAc(H_2O)_3]$	3400-3100br	1629s	1450m	1320s	870m	780,740w	600w	430w
$[NiL'''OAc(H_2O)_3]$	3400-3100br	1630s	1443m	1340s	860m	770,730w	590w	450w
$[CuL_2'''(H_2O)_2]$	3400-3100br	1615s	1440m	1340s	850m	780,740w	580w	440w
$[ZnL''OAc(H_2O)_3]$	3400-3100br	1639s	1440m	1350s	855m	770,735w	560w	460w
$[CdL'''OAcH_2O]$	3400-3100br	1631s	1445m	1330s	890m	770,730w	590w	445w
$[HgL'''ClH_2O]$	3400-3100br	1620s	1438m	1350s	870m	780,740w	580w	430w
$[ZrOL''NO_3H_2O]$	3400-3100br	1636s	1450m	1320s	860m	780,740w	570w	465w
$[UO_2L'''(H_2O)_2]NO_3$	3400-3100br	1627s	1440m	1320s	900m	780,740w	550w	470w

br - broad; m - medium; s - strong; w - weak

CHAPTER VI

TRANSITION METAL COMPLEXES OF *o*-VANILLIN 2-AMINOTHIAZOLE

o-Vanillin-2-aminothiazole (*o*VAAT), a potentially bidentate Schiff base ligand has been synthesised for the first time. This ligand forms a variety of complexes with various transition metals.

Preparation of the ligand

o-Vanillin-2-aminothiazole was prepared from *o*-vanillin (1.52g) and 2-aminothiazole (1g) following the same procedure adopted for the preparation of the ligand in chapter V. The melting point of the purified sample was found to be 90°C.

Characterization of the ligand

The orange yellow coloured ligand is found to be soluble in common organic solvents like methanol, ethanol, nitrobenzene etc. The characterisation of *o*-VAAT is done on the basis of elemental analysis and spectral data CHN analysis of the ligand is as follows:

Analytical data found : C, 57.39%; H, 4.39%; N, 11.82%.

Calculated for $C_{11}H_{10}N_2SO_2$: C, 56.47%; H, 4.27%; N, 11.97%.

The uv and ir spectra of the ligand showed the characteristic bands.

On the basis of above results, the structure of the ligand is confirmed as given below.

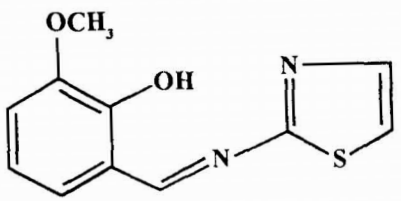

Studies on Mn(II), Fe(II), Co(II), Ni(II), Cu(II), Zn(II), Cd(II), Hg(II), Zro(II) and UO_2(II) complexes of *o*-vanillin-2-aminothiazole

In this section, the studies of the synthesis and characterization of some transition and uranium metal complexes of *o*-vanillin-2-aminothizole are reported.

Preparation of complexes

Mn(II), Fe(II), Co(II), Ni(II), Cu(II), Zn(II), Cd(II), Hg(II), ZrO(II) and UO_2(II) chelates of *o*-vanillin-2-aminothiazole were prepared by applying the same procedure adopted for vanillin-2-aminothiazole complexes. Very good yield was obtained for Hg(II) and UO_2(II) complexes (90-95%) where as others exhibit 80-85% yield.

Characterization of the complexes

The complexes were characterized on the basis of elemental analysis, uv and ir spectral data, magnetic studies and conductance measurements.

RESULTS AND DISCUSSION

The analytical data and physical characteristics of the Mn(II), Fe(II), Co(II), Ni(II), Cu(II), Zn(II), Cd(II), Hg(II), ZrO(II) and UO_2(II) complexes with *o*-VAAT are presented in Table 1.6.1. The room temperature magnetic moments and molar conductivities of the complexes are also reported in this Table. Important ir spectral bands of the ligand and the complexes with their assignments are given in Table 1.6.2. All these complexes are deep coloured, non-hygroscopic solids. Fe(II), Co(II), Ni(II), Zn(II) and

Cd(II) are found to be soluble in methanol, ethanol, nitrobenzene etc. whereas Cu(II), Mn(II), ZrO(II), Hg(II) and UO_2(II) are found to be soluble only in DMSO. From the elemental analysis, it is found that Mn(II), Fe(II), Co(II), Ni(II), Cu(II) and Zn(II) complexes can be represented by the general formula $[MLX(H_2O)_3]$ where X stands for acetate, chloride or sulphate.

Molar conductance

Conductance measurements of the complexes in methanol (10^{-4} M) at room temperature show that these complexes behave as non-electrolytes. The conductance data of the complexes are tabulated in the Table 1.6.1

Magnetic measurements

The magnetic moment calculated from the corrected magnetic suscaptibilities support an octahedral geometry for Mn(II) complex (5.9 BM)[117]. 5.84 BM is the measured magnetic moment for Fe(II) complex. It is in good agreement with the octahedral geometry of the complex[117,118]. Co(II) complex exhibits a μ_{eff} value of 5.25 B.M. It is reported that octahedral, high spin symmetry can be assigned to Co(II) complexes, if the measured magnetic moment values are in the range 4.7 - 5.2 B.M. Therefore high spin, octahedral geometry is suggested for the present Co(II) complex[117]. The magnetic moment value shown by Ni(II) complex (2.83 B.M) is very close to the spin only value indicating the presence of two unpaired electrons with the electronic configuration $t_{2g}^6e_g^2$ ($^3A_2$) That is, an octahedral stereochemistry with sp^3d^2 hybridisation can be assigned to the Ni(II) complex. Based on the μ_{eff} value observed for Cu(II) complex, an octahedral geometry has been suggested with $t_{2g}^6e_g^3$ electronic

configuration[117, 118]. Zn(II), Cd(II), Hg(II), ZrO(II and UO_2(II) complexes are found to be diamagnetic.

Infrared spectral studies

Characteristic ir absorption bands of the ligands and complexes are summarised in Table 1.6.2. The coordination sites of the ligand and the presence of acetate, chloride, nitrate and sulphate groups and water molecules in the complexes were explained on the basis of infrared spectral studies of the ligand and complexes. This ligand acts as bidentate generally but in the Fe(II) complex it acts as monodentate.

The absence of characteristic absorption band of O-H group in the ir spectrum of the ligand clearly suggests the presence of strong intramolecular hydrogen bonding in the ligand molecule.

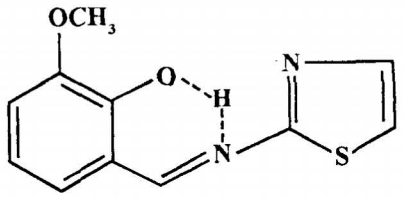

The strong band due to νC=N at 1598 cm^{-1} in the ligand *o*-VAAT is shifted to higher frequency region in the complexes indicating azomathine nitrogen coordination. The shift of the characteristic aborption frequency of phenolic C-O bond, to higher frequency range by about 50 cm^{-1}, in the spectra of the complexes, suggests the involvement of phenolic oxygen atom of the ligand moiety in coordination after deprotonation.

The presence of coordinated water molecules in all of these complexes can be explained by the presence of a strong broad band, ranging between 3500-3100 cm^{-1} in their ir spectra, which are absent in the spectrum of the ligand[120].

In the Co(II), Ni(II), Cu(II), Zn(II) and Cd(II) complexes the asymmetric and symmetric stretching vibrations of the acetate group, occur at 1620-1600 cm^{-1} and 1420-1410 cm^{-1}, respectively with $\Delta\nu$ of 180-170 cm^{-1}. Monodentate acetate groups are, therefore, indicated in the above chelates[121,130].

The band shown in the spectra of ZrO(II) and UO_2(II) complexes at 1450 and 1330 cm^{-1} can be assigned to the vibrations of nitrate groups. The $\Delta\nu$ value of these two bands at ~120 cm^{-1} indicating that the coordinated nitrate ion is monodentate[123, 124].

Fe(II) complex exhibits bands at 1152, 1122, 1105, 1090, 1035,638 and 605 cm^{-1}. This confirm the bidentate nature of sulphate present in the complex[121].

Uranyl complex exhibits very strong band at 915 cm^{-1} due to the asymmetric stretching frequency of O=U=O group[126,127]. The force constant in milidynes 1A° and the bond length in A° were calculated based on Mc Glynn method[128] and was found to be 7.19 and 1.73 respectively.

The presence of Zr=O bond in ZrO(II) complex is confirmed by the presence of narrow bands at 980 cm^{-1} and 970 cm^{-1}[129,136]. The medium to weak bands in the 580-570 cm^{-1} and 450-460 cm^{-1} regions exhibited by the complexes are tentatively assigned to νM-N and νM-O respectively[131].

Electronic spectra

The ligand spectrum showed two characteristic bands at 37736 cm^{-1} and 27400 cm^{-1}. The shift of these bands exhibited in the spectra of complexes can be taken as a proof of coordination of the ligands to metal ions.

The electronic spectum of Mn(II) complex exhibited a band at 24850 cm^{-1} which is taken as an evidence to support the presence of Mn(II) in octahedral geometry[132]. The electronic spectrum of the Fe(II) complex is characterized by a weak band at 16, 140 cm^{-1} which may be attributed to $^5T_{2g} \rightarrow {}^5E_g$ transition, characteristic of octahedral sterochemistry around Fe(II) [133]. Co(II) complex is characterized by two bands at 10965 cm^{-1} and 21322 cm^{-1} due to $^4T_{1g}$ (F) $\rightarrow$ $^4T_{2g}$ (F) and $^4T_{1g}$ (F) $\rightarrow$ $^4T_{2g}$ (P) transitions. Ni(II) complex also exhibits two d-d transitions in the regions at about 10000 and 23500 cm^{-1} due to $^3A_{2g}$ (F) $\rightarrow$ $^3T_{1g}$ (F) and $^3A_{2g}$ (F) $\rightarrow$ $^3T_{1g}$ (P) transitions. The electronic spectrum of Cu(II) complex showed absorption maxima at about 15384 cm^{-1}, which supports a distorted octahedral symmetry[133].

Zn(II), Cd(II), Hg(II) and ZrO(II) chelates show medium intensity charge transfer bands at about 19230 cm^{-1}.

UO_2(II) complex exihibited a band at 27150 cm^{-1}

Electron spin resonance spectra

ESR spectrum of the Cu(II) complex of *o*-VAAT was taken in the solid form. DPPH was the reference. Spectrum showed only one line. It was

analysed and the spin Hamiltonian constant was evaluated. Strong interaction between the ligand and the metal and thereby the covalent character of the complex are established from the small g value (2.1784) obtained[144].

Thermal studies

Complexes of Mn(II), Co(II), Ni(II), Cu(II) and Zn(II) were subjected to thermal studies by nonisothermal method. The complexes decomposed in different stages, ultimately getting converted to the oxides. The determination of kinetic parameters, mechanism of decomposition and probable assignment of each decomposition are discussed in part II.

On the basis of above results, these complexes can be represented by the following structures.

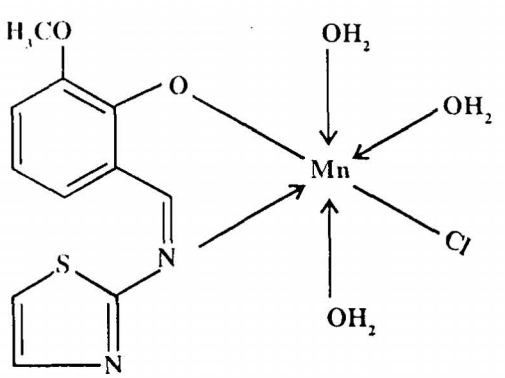

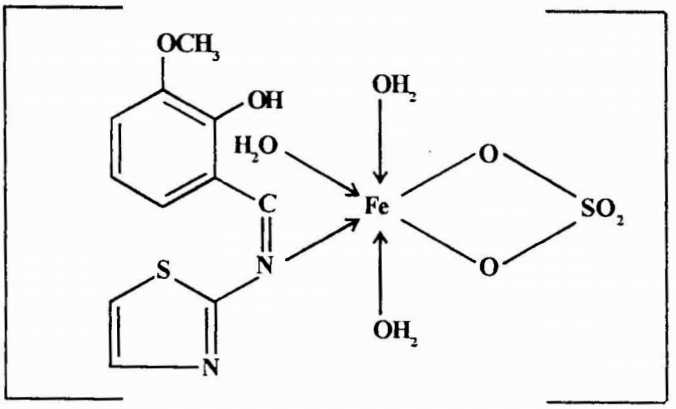

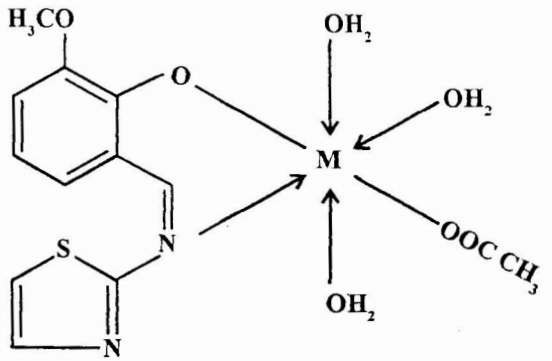

M = Co (II), Ni (II), Cu (II) or Zn (II).

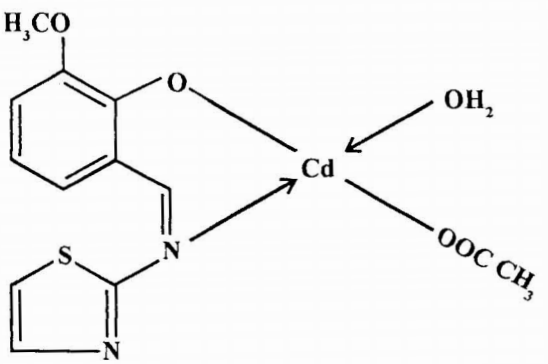

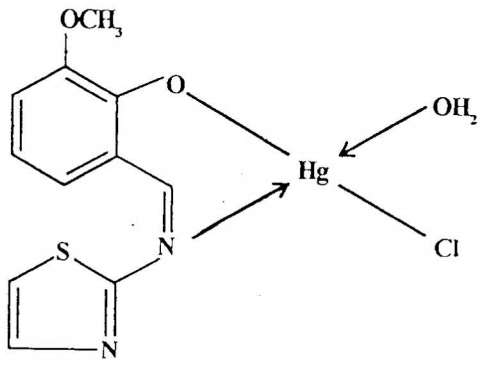
OCH3
O
OH2
Hg
Cl
N
S
N
N

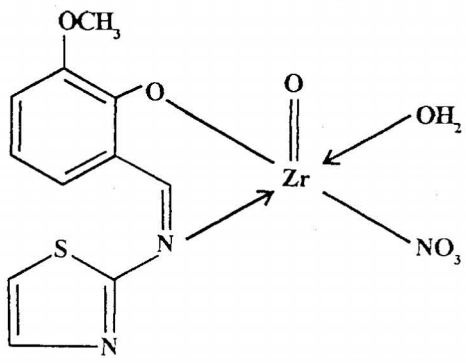
OCH3
O
O
OH2
Zr
NO3
N
S
N
N

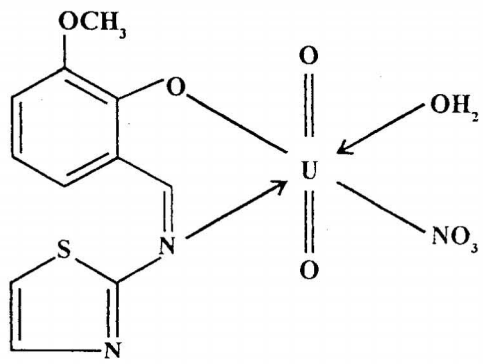
OCH3
O
O
OH2
U
NO3
O
N
S
N
N

TABLE 1.6.1. **Microanalytical, magnetic and conductance data of transition metal chelates of *o*-vanillin-2-aminothiazole ($L^{IV}H$)**

Complex	Colour	M%	C%	H%	N%	S%	Cl%	μ_{eff} (B.M.)	Ω^{-1}
$[MnL^{IV}Cl(H_2O)_3]$	Reddish brown	14.05 (14.56)	34.50 (34.98)	4.82 (4.24)	6.98 (7.42)	7.86 (8.48)	8.87 (9.39)	5.91	1.23
$[FeL^{IV}HSO4(H_2O)_3]$	Black	12.30 (12.70)	30.76 (30.01)	3.51 (3.64)	6.32 (6.36)	14.11 (14.55)	--	5.44	3.21
$[CoL^{IV}(OAc)(H_2O)_3]$	Orange red	14.73 (14.54)	38.23 (38.50)	4.04 (4.69)	6.27 (6.91)	7.38 (7.90)	--	5.25	2.45
$[NiL^{IV}OAc(H_2O)_3]$	Orange	14.52 (14.51)	38.55 (38.55)	4.70 (4.69)	6.81 (6.92)	8.23 (7.91)	--	2.83	1.80
$[CuL^{IV}OAc(H_2O)_3]$	Coffee brown	16.21 (15.51)	37.67 (38.10)	4.01 (4.64)	6.93 (6.84)	7.76 (7.81)	--	1.12	2.24
$[ZnL^{IV}OAc(H_2O)_3]$	Yellow	16.08 (15.89)	37.80 (37.92)	4.88 (4.62)	6.34 (6.81)	7.97 (7.78)	--	D	2.15
$[CdL^{IV}OAcH_2O]$	Orange red	25.97 (26.61)	36.27 (36.93)	3.14 (3.55)	6.21 (6.63)	7.13 (7.58)	--	D	4.17
$[HgL^{IV}ClH_2O]$	Yellow	40.85 (41.19)	27.72 (27.10)	2.87 (2.46)	5.06 (5.75)	6.89 (6.57)	7.89 (7.28)	D	1.52
$[ZrOL^{IV}NO_3H_2O]$	Yellow	21.45 (21.71)	30.86 (31.41)	2.43 (2.86)	9.34 (9.99)	7.31 (7.62)	--	D	5.81
$[UO_2L^{IV}NO_3H_2O]$	Reddish brown	40.32 (40.82)	22.05 (22.64)	2.58 (2.06)	6.83 (7.20)	5.92 (5.49)	--	D	8.28

Calculated values are given in the parenthesis; D - diamagnetic; M - metal; Ω^{-1} - molar conductance in $ohm^{-1}cm^2mol^{-1}$

TABLE 1.6.2. **Characteristic infrared absorption frequencies (cm^{-1}) of transition metal chelates of vanillin-2-aminothiazole ($L^{IV}H$)**

Substance	νH_2O	$\nu C{=}N$ (azomethine)	$\nu C{=}N$ (in ring)	$\nu C{-}O$ (phenolic)	In plane deformation	Out of plane deformation	$\nu M{-}N$	$\nu M{-}O$
LH	--	1598s	1485m	1280s	880m	780,730w	--	--
$[MnL^{IV}Cl_2(H_2O)_3]$	3500-3100br	1620s	1482m	1325s	848m	780,730w	580w	450w
$[FeL^{IV}HSO_4(H_2O)_3]$	3500-3100br	1618s	1480m	1330s	870m	780,730w	575w	460w
$[CoL^{IV}(OAc)(H_2O)_3]$	3500-3100br	1620s	1484m	1320s	850m	770,720w	570w	456w
$[NiL^{IV}OAc(H_2O)_3]$	3500-3100br	1630s	1481m	1335s	852m	770,720w	578w	460w
$[CuL^{IV}OAc(H_2O)_3]$	3500-3100br	1628s	1480m	1340s	850m	790,740w	580w	458w
$[ZnL^{IV}OAc(H_2O)_3]$	3500-3100br	1620s	1480m	1325s	850m	770,720w	580w	450w
$[CdL^{IV}OAcH_2O]$	3500-3100br	1640s	1485m	1340s	848m	780,730w	572w	450w
$[HgL^{IV}ClH_2O]$	3500-3100br	1620s	1485m	1328s	854m	790,740w	576w	460
$[ZrOL^{IV}NO_3H_2O]$	3500-3100br	1628s	1485m	1330s	880m	790,740w	580w	460w
$[UO_2L^{IV}NO_3H_2O]$	3500-3100br	1620s	1480m	1350s	850m	780,730w	570w	460w

br - broad; m - medium; s - strong; w - weak

Ligand	C%	H%	N%
o-Vanillin-L-histidine $C_{14}H_{15}N_3O_4$	53.96 (54.67)	5.17 (4.88)	13.55 (13.67)

Calculated values are given in parenthesis.

Analytical and spectral observations suggest the following structure for the ligand.

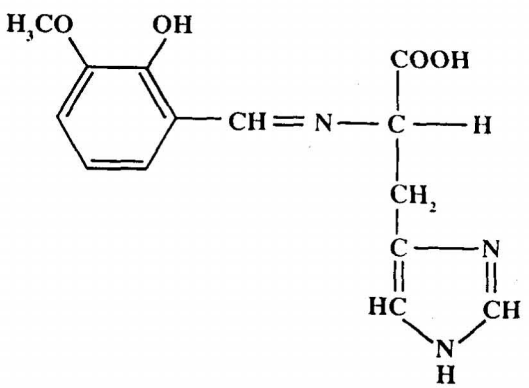

Studies on Mn(II), Fe(II), Co(II), Ni(II), Cu(II), Zn(II), Cd(II), Hg(II), ZrO(II) and UO_2(II) complexes of *o*-vanillin-L-histidine

o-Vanillin-L-histidine (*o*-VALH), a divalent tridentate ligand forms a variety of chelates with transition metals of the type Mn(II), Fe(II), Co(II), Ni(II), Cu(II), Zn(II), Cd(II), Hg(II) and ZrO(II). UO_2(II) complex of the same ligand is also prepared and characterised.

Preparation of complexes

Hot aqueous solution of histidine was mixed with an alcoholic solution of *o*-vanillin taken in an round bottomed flask and refluxed. Appropriate metal salt solution in methanol, ethanol or aqueous medium was added slowly to the boiling solution of the ligand. Cu(II), Zn(II), Cd(II), Hg(II) and ZrO(II) complexes were separated immediately after mixing. Complexes of Mn(II) and Ni(II) were separated only after relfuxing for 2 h.

Co(II), Fe(II) and UO_2(II) complexes were formed only after adding the refluxed solution to distilled water taken in a beaker with constant stirring. The separated complexes were filtered, washed with water and ethanol and dried over anhdydrous $CaCl_2$. The yield was approximately found to be 80%.

Characterization of the complexes

The complexes were characterized on the basis of elemental analysis, uv and ir spectral data, magnetic studies and conductance measurements.

RESULTS AND DISCUSSION

All these complexes are beautifully coloured. Most of them are found to be soluble in hot water and insouble in common organic solvents. On the basis of elemental analysis Mn(II), Fe(II), Co(II), Ni(II), Cu(II), Zn(II) and Cd(II) complexes can be represented by the general formula $ML(H_2O)_3$ where L is the ligand moiety.

The analytical data and physical characteristic of these complexes are presented in Table 1.7.1. The room temperature magnetic moments and molar conductivities of the complexes are also reported in this Table. Important ir spectral bands of the ligand and the complexes with their assignments are given in Table 1.7.2.

Molar conductance

Conductance measurements of the complexes in distilled water (10^{-4} M) at room temperature showed that all the complexes are non-electrolytes. The conductance data of the complexes are tabulated in the Table 1.7.1.

Magnetic measurements

The observed magnetic moment of the Mn(II) complex is 5.8 B.M. which is in accordance with the value expected for octahedral Mn(II) complex[117]. μ_{eff} value of 4.9 B.M. is obtained for the Fe(II) complex. The Co(II) complexexihibitsthe normal magnetic moment 4.4 B.M. Therefore octahedral structure can be assigned to both Fe(II) and Co(II) complexes based on magnetic moment values[117,118]. The magnetic moment value of Ni(II) complex, 2.86 B.M. is in agreement with its ochtaedral geometry[117].

2.02 B.M. is the magnetic moment value obtained for Cu(II) complex. This suggests a $t_{2g}^{6}e_{g}^{3}$ electronic configuration in an octahedral ligand field. The remaining complexes are found to be diamagnetic.

Infrared spectral studies

Characteristic infrared bands of the ligand and complexes were examined in detail and are given in Table 1.7.2.

The ir spectrum of the ligand *o*-VALH shows a strong band at 1720 cm^{-1} and a medium band at 1479 cm^{-1}. The former may be due to the carbonyl stretching frequency of the carboxylate group. A shift of this band at lower frequencies (~ 1590 cm^{-1}) indicates the chelation of the ligand to the metal ion through carbonyl oxygen. The second sharp band of medium intensity at 1489 cm^{-1} in the ligand ir spectrum can be assigned to $\nu_{C=N}$ of the Schiff base residue. In the complexes, this band has shifted to higher frequencies by about 20-40 cm^{-1} showing the coordination of nitrogen atom of the azomethine linkage to metal atom.

The most characteristic feature in the spectrum of a *o*-VALH is the extremely broad O-H absorption occuring in the region 3500-3100 cm^{-1}. This band is attributed to the strong hydrogen bonding present in the ligand. Since this broad hydrogen bonded band is present together with the proper C=O absorption value, a carboxylic acid is certainly indicated.

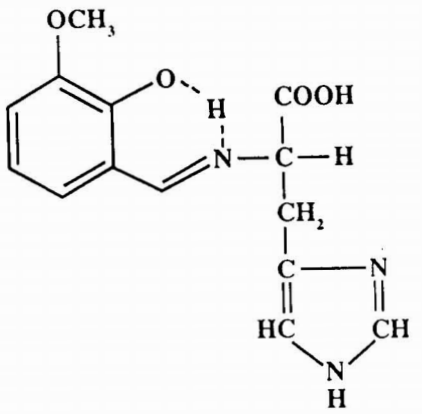

In all the complexes, the asymmetric and symmetric stretching vibrations of the carboxylate groups occur at ~ 1600 and ~ 1400 cm^{-1} respectively, showing a difference of about 200 cm^{-1}. This indicates the monodentate behaviour of the carboxylate group[121,130].

The shift of the characteristic absorption frequency of phenolic C-O bond to higher frequency range by about 40 cm^{-1}, in the spectra of complexes, suggests the involvement of phenolic oxygen atom of the ligand moiety in coordination after deprotonation.

All these complexes show broad absorption bands between 3500-3100 cm^{-1} due to the presence of coordinated water molecules which is further supported by the appearance of rocking mode of medium intensity bands at ~ 860 cm^{-1} [120].

Uranyl complex exhibits a very strong band at 930 cm^{-1} which can be attributed to the asymmetric stretching frequency of O=U=O[127]. The McGlynn method[128] has been used to find out the force constant and bond

length. The $F_{U=O}$ value is 7.19 millidynes/A° and bond length 1.73 angstrom (A°) unit.

The presence of Zr=O bond in ZrO(II) complex is confirmed by the presence of narrow bands at 980 and 970 cm^{-1} [129,136]. The weak bands in the 515-508 cm^{-1} and 415-405 cm^{-1} regions exhibited by the complexes are tentatively assigned to νM-N and νM-O respectively[131].

Electronic spectra

The ligand spectrum showed two characteristic bands near 38000 cm^{-1} and 27500 cm^{-1}. The shift of these bands exhibited in the spectra of complex can be taken as a proof of coordination of the ligand to metal ions. The octahedral environment[132] of ligands around the central Mn(II) ion is confirmed by the appearance of a broad band at 24830 cm^{-1}. The expected $^5T_{2g} \rightarrow {}^5E_g$ electronic transition in the octahedral Fe(II) complex[133] has been recorded at about 18400 cm^{-1}. The $^4T_{1g}(F) \rightarrow {}^4T_{2g}(F)$ and $^4T_{1g}(F) \rightarrow {}^4T_{1g}(P)$ transitions expected for Co(II) complexes with octahedral geometry was very clear in the spectra at 14903 and 23000 cm^{-1} respectively. The two electronic absorption bands at 10482 and 22600 cm^{-1} present in Ni(II) complex are due to $^3A_{2g}(F) \rightarrow {}^3T_{1g}(F)$ and $^3A_{2g}(F) \rightarrow {}^3T_{1g}(P)$ transitions. The octahedral geometry of Cu(II) complex is clear from the absorption bands at 17123 and 23420 cm^{-1}.

For the Zn(II), Cd(II), Hg(II), ZrO(II) and UO_2(II) complexes,d-d transitions are not possible and the bands observed at ~ 25000 cm^{-1} are due to charge transfer.

UO_2(II) complex exhibits a strong band at 29498 cm^{-1}, which is essentially determined by the triatomic UO_2^{2+} entity[142,143].

Nuclear magnetic resonance spectroscopy

The ^1H nmr spectra of the ligand and UO_2(II) chelate in $CDCl_3$/DMSO-d_6 revealed important signals[145-147].

In the vanillin-histidine complex, the bonding of the phenolic oxygen and carboxylate oxygen of the ligand moiety is substantiated by the disappearance of the OH proton signal at δ 14.09 and 10.3.

The proton signal for the azomethine proton at 8.3δ in the ligand shifts upfield in the spectrum of the corresponding 1:1 UO_2(II) complex. Signals observed at δ 3.45 and 2.5 arise due to water molecules and DMSO respectively.

NMR spectra of other complexes could not be determined due to their poor solubility in deuterated solvents.

Electron spin resonance spectra

ESR spectrum of powdered sample of $[CuL^v(H_2O)_3]$ at room temperature showed two bands corresponding to g_{11} and $g_\perp$ with no resolution. g_{11} and $g_\perp$ values calculated are 2.2207 and 2.1640 respectively. Kivelson and Nieman have shown that g_{11} is moderately sensitive function for indicating covalency[148]. The small g value (< 2.3) indicates strong interaction between the ligand and the copper(II) ion which in turn reveals its covalent character[144].

X ray powder diffraction studies

The X ray powder pattern of Fe(II), Ni(II), Cu(II), Cd(II) and UO_2(II) complexes of *o*-VALH were taken to see whether the complex is crystalline and if so to determine the nature of the unit cell.

Thermal studies

Mn(II), Co(II), Ni(II), Cu(II), Zn(II), Cd(II) and ZrO(II) were subjected to thermal studies by nonisothermal method. 2 stage decompositions are observed in Mn(II), Co(II), Ni(II), Cu(II) and Zn(II) complexes whereas Cd(II) complex undergoes a 3 stage decomposition. The determination of kinetic parameters, mechanism of decomposition and probable assignment of each decomposition are discussed in Part II.

Based on the above results, a hexacoordinated structure is assigned to all of these chelates except the chelates of Hg(II) and ZrO(II). Hg(II) forms a tetrahedral complex with *o*-vanillin-L-histidine whereas ZrO(II) complex is found to be square pyramidal. The general structure of these 7 complexes can be represented as

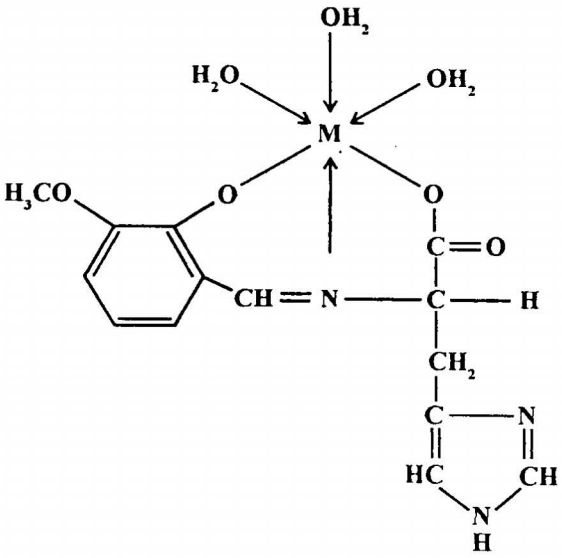

M = Mn (II), Fe (II),Co (II), Ni (II), Cu (II), Zn (II) or Cd (II).

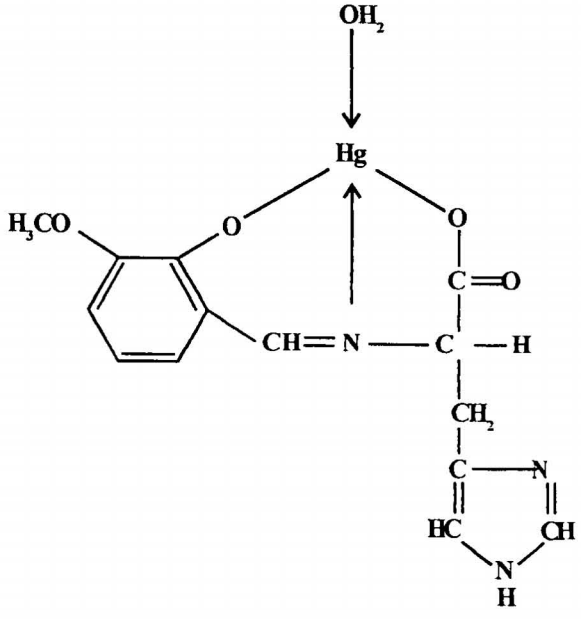

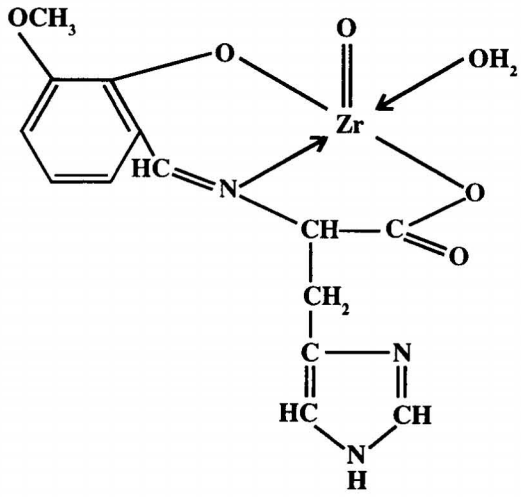
OCH3
O
O
OH2
Zr
HC
N
O
CH
C
O
CH2
C
N
HC
CH
N
H

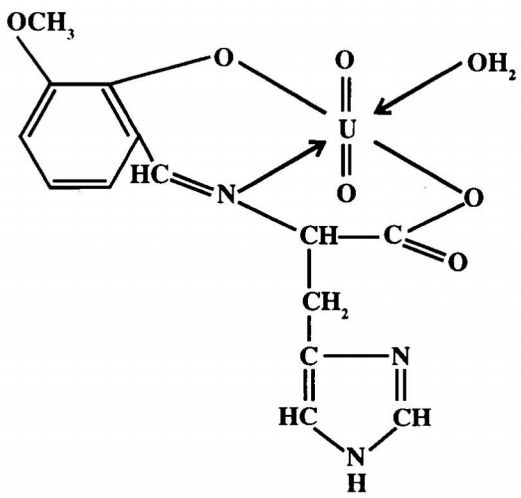
OCH3
O
O
OH2
U
O
HC
N
O
CH
C
O
CH2
C
N
HC
CH
N
H

TABLE 1.7.1. **Microanalytical, magnetic and conductance data of transition metal chelates of *o*-vanillin-L-histidine (L^VH_2)**

Complex	Colour	M%	C%	H%	N%	μ_{eff} (B.M.)	Ω^{-1}
$[ML^V(H_2O)_3]$	Coffee brown	12.67 (13.86)	41.60 (42.40)	4.27 (4.80)	11.24 (10.60)	5.82	2.88
$[FeL^V(H_2O)_3]$	Reddish brown	14.93 (14.06)	42.78 (42.30)	4.31 (4.78)	11.21 (10.58)	4.94	28.62
$[CoL^V(H_2O)_3]$	Brown	15.18 (14.72)	42.71 (41.97)	4.06 (4.75)	10.57 (10.49)	4.41	3.67
$[NiL^V(H_2O)_3]$	Violet	14.86 (14.68)	42.89 (42.00)	4.99 (4.75)	11.24 (10.50)	2.86	3.45
$[CuL^V(H_2O)_3]$	Green	15.52 (15.68)	42.50 (41.50)	4.04 (4.69)	10.31 (10.38)	2.08	1.28
$[ZnL^V(H_2O)_3]$	Lemon yellow	16.68 (16.07)	42.68 (41.31)	4.42 (4.67)	9.81 (10.33)	D	2.54
$[CdL^V(H_2O)_3]$	Lemon yellow	25.35 (24.77)	38.02 (37.03)	3.96 (4.19)	8.87 (9.26)	D	4.68
$[HgL^V(H_2O)]$	Lemon yellow	38.91 (39.68)	34.21 (33.23)	3.18 (2.97)	8.93 (8.31)	D	5.36
$[ZrOL^V(H_2O)]$	Lemon yellow	22.74 (22.13)	41.01 (40.75)	3.78 (3.64)	10.37 (10.19)	D	21.43
$[UO_2L^V(H_2O)]$	Orange red	42.21 (41.39)	30.18 (29.22)	2.57 (2.61)	7.88 (7.30)	D	3.29

Calculated values are given in the parenthesis; D - diamagnetic; M - metal; Ω^{-1} - molar conductance in $ohm^{-1}cm^2mol^{-1}$

TABLE 1.7.2. **Characteristic infrared absorption frequencies (cm^{-1}) of transition metal chelates of *o*-vanillin-L-histidine (L^VH_2)**

Substance	νH_2O	vasy C(=O)O	νC=N (azo-methine)	νC=N (in ring)	vsy C(=O)O	νC-O (phenolic)	Inplane deforma-tion	Out of plane deformation	νM-N	νM-O
L^VH_2	--	1720s	1480m	1440m	1400s	1280m	830m	760, 738m	--	--
$[ML^V(H_2O)_3]$	3500-3100br	1632s	1520m	1445m	1390s	1320m	830m	786,736m	510w	410w
$[FeL^V(H_2O)_3]$	3500-3100br	1630s	1530m	1443m	1370s	1300m	830m	780, 744m	512w	405w
$[CoL^V(H_2O)_3]$	3500-3100br	1625s	1520m	1444m	1368s	1300m	830m	785, 742m	513w	415w
$[NiL^V(H_2O)_3]$	3500-3100br	1628s	1520m	1440m	1390s	1320m	820m	770, 713m	515w	410w
$[CuL^V(H_2O)_3]$	3500-3100br	1635s	1525m	1442m	1330s	1320m	830m	780, 744m	510w	410w
$[ZnL^V(H_2O)_3]$	3500-3100br	1620s	1520m	1446m	1400s	1320,m	820m	770, 743m	510w	410w
$[CdL^V(H_2O)_3]$	3500-3100br	1620s	1520m	1440m	1380s	1300m	840m	780, 742m	508w	415w
$[HgL^V(H_2O)]$	3500-3100br	1620s	1530m	1444m	1397s	1316m	840m	777, 740m	512w	410w
$[ZrOL^V(H_2O)]$	3500-3100br	1630s	1530m	1441m	1362s	1310m	830m	775, 743m	510w	410w
$[UO_2L^V(H_2O)]$	3500-3100br	1630s	1520m	1438m	1340s	1300m	820m	780, 744m	512w	415w

br - broad; m - medium; s - strong; w - weak

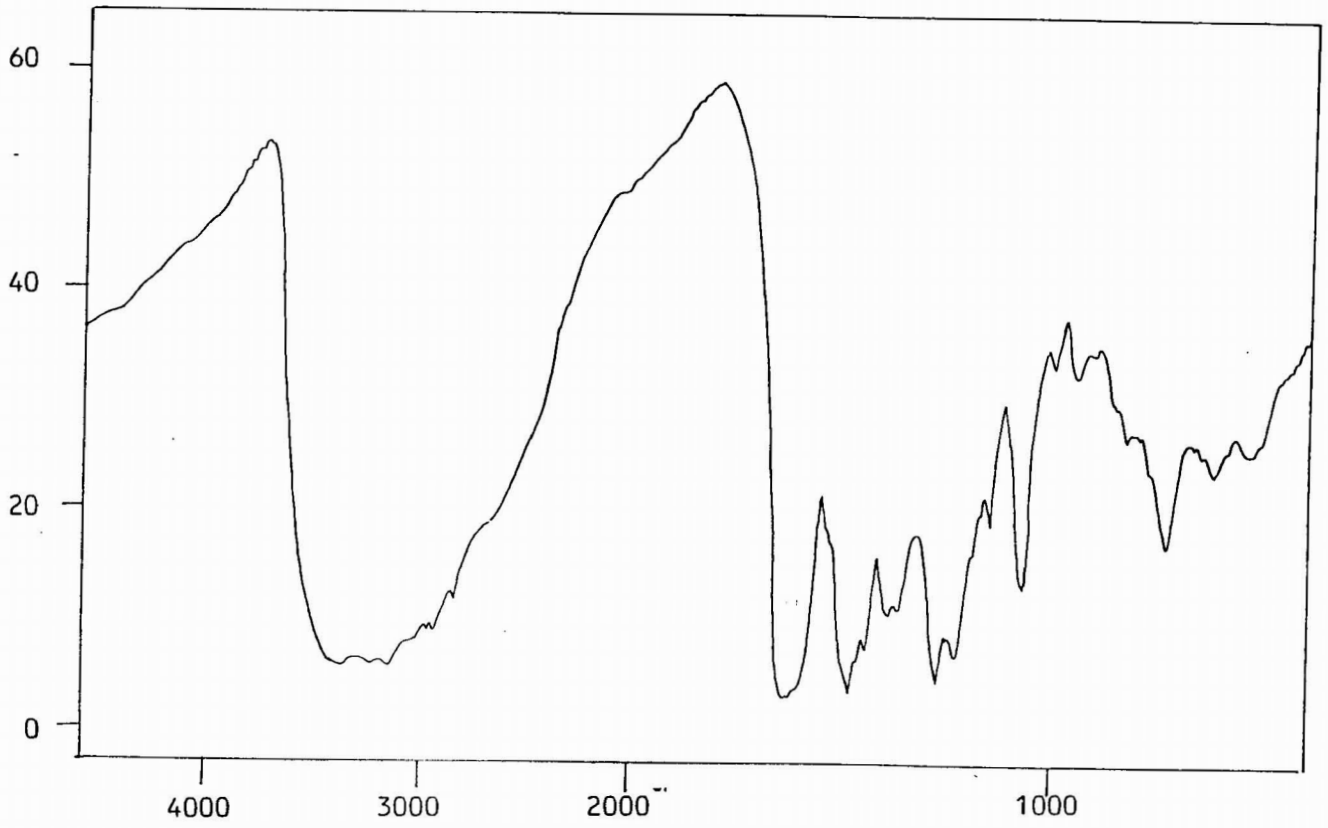

Figure I. 7.1 **IR Spectrum of *o* vanillin-L-histidine**

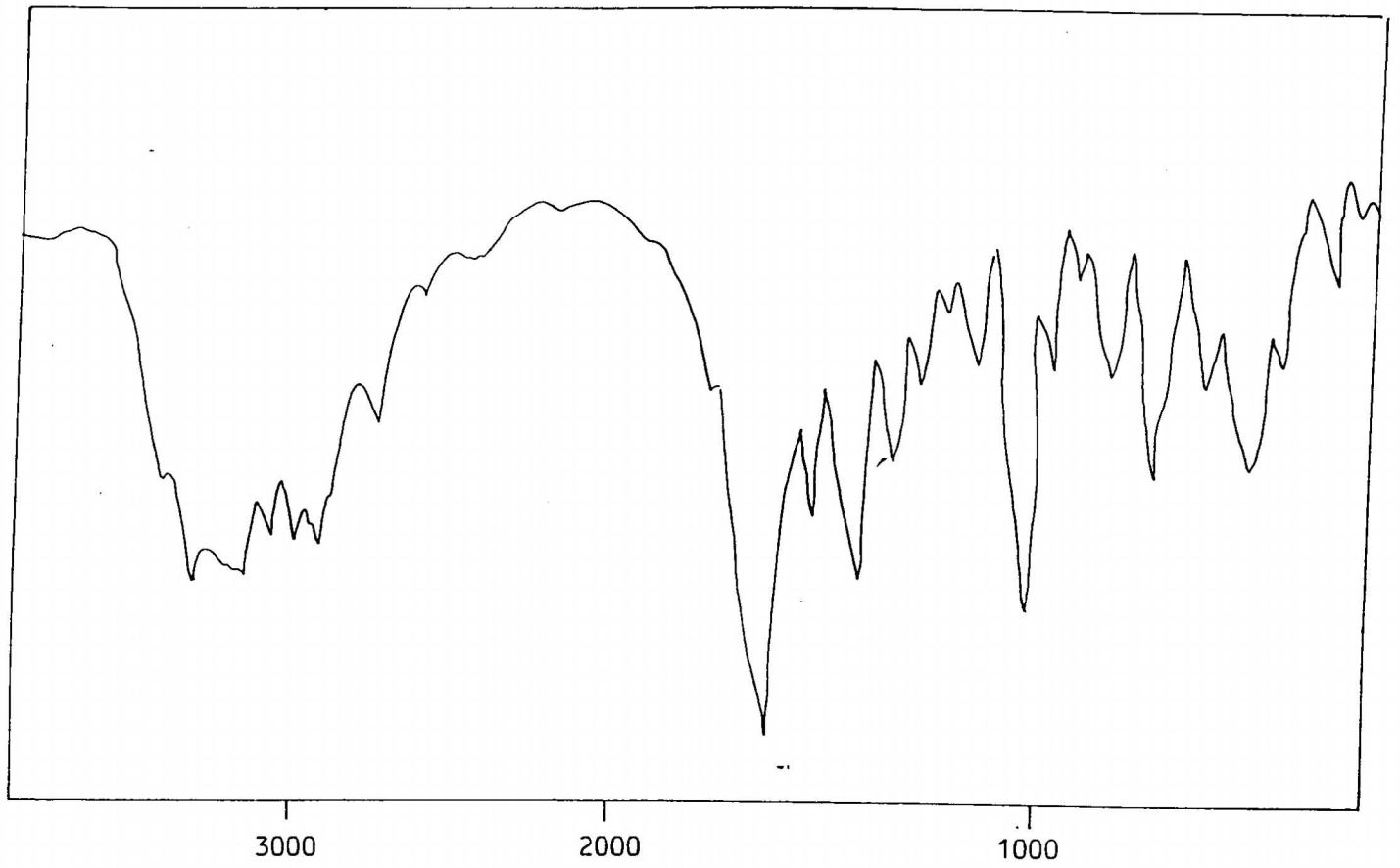

Figure I. 7.2 **IR Spectrum of $[NiL^{V}(H_2O)_3]$**

PART II

THERMOANALYTICAL STUDIES

CHAPTER I

INTRODUCTION

Eventhough spectroscopy and magnetic properties have been the leaders in elucidating structure and bonding in the solid state, thermoanalytical techniques have made much contributions in recent years. Thermal studies include a group of techniques whereby dependence of the parameters of any physical property of a substance on temperature is measured[151]. The study of the thermal decomposition of inorganic metal complexes has been receiving increasing attention recently. The development of techniques such as thermogravimetry (TG), derivative thermogravimetry (DTG), differential thermal analysis (DTA), differential scanning calorimetry (DSC) etc. has been of considerable help in such studies.

Thermogravimetric curves give valuable information on the temperature regions of stability and also of the temperature of inception of maximum rate and of completion of decomposition. Derivative thermogravimetric (DTG) curve is obtained either by manual differentiation of the normal thermogravimetric curve or by suitable instrumentation. The relationship between the rate of weight change and the temperature or time is expressed by the derivative thermogravimetric curve.

$$dw/dt = f(T \text{ or } t)$$

DTA curves give information about the enthalpy changes occurring during heating. The books by Duval[152], Smothers and Yaochiang[153], Garn[154], Schulze[155] etc. can be used for the instruments, principles and techniques of thermal analysis.

Thermogravimetry

Thermogravimetry is defined as a technique whereby the mass of a substance, in an environment heated or cooled at a controlled rate is recorded as a function of time or temperature. The resulting mass change versus temperature curve provides information concerning the thermal stability and composition of the initial sample, the thermal stability and composition of any intermediate compounds that may be formed and the composition of the residue if any.

The first thermobalance was probably the instrument developed by Honda[156] in 1915.

Either by manual differentiation of the normal TG curve or by suitable instrumentation, derivative TG curves (DTG) can be deduced which have certain advantages over normal TG curves. The relationship between the rate of weight change and the temperature or time is expressed by the derivative thermogravimetric curve.

$$\text{i.e. } dw/dt = f(T \text{ or } t)$$

DTG curves have a number of peaks instead of steps and the area under the peaks is proportional to the total change in weight. These curves have certain similarities to the DTA curves, which allows to a certain extent, comparisons to be made[157-159].

Application of thermogravimetry and factors affecting thermogravimetry have been discussed by Wendlandt[160]. TG is the most widely used thermal technique to study the heterogeneous reaction kinetics. The importance of TG method is due to the large amount of information obtainable from single measurement. The factors affecting thermogravimetry have been classified as (i) instrumental and (ii) sample characteristics, and the most important among them are heating rate and sample mass.

Although thermogravimetry has been applied to various problems in chemistry,we have used this technique to study chiefly two aspects.

1. Phenomenological aspect - This study is confined to finding the temperatures of initiation, maximum decomposition and completion of the decomposition. This would also imply ascertaining temperature regions of stability and regime of thermal decomposition.
2. Kinetic aspect - Here one studies kinetic parameters such as the energy of activation, pre-exponential factor and entropy of activation.

Mathematical methods for the evaluation of kinetic parameters

During the past few decades a large number of equations have been formulated for the kinetic analysis of data obtained from thermal methods such as TG, DTA and DSC, in addition to a variety of other methods[161]. In most of these methods, the rate of reaction is followed by measuring the change in some physical property such as mass or enthalpy which varies linearly with the extent of reaction. The change in property may be

measured either isothermally or at a constant linear heating rate. The choice of the property depends on the characteristic type of the solid state reaction[162, 163].

In general, there are two approaches[164] for the evaluation of kinetic parameters of thermal decomposition reactions under non-isothermal conditions.

1. A general kinetic study, which is the simple extension of homogeneous kinetics to solid state kinetics, usually heterogeneous.
2. A mechanism based study, which gives the physico-chemical description of the process.

Non-isothermal kinetic equations

The most widely used thermal technique to study heterogeneous kinetics is TG. The kinetic equation

$$d\alpha/dt = (A)e^{-E/RT}(1-\alpha)^n \qquad (1)$$

may be considered as a general equation relating the parameters A, E and n where A is the pre-exponential factor, E is energy of activation, R is the universal gas constant and n is the order parameter. Several authors have given the solution of equation (1) in simple and more practically useful forms for calculating the kinetic parameters for the thermal decomposition of solid state reation of the type

$$A_{(solid)} \rightarrow B_{(solid)} + C_{(gas)}$$

For monitoring the reaction from mass loss, a dimentionsless quantity, the fractional decomposition α, which at time t, is defined as the fraction of the sample decomposed, is employed. Therefore

$$\alpha = W_t/W_\alpha = \frac{m_o - m_t}{m_o - m_\alpha} \quad \text{in which}$$

W_t = mass loss at time t

W_α = maximum mass loss in the TG experiment for the reaction under investigation.

m_o = initial mass of the sample

m_t = the mass at time t

m_α = the mass at the end of the reaction.

Most of the existing evaluation methods for the calculation of kinetic parameters utilise the equation (1) in some form or other.

The mathematical treatment of kinetic equations make use of one of the following three methods of evaluation; (i) differential methods, (ii) integral methods and (iii) approximation methods.

Using these approaches, a number of equations are derived by different authors. Only one method used in the present study is outlined in this chapter.

Integral methods

Integral methods are generally accepted as the most accurate among the methods available for the determination of kinetic parameters from TG

data[165,166]. On rearranging and integrating the equation (1) between the limits $\alpha=0$ and T_i and α at T we get

$$\int_0^{\alpha} \frac{d\alpha}{(1-\alpha)^n} = \frac{A}{\phi} \int_{Ti}^{T} e^{-E/RT}\, dT = \left[\frac{A}{\phi} \int_0^{T} e^{-E/RT}\, dT\right] \qquad (2)$$

For convenience of integration, the lower limit T_i of equation (2) is usually taken as zero[167]. This is justifiable because the extent of reaction which occurs between the temperatures 0 and Ti would be negligibly small, Ti, being the temperature at the inception of reaction.

The left hand side of the equation (2) can be readily integrated to get the expression $1-(1-\alpha)^{(1-n)}/(1-n)$. For convenience, the expression will be denoted hereafter by $g(\alpha)$,

$$g(\alpha) = 1-(1-\alpha)^{1-n}/1-n \qquad (3)$$

This is valid when $n\neq1$. When $n=1$, $g(\alpha)$ gets reduced to the form

$$g(\alpha) = -\ln(1-\alpha) \qquad (4)$$

The temperature integral on the right hand side of the equation (2) cannot be integrated in a closed form. Several authors have employed different techniques for the evaluation of the temperature integral[168].

Coats-Redfern method is a typical integral method.

Coats-Redfern method

Coats and Redfern[169] evaluated the temperature integral with the aid of the Rainville function[170],

$$\ln\left[\frac{g(\alpha)}{T^2}\right] = \ln\left[\frac{AR}{\phi E}\left(1-\frac{2RT}{E}\right)\right] - \frac{E}{RT} \qquad (5)$$

This is the Coats-Redferm equation. These authors have shown that for the usual value of E and temperature range in which the reaction generally occurs, the term, ln [AR/ϕE (1-2RT/E)] is sensibly constant, since 2RT/E <<1. A plot of ln [g(α)/T^2] against 1/T would therefore be linear. E and A can be evaluated from the slope and the intercept of the linear plot. These authors have recommended a trial and error method for determining the form of g(α), i.e., the value of n is determined by trial and error. The parameter, entropy of activation, ΔS, can be evaluated from the pre-exponential factor, A, using the equation

$$A = kT_s/h \exp.(\Delta S/R) \qquad (6)$$

where k is the Boltzmann constant, h is the Planck constant, T_s is the peak temperature and R is the universal gas constant.

Mechanism of reaction from non-isothermal TG traces

The procedure for deducing the mechanism of the reaction using nonisothermal kinetic methods has been discussed by Sestak and Berggren[171] and Satava[172]. According to Satava, a non-isothermal reaction proceeds in an infinitesimal time interval isothermally, where the rate can be expressed by an Arrhenius type equation.

$$\frac{d\alpha}{dt} = A \exp.(-E/RT)\, f(\alpha) \qquad (7)$$

A is the pre-exponential factor, t is the time and f(α) depends on the mechanism of the process.

For a linear heating rate, $\phi = \frac{dT}{dt}$

substitution into equation (7) gives

$$\frac{d\alpha}{f(\alpha)} = \frac{A}{\phi} e^{-E/RT} dT \qquad (8)$$

Integration of the LHS of the equation (8) gives

$$\int_0^{\alpha} \frac{d\alpha}{f(\alpha)} = g(\alpha) = \int_0^{T} \frac{A}{\phi} e^{-E/RT} dT \qquad (9)$$

Where g(α) is the integrated form of f(α). A series of f(α) forms are proposed and the mechanism is obtained from that which gives the best representation of the experimental data. Nine probable reaction mechanisms given by Satava are given in Table II.1. For evaluating kinetic parameters from the mechanistic equations, the right hand side of equation (9), the temperature integral, which is an incomplete gamma function, was used in the form given by Coats and Redfern which is one of the best solutions, recommended by several authors[173, 174]. The general form of the equation used is

$$\ln\left[\frac{g(\alpha)}{T^2}\right] = \ln\left[\frac{AR}{\phi E} - \frac{E}{RT}\right]$$

Using the computer, linear plots were drawn for the nine forms of $\ln[g(\alpha)/T^2]$ versus $1/T$, by the method of least squares. E, A, ΔS and the corresponding correlation coefficient, r, for the linear plots were calculated.

Scope of present investigation

The results of the studies on thermal decomposition of Mn(II), Co(II), Ni(II), Cu(II) and Zn(II) complexes of vanillin-2-aminopyridine, vanillin-2-aminothiazole, *o*-vanillin-2-aminopyridine, *o*-vanillin-2-aminothiazole and *o*-vanillin-L-histidine are presented in this part using TG technique. UO_2(II) complex of *o*-vanillin-2-aminopyridine, Cd(II) and ZrO(II) complexes of *o*-vanillin-L-histidine are also presented along with the above chelates. DTG and DTA techniques are also used in the study of few complexes.

The temperature regions of stability have been noted from the TG traces. The temperature of inception and decomposition and the temperatures of maximum rate of decomposition have also been noted. The thermal stability and the decomposition stages of the complexes have been discussed. The intermediate products are confirmed by chemical analysis and infrared spectral analysis. X ray diffractometry has been used for the characterization of the ultimate decomposition products.

The non-isothermal TG curves have been subjected to mathematical analysis using the integral method of Coats Redfern[169] and the activation parameters have been evaluated for all the complexes. The mechanism of the decomposition has been established from TG data using mechanistic equations.

Table II.1. **Mechanistic Equations**

Function	Equation	Rate controlling Process
D_1	$\alpha^2 = kt$	One-dimensional diffusion
D_2	$(1-\alpha)\ln(1-\alpha)+\alpha = kt$	Two-dimensional diffusion, cylindrical symmetry
D_3	$[1-(1-\alpha)^{1/3}]^2 = kt$	Three-dimensional diffusion, spherical symmetry, Jander equations
D_4	$(1-2/3\alpha)-(1-\alpha)^{2/3} = kt$	Three-dimensional diffusion, spherical symmetry, Ginstling Brounshtein equation
F_1	$-\ln(1-\alpha) = kt$	Random nucleation, one nucleus at each particle, Mampel equation.
A_2	$-\ln(1-\alpha)^{1/2} = kt$	Random nucleation; Avrami equation I
A_3	$-\ln(1-\alpha)^{1/3} = kt$	Random nucleation; Avrami equation II
R_2	$1 - (1-\alpha)^{1/2} = kt$	Phase boundary reaction; cylindrical symmetry
R_3	$1 - (1-\alpha)^{1/3} = kt$	Phase boundary reaction; spherical symmetry

CHAPTER III

THERMAL DECOMPOSITION KINETICS OF Mn(II), Co(II), Ni(II), Cu(II) AND Zn(II) COMPLEXES OF VANILLIN-2-AMINOPYRIDINE

Thermoanalytical techniques have an important role in elucidating the bonding and structure of complexes. They can help to define the stoichiometry, kinetics and mechanisms of the decomposition of these materials, along with a variety of other analytical techniques. Understanding these aspects is highly desirable in utilizing such coordination compounds as precursors in synthetic inorganic chemistry.

Wendlandt and coworkers[175-177] as well as Hill and coworkers[178,179] studied the thermal properties of metal chelates with different types of complexing ligands. Such studies on thermal decomposition and kinetics of metal chelates with azomethine ligands have been carried out by a few workers[180-183]. The use of thermoanalytical technique to follow the reaction of the metal ion during the course of a thermal decomposition has been reported by Wendlandt[184].

Studies on the thermal decomposition of five typical complexes viz., vanillin-2-aminopyridine complexes of Mn(II), Co(II), Ni(II), Cu(II) and Zn(II) are described in this chapter. Interpretation and mathematical analysis of these thermal decomposition data and evaluation of order of reaction, energy and entropy of activation and pre-exponential factor based on the Coats-Redfern method is also described. Evaluation of the reaction mechanism by non-isothermal methods has been discussed using the nine mechanistic equations by Sestak and Berggren[171] and Satava[172].

Experimental

Thermogravimetric curves were traced using a Shimadzu DT40 thermobalance, in an atmosphere of static air. A constant heating rate of $10^{o}C\ min^{-1}$ and a sample of 5-10 mg were employed for the entire study. Mass loss considerations and X ray diffraction data confirmed the products to be the corresponding oxides. The preparative procedures for the ligand and the complexes were described in Part I. Mechanistic and non-mechanistic calculations were performed with a Horizon III mini computers using the programming language Fortran.

Treatment of data

The instrumental TG curves were redrawn as percentage weight versus temperature. They are represented in Figures II.3.1 - II.3.5. The thermal behaviour of above chelates were studied in detail. Nine mechanistic equations and non-mechanistic equation were employed to evaluate kinetic data from these TG traces. The thermal data for the metal chelates are given in Tables II.3.1 and II.3.2. Data from independent pyrolytic experiments are also included in these Tables. The kinetic parameters calculated from TG data for the nine mechanistic equations are given in Tables II.3.3-II.3.5. The corresplonding values of E, A, ΔS and r from non-mechanistic equation (Coats-Redfern) and the mechanistic equations suggested are given in Tables II.3.6 - II.3.8.

RESULTS AND DISCUSSION

From the physicochemical studies of complexes, the molecular formula have been found to be $[MnL'HCl(H_2O)_4]Cl$, $[CoL'H(OAc)_2(H_2O)_3]$,

$[NiL'H(OAc)_2(H_2O)_3]$, $[CuL'H(OAc)_2(H_2O)_3]$ and $[ZnL'H(OAc)_2(H_2O)_3]$ where L = VAAP. Mn(II), Ni(II), Cu(II) and Zn(II) complexes decomposed in three stages whereas Co(II) complex decomposed in four stages. The first stage, in all the above chelates represents the loss of 2-3 water molecules above 150°C. According to Nikolaev *et al.*[185], water eliminated above 150°C can be considered as coordinated water. The temperature ranges of decomposition, peak temperature and probable assignment of the decomposition of the complexes are given in Tables II.3.1 - II.3.2.

The total mass loss for each complex is in agreement with theoretical values and those obtained by independent pyrolytic experiment.

The activation energies obtained for the main decomposition stages of these five complexes are also comparable to those of coordination compounds of 3d transition metals having similar structures[186,187].

Initial decomposition temperature and inflection temperature have been used to determine the thermal stability of metal chelates. In the present course of studies, based on observations made by earlier workers[187,188], the relative thermal stabilities of the metal chelates can be given as $[CuL'H(OAc)_2(H_2O)_3]$ < $[CoL'H(OAc)_2(H_2O)_3]$ < $[NiL'H(OAc)_2(H_2O)_3]$ < $[ZnL'H(OAc)_2(H_2O)_3]$ < $[MnL'HCl(H_2O)_4]Cl$.

Decomposition kinetics

Tables II.3.3 II.3.5 show that more than one equation give good linear curves with high correlation coefficient, making the assignment of reaction mechanism a difficult task. In such cases the function ($g\alpha$) which gives

kinetic parameter in agreement with those obtained by non-mechanistic equation are considered.

In the present study it is observed that the values of E, A and ΔS for the second stage decomposition of $[MnL'HCl(H_2O)_4]Cl$ and first stage decomposition of $[NiL'H(OAc)_2(H_2O)_3]$ obtained from Coats-Redfern with n = 1/3 are in good agreement with the corresponding values obtained for A_2 mechanism based on Random nucleation, Avrami equation 1.

First and fourth stage of the $[CoL'H(OAc)_2(H_2O)_3]$ and the first stage of $[CuL'H(OAc)_2(H_2O)_3]$ follows 1/2 order of reaction. First stage decomposition of $[CoL'H(OAc)_2(H_2O)_3]$ and $[CuL'H(OAc)_2(H_2O)_3]$ follows R_2 mechanism based on phase boundary reaction, cylindrical symmetry and the fourth stage decomposition of $[CoL'H(OAc)_2(H_2O)_3]$ follows A_2 mechanism based on Random nucleation, Avrami equation 1.

Order of the reaction is found to be 2/3 for the third stage of $[MnL'HCl(H_2O)_4]Cl$ and for the second stage of $[CoL'H(OAc)_2(H_2O)_3]$. Of these $[MnL'HCl(H_2O)_4]Cl$ follows D_1 mechanism with one-dimensional diffusion and $[CoL'H(OAc)_2(H_2O)_3]$ follows A_3 mechanism based on Random nucleation, Avrami equation II.

For the first stage decomposition of $[MnL'HCl(H_2O)_4]Cl$ and third stage decomposition of $[NiL'H(OAc)_2(H_2O)_3]$ and $[CuL'H(OAc)_2(H_2O)_3]$ the values of kinetic parameters obtained for Coats-Redfern equation with n=1 are in good agreement with those values obtained for F_1 mechanism based on random nucleation (Mampel equation).

Second and third stage decomposition of $[ZnL^1H(OAc)_2(H_2O)_3]$ also follows first order reaction which is in agreement with F_1 mechanism based on random nucleation.

All these mechanisms are proposed since the values of E, A and ΔS computed from the mechanistic equation agree well with those from the nonmechanistic equation (Coats-Redfern) having maximum correlation coefficient.

TABLE II.3.1. **Thermal decomposition data of Mn(II), Co(II) and Ni(II) complexes of Vanillin-2-aminopyridine (L'H)**

Complex	Stage	Temp. range in TG (°C)	Peak temp. in TG (°C)	Loss of mass (%)			Probable assignment
				From TG	Theo-retical	From Pyrolysis	
$[MnL'HCl(H_2O)_4]Cl$	I	170 - 200	190	8.00	8.40	--	Loss of $2H_2O$
	II	260 - 320	320	40.00	40.40	--	Loss of $2H_2O$ + vanillin part
	III	390 - 490	450	32.00	33.20	--	Loss of aminopyridine part + 2Cl
				80.00	82.00	81.00	
$[CoL'H(OAc)_2(H_2O)_3]$	I	110 - 200	160	10.00	11.80	--	Loss of $3H_2O$
	II	210 - 330	240	27.00	29.70	--	Loss of vanillin part
	III	330 - 340	338	24.00	20.10	--	Loss of aminopyridine part
	IV	340 - 400	350	22.00	21.20	--	Loss of 2 acetate
				83.00	82.80	83.10	
$[NiL'H(OAc)_2(H_2O)_3]$	I	120 - 300	150	41.00	41.50	--	Loss of $3H_2O$ + vanillin part
	II	300 - 310	302	29.00	26.50	--	Loss of aminopyridine part + 0.5 acetate
	III	310 - 390	340	15.50	16.00	--	Loss of 1.5 acetate
				85.50	84.00	84.98	

TABLE II.3.2. **Thermal decomposition data of Cu(II) and Zn(II) complexes of Vanillin-2-aminopyridine (L'H)**

Complex	Stage	Temp. range in TG (°C)	Peak temp. in TG (°C)	Loss of mass (%)			Probable assignment
				From TG	Theore-tical	From Pyrolysis	
$[CuL'H(OAc)_2(H_2O)_3]$	I	90 - 120	120	8.00	7.70	--	Loss of $2H_2O$
	II	130 - 260	254	60.00	60.00	--	Loss of $1H_2O$ + L + 0.5 acetate
	III	260 - 400	300	14.00	15.60	--	Loss of 1.5 acetate
				82.00	83.30	82.80	
$[ZnL'H(OAc)_2(H_2O)_3]$	I	130 - 200	180	11.00	11.60	--	Loss of $3H_2O$
	II	230 - 340	250	20.00	19.77	--	Loss of aminopyriidne part
	III	340 - 450	420	50.50	51.14	--	Loss of vanillin part + 2 acetate
				81.50	82.51	81.78	

TABLE II.3.3. **Kinetic parameters for the decomposition of Mn(II) and Co(II) complexes of vanillin-2-aminopyridine (L'H) from TG using mechanistic equations**

Complex	Para-meter*	Mechanistic Equations								
		1	2	3	4	5	6	7	8	9
$[MnL'HCl(H_2O)_4]Cl$	E	52.9164	53.2949	53.6711	40.2618	26.1203	26.1070	26.1082	25.8336	25.9288
	A	6.8824×10^{20}	5.3505×10^{20}	1.8352×10^{20}	7.1625×10^{13}	1.3356×10^{9}	6.5816×10^{8}	4.3935×10^{8}	4.7538×10^{8}	3.5439×10^{8}
I Stage	ΔS	-9.8216	-10.3219	-12.4481	-41.7690	-63.4070	-63.4070	-65.6163	-65.4597	-66.0433
	γ	0.9543	0.9547	0.9555	0.9783	0.9525	0.9525	0.9527	0.9518	0.9521
	E	6.1064	13.8800	16.5950	16.1674	7.5124	7.5164	7.5162	7.0370	7.1937
II Stage	A	4.7072×10^{-6}	4.7646×10^{1}	4.0373×10^{1}	2.5887×10^{1}	2.9620×10^{-1}	1.4680×10^{-1}	9.7900×10^{-2}	8.5500×10^{-2}	6.8000×10^{-2}
	ΔS	-130.0243	-97.9736	-98.3027	-99.1857	-108.0929	-109.4627	-110.2687	-110.5379	-110.9925
	γ	0.9474	0.9189	0.9356	0.9376	0.9163	0.9164	0.9164	0.9182	0.9176
	E	3.2780	5.6808	9.7468	6.9756	5.8811	5.8986	5.8807	2.4613	3.4602
III Stage	A	3.6650×10^{-3}	2.6600×10^{-2}	3.0790×10^{-1}	2.1680×10^{-2}	1.0990×10^{-1}	5.5800×10^{-2}	3.6600×10^{-2}	1.3437×10^{-3}	2.9109×10^{-3}
	ΔS	-117.1897	-113.2470	-108.3853	-113.6578	-110.4319	-111.7795	-112.6157	-119.1835	-117.6475
	γ	0.9928	0.9893	0.9803	0.9862	0.9593	0.9600	0.9593	0.9645	0.9637
$[CoL'H(OAc)_2(H_2O)_3]$	E	31.0870	29.8799	31.5112	22.4509	15.0187	15.0183	15.0185	14.8578	14.9176
	A	1.8282×10^{11}	2.3764×10^{10}	3.5585×10^{10}	9.2245×10^{5}	1.3779×10^{4}	6.8872×10^{3}	4.5918×10^{3}	5.5346×10^{3}	3.9946×10^{3}
I Stage	ΔS	-53.4997	-105.0261	-56.7516	-77.7351	-86.0881	-87.4662	-88.2717	-87.9006	-88.5488
	γ	0.9348	0.9220	0.9363	0.9584	0.9300	0.9300	0.9300	0.9287	0.9291
	E	9.7212	10.5422	11.2124	10.8427	4.8769	4.9053	4.8769	4.6394	4.5353
II Stage	A	1.6707	2.1405	1.0539	6.6940×10^{-1}	4.0700×10^{-2}	2.1100×10^{-2}	1.3600×10^{-2}	1.0400×10^{-2}	8.6729×10^{-3}
	ΔS	-104.3431	-103.8508	-105.2587	-106.1604	-111.7232	-113.0252	-113.9057	-120.9268	-114.7964
	γ	0.9443	0.9595	0.9629	0.9601	0.9491	0.9437	0.9491	0.9401	0.9433
III Stage	So rapid that could not be studied.									
	E	9.5940	14.5132	26.8714	18.2581	20.4172	20.4172	20.4172	9.0937	12.1958
	A	3.1515	1.9864×10^{2}	1.6822	1.3647×10^{3}	1.1353×10^{5}	5.6768×10^{4}	3.7844×10^{4}	1.7673	2.2084×10^{1}
IV Stage	ΔS	-103.4681	-95.2348	-104.7155	-91.4055	-82.6206	-83.9978	-84.8036	-104.6175	-99.5995
	γ	0.9348	0.9955	0.9990	0.9991	0.9908	0.9908	0.9908	0.9998	0.9989

*E in kCals mol^{-1}; A in s^{-1}; ΔS in eu.

TABLE II.3.4. **Kinetic parameters for the decomposition of Ni(II) and Cu(II) complexes of vanillin-2-aminopyridine (L'H) from TG using mechanistic equations**

Complex	Para-meter*	Mechanistic Equations								
		1	2	3	4	5	6	7	8	9
$[NiL'H(OAc)_2(H_2O)_3]$	E	13.3163	13.5964	14.2436	16.4655	6.4244	6.4246	6.4246	6.0635	6.0882
	A	1.6363×10^{2}	1.2355×10^{2}	6.145×10^{1}	5.8994×10^{2}	3.8310×10^{-1}	1.9160×10^{-1}	1.2770×10^{-1}	1.1550×10^{-1}	8.0200×10^{-2}
I Stage	ΔS	-94.85	-95.41	-96.80	-92.3026	-106.8860	-108.2612	-109-0782	-109.2718	-109.9900
	γ	0.9435	0.9504	-0.9528	0.8912	0.9426	0.9426	0.9426	0.9334	0.9362
II Stage	So rapid that could not be studied									
	E	1.5379	4.1832	10.7018	6.0979	8.7786	8.7788	8.7784	2.4696	4.1163
III Stage	A	9.8062×10^{-4}	1.9700×10^{-2}	4.8563	3.8800×10^{-2}	6.6700	3.3394	2.2254	2.9281×10^{-3}	1.5000×10^{-2}
	ΔS	-118.7443	-112.7848	-101.8397	-111.4378	-101.2070	-102.5838	-103.3902	-116.5706	-113.3211
	γ	0.8229	0.9390	0.9760	0.9602	0.9753	0.9753	0.9753	0.9315	0.9605
$[CuL'H(OAc)_2(H_2O)_3]$	E	37.9847	38.1595	38.4784	41.668	18.6118	18.6033	18.6035	18.4270	18.4886
	A	1.8027×10^{17}	1.2101×10^{17}	4.0144×10^{16}	2.0010×10^{18}	1.9095×10^{7}	9.4327×10^{6}	6.2908×10^{6}	7.3152×10^{6}	5.3244×10^{6}
I Stage	ΔS	-25.8836	-26.6756	-28.8680	-21.1010	-71.5216	-72.9229	-73.7278	-73.4281	-74.0592
	γ	0.9627	0.9806	0.9624	0.792	0.9595	0.9594	0.9594	0.9595	0.9595
II Stage	So rapid that could not be studied.									
	E	0.9635	1.3722	4.6957	2.4460	3.5301	2.7017	3.5299	0.3185	1.1684
	A	8.8260×10^{-5}	7.4589×10^{-4}	2.0300×10^{-2}	9.3581×10^{-4}	4.5333×10^{-2}	8.4443×10^{-3}	1.5109×10^{-2}	7.1332×10^{-5}	4.3558×10^{-4}
III Stage	ΔS	-124.1318	-119.8910	-113.3209	-119.4403	-111.7300	-115.0692	-113.9131	-124.5411	-120.9594
	γ	0.9753	0.9372	0.9905	0.9847	0.9716	0.9079	0.9716	0.8128	0.9674

*E in kCals mol^{-1}; A in s^{-1}; ΔS in eu.

TABLE II.3.5. **Kinetic parameters for the decomposition of Zn(II) complex of vanillin-2-aminopyridine (L'H) from TG using using mechanistic equations**

Complex	Para-meter*	Mechanistic Equations								
		1	2	3	4	5	6	7	8	9
$[ZnL'H(OAc)_2(H_2O)_3]$ I Stage		So rapid that could not be studied.								
II Stage	E	14.7624	15.5014	16.2914	14.5655	7.5041	7.5013	6.7085	6.9104	7.1055
	A	7.0053×10^{2}	8.1573×10^{2}	4.4412×10^{2}	6.8787×10^{1}	1.6425	8.1880×10^{-1}	2.2296×10^{-2}	3.3967×10^{-2}	3.3757×10^{-1}
	ΔS	3.6971	3.9997	2.7916	-0.9143	-8.3354	-9.7185	-12.3034	-11.1437	-11.4792
	γ	0.9770	0.9781	0.9793	0.9801	0.9742	0.9742	0.9626	0.9717	0.9726
III Stage	E	7.8661	9.2370	10.8639	9.7969	5.0112	5.0112	5.0112	3.7558	4.1592
	A	3.9050×10^{-1}	8.2810×10^{-1}	9.7150×10^{-1}	3.2562×10^{-1}	7.3346×10^{-2}	3.6670×10^{-2}	2.4446×10^{-2}	8.6401×10^{-3}	9.2519×10^{-3}
	ΔS	-10.7586	-9.2649	-8.9475	-11.1135	-1.0813	-15.4587	-16.2644	-18.3310	-18.1951
	γ	0.9780	0.9807	0.9827	0.9809	0.9754	0.9754	0.9754	0.9673	0.9706

*E in kCals mol^{-1}; A in s^{-1}; ΔS in eu.

TABLE II.3.6. **Kinetic Parameters for the decomposition of Mn(II) and Co(II) complexes of vanillin-2-aminopyridine (L'H) from TG using Coats-Redfern equation and accepted mechanistic equations**

Complex	Parameters	From Coats-Redfern equation	From mechanistic equation	Reaction mechanism	Order of reaction
$[MnL'HCl(H_2O)_4]Cl$					
	E kCal/mole	26.1203	26.1203	Equation V	
I Stage	A sec^{-1}	1.3356×10^{9}	1.3356×10^{9}	F_1 mechanism	
	ΔS eu	-63.4070	-63.4070	Random nucleation	
	γ	0.9525	0.9525	Mampel equation	1
	E kCal/mole	6.9828	7.5164	Equation VI	
	A sec^{-1}	1.4553×10^{-1}	1.4680×10^{-1}	A_2 mechanism	
II Stage	ΔS eu	-109.5093	-109.4627	Random nucleation	1/3
	γ	0.9189	0.9164	Avrami equation I	
	E kCal/mole	3.4610	3.2780	Equation 1	
	A sec^{-1}	4.3443×10^{-3}	3.6650×10^{-3}	D_1 mechanism	
III Stage	ΔS eu	-116.4610	-117.1897	one-dimensional diffusion	2/3
	γ	0.9637	0.9928		
$[CoL'H(OAc)_2(H_2O)_3]$					
	E kCal/mole	14.6587	14.8578	Equation VIII	
I Stage	A sec^{-1}	5.4165×10^{3}	5.5346×10^{3}	R_2 mechanism	
	ΔS eu	-87.9435	-87.9006	Phase boundary reaction	1/2
	γ	0.9246	0.9287	Cylindrical symmetry	
	E kCal/mole	4.8355	4.8769	Equation VII	
II Stage	A sec^{-1}	1.3617×10^{-2}	1.3600×10^{-2}	A_3 mechanism	
	ΔS eu	-113.2785	-113.9057	Random nucleation	2/3
	γ	0.9433	0.9491	Avrami equation II	
III Stage	So rapid that could not be studied.				
	E kCal/mole	20.4180	20.4172	Equation VI	
IV Stage	A sec^{-1}	5.7842×10^{4}	5.6768×10^{4}	A_2 mechanism	
	ΔS eu	-83.3645	-83.9978	Random nucleation	1/2
	γ	0.9908	0.9908	Avrami equation 1	

TABLE II.3.7. **Kinetic Parameters for the decomposition of Ni(II) and Cu(II) complexes of vanillin-2-aminopyridine (L'H) from TG using Coats-Redfern equation and accepted mechanistic equations**

Complex	Parameters	From Coats-Redfern equation	From mechanistic equation	Reaction mechanism	Order of reaction
$[NiL'H(OAc)_2(H_2O)_3]$					
I Stage	E kCal/mole	6.0238	6.4246	Equation VI	
	A sec^{-1}	1.9005×10^{-1}	1.9160×10^{-1}	A_2 mechanism	
	ΔS eu	-108.2790	-108.2612	Random nucleation	1/3
	γ	0.9300	0.9426	Avrami equation I	
II Stage	So rapid that could not be studied				
III Stage	E kCal/mole	8.7786	8.7786	Equation V	
	A sec^{-1}	6.6770	6.6770	F_1 mechanism	
	ΔS eu	-101.2070	-101.2070	Random nucleation	1
	γ	0.9753	0.9753	Mampel equation	
$[CuL'H(OAc)_2(H_2O)_3]$					
I Stage	E kCal/mole	18.4278	18.4270	Equation VIII	
	A sec^{-1}	7.2740×10^{6}	7.3152×10^{6}	R_2 mechanism	
	ΔS eu	-73.4393	-73.4281	Phase boundary reaction	1/2
	γ	0.9595	0.9595	Cylindrical symmetry	
II Stage	So rapid that could not be studied.				
III Stage	E kCal/mole	3.5301	3.5301	Equation V	
	A sec^{-1}	4.5333×10^{-2}	4.5333×10^{-2}	F_1 mechanism	
	ΔS eu	-111.7300	-111.7300	Random nucleation	1
	γ	0.9716	0.9716	Mampel equation	

TABLE II.3.8. **Kinetic Parameters for the decomposition of Zn(II) complex of vanillin-2-aminopyridine (L'H) from TG using Coats-Redfern equation and accepted mechanistic equations**

Complex	Parameters	From Coats-Redfern equation	From mechanistic equation	Reaction mechanism	Order of reaction
$[ZnL'H(OAc)_2(H_2O)_3]$ I Stage	So rapid that could not be studied.				
II Stage	E kCal/mole	7.5041	7.5041	Equation V	1
	A sec^{-1}	1.6425	1.6425	F_1 mechanism	
	ΔS eu	-8.3354	-8.3354	Random nucleation	
	γ	0.9742	0.9742	Mampel equation	
III Stage	E kCal/mole	5.0112	5.0112	Equation V	1
	A sec^{-1}	7.3346×10^{-2}	7.3346×10^{-2}	F_1 mechanism	
	ΔS eu	-14.0813	-14.0813	Random nucleation	
	γ	0.9754	0.9754	Mampel equation	

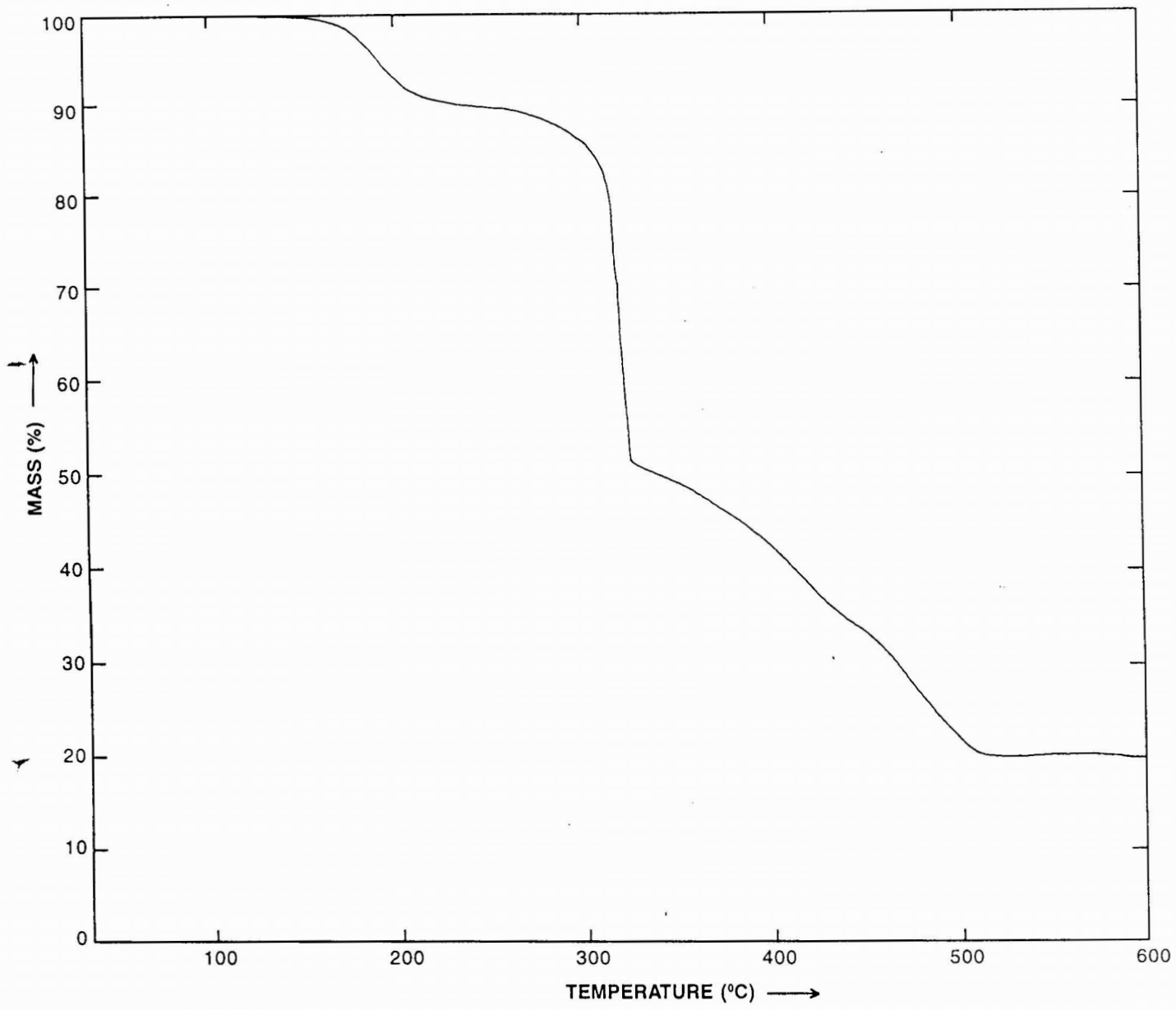

Figure II. 3.1 **TG Traces of $[MnL^1 HCl (H_2O)_4]Cl$**

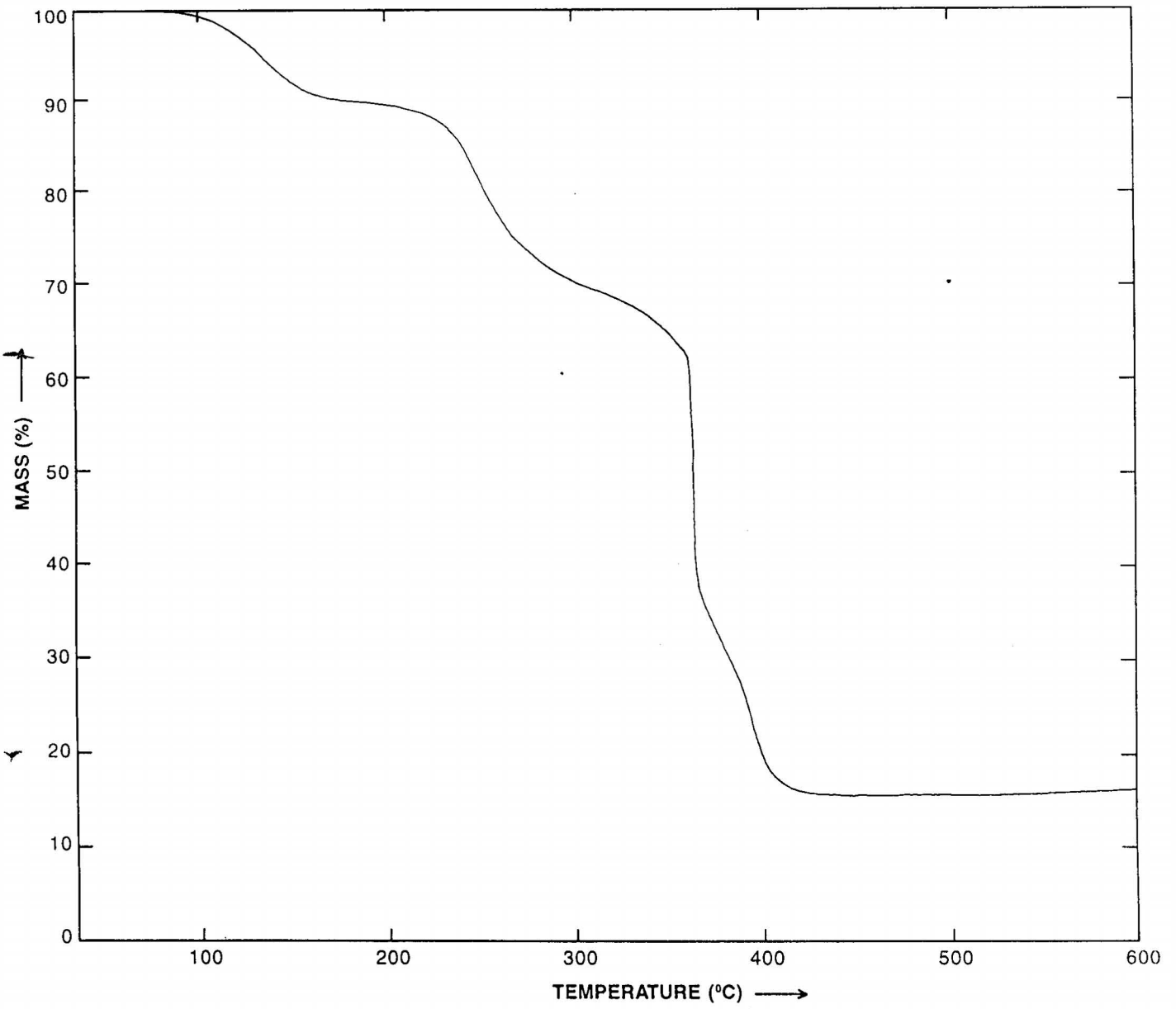

Figure II. 3.2 **TG Traces of $[CoL^{I}H(OAc)_2(H_2O)_3]$**

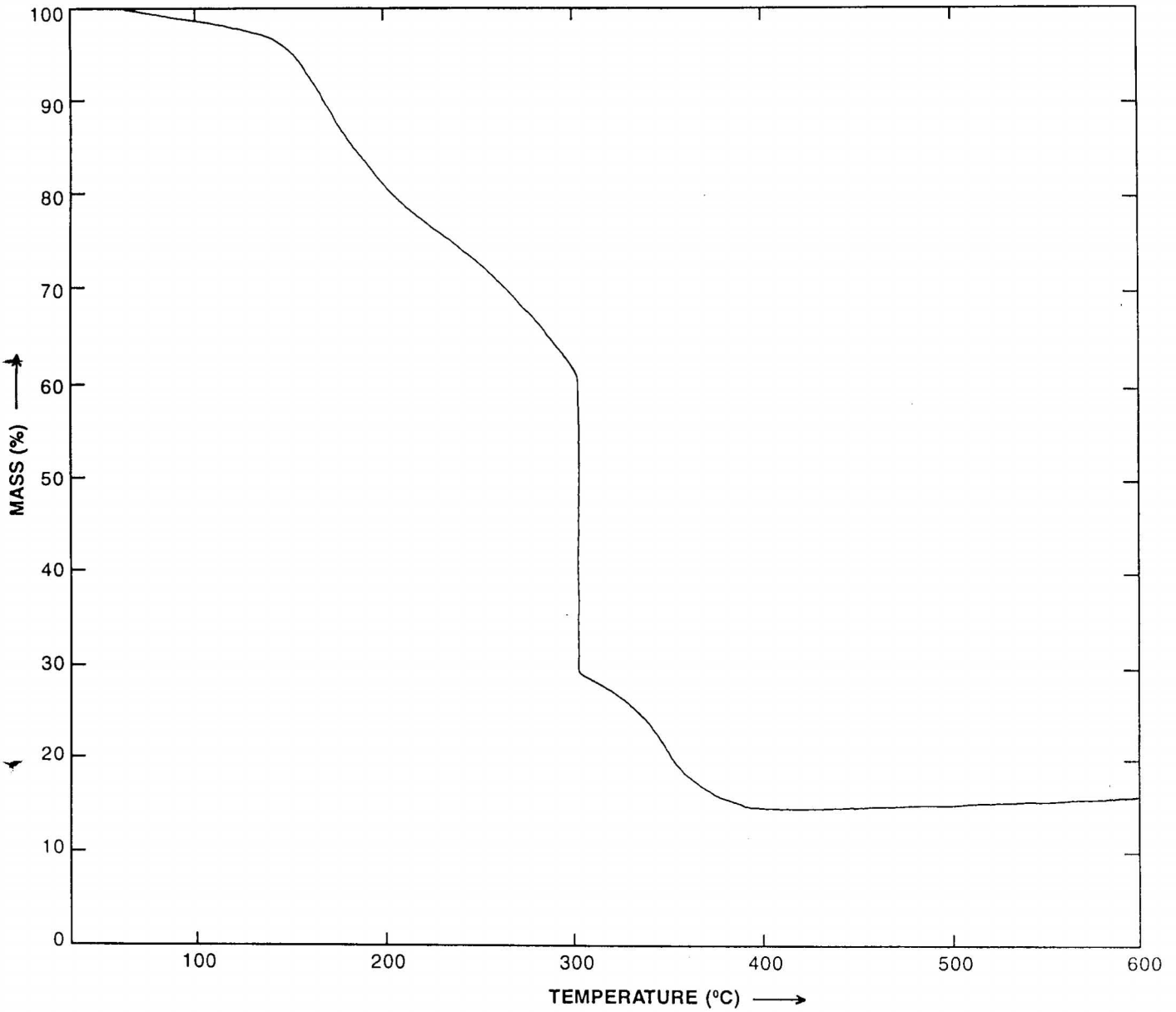

Figure II. 3.3 **TG Traces of [Ni L^1 H $(OAc)_2$ $(H_2O)_3$]**

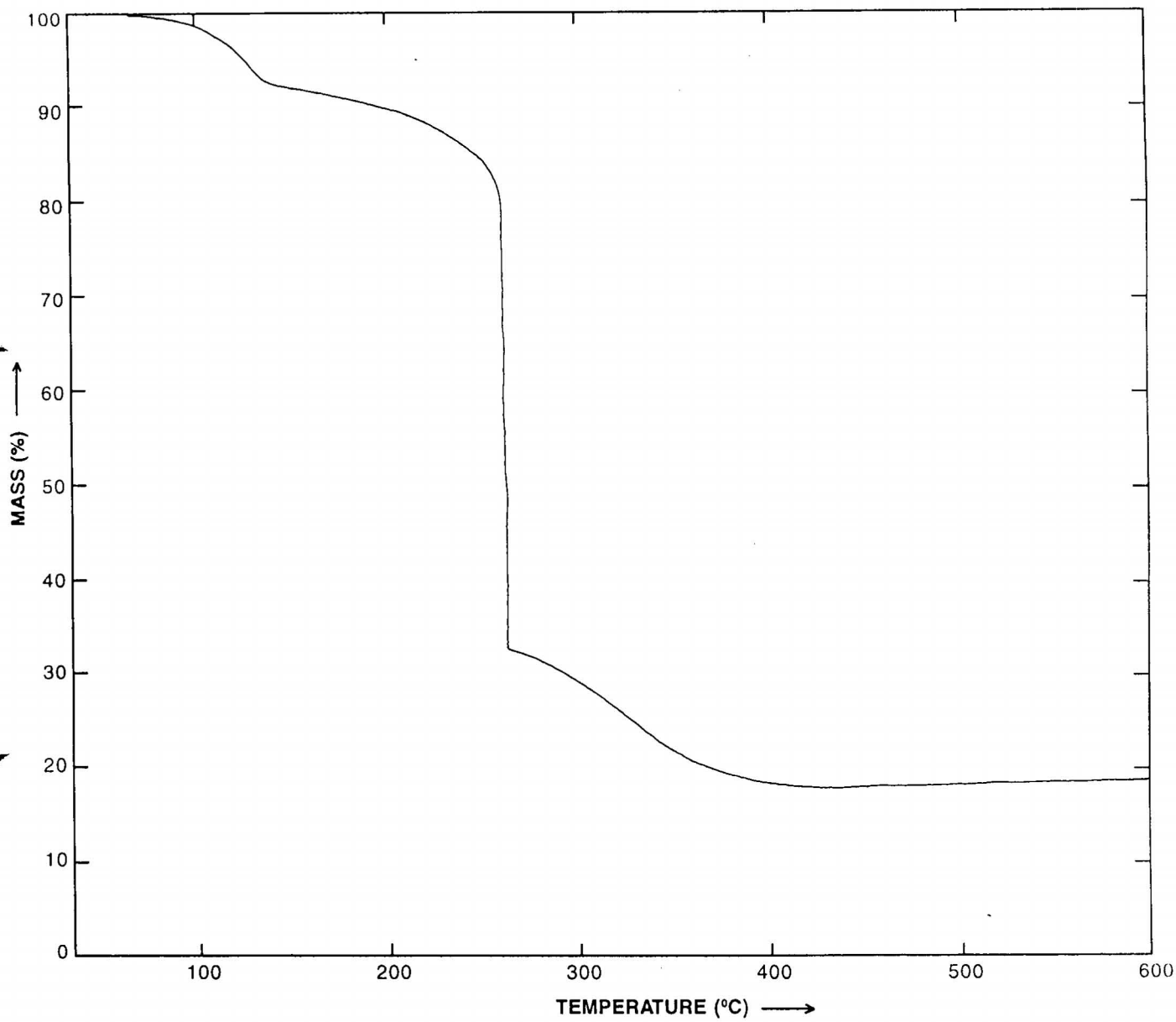

Figure II. 3.4 **TG Traces of [Cu L^1H $(OAc)_2$ $(H_2O)_3$]**

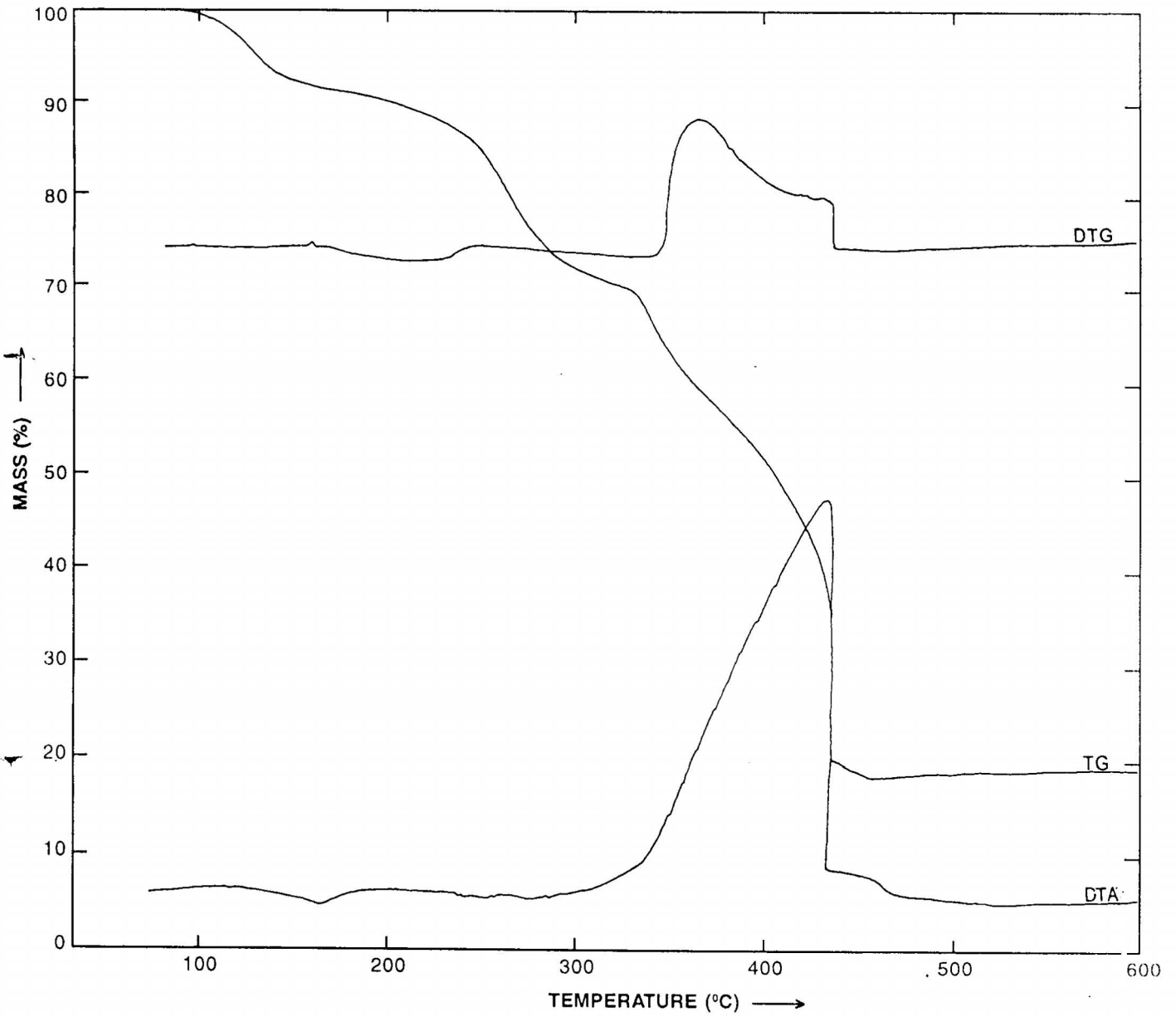

Figure II. 3.5 **TG, DTG and DTA Traces of [Zn L^1H $(OAc)_2$ $(H_2O)_3$]**

CHAPTER IV

THERMAL DECOMPOSTION KINETICS OF Mn(II), Co(II), Ni(II), Cu(II) AND Zn(II) COMPLEXES OF VANILLIN-2-AMINOTHIAZOLE

In this chapter, results of thermal decomposition studies on Mn(II), Co(II), Ni(II), Cu(II) and Zn(II) chelates of vanillin-2-aminothiazole are presented. The kinetic parameters like energy of activation E, pre-exponential factor A and entropy of activation ΔS, of the decomposition reactions were calculated based on various mechanistic and non-mechanistic kinetic equations. The order of reaction and mechanism of decomposition are also interpreted.

Experimental

The metal complexes concerned were prepared and characterized according to the procedure described in Part I. The TG curves were recorded in static air atmosphere at a heating rate of 15°C $min.^{-1}$ Calculation of kinetic parameters and order of decompositions were carried out using a Horizon III mini computer.

Treatment of data

The instrumental TG curves were redrawn as mass vs temperature and are given in Figures II.4.1 - II.4.5. The temperature ranges, peak temperature, probable assignments and total mass loss from TG along with the independent pyrolytic experimental data are presented in Tables II.4.1 and II.4.2. The kinetic parameters calculated using nine mechanistic

equations are summarised in Tables II.4.3. - II.4.5. Tables II.4.6 - II.4.8 include the suggested mechanism of decomposition, order of decomposition and the kinetic parameters evaluated by applying Coats-Redfern non-mechanistic method.

RESULTS AND DISCUSSION

For Mn(II) complex, a two stage decomposition pattern was observed. The stage 1 in the case of Mn(II) complex represents the loss of two water molecules and aminothiazole part of the first ligand. The second stage represents the loss of a combination of two chlorine atoms, vanillin part of the first ligand and second ligand part. The mass loss at the end of decomposition as read from TG curve is 90%.

The TG curve of $[Co(L"H)_2(OAc)_2(H_2O)_2]$ gave a three stage decomposition pattern, though stages II and III are overlapping. The first stage, represents the loss of two water molecules and aminothiazole part of the first ligand and the second stage, the loss of vanillin part of the first ligand and aminothiazole part of the second ligand. The third stage represents the loss of vanillin part of the second ligand and two acetate groups. The overall loss of mass from the curve is 90% while the theoretical loss in mass for the conversion of complex to Co_3O_4 is 88.29%.

$[NiL"H(OAc)_2(H_2O)_3]$ showed three stage decomposition pattern in its TG graph. The first stage represents the loss of three water molecules. The second stage corresponds to the loss of aminothiazole part of the ligand and the third stage, the loss of vanillin part of the ligand and, two acetate

groups. The overall mass loss from the curve is 84% while the theoretical loss in mass for the conversion to NiO is 83.91.

During thermal decomposition of $[CuL''H(OAc)_2(H_2O)_3]$ only one water molecule was lost in the first stage while the remaining two water molecules and vanillin part of the ligand were lost during the second stage of decomposition. The third stage represents the loss of aminothiazole part of the ligand and two acetate groups. Well-defined peaks in the appropriate region were obtained in the DTA and DTG curve. The mass loss at the end of the third stage as read from the TG is 85% while the theoretical mass loss appeared to be 83%.

A four stage decomposition pattern was observed in Zn(II) complex. Two water molecules and one acetate group were lost in the first stage while the remaining water molecule and the other acetate group were lost during the second stage of decomposition. Third stage represents the loss of aminothiazole part of the ligand and the fourth step represents the loss of vanillin part of the ligand.

The activation energies obtained for the main decomposition stages of these four complexes were also comparable to those of coordination compounds of 3d transition metals having similar structures[186, 187]. In all the cases the final products of decomposition were found to be corresponding metal oxides such as Mn_3O_4, Co_3O_4, NiO CuO and ZnO which were identified by X ray diffraction studies.

Decomposition kinetics

Kinetic parameters such as activation energy, E, preexponential factor, A, entropy of activation, ΔS and order of decomposition were evaluated using mechanistic and non mechanistic equations.

In the present investigation it is seen that R_2 mechanism based on phase boundary reaction, cylindrical symmetry gives the maximum correlation for the first stage of Ni(II), second stage of Mn(II) and third stage of Zn(II) complexes. The order of decomposition of all the above stage were found to be ½.

Order of the reaction is found to be 2/3 for first and second stage of $[Co(L"H)_2(OAc)_2(H_2O)_2]$ and for the fourth stage of $[ZnL"H(OAc)_2(H_2O)_3]$. First stage of Co(II) complex followed A_2 mechanism while the second stage A_3 mechanism. Both the mechanisms are based on Random nucleation. The fourth stage decomposition of Zn(II) complex show good agreement with the D_1 mechanism based on one dimensional diffusion.

Kinetic parameters computed for F_1 mechanism based on random nucleation (Mampel equation) gives the maximum correlation with the corresponding values obtained for Coats Redfern equation with n=1, for the first stage decomposition of $[Mn(L"H)_2Cl_2(H_2O)_2]$, second stage decomposition of $[NiL"H(OAc)_2(H_2O)_3]$, $[CuL"H(OAc)_2(H_2O)_3]$ and the for the first and second stage decomposition of $[ZnL"H(OAc)_2(H_2O)_3]$.

TABLE II.4.1. **Thermal decomposition data of Mn(II), Co(II) and Ni(II) complexes of vanillin-2-aminothiazole (L"H)**

Complex	Stage	Temp. range in TG (°C)	Peak temp. in TG (°C)	Loss of mass (%)			Probable assignment
				From TG	Theo-retical	From Pyrolysis	
$[Mn(L"H)_2Cl_2(H_2O)_2]$	I	70-260	160	22.00	21.28	--	Loss of $2H_2O$ + aminothiazole part
	II	270-520	430	68.00	66.72	--	Loss of 2(vanillin part)+L+2 chlorine atoms
				90.00	88.00	89.20	
$[Co(L"H)_2(OAc)(H_2O)_2]$	I	110-300	190	20.00	19.68	--	Loss of $2H_2O$+Aminothiazole part of Ist ligand
	II	310-450	330	30.00	34.36	--	Loss of vanillin part of Ist ligand +Aminothiazole part of 2nd ligand
	III	450-520	480	40.00	34.25	--	Loss of vanillin part of 2nd ligand + 2 acetate
				90.00	88.29	88.90	
$[NiL"H(OAc)_2(H_2O)_3]$	I	100-300	230	13.00	11.62	--	Loss of $3H_2O$
	II	300-450	410	20.00	21.08	--	Loss of aminothiazole part
	III	450-550	490	51.00	51.21	--	Loss of vanillin part +2 acetate
				84.00	83.91	84.02	

TABLE II.4.2. **Thermal decomposition data of Cu(II) and Zn(II) complexes of vanillin-2-aminothiazole (L"H)**

Complex	Stage	Temp. range in TG (°C)	Peak temp. in TG (°C)	Loss of mass (%)			Probable assignment
				From TG	Theo-retical	From Pyrolysis	
$[CuL"H(OAc)_2(H_2O)_2]$	I	80-150	150	3.50	3.80	--	Loss of $1H_2O$
	II	160-530	530	36.50	36.60	--	Loss of $2H_2O$+vanillin part
	III	530-620	600	45.00	42.60		Loss of aminothiazole part+2 acetate
				85.00	83.00	84.02	
$[ZnL"H(OAc)_2(H_2O)_3]$	I	150-240	170	20.50	20.20	--	Loss of $2H_2O$+1 acetate
	II	250-320	270	16.00	16.30	--	Loss of $1H_2O$+1 acetate
	III	340-420	360	21.40	20.80	--	Loss of 2-aminothiazole part
	IV	440-500	450	26.00	25.40	--	Loss of vanillin part
				83.90	82.70	83.50	

TABLE II.4.3. Kinetic parameters for the decomposition of Mn(II) and Co(II) complexes of vanillin-2-aminothiazole (L"H) from TG using mechanistic equations

Complex	Para-meter*	Mechanistic Equations								
		1	2	3	4	5	6	7	8	9
$[Mn(L"H)_2Cl_2(H_2O)_2]$	E	12.2355	12.5030	12.7798	12.6232	5.6222	5.6222	5.6222	5.4138	5.4827
	A	6.6334×10^{1}	4.7867×10^{1}	1.5506×10^{1}	1.2384×10^{1}	2.0030×10^{-1}	1.0010×10^{-1}	6.6800×10^{-2}	7.3700×10^{-2}	5.4300×10^{-2}
I Stage	ΔS	-96.6100	-97.2620	-99.5018	-99.9485	-108.1436	-109.5211	-110.3266	-110.1297	-110.7356
	γ	0.9372	0.9393	0.9413	0.9398	0.9235	0.9235	0.9235	0.9189	0.9204
	E	8.4809	17.6952	14.4238	11.9121	4.6402	4.6402	4.6402	4.9991	5.9117
II Stage	A	5.1780×10^{-1}	9.0928×10^{2}	1.9932×10^{1}	1.7809	3.7170×10^{-2}	1.8600×10^{-2}	1.2400×10^{-2}	2.4600×10^{-2}	4.3500×10^{-2}
	ΔS	-107.2970	-92.4523	-100.0433	-104.8423	-112.5306	-113.9078	-114.7133	-113.3499	-112.2161
	γ	0.9792	0.9854	0.9853	0.9861	0.9739	0.9739	0.9739	0.9794	0.9795
$[Co(L"H)_2(OAc)_2(H_2O)_2]$	E	13.8607	14.2921	14.1943	14.0334	6.7220	6.7220	6.7220	6.5740	6.6233
	A	1.0717×10^{2}	9.0158×10^{1}	1.9123×10^{1}	1.5809×10^{1}	3.6640×10^{-1}	1.8320×10^{-1}	1.2210×10^{-1}	1.4860×10^{-1}	1.0610×10^{-1}
I Stage	ΔS	95.7935	-96.1370	-99.2181	-99.5963	-107.0764	108.4539	-109.2596	-108.8698	-109.539
	γ	0.9467	0.9436	0.9476	0.9353	0.9417	0.9417	0.9417	0.9386	0.9396
	E	2.1708	2.7057	3.3254	2.9129	1.3788	1.3786	1.3788	0.8655	0.7372
II Stage	A	7.4216×10^{-4}	8.4533×10^{-4}	4.5644×10^{-4}	2.5389×10^{-4}	7.6745×10^{-4}	3.8357×10^{-4}	2.5582×10^{-4}	3.7059×10^{-5}	2.4456×10^{-5}
	ΔS	-119.9248	-119.6662	-120.8907	-122.0562	-119.8582	-121.2363	-122.0411	-125.8799	-126.7058
	γ	0.9509	0.9648	0.9745	0.9686	0.9656	0.9658	0.9657	0.9591	0.9391
III Stage	So rapid that could not be studied									

*E in k Cals mol^{-1}; A in s^{-1}; ΔS in eu

TABLE II.4.4. **Kinetic parameters for the decomposition of Ni(II) and Cu(II) complexes of vanillin-2-aminothiazole (L"H) from TG using mechanistic equations**

Complex	Para-meter*	Mechanistic Equations								
		1	2	3	4	5	6	7	8	9
$[NiL"H(OAc)_2(H_2O)_3]$	E	13.4470	13.6330	13.8430	12.8392	3.8584	6.0613	6.0607	5.9246	5.9713
	A	8.0420×10^{1}	5.0909×10^{1}	1.4694×10^{1}	4.6737	1.2904×10^{-2}	1.0406×10^{-1}	6.9327×10^{-2}	8.6325×10^{-2}	6.1269×10^{-2}
I Stage	ΔS	-96.4259	-97.3400	-99.8044	-102.0805	-113.7881	-109.6405	-110.4475	-110.0117	-110.6930
	γ	0.9960	0.9961	0.9963	0.9910	0.9672	0.9950	0.9950	0.9947	0.9948
	E	5.0285	5.6314	6.2977	5.9397	2.1171	2.1171	2.1142	1.6097	1.7720
II Stage	A	8.5057×10^{-3}	8.4509×10^{-3}	3.9220×10^{-3}	2.5988×10^{-3}	1.5066×10^{-3}	7.5326×10^{-4}	5.0047×10^{-4}	3.5574×10^{-4}	3.0410×10^{-4}
	ΔS	-115.4038	-115.4166	-116.9420	-117.7597	-118.8430	-120.2204	-121.0328	-121.7110	-122.0227
	γ	0.9634	0.9672	0.9697	0.9691	0.9280	0.9280	0.9276	0.9001	0.9110
III Stage	So rapid that could not be studied									
$[CuL"H(OAc)_2(H_2O)_3]$ I Stage	Weight loss is too small to carry out the kinetic study									
	E	5.1340	4.7541	6.3697	5.9125	2.2481	2.2431	2.2415	1.7478	1.4253
II Stage	A	1.3821×10^{-2}	5.4451×10^{-3}	6.5546×10^{-3}	3.8864×10^{-3}	2.2474×10^{-3}	1.1168×10^{-3}	7.4316×10^{-4}	5.3194×10^{-4}	2.3312×10^{-4}
	ΔS	-114.3798	-116.2307	-115.9622	-115.9008	-117.9890	-119.3786	-120.1879	-120.9523	-122.4916
	γ	0.9287	0.9757	0.9333	0.9296	0.9615	0.9609	0.9610	0.9322	0.9295
III Stage	So rapid that could not be studied.									

*E in kCals mol^{-1}; A in s^{-1}; ΔS in eu.

TABLE II.4.5. **Kinetic parameters for the decomposition of Zn(II) complex of vanillin-2-aminothiazole (L"H) from TG using mechanistic equations**

Complex	Para-meter*	Mechanistic Equations								
		1	2	3	4	5	6	7	8	9
$[ZnL"H(OAc)_2(H_2O)_3]$										
I Stage	E	7.9691	8.2222	8.4791	8.1248	3.4166	3.4146	3.4145	3.2354	3.2956
	A	4.6060×10^{-1}	3.2770×10^{-1}	1.0540×10^{-1}	6.7100×10^{-2}	1.1501×10^{-2}	5.7533×10^{-3}	3.8353×10^{-3}	4.3226×10^{-3}	3.1702×10^{-3}
	ΔS	-106.5342	-107.2100	-109.4612	-110.3607	-113.8599	-115.2428	-116.0486	-115.8109	-116.4270
	γ	0.9626	0.9650	0.9642	0.9612	0.9460	0.9459	0.9459	0.9414	0.9430
II Stage	E	9.0045	9.7933	11.0406	10.0836	5.8771	4.6744	4.6752	4.0120	4.2277
	A	1.4072	1.7801	1.5449	5.5551×10^{-1}	2.0551×10^{-1}	2.6667×10^{-2}	1.7792×10^{-2}	1.1329×10^{-2}	1.0002×10^{-2}
	ΔS	-104.7972	-104.3301	-104.6117	-106.6441	-108.6199	-112.6775	-113.4815	114.3784	-114.6260
	γ	0.9625	0.9659	0.9546	0.9667	0.9771	0.9568	0.9568	0.9474	0.9509
III Stage	E	4.7744	5.9825	7.4838	6.3826	3.2430	3.2430	3.2444	2.7162	3.1112
	A	1.9010×10^{-2}	3.8910×10^{-2}	4.5558×10^{-2}	1.3839×10^{-2}	1.0271×10^{-2}	5.1357×10^{-3}	3.4282×10^{-3}	2.3451×10^{-3}	2.6037×10^{-3}
	ΔS	-113.6576	-112.2314	-111.9180	-114.2855	-114.8780	-116.2552	-116.8596	-117.8127	-117.6049
	γ	0.9678	0.9754	0.9814	0.9755	0.9701	0.9700	0.9700	0.9864	0.9890
IV Stage	E	8.8469	7.5178	12.3202	9.0671	7.5017	7.5005	12.1531	3.5078	4.6865
	A	6.0849×10^{-1}	1.5232×10^{-1}	2.4957	1.3996×10^{-1}	5.6109×10^{2}	2.5559×10^{-1}	6.8519	5.1753×10^{-3}	1.1734×10^{-2}
	ΔS	-107.0318	-109.7838	-104.2275	-109.9520	-107.3763	-108.7554	-102.2207	-116.5041	-114.8775
	γ	0.9686	0.9305	0.9581	0.9427	0.9583	0.9583	0.9128	0.9018	0.9296

*E in kCals mol^{-1}; A in s^{-1}; ΔS in eu.

TABLE II.4.6. Kinetic Parameters for the decomposition of Mn(II) and Co(II) complexes of vanillin-2-aminothiazole (L"H) from TG using Coats-Redfern equation and accepted mechanistic equation

Complex	Parameters	From Coats-Redfern equation	From mechanistic equation	Reaction mechanism	Order of reaction
$[Mn(L"H)_2Cl_2(H_2O)_2]$					
I Stage	E kCal/mole	5.6222	5.6222	Equation V	
	A sec^{-1}	2.0030×10^{-1}	2.0030×10^{-1}	F_1 mechanism	
	ΔS eu	-108.1436	-108.1436	Random nucleation	
	γ	0.9206	0.9235	Mampel equation	1
II Stage	E kCal/mole	4.9993	4.9991	Equation VIII	
	A sec^{-1}	2.9860×10^{-2}	2.4600×10^{-2}	R_2 mechanism	
	ΔS eu	-113.0972	-113.3499	Phase boundary reaction	1/2
	γ	0.9794	0.9794	Cylindrical symmetry	
$[Co(L"H)_2(OAc)_2(H_2O)_2]$					
I Stage	E kCal/mole	6.7233	6.7220	Equation VI	
	A sec^{-1}	3.1860×10^{-1}	1.8320×10^{-1}	A_2 mechanism	
	ΔS eu	-107.3542	-108.4539	Random nucleation	2/3
	r	0.9396	0.9417	Avrami equation I	
II Stage	E kCal/mole	1.3822	1.3788	Equation VII	
	A sec^{-1}	2.5092×10^{-4}	2.5582×10^{-4}	A_3 mechanism	
	ΔS eu	-122.0860	-122.0411	Random nucleation	2/3
	γ	0.9658	0.9657	Avrami equation II	
III Stage	So rapid that could not be studied				

TABLE II.4.7. **Kinetic Parameters for the decomposition of Ni(II) and Cu(II) complexes of vanillin-2-aminothiazole (L"H) from TG using Coats-Redfern equation and accepted mechanistic equations**

Complex	Parameters	From Coats-Redfern equation	From mechanistic equation	Reaction mechanism	Order of reaction
$[Ni"LH(OAc)_2(H_2O)_3]$					
I Stage	E kCal/mole	5.9284	5.9246	Equation VIII	
	A sec^{-1}	1.7353×10^{-1}	-8.6325×10^{-2}	R_2 mechanism	
	ΔS eu	-108.6243	-110.0117	Phase boundary reaction	1/2
	γ	0.9946	0.9947	Cylindrical symmetry	
II Stage	E kCal/mole	2.1171	2.1171	Equation V	
	A sec^{-1}	1.5066×10^{-3}	1.5066×10^{-3}	F_1 mechanism	
	ΔS eu	-118.8430	-118.8430	Random nucleation	1
	γ	0.9280	0.9280	Mampel equation	
III Stage	So rapid that could not be studied				
$[CuL"H(OAc)_2(H_2O)_3]$ I Stage	Weight loss is too small to carry out the kinetic study				
II Stage	E kCal/mole	2.2481	2.2481	Equation V	
	A sec^{-1}	2.2474×10^{-3}	2.2474×10^{-3}	F_1 mechanism	
	ΔS eu	-117.9890	-117.9890	Random nucleation	1
	γ	0.9615	0.9615	Mampel equation	
III Stage	So rapid that could not be studied.				

TABLE II.4.8. **Kinetic Parameters for the decomposition of Zn(II) complex of vanillin-2-aminothiazole (L"H) from TG using Coats-Redfern equation and accepted mechanistic equations**

Complex	Parameters	From Coats-Redfern equation	From mechanistic equation	Reaction mechanism	Order of reaction
$[ZnL"H(OAc)_2(H_2O)_3]$					
	E kCal/mole	3.4166	3.4166	Equation V	
	A sec^{-1}	$1.1501x10^{-2}$	$1.1501x10^{-2}$	F_1 mechanism	
I Stage	ΔS eu	-113.8599	-113.8599	Random nucleation	1
	γ	0.9460	0.9460	Mampel equation	
	E kCal/mole	5.8771	5.8771	Equation V	
II Stage	A sec^{-1}	$2.0551x10^{-1}$	$2.0551x10^{-1}$	F_1 mechanism	
	ΔS eu	-108.6199	-108.6199	Random nucleation	1
	γ	0.9771	0.9771	Mampel equation	
III State	E kCal/mole	2.7162	2.7162	Equation VIII	
	A sec^{-1}	$4.6905x10^{-3}$	$2.3451x10^{-3}$	R_2 mechanism	
	ΔS eu	-116.4353	-117.8127	Phase boundary reaction	1/2
	γ	0.9864	0.9864	Cylindrical symmetry	
IV Stage	E kCal/mole	8.0634	8.8469	Equation 1	
	A sec^{-1}	$6.3235x10^{-1}$	$6.0849x10^{-1}$	D_1 mechanism	
	ΔS eu	-106.0046	-107.0318	One dimensional diffusion	2/3
	γ	0.9783	0.9686		

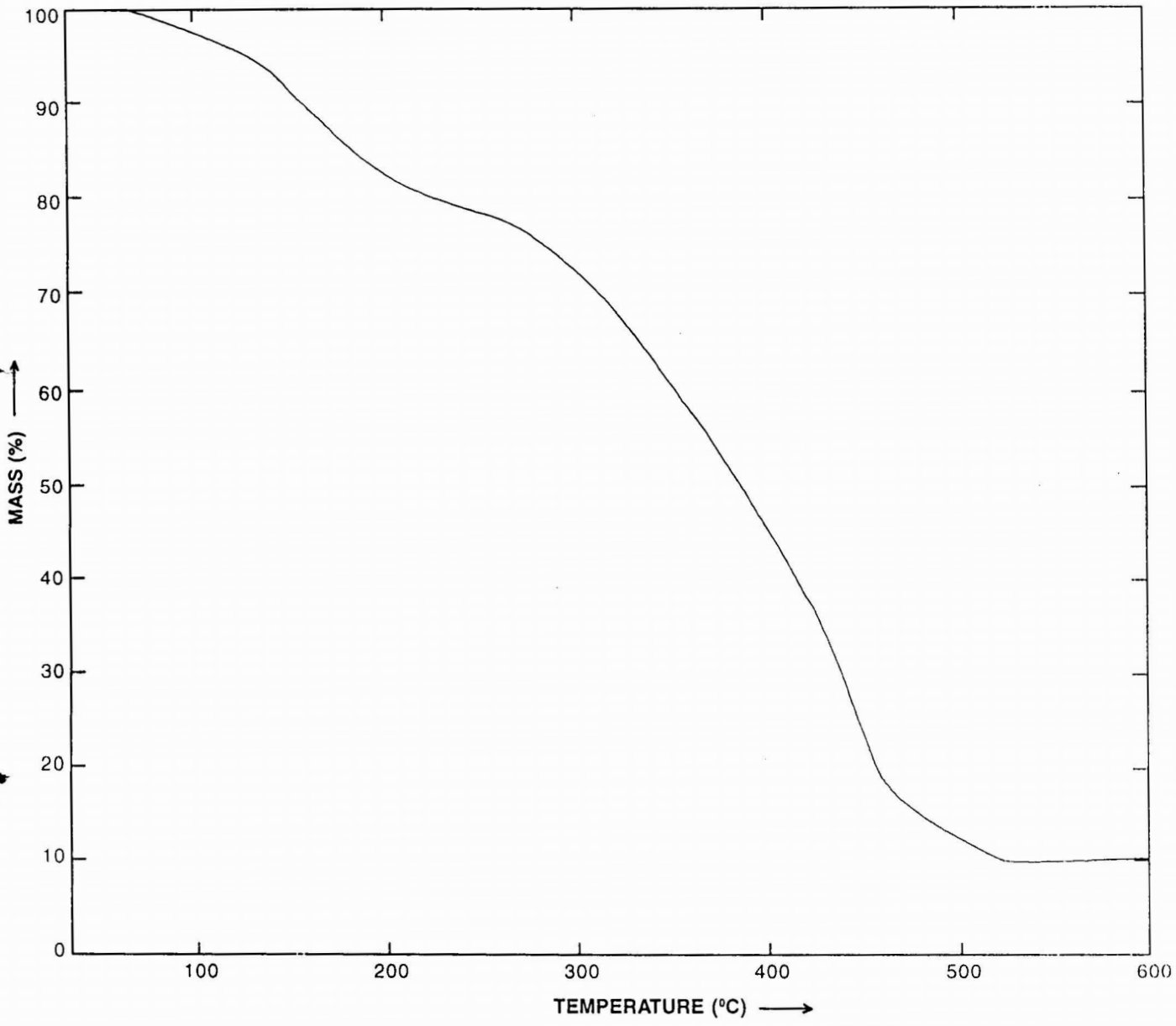

Figure II. 4.1 **TG Traces of [Mn $(L^{II}H)_2$ Cl_2 $(H_2O)_2$]**

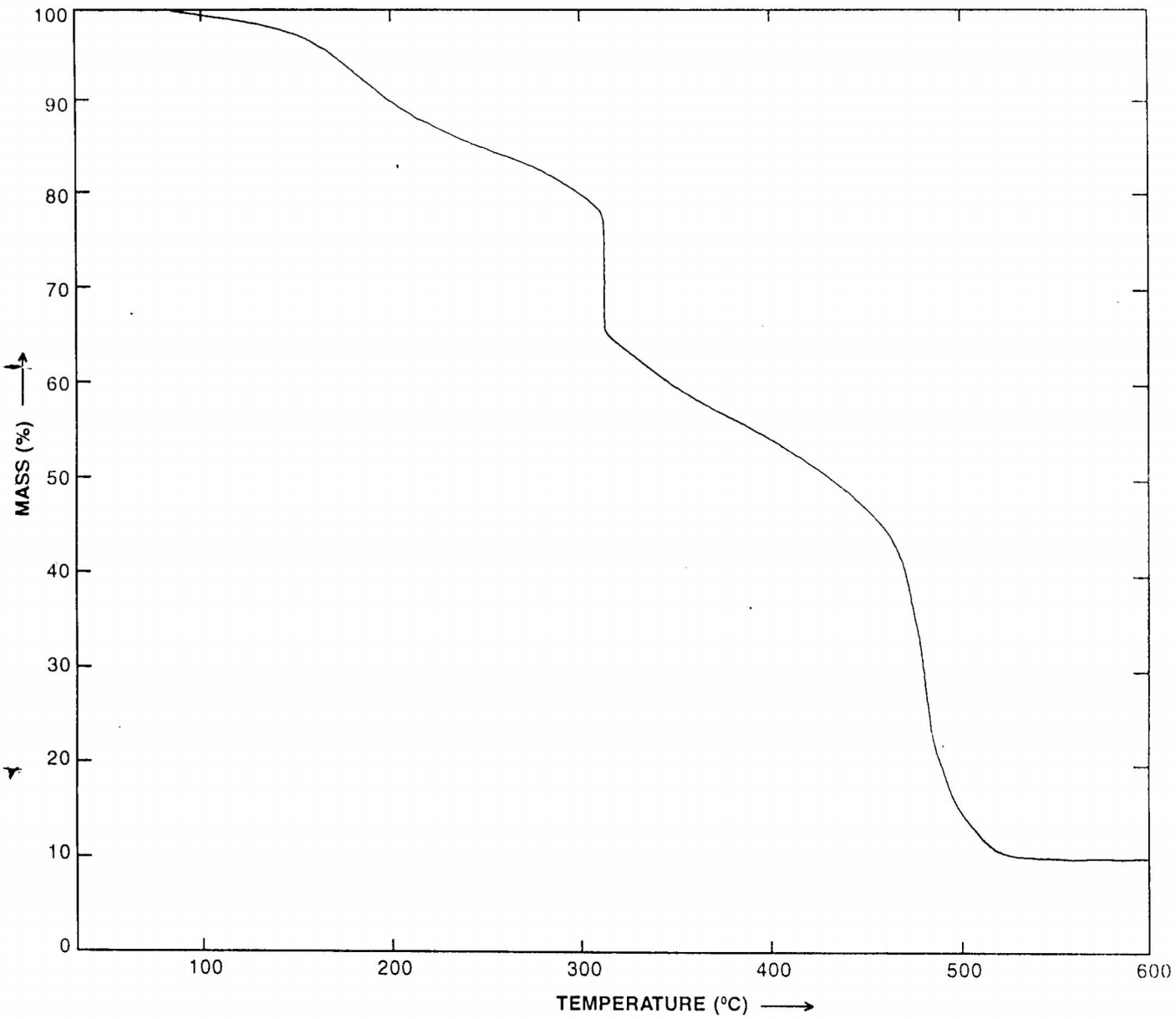

Figure II. 4.2 **TG Traces of [Co $(L^{II}H)_2$ $(OAc)_2$ $(H_2O)_2$]**

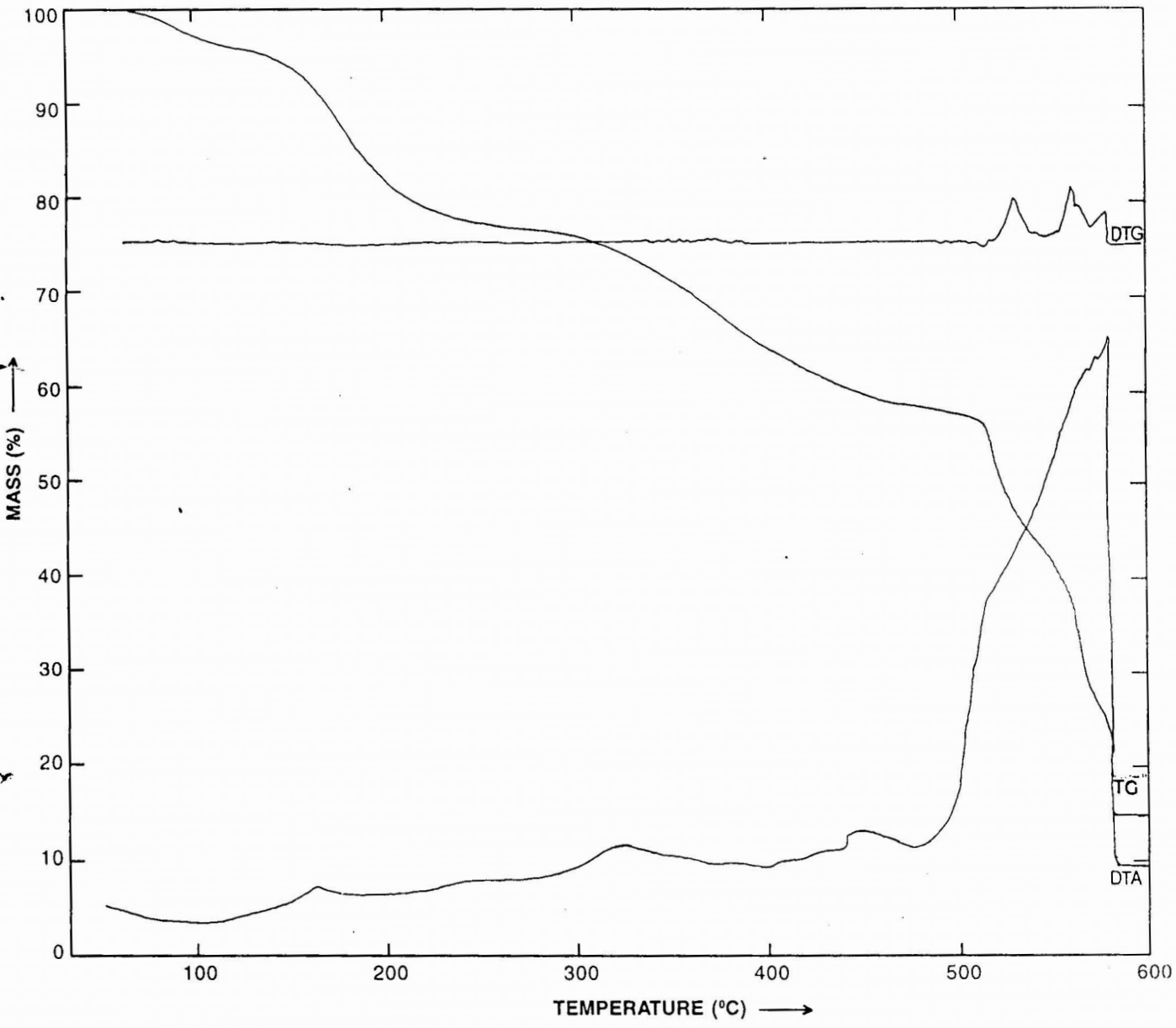

Figure II. 4.4 **TG, DTG and DTA Traces of** [Cu L^{II} H $(OAc)_2 (H_2O)_3$]

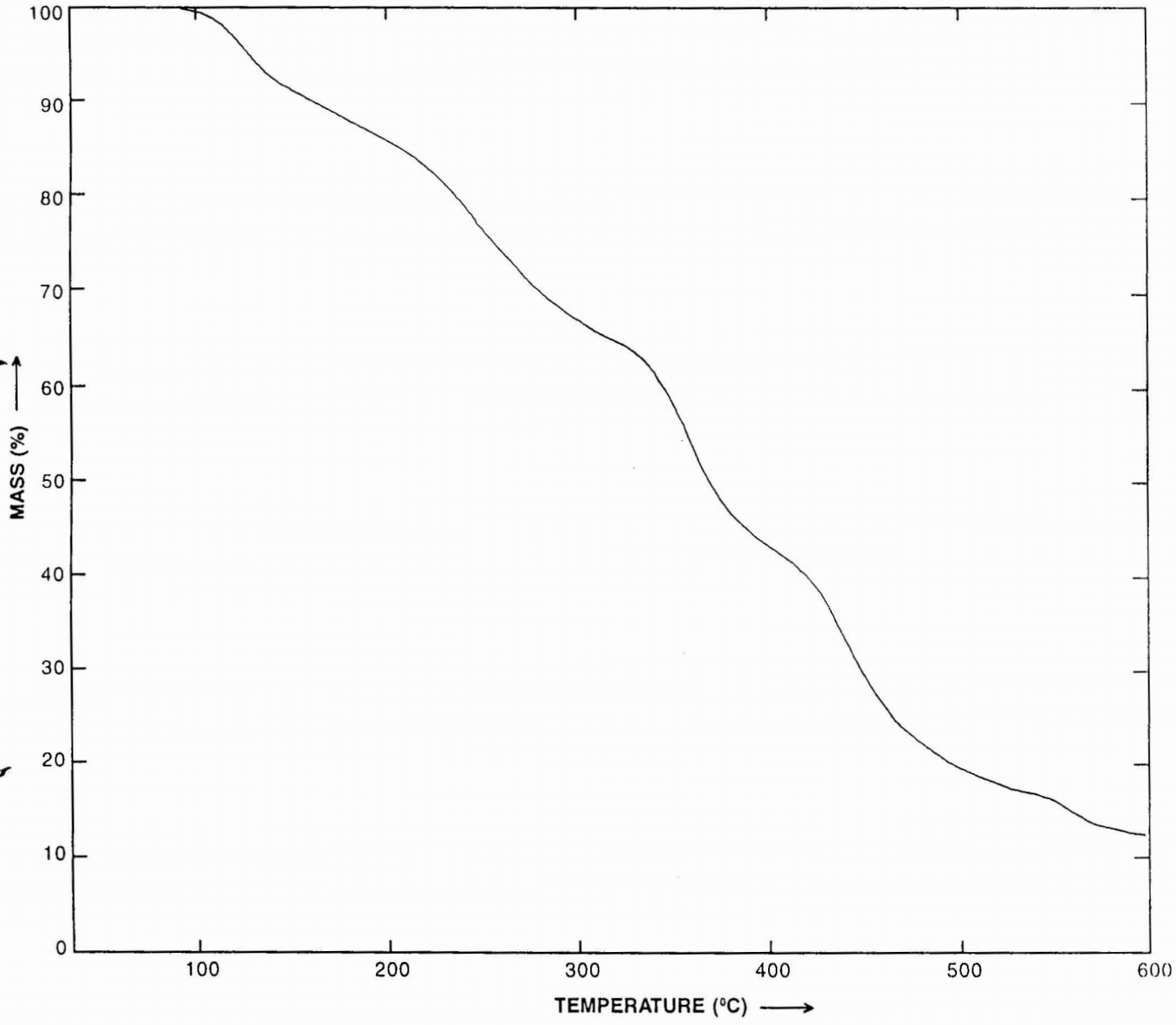

Figure II. 4.5 **TG Traces of [Zn L^{II} H $(OAc)_2$ $(H_2O)_3$]**

CHAPTER V

THERMAL DECOMPOSITION KINETICS OF Mn(II), Co(II), Ni(II), Cu(II), Zn(II) AND UO_2(II) COMPLEXES OF *o*-VANILLIN-2-AMINOPYRIDINE

The thermal behaviour of *o*-vanillin-2-aminopyridine complexes of Mn(II), Co(II), Ni(II), Cu(II), Zn(II) and UO_2(II) was studied by TG. The energy of activation, change in entropy and frequency factor of the various stages of decompositions of these complexes were calculated based on non-mechanistic Coats-Redfern and nine mechanistic equations.

Experimental

The method of preparation and characterization of the above mentioned complexes are given in Part I. The substance was taken in a platinum crucible and heated in static air atmosphere at a heating rate of 15°C min^{-1}.

Treatment of data

The typical TG curves in which mass is plotted against temperature are shown in Figures II.5.1 - II.5.6. The temperature ranges in which decomposition of the complexes take place are given in Tables II.5.1 - II.5.2. Data from independent pyrolytic experiments are also included in these Tables. These tables also summarise the probable assignments for the various stages of decomposition of these complexes. The kinetic parameters n, E, A and ΔS ae calculated and the results are given in Tables II.5.3 - II.5.8.

RESULTS AND DISCUSSION

The TG curve of $[MnL(H_2O)_4]$ Cl gives a two-stage decomposition pattern. The first stage, represents the loss of $4H_2O$ molecules and the *o*-vanillin part of the ligand moiety. According to Nikolaev *et al.*[185], water eliminated above 150°C can be considered as coordinated water. The second stage represents the loss of aminopyridine part and chlorine. The overall loss of mass from the curve is 78% while the theoretical loss in mass for the conversion of $[MnL'''(H_2O)_4]Cl$ to Mn_3O_4 is 82.10%.

$[CoL'''OAc(H_2O_3]$ also gives a two-stage decomposition pattern in it's TG curve. The first stage, which is a rapid one, represents the loss of $3H_2O$ molecules and the acetate group . Since water is eliminated above 150°C, it can be considered as coordinated water. The second stage represents the loss of ligand moiety. The overall mass loss from the curve is 83% while the theoretical loss in mass for the conversion of $[CoL'''OAc(H2O)_3]$ to Co_3O_4 is 80.02%.

In the case of $[NiL'''OAc(H_2O)_3]$, $[CuL_2'''(H_2O)_2]$, $[ZnL'''OAc(H_2O)_3]$ and $[UO_2L'''(H_2O)2]NO_3$ chelates, a three stage decomposition pattern is observed. These four complexes lose one to three water molecules in the first stage at about 165°C. Acetate group is lost in the second stage of $[NiL'''OAc(H_2O)_3]$. While the *o*-vanillin part of the ligand moiety is lost in the second stage of $[CuL_2'''(H_2O)_2]$, $[ZnL'''OAc(H_2O)_3]$ and $[UO_2L'''(H_2O)2]NO_3$.

In the third stage ligand moiety is eliminated in $[NiL'''OAc(H_2O)_3]$; *o*-vanillin part of the ligand and acetate group are eliminated in

$[ZnL'''OAc(H_2O)_3]$ and amino pyridine part of the ligand is eliminated in $[CuL_2'''(H_2O)_2]$, and $[UO_2L'''(H_2O)_2]NO_3$. The mass loss at the end of this stage as read from the TG curve is 83%, 86%, 79% and 54.5% for Ni(II), Cu(II), Zn(II) and UO_2(II) complexes respectively.

The initial decomposition temperature of complexes indicated the stability order as $[ZnL'''OAc(H_2O)_3] < [CuL_2'''(H_2O)_2] \approx [UO_2L'''(H_2O)_2]NO_3 < [CoL'''OAc(H_2O)_3] < [NiL'''OAc(H_2O)_3] < [MnL'''(H_2O)_4]$ Cl.

Decomposition kinetics

From the Tables II.5.3 - II.5.5, it can be seen that more than one equation gives good linear curves with high correlation coefficient. It thus becomes difficult to assign the reaction mechanism unequivocally from the linearity of the curve alone. In such cases, some authors have chosen the function $g(\alpha)$ which gives the kinetic parameters in agreement with those obtained by numerical method.

In the present case it is observed that the order of decomposition is 1/2 for the third stage of $[CuL_2'''(H_2O)_2]$ and the second stage of $[ZnL'''OAc(H_2O)_3]$. Of these $[CuL_2'''(H_2O)_2]$ followed D_1 mechanism based on one dimensional diffusion and $[ZnLOAc(H_2O)_3]$ followed A_2 mechanism based on Random nucleation.

Second stage decomposition of $[CoL'''OAc(H_2O)_3]$ and $[UO_2L'''(H_2O)_2]NO_3$ also followed A_2 mechanism based on Random nucleation. First stage decomposition of $[NiL'''OAc(H_2O)_3]$ is according to A_2 mechanism based on Random nucleation. R_3 mechanism based on phase boundary reaction with cylindrical symmetry is observed in the first

TABLE II.5.1. **Thermal decomposition data of Mn(II), Co(II) and Ni(II) complexes of *o*-vanillin-2-aminopyridine (L"'H)**

Complex	Stage	Temp. range in TG (°C)	Peak temp. in TG (°C)	Loss of mass (%)			Probable assignment
				From TG	Theo-retical	From Pyrolysis	
$[MnL'''(H_2O)_4]Cl$	I	190 - 410	350	50.00	53.45	--	Loss of $4H_2O$ + vanillin part
	II	410 - 520	470	28.00	28.65	--	Loss of 2-aminopyridine part + chlorine
				78.00	82.10	80.99	
$[CoL'''OAc(H_2O)_3]$	I	120 - 330	280	26.00	28.33	--	Loss of $3H_2O$ + acetate
	II	330 - 380	340	57.00	51.69	--	Loss of L
				83.00	80.02	80.48	
$[NiL'''OAc(H_2O)_3]$	I	160 - 200	180	14.00	13.50	--	Loss of $3H_2O$
	II	210 - 310	240	13.50	14.70	--	Loss of acetate
	IIII	320 - 420	380	55.50	53.02	--	Loss of L
				83.00	81.22	82.66	

TABLE II.5.2. **Thermal decomposition data of Cu(II), Zn(II) and UO_2(II) complexes of *o*-vanillin-2-aminopyridine (L'''H)**

Complex	Stage	Temp. range in TG (°C)	Peak temp. in TG (°C)	Loss of mass (%)			Probable assignment
				From TG	Theoretical	From Pyrolysis	
$[CuL_2'''(H_2O)_2]$	I	110-160	160	6.50	6.50	--	Loss of $2H_2O$
	II	160-280	280	47.00	49.09	--	Loss of 2(vanillin part)
	III	290-410	340	32.50	30.36	--	Loss of 2(aminopyridine part)
				86.00	85.95	86.20	
$[ZnL'''OAc(H_2O)_3]$	I	90 - 180	170	13.00	13.30	--	Loss of $3H_2O$
	II	190 - 370	270	31.00	33.58	--	Loss of vanillin part
	III	370 - 450	430	35.00	33.33	--	Loss of aminopyridine part + acetate
				79.00	80.21	80.68	
$[UO_2L'''(H_2O)_2]NO_3$	I	110 - 190	190	3.50	3.10	--	Loss of $1H_2O$
	II	210 - 480	320	24.00	23.57	--	Loss of vanillin part
	III	480 - 520	500	27.00	23.93	--	Loss of aminopyridine part
				54.50	50.60	51.80	

TABLE II.5.3. **Kinetic parameters for the decomposition of Mn(II), Co(II) and Ni(II) complexes of *o*-vanillin-2-aminopyridine (L"'H) from TG using using mechanistic equations**

Complex	Para-meter*	Mechanistic equations								
		1	2	3	4	5	6	7	8	9
$[MnL'''HCl(H_2O)_4]Cl$	E	42.8111	45.8615	48.8655	51.0560	56.1498	24.8566	56.1520	51.6656	53.2880
	A	2.9035×10^{17}	5.3943×10^{18}	2.5613×10^{19}	2.7908×10^{18}	4.3883×10^{17}	9.7268×10^{16}	1.4656×10^{17}	4.5844×10^{15}	1.2395×10^{16}
I Stage	ΔS	-25.8520	-20.0460	-16.9507	-21.3554	-25.0313	-28.0250	-27.2104	-34.0949	-32.1186
	γ	0.9001	0.9071	0.9060	0.9041	0.9627	0.9627	0.9627	0.9670	0.9640
II Stage	So rapid that could not be studied									
$[CoL'''OAc(H_2O)_3]$	So rapid that could not be studied									
I stage										
	E	6.2350	6.7228	7.2518	6.8889	.7375	2.7395	2.7403	2.3375	2.4676
	A	3.9001×10^{-2}	3.5502×10^{-2}	1.4900×10^{-2}	9.6790×10^{-3}	3.5207×10^{-3}	1.7645×10^{-3}	1.7775×10^{-3}	9.8123×10^{-4}	7.9293×10^{-4}
II Stage	ΔS	-112.03	-112.2158	-113.9343	-114.7981	-116.8075	-118.1801	-118.9838	-119.3461	-119.7695
	γ	0.9895	0.9902	0.9909	0.9903	0.9826	0.9828	0.9829	0.9790	0.9802
$[NiL'''OAc(H_2O)_3]$	E	53.0038	40.1517	52.8931	39.8096	25.9158	25.8646	25.8650	25.3939	25.5446
	A	5.4445×10^{21}	1.8096×10^{15}	5.8587×10^{20}	1.4135×10^{8}	3.6010×10^{9}	1.7001×10^{9}	1.1002×10^{9}	9.6500×10^{8}	7.7001×10^{8}
I Stage	ΔS	-5.6687	-35.2313	-10.0207	-52.6654	-61.3920	-62.8800	-63.7500	-64.0100	-64.4600
	γ	0.9464	0.9148	0.9517	0.9066	0.9491	0.9493	0.9493	0.9479	0.9484
	E	5.7544	6.1488	6.5700	6.2964	2.4458	2.4462	2.4460	2.1269	2.2318
	A	3.7801×10^{-2}	3.2280×10^{-2}	1.2600×10^{-2}	8.7186×10^{-3}	3.2152×10^{-3}	1.6081×10^{-3}	1.0720×10^{-3}	9.5940×10^{-4}	7.5908×10^{-4}
II Stage	ΔS	-111.8710	-112.1800	-114.0512	-114.7827	-116.7682	-118.1431	-118.9566	-119.1716	-119.6471
	γ	0.9716	0.9731	0.9747	0.9747	0.9516	0.9516	0.9516	0.9430	0.9461

*E in kCals mol^{-1}; A in s^{-1}; ΔS in eu.

TABLE II.5.4. **Kinetic parameters for the decomposition of Cu(II) and Zn(II) complexes of *o*-vanillin-2-aminopyridine (L"'H) from TG using mechanistic equations**

Complex	Para-meter*	Mechanistic equations								
		1	2	3	4	5	6	7	8	9
$[CuL_2'''(H_2O)_2]$ I Stage		So rapid that could not be studied.								
II Stage		So rapid that could not be studied.								
III Stage	E	4.0966	5.7261	11.2546	7.4010	8.1209	8.1766	8.1208	3.0238	4.4084
	A	2.9443×10^{-2}	1.2301×10^{-1}	9.7376	1.7290×10^{-1}	4.6781	2.4415	1.5592	7.7216×10^{-3}	2.7501×10^{-2}
	ΔS	-112.7216	-109.8807	-101.1944	-109.2041	-102.6511	-103.9432	-104.8343	-115.3811	-112.8572
	γ	0.9887	0.9824	0.9965	0.9919	0.9875	0.9780	0.9876	0.9896	0.9946
$[ZnL'''OAc(H_2O)_3]$ I Stage	E	20.6886	20.9983	21.2653	21.2147	10.0478	10.0479	10.0481	9.8100	9.8891
	A	6.5263×10^{7}	5.1423×10^{7}	1.6752×10^{7}	1.5441×10^{7}	2.5355×10^{6}	1.2653×10^{6}	8.4428×10^{5}	7.7860×10^{5}	6.0980×10^{5}
	ΔS	-69.0280	-69.5019	-71.7305	-71.8924	-75.4843	-76.8633	-77.6672	-77.8281	-78.3137
	γ	0.9099	0.9108	0.9108	0.9100	0.9843	0.9843	0.9843	0.9838	0.9840
II Stage	E	6.7570	7.4302	8.1972	7.7080	3.3972	3.3974	3.3974	2.8174	3.0055
	A	1.6037×10^{-1}	1.8910×10^{-1}	1.0910×10^{-1}	5.9101×10^{-2}	1.3602×10^{-2}	6.8116×10^{-3}	4.5413×10^{-3}	2.9512×10^{-3}	2.5895×10^{-3}
	ΔS	-109.1126	-108.7854	-109.8778	-111.0955	-114.0126	-115.3893	-116.1948	-117.0512	-117.3111
	γ	0.9579	0.9624	0.9668	0.9644	0.9474	0.9475	0.9475	0.9323	0.9380
III Stage	E	4.8898	6.4407	8.4714	7.1085	3.9949	3.9955	3.9945	2.4011	2.8996
	A	2.0580×10^{-2}	5.7142×10^{-2}	1.0424×10^{-1}	2.5631×10^{-2}	2.1784×10^{-2}	1.0898×10^{-2}	7.2582×10^{-3}	1.5630×10^{-3}	1.9733×10^{-3}
	ΔS	-113.7055	-111.6762	-110.4818	-113.2693	-113.5925	-114.9686	-115.7763	-118.8273	-118.3642
	γ	0.8638	0.8725	0.8765	0.8741	0.8106	0.8106	0.8105	0.7597	0.7818

*E in kCals mol^{-1}; A in s^{-1}; ΔS in eu.

TABLE II.5.5. **Kinetic parameters for the decomposition of UO_2(II) complex of *o*-vanillin-2-aminopyridine (L"'H) from TG using mechanistic equations**

Complex	Para-meter*	Mechanistic equations								
		1	2	3	4	5	6	7	8	9
$[UO_2L'''(H_2O)_2]NO_3$ I Stage	Weight loss is too small to carry out the kinetic study.									
II Stage	E	8.2317	8.7295	9.2924	8.9194	3.7286	3.7463	3.7461	3.3225	3.4600
	A	1.4899×10^{-1}	1.3229×10^{-1}	5.5761×10^{-2}	3.6520×10^{-2}	7.8848×10^{-3}	4.0098×10^{-3}	2.6725×10^{-3}	2.2966×10^{-3}	1.8373×10^{-3}
	ΔS	-109.6300	-109.8616	-111.5782	-112.4191	-115.4651	-116.8088	-117.6149	-117.9161	-118.3595
	γ	0.9937	0.9948	0.9950	0.9950	0.9906	0.9915	0.9915	0.9903	0.9909
II Stage	So rapid that cold not be studied									

*E in kCals mol^{-1}; A in s^{-1}; ΔS in eu.

TABLE II.5.7. **Kinetic Parameters for the decomposition of Cu(II) and Zn(II) complexes of *o*-vanillin-2-aminopyridine (L"'H) from TG using Coats-Redfern equation and accepted mechanistic equation**

Complex	Parameters	From Coats-Redfern equation	From mechanistic equation	Reaction mechanism	Order of reaction
$[CuL_2'''(H_2O)_2]$ I Stage	So rapid that could not be studied				
II Stage	So rapid that could not be studied				
III Stage	E kCal/mole	3.0237	2.9443×10^{-2}	Equation I	
	A sec^{-1}	2.3034×10^{-2}	2.9443×10^{-2}	D_1 mechanism	1/2
	ΔS eu	-113.2093	-113.3250	One-dimensional diffusion	
	γ	0.9896	0.9887		
$[ZnL'''OAc(H_2O)_3]$ I Stage	E kCal/mole	9.8891	9.8891	Equation IX	
	A sec^{-1}	6.2812×10^{5}	6.0980×10^{5}	R_3 mechanism	
	ΔS eu	-78.1158	-78.3137	Phase boundary reaction	2/3
	γ	0.9840	0.9840	Spherical symmetry	
II Stage	E kCal/mole	2.8172	3.3974	Equation VI	
	A sec^{-1}	5.9012×10^{-3}	6.8116×10^{-3}	A_2 mechanism	
	ΔS eu	-115.6744	-115.3893	Random nucleation	1/2
	γ	0.9323	0.9475	Avrami equation I	
III Stage	E kCal/mole	3.9949	3.9949	Equation V	
	A sec^{-1}	2.1784×10^{-2}	2.1784×10^{-2}	F_1 mechanism	
	ΔS eu	-113.5925	-113.5925	Random nucleation	1
	γ	0.8106	0.8106	Mampel equation	

TABLE II.5.8. **Kinetic Parameters for the decomposition of UO_2(II) complex of *o*-vanillin-2-aminopyridine (L'''H) from TG using Coats-Redfern equation and accepted mechanistic equation**

Complex	Parameters	From Coats-Redfern equation	From mechanistic equation	Reaction mechanism	Order of reaction
$[UO_2L'''(H_2O)_2]NO_3$ I Stage	Weight loss is too small to carry out the kinetic study.				
II Stage	E kCal/mole A sec^{-1} ΔS eu γ	3.6612 4.3293×10^{-3} -116.6564 0.9910	3.7463 4.0098×10^{-3} -116.8088 0.9915	Equation VI A_2 mechanism Random nucleation Avrami equation 1	2/3
III Stage	So rapid that could not be studied.				

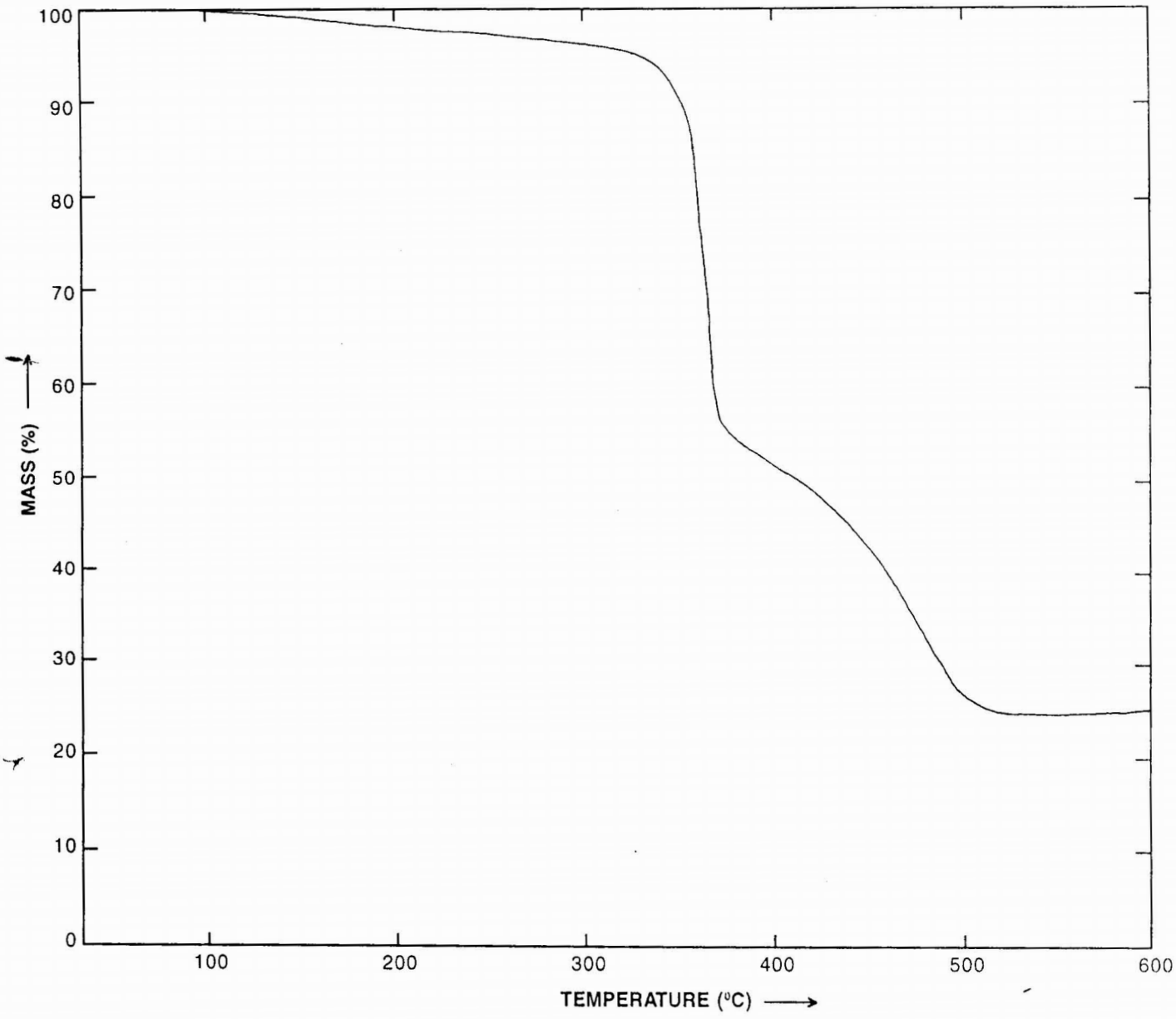

Figure II. 5.1 **TG Traces of [Mn L^{III} $(H_2O)_4$] Cl**

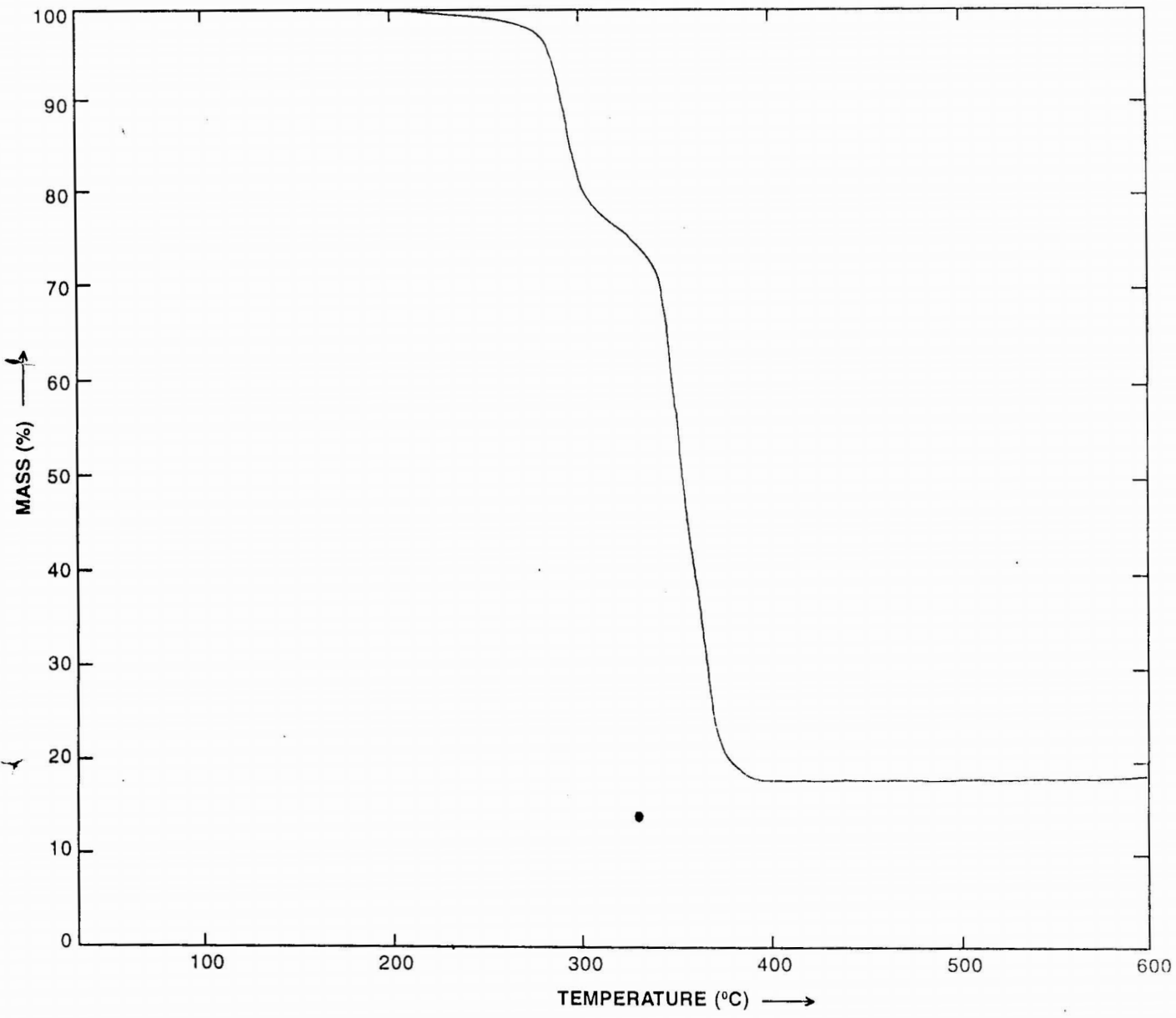

Figure II. 5.2 **TG Traces of [Co L^{III} OAc $(H_2O)_3$]**

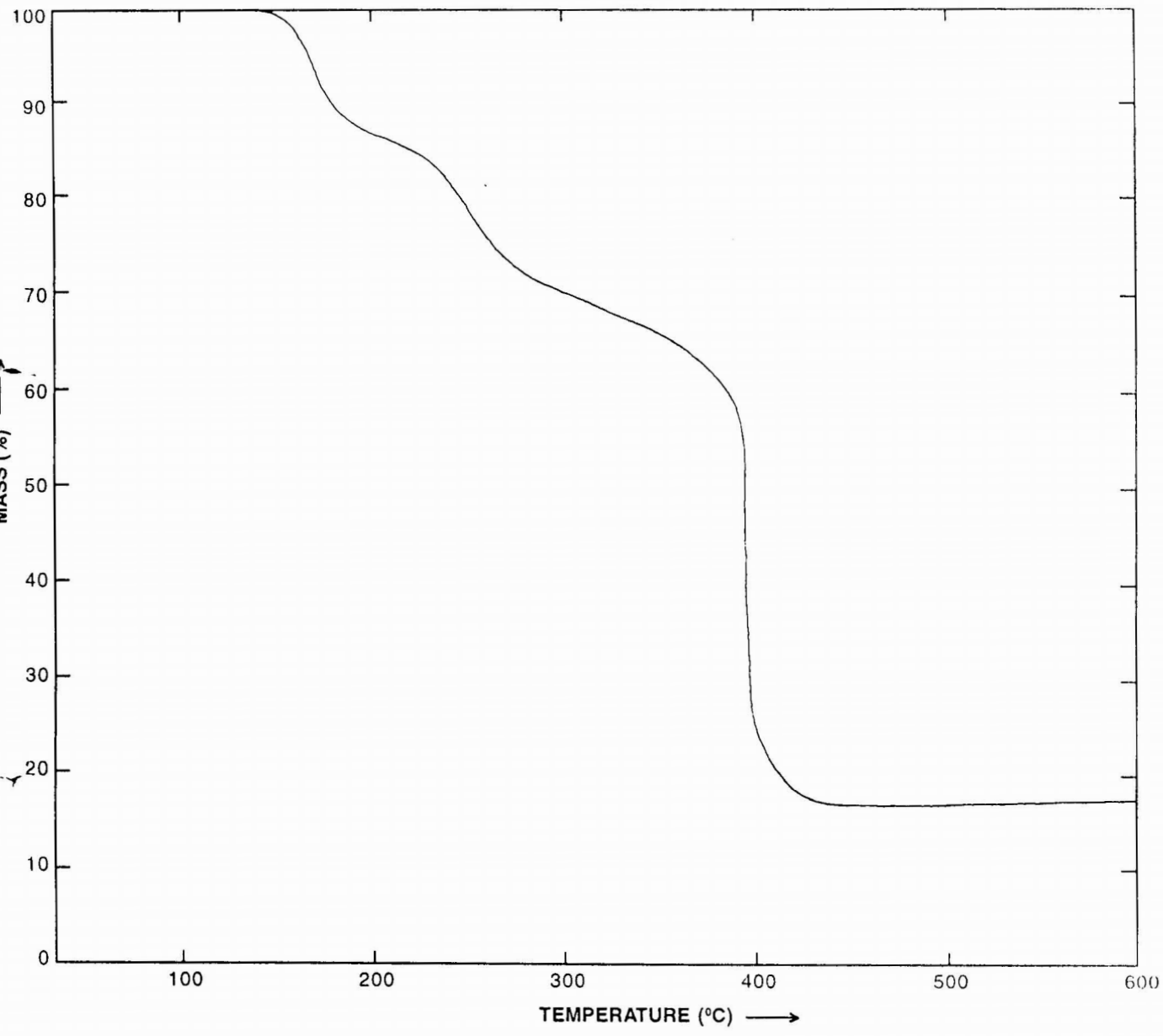

Figure II. 5.3 **TG Traces of [Ni L^{III} OAc $(H_2O)_3$]**

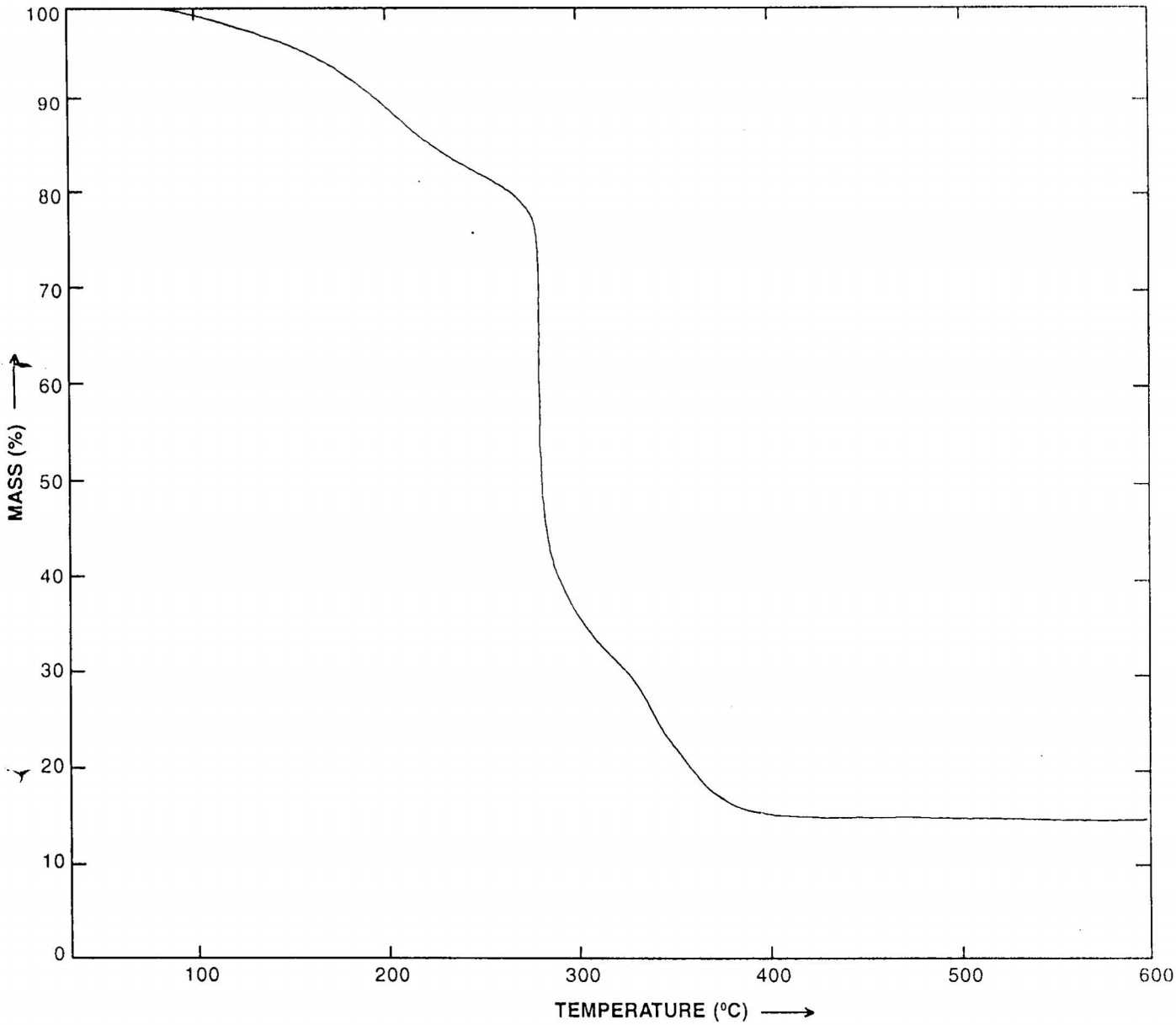

Figure II. 5.4 **TG Traces of [Cu L_2^{III} $(H_2O)_2$]**

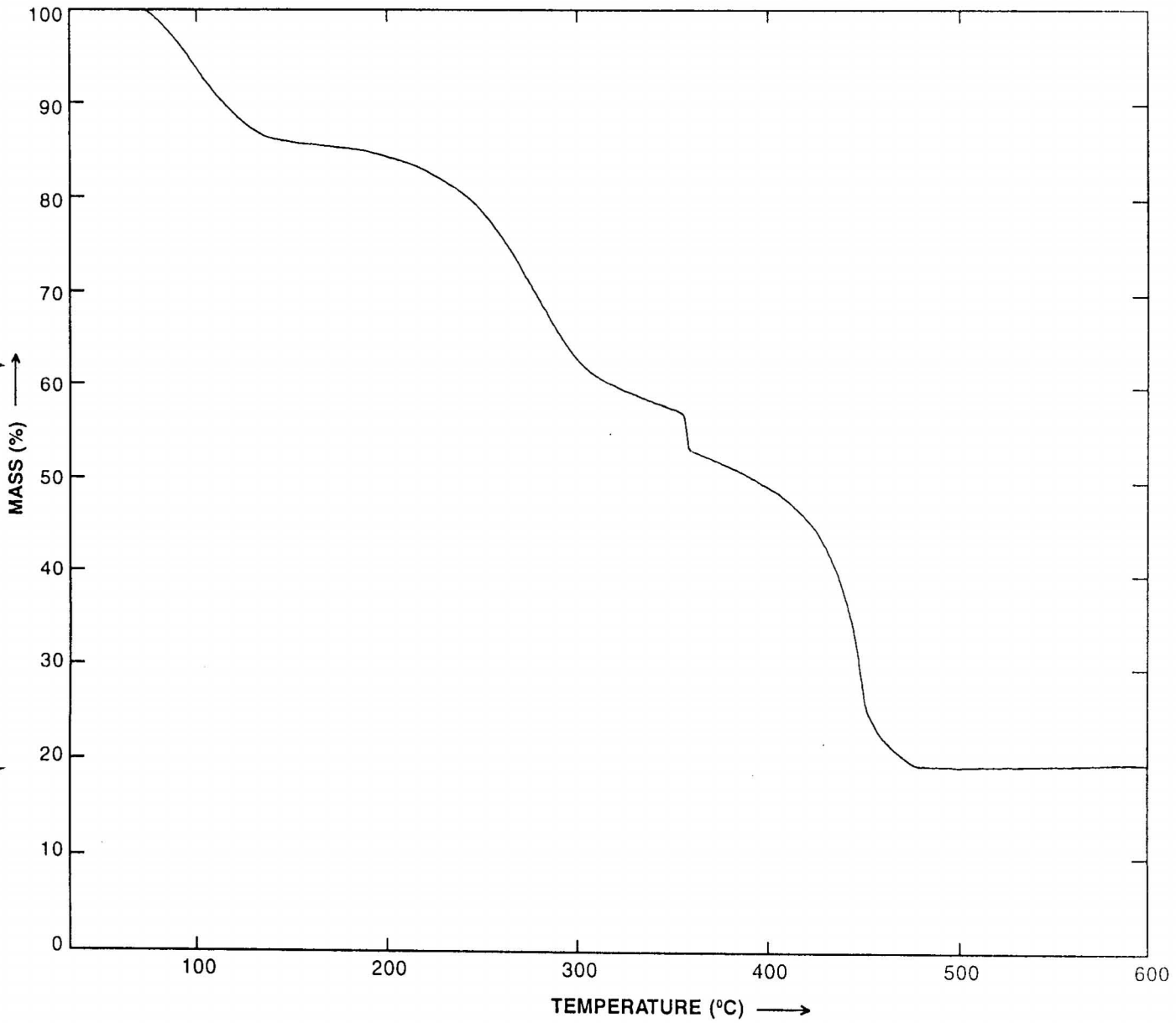

Figure II. 5.5 **TG Traces of [Zn L^{III} OAc $(H_2O)_3$]**

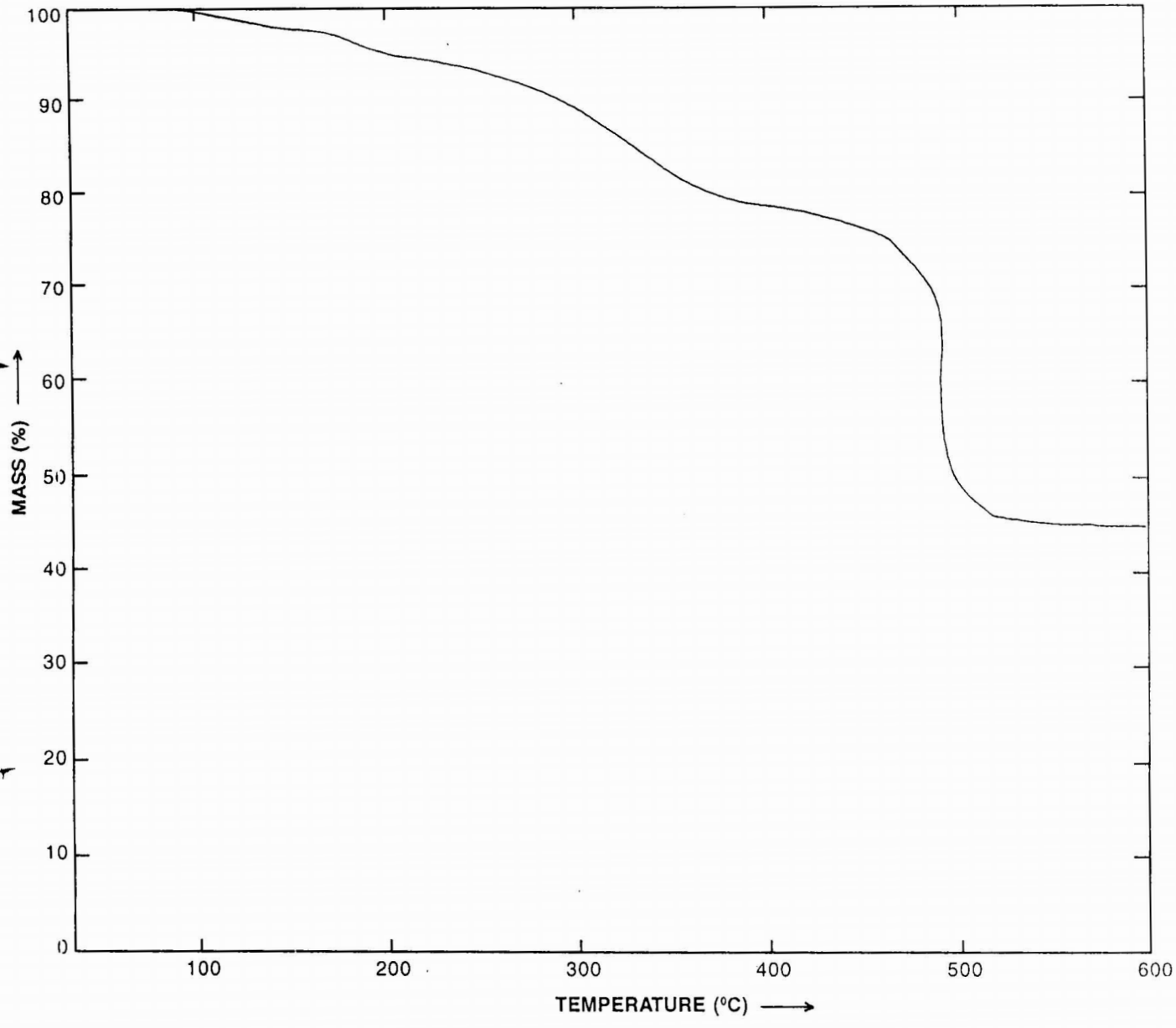

Figure II. 5.6 **TG Traces of $[UO_2 L^{III} (H_2O)_2] NO_3$**

CHAPTER VI

THERMAL DECOMPOSITION KINETICS OF Mn(II), Co(II), Ni(II), Cu(II) AND Zn(II) COMPLEXES OF *o*-VANILLIN-2-AMINOTHIAZOLE

This chapter deals with the thermal decomposition kinetics of Mn(II), Co(II), Ni(II), Cu(II) and Zn(II) chelates of *o*-vanillin-2-aminothiazole. Kinetic parameters are calculated using various mechanistic and non-mechanistic equations. Mechanism of decomposition of these complexes are also interpreted.

Experimental

Preparation and characterisation of the metal complexes are given in Part I. The substance heated in a platinum crucible in an atmosphere of static air at a rate of 15^{o} $min.^{-1}$

Treatment of data

The thermograms recorded were used as such and are shown in figures II.6.1 - II.6.5. Decomposition temperature ranges for this metal chelates are given in Table II.6.1. Data from independent pyrolytic experiments are also included in this Table. The kinetic parameters calculated from TG data for the nine mechanistic equations are given in Tables II.6.2 - II.6.4. The corresponding values of E, A, ΔS and γ from Coats-Redfern and the mechanistic equations suggested are given in Tables II.6.5 - II.6.7.

RESULTS AND DISCUSSION

Metal percentage from independent pyrolytic experiments and from thermal studies were found to be agreeable with the calculated values. The thermal data have supported the structure of complexes as $[ML^{IV}X(H_2O)_3]$ where M = Mn(II), Co(II), Ni(II), Cu(II) and Zn(II) and L, the deprotonated ligand as proposed by the physicochemical studies X stands for Cl for Mn(II) chelate and OAc for the rest of the complexes.

$[MnL^{IV}Cl(H_2O)_3]$ decomposed in two stages of which first one is attributed to the loss of three water molecules and *o*-vanillin part of the ligand while the second to loss of aminothiazole part of the ligand along with the chlorine atom.

The TG curve of $[Co^{IV}OAc(H_2O)_3]$ gave a two stage decomposition pattern which is supported by the DTA and DTG pattern. The first stage, represents the loss of three water molecules and the second stage, the loss of ligand part and acetate group.

Ni(II) complex exhibited three stage decomposition pattern. Stage I stands for the removal of three coordinated water molecules and stage II, the loss of acetate group and aminothiazole part of the ligand. Since water is eliminated above 150°C it can be considered as coordinated water[185].

Cu(II) and Zn(II) complexes of o-VAAT show two stage decomposition pattern. In the case of Cu(II) complex, first stage represents the loss of three coordinated water molecules and the acetate group. The second stage is assigned to the loss of ligand part. First stage of Zn(II) complex represents the loss of three coordinated water and vanillin part of

the ligand while the second stage stands for the removal of aminothiazole part of the ligand and acetate group.

The total mass loss considerations and X ray diffraction pattern confirmed the final products as the respective oxides. The final products of decomposition of all the five complexes were found to be Mn_3O_4, Co_3O_4, NiO, CuO and ZnO.

The thermal decomposition studies of all the above five complexes were found to follow the thermal stability order as

$[MnL^{IV}Cl(H_2O)_3] \approx [NiL^{IV}OAc(H_2O)_3] < [CoL^{IV}OAc(H_2O)_3] < [CuL^{IV}OAc(H_2O)_3] \approx [ZnL^{IV}OAc(H_2O)_3]$

Decomposition kinetics

The summarised data of kinetic parameters like energy of activation E, entropy of activation ΔS and Arrhenius frequency factor A, represented in Tables II.6.3 - II.6.7.

Order of the reaction is found to be 1/2 for the second thermal decomposition step of $[CoL^{IV}OAc(H_2O)_3$ which is based on D_1 mechanism with one dimensional diffusion. First thermal decomposition of $[ZnL^{IV}OAc(H_2O)_3]$ based on R_2 mechanism on phase boundary reaction also follows the same order of the reaction 1/2.

Maximum correlation between the R_3 mechanism based on phase boundary reaction, spherical symmetry and the Coats-Redfern equation with n=2/3 is observed for the first stage decomposition of $[CoL^{IV}OAc(H_2O)_3]$, third stage decomposition of $[NiL^{IV}OAc(H_2O)_3$ and

second stage decomposition of $[ZnL^{IV}OAc(H_2O)_3]$. Second stage decomposition of Ni(II) complex based on A_2 mechanism with Random nucleation also follows 2/3 order of the reaction.

First order reaction is observed in the first stage decomposition of $[MnL^{IV}Cl(H_2O)_3]$ and first and second stage decomposition of $[CuL^{IV}OAc(H_2O)_3]$. All the decomposition stages followed F_1 mechanism based on Mampel equation, the rate controlling process being random nucleation, by the formation of a nucleus on each particle. The negative values of ΔS indicate that the activated complexes have a more ordered structure than the reactants and the reactions are slower than the normal.

TABLE II.6.1. **Thermal decomposition data of Mn(II), Co(II), Ni(II), Cu(II) and Zn(II) complexes of *o*-vanillin-2-aminothiazole ($L^{IV}H$)**

Complex	Stage	Temp. range in TG (°C)	Peak temp. in TG (°C)	Loss of mass (%)			Probable assignment
				From TG	Theo-retical	From Pyrolysis	
$[MnL^{IV}Cl(H_2O)_3]$	I II	90-510 510-540	340 540	50.00 30.00	50.00 30.20	-- --	Loss of $3H_2O$ + vanillin part Loss of aminothiazol part + Chlorine
				80.00	80.20	79.80	
$[CoL^{IV}OAc(H_2O)_3]$	I II	110-310 310-580	210 580	11.00 71.00	13.32 67.00	-- --	Loss of $3H_2O$ Loss of ligand part + acetate
				82.00	80.00	80.77	
$[NiL^{IV}OAc(H_2O)_3]$	I II III	90-200 200-390 390-540	170 320 400	11.00 44.00 27.00	13.30 39.30 29.60	-- -- --	Loss of $3H_2O$ Loss of acetate + aminothiazole part Loss of vanillin part
				82.00	82.20	81.52	
$[CuL^{IV}OAc(H_2O)_3]$	I II	120-330 330-690	310 430	25.00 56.00	27.50 53.00	-- --	Loss of $3H_2O$+ acetate Loss of ligand part
				81.00	80.50	80.25	
$[ZnL^{IV}OAc(H_2O)_3]$	I II	120-380 380-600	380 590	48.00 34.00	46.20 34.80	-- --	Loss of $3H_2O$+ vanillin part Loss of aminothiazole part + acetate
				82.00	81.00	80.8	

TABLE II.6.2. **Kinetic parameters for the decomposition of Mn(II) and Co(II) complexes of *o*-vanillin-2-aminothiazole ($L^{IV}H$) from TG using mechanistic equations**

Complex	Para-meter*	Mechanistic equations								
		1	2	3	4	5	6	7	8	9
$[MnL^{IV}Cl(H_2O)_3]$	E	11.7533	12.9656	14.8232	13.3566	6.5072	6.5078	6.5082	5.4865	5.8140
	A	3.1947	5.1529	6.1975	1.6825	1.1801×10^{-1}	5.9040×10^{-2}	3.9371×10^{-2}	2.0150×10^{-2}	1.9064×10^{-2}
I Stage	ΔS	-103.4090	-102.4590	-102.0922	-104.6831	-109.9630	-111.3391	-112.1441	-113.4752	-113.5853
	γ	0.9660	0.9711	0.9812	0.9730	0.9698	0.9698	0.9698	0.9610	0.9628
II Stage	So rapid that could not be studied									
$[CoL^{IV}OAc(H_2O)_3]$	E	4.8574	5.0126	5.1455	10.0832	2.9072	1.5954	2.9203	2.8119	2.7391
	A	2.8580×10^{-3}	1.7760×10^{-3}	4.7603×10^{-4}	1.4597×10^{-1}	3.1531×10^{-3}	2.2622×10^{-4}	1.0698×10^{-3}	1.3556×10^{-3}	2.4450×10^{-4}
I Stage	ΔS	116.8826	-117.8279	120.4440	-109.0672	-116.6873	-121.9224	-118.8350	-118.3646	-121.7680
	γ	0.9661	0.9686	0.9683	0.9565	0.9433	0.9183	0.9439	0.9413	0.9854
	E	7.2080	7.7404	8.2852	7.8121	3.0773	3.1233	3.1233	2.6542	2.7915
II Stage	A	3.4285×10^{-2}	3.0098×10^{-2}	1.1775×10^{-2}	7.4111×10^{-3}	3.1768×10^{-3}	1.6854×10^{-3}	1.1236×10^{-3}	9.2733×10^{-4}	7.3763×10^{-4}
	ΔS	-112.8801	-113.1388	-115.0036	-115.9236	-117.6068	-118.8663	-119.6720	-120.0534	-1205082
	γ	0.9887	0.9878	0.9869	0.9874	0.9726	0.9979	0.9979	0.9732	0.9730

*E in kCals mol^{-1}; A in s^{-1}; ΔS in eu.

TABLE II.6.3. **Kinetic parameters for the decomposition of Ni(II) and Cu(II) complexes of *o*-vanillin-2-aminothiazole ($L^{IV}H$) from TG using mechanistic equations**

Complex	Para-meter*	Mechanistic equations								
		1	2	3	4	5	6	7	8	9
$[NiL^{IV}(OAc)_2(H_2O)_3]$										
I Stage		Weight loss is too small to carryout the kinetic study								
II Stage	E	7.3845	7.8107	8.1874	7.7334	3.2618	3.2613	3.2613	2.9525	3.0542
	A	1.8280×10^{-1}	1.5751×10^{-1}	5.7201×10^{-2}	3.3302×10^{-2}	8.2046×10^{-3}	4.0990×10^{-3}	2.7328×10^{-3}	2.5921×10^{-3}	2.0102×10^{-3}
	ΔS	-108.7778	-109.9738	-111.0880	-112.1609	-114.9450	-116.3239	-117.1294	-117.2345	-117.7397
	γ	0.9924	0.9928	0.9922	0.9906	0.9869	0.9869	0.9869	0.9865	0.9866
IIIStage	E	3.6694	6.4756	11.6148	8.0895	7.5593	7.5709	7.5593	3.1083	4.3774
	A	8.1861×10^{-3}	8.1601×10^{-2}	2.1678	8.5402×10^{-2}	7.2601×10^{-1}	3.6698×10^{-1}	2.4202×10^{-1}	4.0918×10^{-3}	1.0801×10^{-2}
	ΔS	-115.4505	-110.8810	-104.3650	-110.7917	-106.5386	-107.8942	-108.7214	-116.8284	-114.8945
	γ	0.9487	0.9824	0.9973	0.9907	0.9974	0.9973	0.9974	0.9857	0.9949
$[CuL^{IV}OAc(H_2O)_3]$										
I Stage	E	6.3695	6.6612	6.9360	6.7274	2.5644	2.5644	2.5644	2.3490	4.4200
	A	3.5796×10^{-2}	2.6301×10^{-2}	8.4202×10^{-3}	6.4501×10^{-3}	2.4834×10^{-3}	1.2416×10^{-3}	8.2782×10^{-4}	8.8250×10^{-4}	6.5848×10^{-4}
	ΔS	-110.9787	-111.5913	-113.8542	-114.3839	-116.2804	-117.6578	-118.4623	-118.3362	-118.9180
	γ	0.9706	0.9715	0.9707	0.9669	0.9454	0.9453	0.9453	0.9426	0.9436
	E	25.5204	5.1406	5.7637	5.3480	1.9429	1.9437	1.9437	1.4664	1.6214
	A	6.0298×10^{5}	6.5981×10^{3}	3.1031×10^{-3}	1.8875×10^{-3}	1.2199×10^{-3}	6.1061×10^{-4}	4.0702×10^{-4}	2.8321×10^{-4}	2.4434×10^{-4}
	ΔS	-78.5193	-1149422	-116.4412	-117.4291	-118.2963	-119.6714	-120.4774	-121.1980	-121.4914
	γ	0.9535	0.9812	0.9813	0.9807	0.9535	0.9535	0.9535	0.9432	0.9473

*E in kCals mol^{-1}; A in s^{-1}; ΔS in eu.

TABLE II.6.4 **Kinetic parameters for the decomposition of Zn(II) complex of *o*-vanillin-2-aminothiazole ($L^{IV}H$) from TG using using mechanistic equations**

Complex	Para-meter*	Mechanistic equations								
		1	2	3	4	5	6	7	8	9
$[ZnL^{IV}OAc(H_2O)_3]$										
I Stage	E	2.5857	2.8394	3.1158	2.7903	0.6450	0.6458	0.6458	0.7819	0.8463
	A	9.5324×10^{-4}	7.3595×10^{-4}	2.5820×10^{-4}	1.5808×10^{-4}	1.6482×10^{-4}	8.2566×10^{-5}	5.5042×10^{-5}	1.0769×10^{-4}	8.4672×10^{-5}
	ΔS	-119.4718	-119.9858	-122.0670	-123.0419	-122.9590	-124.3325	-125.1382	-123.8046	-124.2825
	γ	0.9843	0.9857	0.9870	0.9876	0.9188	0.9189	0.9188	0.9977	0.9983
II Stage	E	1.1922	0.5595	0.4173	0.4111	0.8997	0.8783	0.8993	1.6190	1.3945
	A	6.8181×10^{-5}	3.5137×10^{-5}	1.7108×10^{-5}	7.3217×10^{-6}	1.5430×10^{-4}	7.6336×10^{-5}	5.1420×10^{-5}	6.1619×10^{-5}	4.5659×10^{-5}
	ΔS	-125.4118	-126.7291	-128.1591	-129.8455	-123.7891	-125.1874	-125.9725	-125.6129	-126.2086
	γ	0.9999	0.9998	0.9970	0.9728	0.9994	0.9995	0.9994	0.9999	0.9999

*E in $kCs\ mol^{-1}$; A in s^{1}; ΔS in eu.

TABLE II.6.5 **Kinetic Parameters for the decomposition of Mn(II) and Co(II) complexes of *o*-vanillin-2-aminothiazole ($L^{IV}H$) from TG using Coats-Redfern equation and accepted mechanistic equation**

Complex	Parameters	From Coats-Redfern equation	From mechanistic equation	Reaction mechanism	Order of reaction
$[MnL^{IV}Cl(H_2O)_3$					
I Stage	E kCal/mole	6.5072	6.5072	Equation V	
	A sec^{-1}	1.1801×10^{-1}	1.1801×10^{-1}	F_1 mechanism	1
	ΔS eu	-109.9630	-109.9630	Random nucleation	
	γ	0.9698	0.9698	Mampel equation	
II Stage	So rapid that could not be studied				
$[CoL^{IV}(OAc)(H_2O)_3]$					
I Stage	E kCal/mole	2.8420	2.7391	Equation IX	
	A sec^{-1}	2.5085×10^{-4}	2.4450×10^{-4}	R_3 mechanism	
	ΔS eu	-121.7718	-121.7680	Phase boundary reaction	2/3
	γ	0.9899	0.9854	Spherical symmetry	
II Stage	E kCal/mole	7.2084	7.2080	Equation I	
	A sec^{-1}	3.4280×10^{-2}	3.4285×10^{-2}	D_1 mechanism	
	ΔS eu	-112.8142	-112.8801	One dimensional diffusion	1/2
	γ	0.9898	0.9887		

TABLE II.6.6. **Kinetic Parameters for the decomposition of Ni(II) and Cu(II) complexes of *o*-vanillin-2-aminothiazole ($L^{IV}H$) from TG using Coats-Redfern equation and accepted mechanistic equation**

Complex	Parameters	From Coats-Redfern equation	From mechanistic equation	Reaction mechanism	Order of reaction
$[NiL^{IV}OAc(H_2O)_3]$					
I Stage	Weight loss is too small to carryout the kinetic study				
II Stage	E kCal/mole	3.0604	3.2613	Equation VI	
	A sec^{-1}	3.9400×10^{-3}	4.0990×10^{-3}	A_2 mechanism	
	ΔS eu	-116.4026	-116.3239	Random nucleation	2/3
	γ	0.9867	0.9869	Avrami equation I	
III Stage	E kCal/mole	4.3766	4.3774	Equation IX	
	A sec^{-1}	1.1956×10^{-2}	1.0801×10^{-2}	R_3 mechanism	
	ΔS eu	-114.6978	-114.8945	Phase boundary reaction	2/3
	γ	0.9949	0.9949	Spherical symmetry	
$[CuL^{IV}HOAc(H_2O)_3]$					
I Stage	E kCal/mole	2.5644	2.5644	Equation V	
	A sec^{-1}	2.4834×10^{-3}	2.4834×10^{-3}	F_1 mechanism	
	ΔS eu	-116.2804	-116.2804	Random nucleation	1
	γ	0.9454	0.9454	Mampel equation	
II Stage	E kCal/mole	1.9429	1.9429	Equation V	
	A sec^{-1}	1.2199×10^{-3}	1.2199×10^{-3}	F_1 mechanism	
	ΔS eu	-118.2963	-118.2963	Random nucleation	1
	γ	0.9535	0.9535	Mampel equation	

TABLE II.6.7. **Kinetic Parameters for the decomposition of Zn(II) complex of *o*-vanillin-2-aminothiazole ($L^{IV}H$) from TG using Coats-Redfern equation and accepted mechanistic equation**

Complex	Parameters	From Coats-Redfern equation	From mechanistic equation	Reaction mechanism	Order of reaction
$[ZnL^{IV}OAc(H_2O)_3]$					
	E kCal/mole	0.8111	0.7819	Equation VIII	
	A sec^{-1}	1.1432×10^{-4}	1.0769×10^{-4}	R_2 mechanism	
I Stage	ΔS eu	-123.6860	-123.8046	Phase boundary reaction	1/2
	γ	0.9978	0.9977	Cylindrical symmetry	
	E kCal/mole	1.3949	1.3945	Equation IX	
II Stage	A sec^{-1}	4.5645×10^{-5}	4.5659×10^{-5}	R_3 mechanism	
	ΔS eu	-126.2092	-126.2086	Phase boundary reaction	2/3
	γ	0.9999	0.9999	Spherical symmetry	

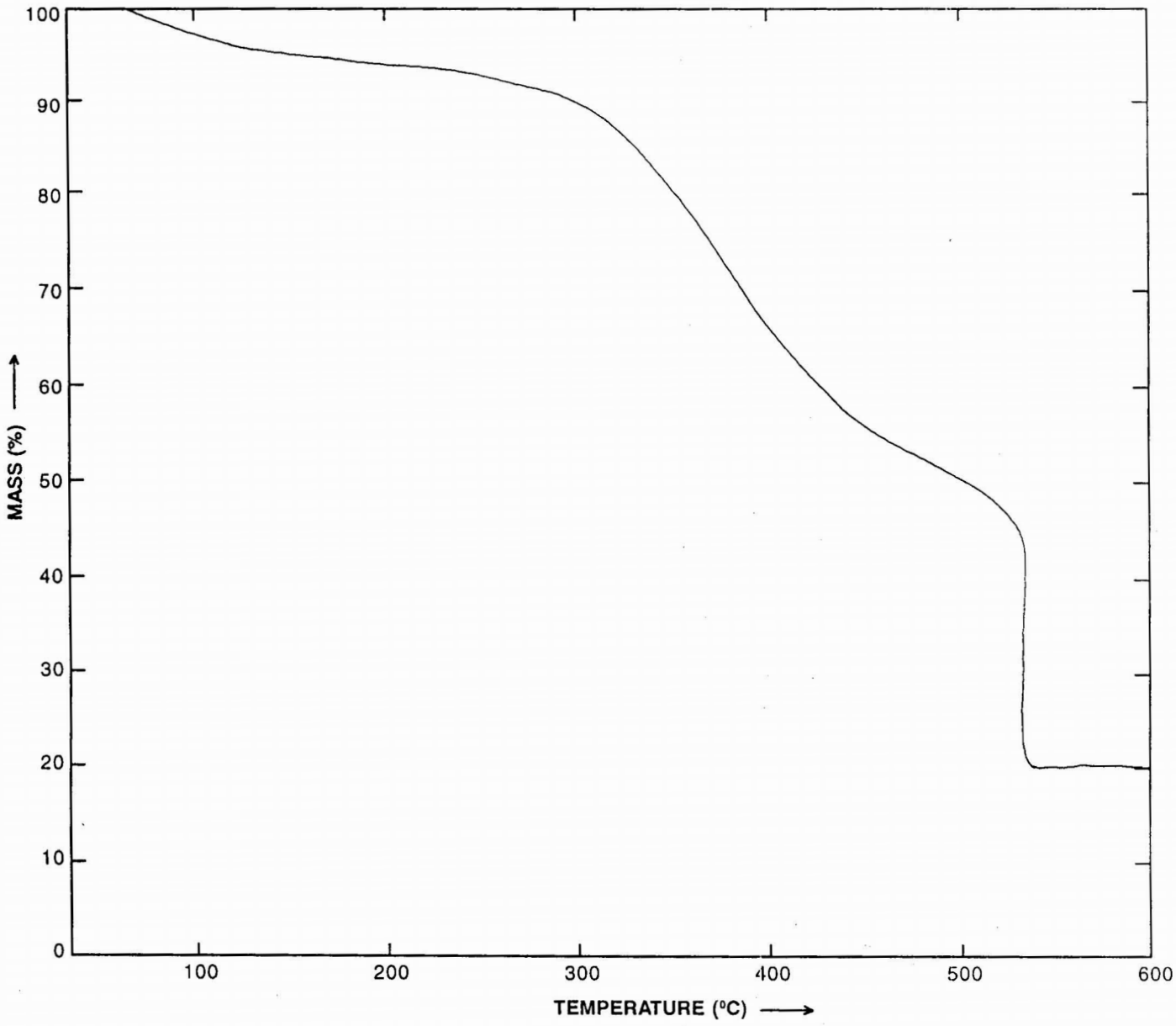

Figure II. 6.1 **TG Traces of [Mn L^{IV} Cl $(H_2O)_3$]**

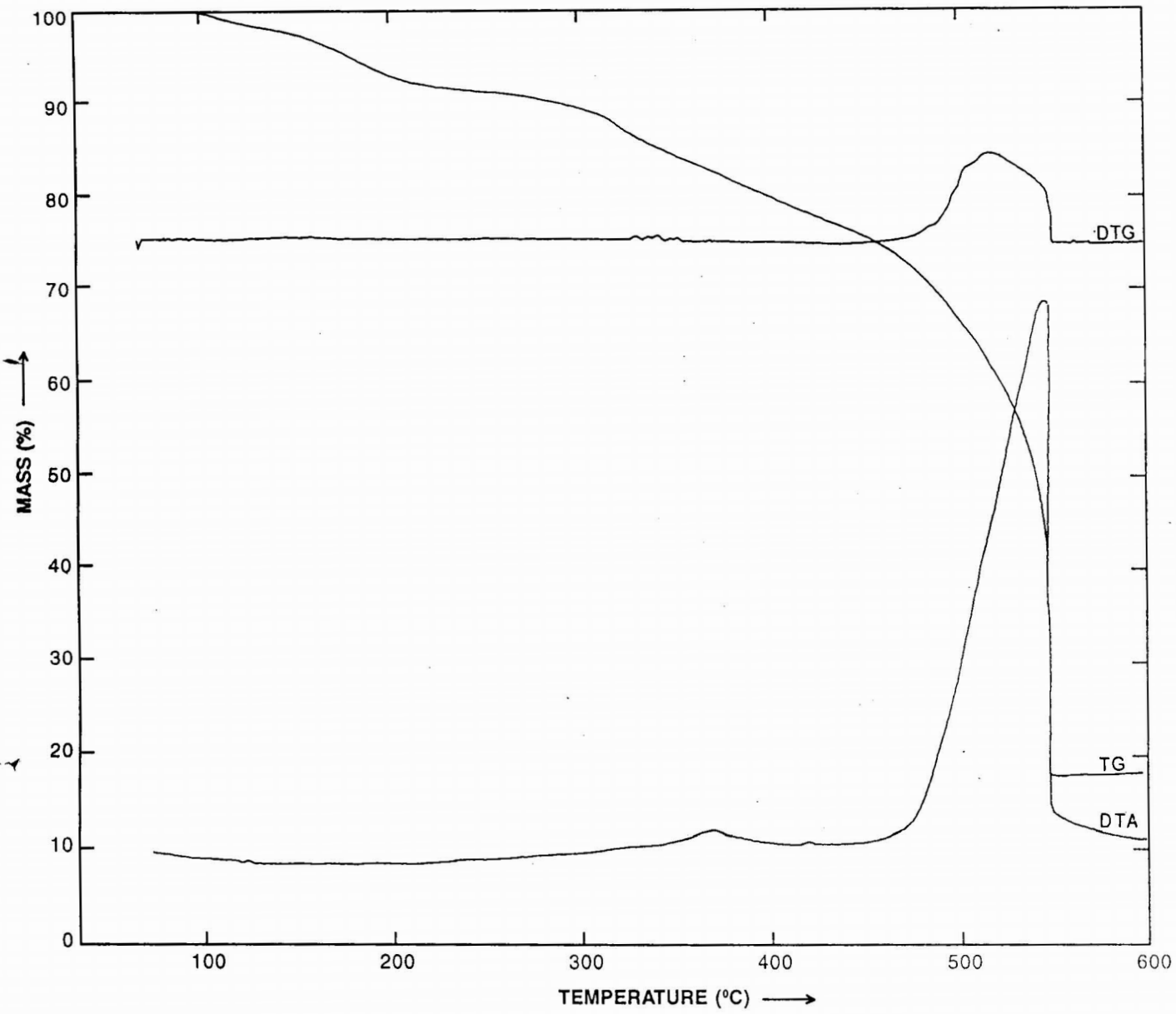

Figure II. 6.2 **TG, DTG and DTA Traces of [Co L^{IV} OAc $(H_2O)_3$]**

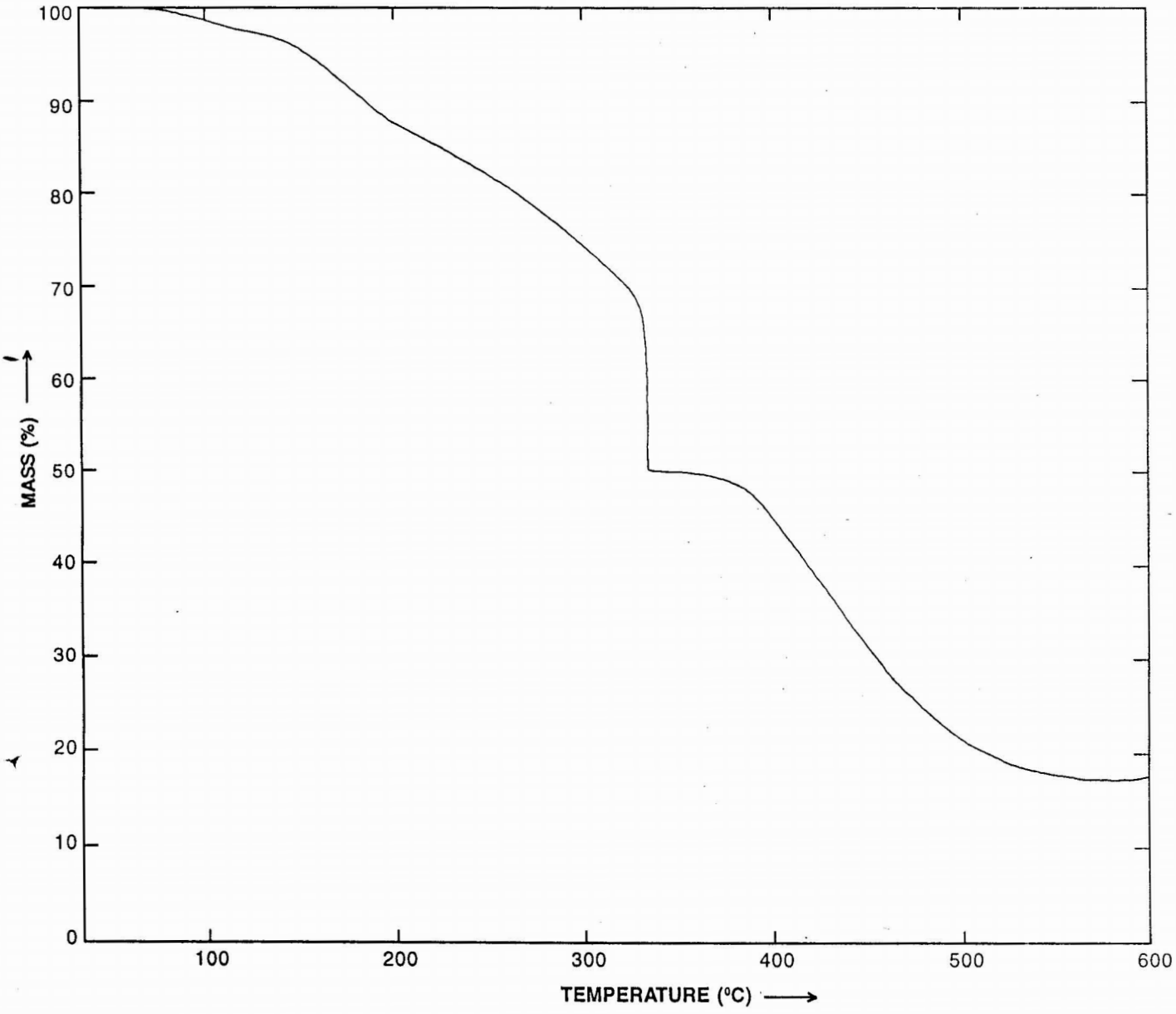

Figure II. 6.3 **TG Traces of [Ni L^{IV} OAc $(H_2O)_3$]**

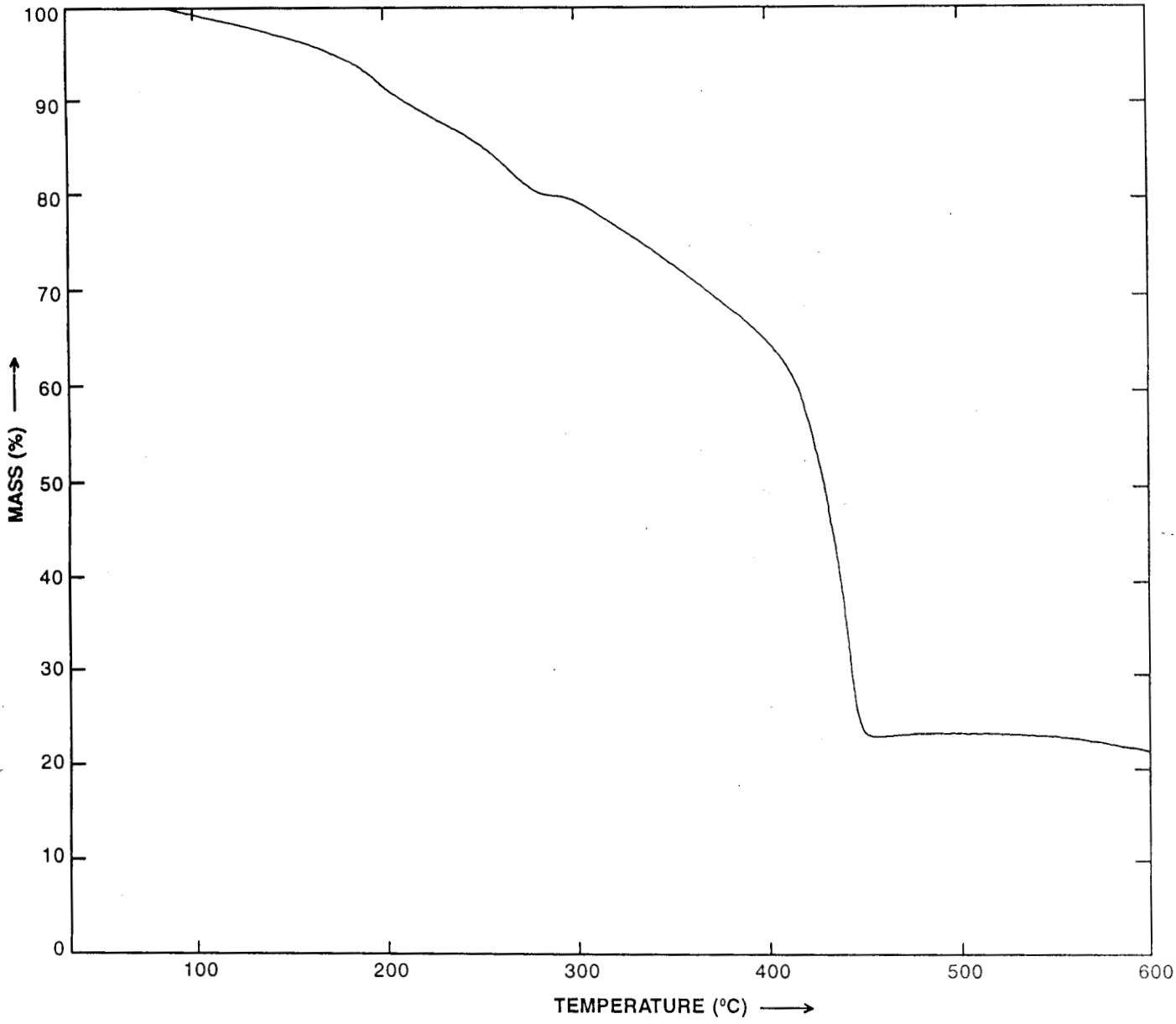

Figure II. 6.4 **TG Traces of [Cu L^{IV} OAc $(H_2O)_3$]**

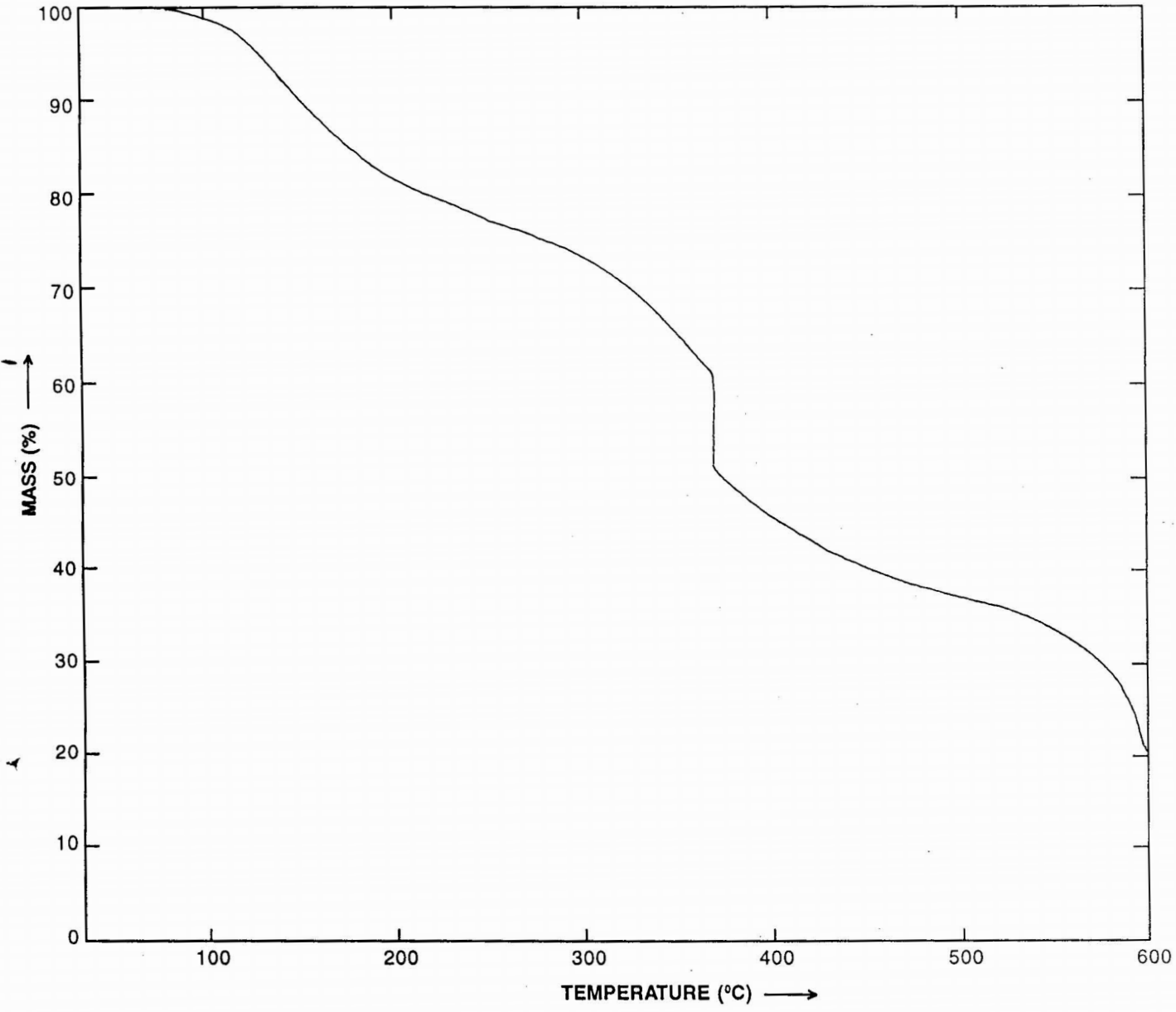

Figure II. 6.5 **TG Traces of [Zn L^{IV} OAc $(H_2O)_3$]**

CHAPTER VII

THERMAL DECOMPOSITION KINETICS OF Mn(II), Co(II), Ni(II), Cu(II), Zn(II), Cd(II) and ZrO(II) COMPLEXES OF *o*-VANILLIN-L-HISTIDINE

Solid state thermal decomposition studies on some transition metal complexes viz. Mn(II), Co(II), Ni(II), Cu(II), Zn(II), Cd(II) and ZrO(II) with Schiff base derived from *o*-vanillin and L-histidine have been carried out by thermogravimetry. Interpretation and mathematical analysis of order of reaction, entropy and energy of activation based on the integral method using the Coats-Redfern equation and nine mechanistic equations given by Satava[172]. The mechanism of decomposition has been also established from TG data.

Experimental

The complexes were prepared and characterized by the methods reported in part I. TGA traces of the complexes were recorded on a Shimadzu thermobalance at a constant heating rate of 10°C min^{-1}. Static air atmosphere was employed during the experiment. Using the programming language Fortran, the mathematical calculations were performed with a Horizon II mini computer.

Treatment of data

The instrumental TG curves are redrawn and presented in Figures II.7.1 - II.7.7. Independent pyrolytic decomposition was carried out with each sample for checking the mass loss obtained from thermogravimetric experiments. The temperature ranges of decomposition, peak temperatures

in TG and the pyrolytic experimental data compared with mass loss in TG are given in Tables II.7.1 and II.7.2.

Standard mechanistic and non-mechanistic equations were employed to obtain the values of kinetic parameters, order of reaction and also to interpret the probable mechanism of decomposition. The results are summarised in Tables II.7.3 - II.7.8.

RESULTS AND DISCUSSION

Structural analysis using various analytical techniques established that all the above complexes have the general formula ($ML^{v}(H_2O)_3$ except the zirconyl complex which can be represented as [$ZrOL(H_2O)$].

The TG curves of Mn(II), Co(II), Ni(II), Cu(II), Zn(II) and ZrO(II), chelates show a two-stage decomposition. Mass loss considerations from TG curves indicate that the first step of decomposition consists of the removal of the water molecules. It may be one, two or three. The loss of ligand moiety takes place only in the second step except in ZrO(II) complex in which *o*-vanillin part of the ligand also removed along with water molecule in the first step.

In the case of [$CdL^{v}(H_2O)_3$] a three stage decomposition pattern is observed. The first stage, represents the loss of three H_2O molecules. And these water molecules can be considered as coordinated water. The second stage represents the loss of histidine part of the ligand, and the loss of *o*-vanillin part of the ligand can be observed in the third stage.

The activation energies obtained for the main decomposition stages of these seven complexes are also comparable to those of coordination compounds of transition metals having similar structure[186,187].

Initial composition temperature and inflection temperature have been used to determine the thermal stability of metal chelates. In the present course of studies, based on observations made by earlier workers[187,188], the relative thermal stabilities of the metal chelates can be given as $[CoL^{v}(H_2O)_3] \approx [CuL^{v}(H_2O_3)] < ZnL^{v}(H_2O)_3 < [CdL^{v}(H_2O_3] \approx [MnL^{v}(H_2O)_3] < [ZrOL^{v}(H_2O)] < [NiL^{v}(H_2O)_3]$.

Decomposition kinetics

The order parameter, n and the kinetic parameters, viz., activation energy E, pre-exponential factor A and entropy of activation ΔS, for the thermal decomposition of the six complexes Mn(II), Co(II), Ni(II), Zn(II), Cd(II) and ZrO(II) were evaluated and summarised in Tables II.7.3 - II.7.8. First stage decomposition of Cu(II) complex involves a very small mass loss and the second stage is very steep. So these stages cannot be subjected to kinetic analysis. It can be seen from these data that more than one equation gives a good linear curve with a high value of correlation coefficient. It is also found that, the greater the thermal stability of a complex, the larger the activation energy for decomposition.

In the present course of studies, based on these mathematical evaluations, it is observed that the kinetic parameters calculated for the second stage of decomposition of Zn(II) complex, from the Coats Redfern equation with n=1/3 are in good agreement with those obtained for the R_2

mechanism based on phase boundary reaction with cylindrical symmetry. Same order is followed by the second stage decomposition of Cd(II) complex based on A_3 mechanism with random nucleation.

The second stage decomposition of Co(II) and ZrO(II) complexes give good correlation with R_3 mechanism based on phase boundary reaction, spherical symmetry thereby establishing the order of reaction to be 2/3. A_2 mechanism based on Avrami equation 1 with random nucleation gives the maximum correlation for the second stage of decomposition of Mn(II) complex with n=2/3 from the Coats Redfern equation.

For the first stage of decomposition of the ZrO(II) complex, second stage of decomposition of the Ni(II) complex and the third stage decomposition of the Cd(II) complex, good agreement is resulted between the kinetic parameters obtained from Coats Redfern method with n=1 and F_1 mechanism (Mampel equation) which is based on random nucleation. We can thus infer that the rate controlling process for the reaction is random nucleation with the formation of one nucleus on each particle and is independent of the thermal technique used.

TABLE II.7.1. **Thermal decomposition data of Mn(II), Co(II) and Ni(II) complexes of *o*-vanillin-L-histidine ($L^{V}H_2$)**

Complex	Stage	Temp. range in TG (°C)	Peak temp. in TG (°C)	Loss of mass (%)			Probable assignment
				From TG	Theoretical	From Pyrolysis	
$[MnL^{V}(H_2O)_3]$	I	60 - 240	180	11.00	13.60	--	Loss of $3H_2O$
	II	240 - 470	390	71.00	67.00	--	Loss of ligand part
				82.00	80.60	81.20	
$[CoL^{V}(H_2O)_3]$	I	40 - 110	105	5.00	5.00	--	Loss of $1H_2O$
	II	120 - 380	370	80.00	75.00	--	Loss of $2H_2O$ + ligand part
				85.00	80.00	81.50	
$[NiL^{V}(H_2O)_3]$	I	140 - 160	160	5.00	4.50	--	Loss of 1 H_2O
	II	160 - 390	390	80.00	80.80	--	Loss of $2H_2O$ + ligand part
				85.00	85.30	83.30	

TABLE II.7.2. **Thermal decomposition data of Cu(II), Zn(II), Cd(II) and ZrO(II) complexes of *o*-vanillin-L-histidine ($L^{V}H_2$)**

Complex	Stage	Temp. range in TG (°C)	Peak temp. in TG (°C)	Loss of mass (%)			Probable assignment
				From TG	Theore-tical	From Pyrolysis	
$[CuL^{V}(H_2O)_3]$	I	40 - 140	120	5.00	5.00	--	Loss of 1 H_2O
	II	250 - 350	320	75.00	75.00	--	Loss of $2H_2O$ + ligand part
				80.00	80.00	80.80	
$[ZnL^{V}(H_2O)_3]$	I	50 - 190	180	9.00	8.80	--	Loss of $2H_2O$
	II	200 - 510	330	74.00	71.00	--	Loss of $1H_2O$ + ligand part
				83.00	79.80	79.30	
$[CdL^{V}(H_2O)_3]$	I	60 - 260	170	10.00	11.90	--	Loss of $3H_2O$
	II	260 - 410	330	30.00	33.70	--	Loss of histidine part
	III	410 - 510	460	34.00	26.00	--	Loss of *o*-vanillin part
				74.00	71.60	72.80	
$[ZrOL^{V}(H_2O)]$	I	80 - 410	260	38.00	37.40	--	Loss of H_2O + *o*-vanillin part
	II	410 - 520	450	31.00	29.30	--	Loss lof histidine part
				69.00	66.70	68.20	

TABLE II.7.3. **Kinetic parameters for the decomposition of Mn(II), Co(II) and Ni(II) complexes of *o*-vanillin-L-histidine (L^VH_2) from TG using mechanistic equations**

Complex	Para-meter*	Mechanistic equations								
		1	2	3	4	5	6	7	8	9
$[MnL^v(H_2O)_3]$ I Stage	Weight loss is too small to carry out the kinetic study.									
II Stage	E	13.2068	14.4091	15.8785	14.8055	7.4016	7.4010	7.4010	6.3727	6.7069
	A	2.8905×10^{1}	5.0699×10^{1}	5.0210×10^{1}	1.7120×10^{1}	4.1960×10^{-1}	2.0970×10^{-1}	1.3980×10^{-1}	6.6960×10^{-2}	6.4801×10^{-2}
	ΔS	-2.8529	-1.7364	-1.7556	-3.8936	-11.2626	-12.6411	-13.4468	-14.9092	-14.9738
	γ	0.9926	0.9944	0.9953	0.9950	0.9958	0.9958	0.9958	0.9929	0.9940
$[CoL^v(H_2O)_3]$ I stage	Weight loss is too small to carry out the kinetic study.									
II Stage	E	15.6049	17.6585	20.2890	18.5091	10.4196	10.4156	10.3000	8.3458	8.9938
	A	4.7763×10^{2}	1.9592×10^{3}	6.1452×10^{3}	1.0295×10^{3}	1.2271×10^{1}	6.1120	3.6587	1.4661	1.2272×10^{1}
	ΔS	-93.5500	30.1200	-88.4800	-92.0300	-100.8300	-102.2100	-103.2300	-105.0500	-106.0018
	γ	0.9930	0.9914	0.9842	0.9895	0.9676	0.9675	0.9669	0.9848	0.9803
$[NiL^v(H_2O)_3]$ I Stage	Weight loss is too small to carry out the kinetic study.									
II Stage	E	87.8248	95.0442	103.2195	97.6567	54.5541	54.5622	54.5582	48.3139	50.3309
	A	1.6900×10^{27}	3.0660×10^{29}	5.2900×10^{31}	5.7300×10^{29}	1.8311×10^{16}	9.2158×10^{5}	6.1200×10^{15}	5.3700×10^{13}	1.8870×10^{14}
	ΔS	18.7000	29.0400	39.2700	30.2800	-31.4700	-32.8300	-33.6400	-43.0600	-40.5600
	γ	0.9566	0.9602	0.9641	0.9616	0.9660	0.9660	0.9660	0.9604	0.9623

*E in kCals mol^{-1}; A in s^{-1}; ΔS in eu.

TABLE II.7.4. **Kinetic parameters for the decomposition of Zn(II) and Cd(II) complexes of *o*-vanillin-L-histidine (L^VH_2) from TG using mechanistic equations**

Complex	Para-meter*	Mechanistic equations								
		1	2	3	4	5	6	7	8	9
$[ZnL^{v'}(H_2O)_3]$ I Stage		Weight loss is too small to carry out the kinetic study.								
II Stage	E	9.5314	11.2275	13.5488	11.9904	6.7969	6.7727	6.7725	4.9321	5.5038
	A	7.3880×10^{-1}	1.5001×10^{-2}	5.1300×10^{-2}	2.0570×10^{-1}	2.0570×10^{-1}	1.0070×10^{-1}	6.7101×10^{-2}	1.3600×10^{-2}	1.7100×10^{-2}
	ΔS	-106.38	-114.1254	-111.6821	-108.9230	-108.9230	-110.3426	-111.1484	-114.3189	-113.8668
	γ	0.9896	0.9962	0.9974	0.9975	0.9895	0.9890	0.9890	0.9962	0.9963
$[CdL^{v}(H_2O)_3]$ I Stage		Weight loss is too small to carry out the kinetic study.								
II Stage	E	11.6893	12.5741	13.5823	13.1249	6.1078	6.1086	6.1090	5.3506	5.5974
	A	3.9567	5.0749	3.2323	1.9650	8.2101×10^{-2}	4.1100×10^{-2}	2.7400×10^{-2}	1.7201×10^{-2}	1.5202×10^{-2}
	ΔS	-6.8712	-6.3767	-7.2730	-8.2620	-14.5711	-15.9473	-16.7520	-17.6740	-113.8668
	γ	0.9873	0.9892	0.9906	0.9900	0.9878	0.9878	0.9878	0.9843	0.9857
III Stage	E	19.7538	27.1180	39.4815	31.0262	25.7477	25.7468	25.7468	15.2562	18.3052
	A	1.6120×10^{3}	2.7674×10^{5}	8.1597×10^{8}	1.2635×10^{6}	3.8636×10^{5}	1.9301×10^{5}	1.2868×10^{5}	5.1208×10^{1}	3.8797×10^{2}
	ΔS	4.6823	14.9067	30.78	17.92	15.5697	14.1906	13.3851	-2.1715	1.8523
	γ	0.9695	0.9711	0.9700	0.9711	0.9625	0.9625	0.9625	0.9657	0.9655

*E in kCals mol^{-1}; A in s^{-1}; ΔS in eu.

TABLE II.7.5. **Kinetic parameters for the decomposition of ZrO(II) complex of *o*-vanillin-L-histidine (L^VH_2) from TG using mechanistic equations**

Complex	Para-meter*	Mechanistic equations								
		1	2	3	4	5	6	7	8	9
$[ZrOL^V((H_2O)]$										
I Stage	E	8.5036	9.0663	18.2603	10.1667	4.0251	4.0239	4.0241	3.5522	3.7206
	A	2.7620×10^{-1}	2.7120×10^{-1}	5.3367×10^{2}	2.0040×10^{-1}	1.1401×10^{-2}	5.6683×10^{-3}	3.7800×10^{-3}	3.0297×10^{-3}	2.5088×10^{-3}
	ΔS	-107.9954	-108.0314	-92.9610	-108.6333	-114.3377	-115.7174	-116.5225	-116.9621	-117.3370
	γ	0.9837	0.9862	0.9833	0.9874	0.9833	0.9833	0.9833	0.9688	0.9800
II Stage	E	14.3072	20.2755	30.4466	23.5044	19.9105	19.9099	19.9099	11.2709	13.7775
	A	2.7249×10^{1}	1.5852×10^{3}	5.4752	7.4192×10^{2}	5.4310×10^{2}	6.9909	1.6299×10^{3}	2.3917	1.2616×10^{1}
	ΔS	-103.6694	-91.1235	-78.2450	-89.0277	-89.0672	-90.4455	-91.2510	-104.3121	-101.0078
	γ	0.9809	0.9901	0.9957	0.9932	0.9941	0.9941	0.9941	0.9929	0.9948

*E in kCals mol^{-1}; A in s^{-1}; ΔS in eu.

TABLE II.7.6. **Kinetic Parameters for the decomposition of Mn(II), Co(II) and Ni(II) complexes of o-vanillin-L-histidine (L^VH_2) from TG using Coats-Redfern equation and accepted mechanistic equation**

Complex	Parameters	From Coats-Redfern equation	From mechanistic equation	Reaction mechanism	Order of reaction
$[MnL(H_2O)_3]$ I Stage	Weight loss is too small to carry out the kinetic study				
II Stage	E kCal/mole	6.7071	7.4010	Equation VI	
	A sec^{-1}	$1.9468x10^{-1}$	$2.0970x10^{-1}$	A_2 mechanism	
	ΔS eu	-12.7887	-12.6411	Random nucleation	2/3
	γ	0.9941	0.9958	Avrami equation I	
$[CoL(H_2O)_3]$ I Stage	Weight loss is too small to carry out the kinetic study.				
II Stage	E kCal/mole	8.9940	8.9938	Equation IX	
	A sec^{-1}	1.0042	$1.2272x10^{1}$	R_3 mechanism	
	ΔS eu	-105.8034	-106.0018	Phase boundary reaction	2/3
	γ	0.9803	0.9803	Spherical symmetry	
$[NiL^V(H_2O)_3]$ I Stage	Weight loss is too small to carry out the kinetic study.				
II Stage	E kCal/mole	54.5540	54.5541	Equation V	
	A sec^{-1}	$1.8311x10^{16}$	$1.8311x10^{16}$	F_1 mechanism	
	ΔS eu	-31.4667	-31.4667	Random nucleation	1
	γ	0.9660	0.9660	Mampel equation	

TABLE II.7.7. **Kinetic Parameters for the decomposition of Zn(II) and Cd(II) complexes of *o*-vanillin-L-histidine (L^VH_2) from TG using Coats-Redfern equation and accepted mechanistic equation**

Complex	Parameters	From Coats-Redfern equation	From mechanistic equation	Reaction mechanism	Order of reaction
$[ZnL^V(H_2O)_3]$ I Stage	Weight loss is too small to carry out the kinetic study.				
II Stage	E kCal/mole	4.4086	4.9321	Equation VIII	1/3
	A sec^{-1}	1.5001×10^{-2}	1.3600×10^{-2}	R_2 mechanism	
	ΔS eu	-114.1234	-114.3189	Phase boudnary reaction	
	γ	0.9933	0.9962	Cylindrical symmetry	
$[CdL^V(H_2O)_3]$ I Stage	Weight Loss is too small to carry out the kinetic study.				
II Stage	E kCal/mole	6.1106	6.1090	Equation VII	1/3
	A sec^{-1}	3.1132×10^{-2}	2.7400×10^{-2}	A_3 mechanism	
	ΔS eu	-16.7532	-16.7520	Random nucleation	
	γ	0.9878	0.9878	Avrami equation II	
III Stage	E kCal/mole	25.7477	25.7477	Equation V	1
	A sec^{-1}	3.8636×10^5	3.8636×10^5	F_1 mechanism	
	ΔS eu	15.5697	15.5697	Random nucleation	
	γ	0.9625	0.9625	Mampel equation	

TABLE II.7.8. **Kinetic Parameters for the decomposition of ZrO(II) complex of *o*-vanillin-L-histidine (L^VH_2) from TG using Coats-Redfern equation and accepted mechanistic equations**

Complex	Parameters	From Coats-Redfern equation	From mechanistic equation	Reaction mechanism	Order of reaction
$[ZrOL(H_2O)]$					
	E kCal/mole	4.0251	4.0251	Equation V	
I Stage	A sec^{-1}	1.1401×10^{-2}	1.1401×10^{-2}	F_1 mechanism	
	ΔS eu	-114.3377	-114.3377	Random nucleation	1
	γ	0.9833	0.9833	Mampel equation	
II Stage	E kCal/mole	13.7794	13.7775	Equation IX	
	A sec^{-1}	3.7941×10^{1}	1.2616×10^{1}	R_3 mechanism	
	ΔS eu	-98.8200	-101.0078	Phase boundary reaction	2/3
	γ	0.9948	0.9948	Spherical symmetry	

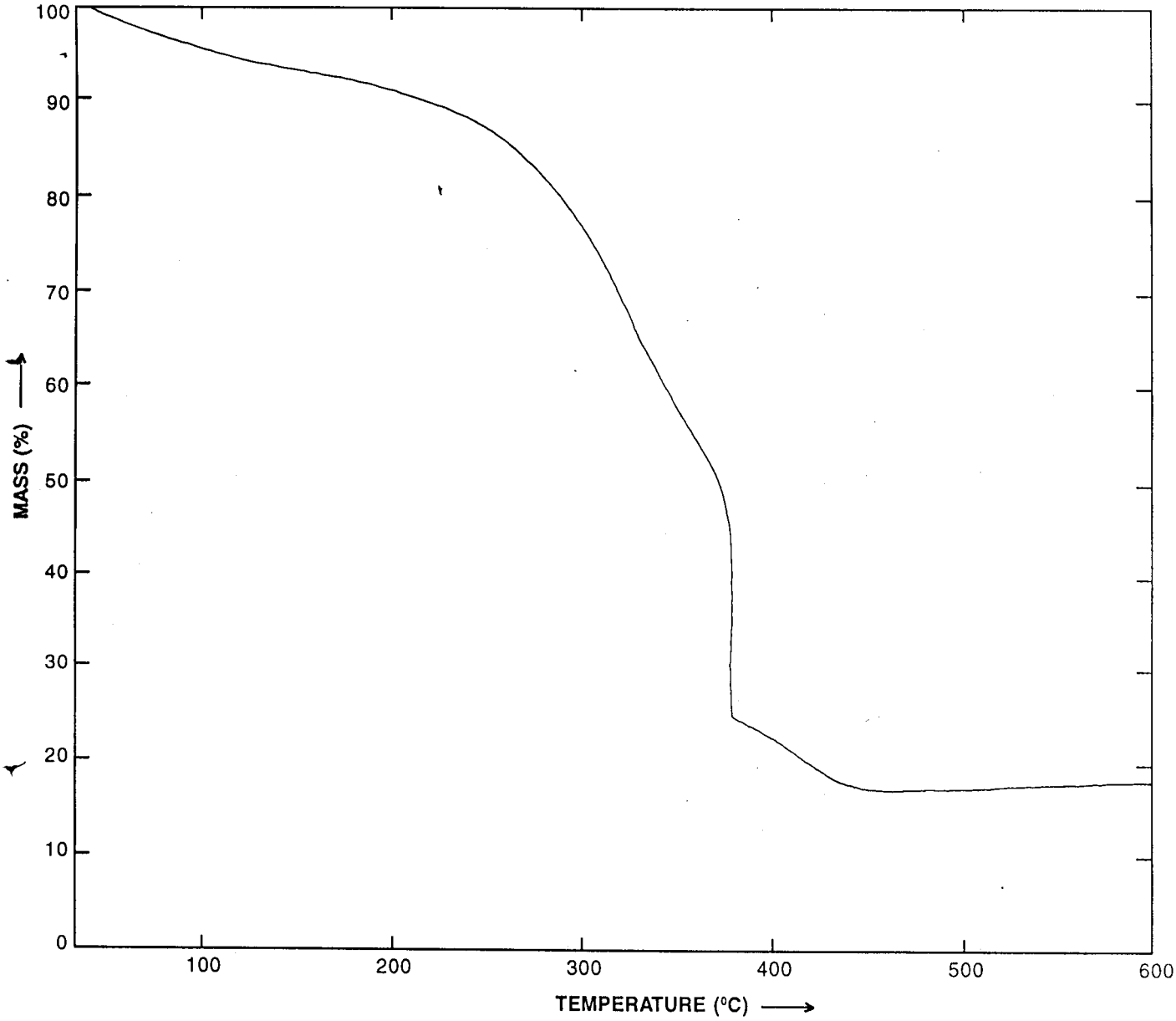

Figure II. 7.1 **TG Traces of [Mn L^V $(H_2O)_3$]**

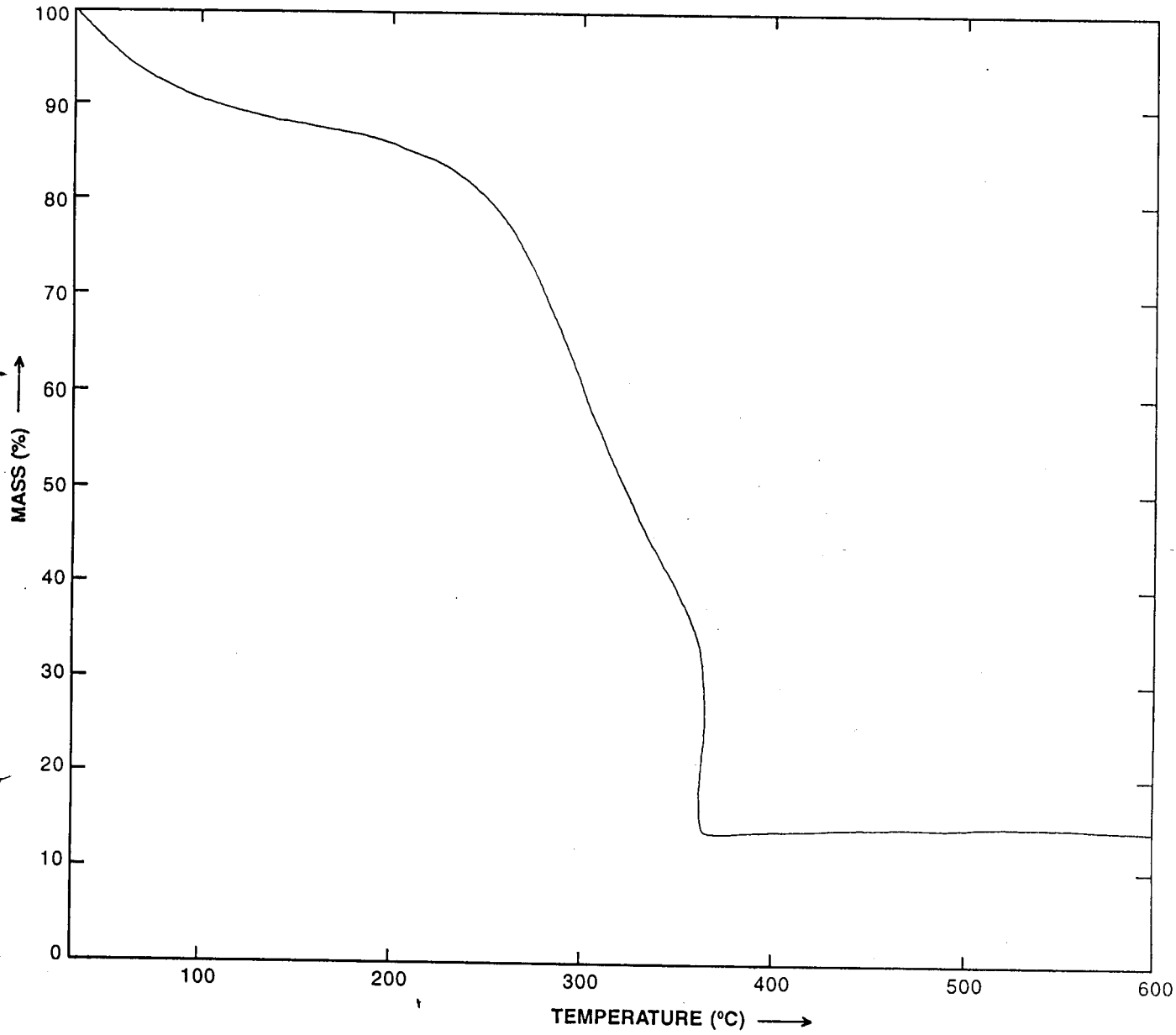

Figure II. 7.2 **TG Traces of [Co L^V $(H_2O)_3$]**

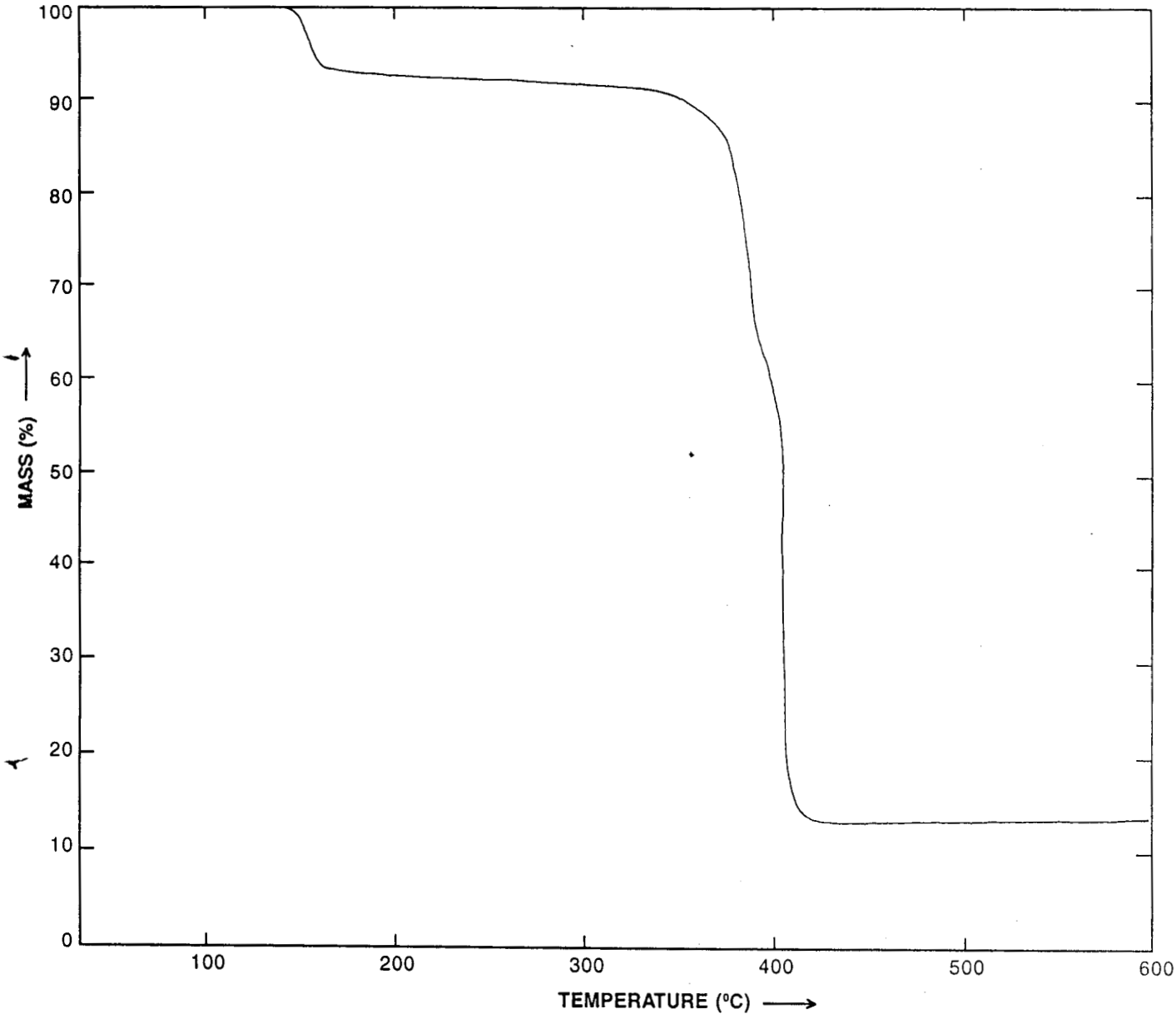

Figure II. 7.3 **TG Traces of [Ni L^V $(H_2O)_3$]**

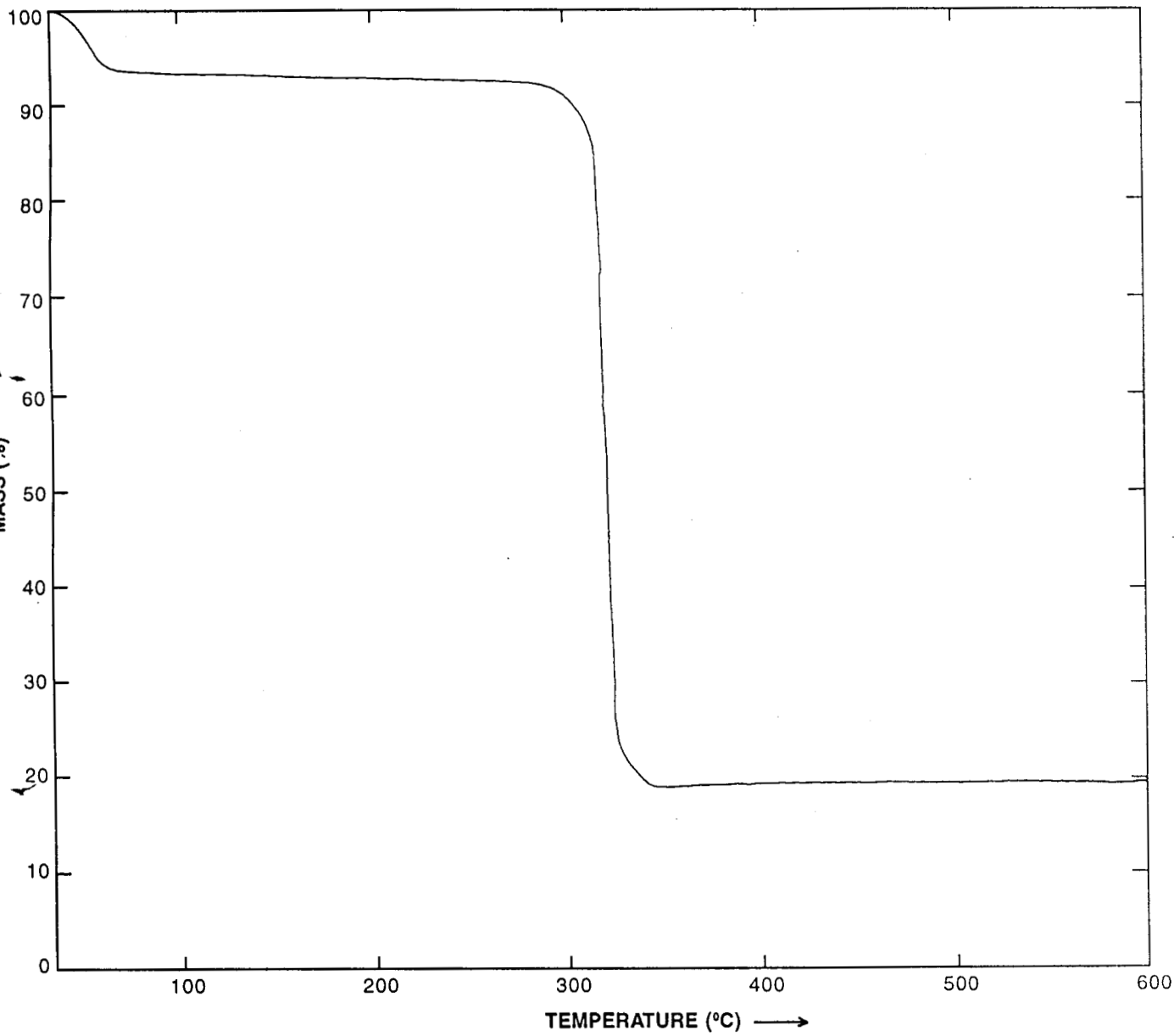

Figure II. 7.4 **TG Traces of [Cu L^V $(H_2O)_3$]**

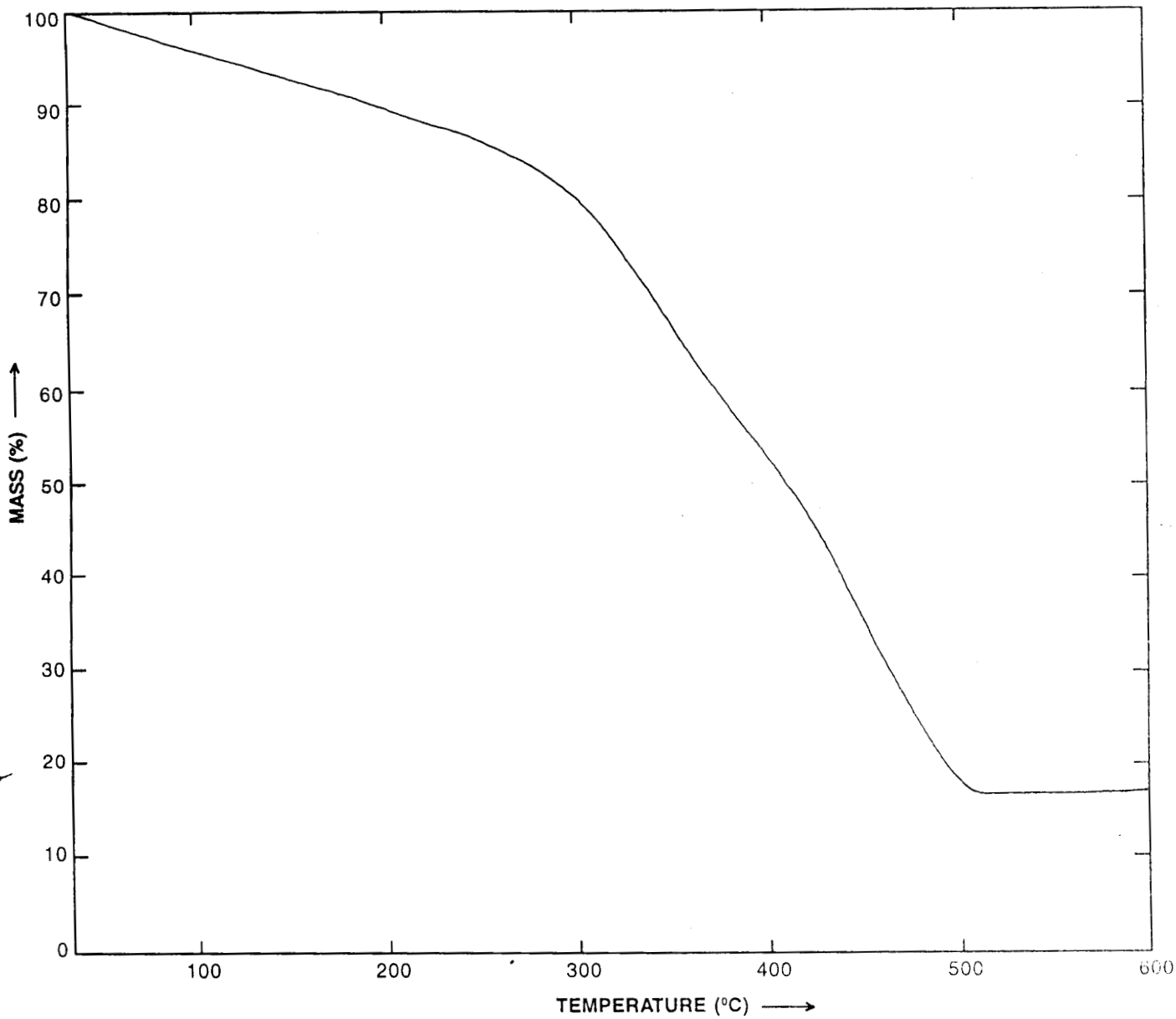

Figure II. 7.5 **TG Traces of [Zn L^V $(H_2O)_3$]**

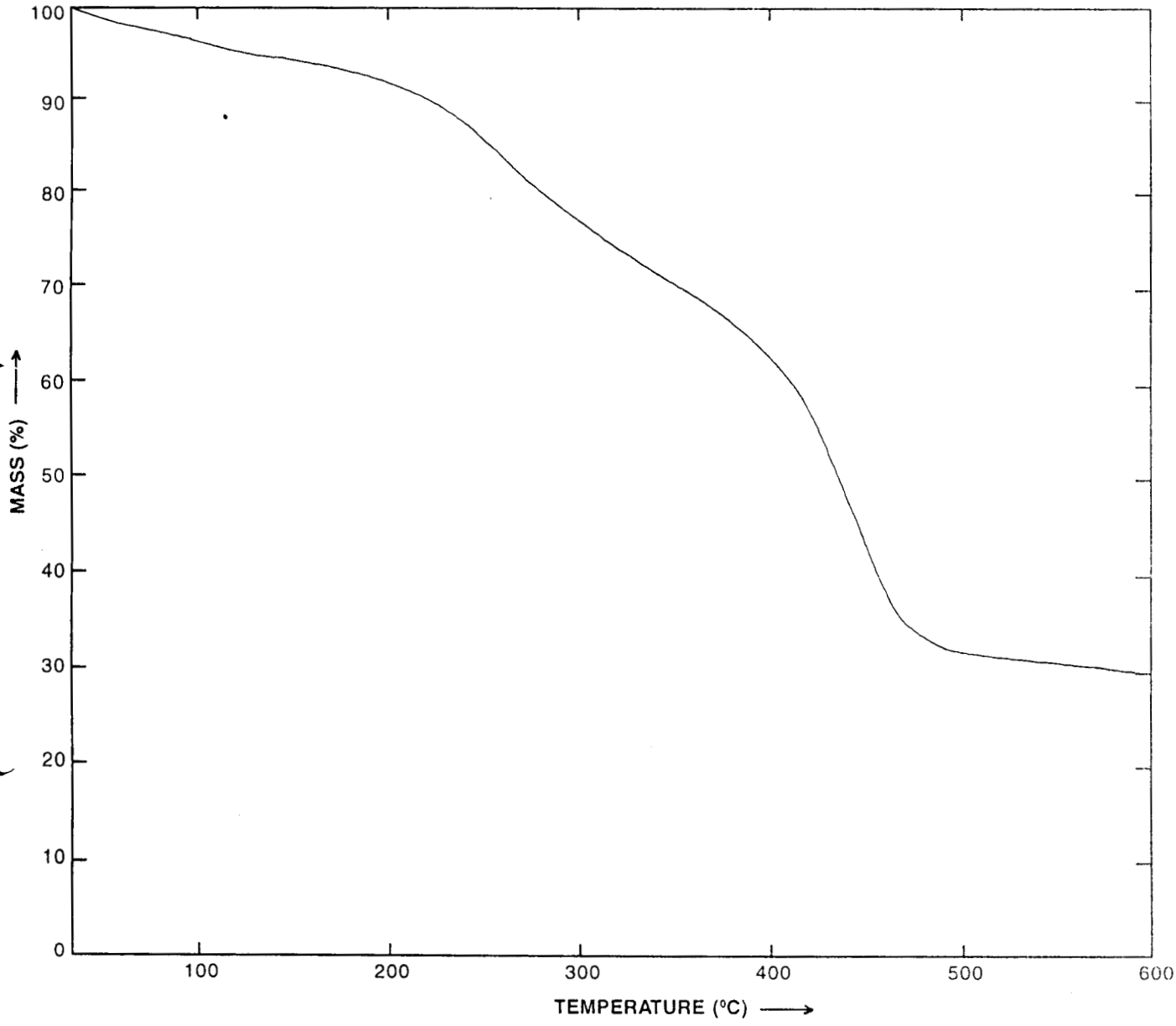

Figure II. 7.7 **TG Traces of [Zr O L^V $(H_2O)_3$]**

PART III

X RAY CRYSTALLOGRAPHIC STUDIES

CHAPTER I

INTRODUCTION

X ray powder diffraction study is a modern method used for the determination of lattice type and unit cell dimensions of complexes. In the earlier stages of X ray crystallographic studies, graphical methods have been used by Hull and Davey[189], Bjurstrom[190] and Bunn[191] for indexing powder photographs. The numerical methods of Runge[192], Johnsen and Toeplitz[193] deserve special mentioning though they were of mainly theoretical interest. Later Hesse[194] and Lipson[195] introduced more easier methods for studying crystallographic pattern. Henry, Lipson and Wooster[196] introduced equations, for studying powder crystallographs in 1951 which are found to be useful and easy to handle.

X-ray diffraction study

The arrangement of atoms extending as a repeating three dimensional pattern enables one to classify the crystals on the basis of axial lengths and axial angles. The relationship between axial lengths and axial angles gives rise to seven distinct crystalline forms as explained below.

Crystal system	Axial length	Axial angle
Cubic	$a = b = c$	$\alpha = \beta = \gamma = 90^{o}$
Tetragonal	$a = b \neq c$	$\alpha = \beta = \gamma = 90^{o}$
Orthorhombic	$a \neq b \neq c$	$\alpha = \beta = \gamma = 90^{o}$
Monoclinic	$a \neq b \neq c$	$\alpha = \gamma = 90^{o}, \beta \neq 90^{o}$
Triclinic	$a \neq b \neq c$	$\alpha = \beta = \gamma = 90^{o}$

Hexagonal	$a = b \neq c$	$\alpha = \beta = 90^{o}, \gamma = 120^{o}$
Trigonal	$a = b = c$	$\alpha = \beta = \gamma = 90^{o}$

X ray crystallographic study of single crystals is an easy method and amongst the useful summary articles available about the study of elastic constants of such compounds, mention may be made of those of Bhagavantam[197], Hearmon[198], Krishnan[199] and Suryanarayana[200]. But materials which cannot be obtained in suitable single crystalline form, can only be studied by powder methods.

The X-rays produced as a result of bombardment of electrons of sufficient energy on any matter is passed through a monochromator and suitable filter to get rays of required wavelength. These rays on falling on a crystal, scattering occurs and these rays from neighbouring atoms cause diffraction' by interference giving peaks. These diffracted rays obey the Bragg's equation

$$n\lambda = 2d \sin \theta$$

where n - an integer

λ - wavelength of incident light

d - interplanar distance; and

θ - angle at diffraction

The X ray crystallographic pattern which plots 2θ against intensity of diffraction can be used for finding the following informations

1. The interplanar (d-) spacing of the lattice planes

2. The intensities of reflections
3. The miller indices of reflection planes
4. The unit cell dimensions and the lattice type

Determination of the crystal system

For the determination of the crystal system the following relationships of d and h, k, l values are employed, where d is interplanar spacing and h, k, l are miller indices. a, b, c are the unit cell dimensions.

For cubic system

$$\frac{1}{d^2} = \frac{h^2 + k^2 + l^2}{a^2} \quad \text{and} \quad d^2 = \lambda^2 / (4\sin^2\theta)$$

$$\sin^2\theta = \frac{\lambda^2}{4a^2}(h^2 + k^2 + l^2) \qquad (1)$$

$h^2 + k^2 + l^2$ will be a constant and will have values other than forbidden numbers 7, 15, 23, 28, 32, etc. From measured Bragg angles, θ's, a set of $\sin^2\theta$ values would be obtained which will be the integral multiples of constant $\lambda^2/4a^2$.

Tetragonal System

$$\text{Sin}^2\theta = \frac{\lambda^2}{4a^2}(h^2 + k^2) + \frac{\lambda^2}{4c^2} l^2 \qquad (2)$$

Orthorhombic system

$$\sin^2\theta = \frac{\lambda^2}{4a^2} h^2 + \frac{\lambda^2}{4b^2} k^2 + \frac{\lambda^2}{4c^2} l^2 \qquad (3)$$

Hexagonal System

$$\sin^2\theta = \frac{\lambda^2}{3a^2} (h^2 + hk + k^2) + \frac{\lambda^2}{4c^2} l^2 \qquad (4)$$

A plane hkl intercepts the crystallographic axes at a/h, b/k and c/l distances and hence the interplanar distance of a crystal can be obtained by the equation

$$d = 1 / \sqrt{h^2/a^2 + k^2/b^2 + l^2/c^2} \qquad (5)$$

For a cubic system,a = b = c and hence

$$d = a / \sqrt{(h^2 + k^2 + l^2)} \qquad (6)$$

The number of molecules per unit cell and the density of the complex have been calculated by using the formula

$$n = \frac{\rho VN}{M} \qquad (7)$$

where n - number of molecules in the unit cell

ρ - density of the complex

N - Avagadro number

V - Unit cell volume

and M - Molecular mass of complex

The relative density of each peak can be calculated using the equation

$$I / I_o \times 100$$

where I - intensity of diffracted beam

and I_o - the intensity of incident beam

The above method of X ray powder crystallography has successfully been applied in the field of coordination chemistry and there are reports on study of different types of crystalline systems of coordination compounds[201-205].

The scope of present investigation

In this thesis attempt has been made to determine the crystalline systems of Fe(II), Ni(II), Cu(II), Cd(II) and UO_2(II) complexes of o-vanillin-L-histidine. The unit cell dimension, a, b, c and number of molecules per unit cell of Fe(II), Ni(II) and Cu(II) have been found out. The densities of these complexes have been measured by making pellets under 7 ton pressure[202].

CHAPTER II

MATERIALS, METHODS AND INSTRUMENTS

Materials

Analar grade chemicals supplied by Sigma, BDH or E. Merck were used for synthetic purpose. Commercial solvents were purified by distillation.

Methods

The ligand *o*-vanillin-L-histidine was synthesised by the procedure described in Part I. The detailed methods of preparation of complexes are also discussed in the same part.

Instruments

Instruments used for studying crystalline systems are:

1. Philips PW 1712 X ray powder diffractometer
2. Screw Gauge
3. Pelletiser
4. Horizon III mini computer

CHAPTER III

X RAY DIFFRACTION STUDIES OF Fe(II), Ni(II) AND Cu(II) COMPLEXES OF *o*-VANILLIN-L-HISTIDINE

X ray powder diffraction method is found to be applicable in determining the structure of complexes in solid state when they are not obtained in single crystal form. Lipson *et al.*[196] have proposed useful equations for studying the X ray powder pattern of each type of crystalline systems. The application to three complexes of *o*-VALH shows that all of them are orthorhombic.

Experimental

The reagents used for the preparation of complexes were of analar grade and the detailed methods of preparation are explained in Part I. The diffraction pattern was obtained using Philips PW 1712 X ray diffractometer. The powder lines were recorded for 2θ values from 5° to 60° at a chart speed of 20 mm min^{-1} and scan speed 2° min^{-1} with Cuk_{α} (λ = 1.5418 A°) radiation. The density of each complex was found out by making pellets at a pressure of 7 ton.

Treatment of data

Eventhough powder diffraction pattern between 2θ values of 5° and 60° is recorded, for simplicity first few peaks are considered. Using the Lipson's equation[196] the nature of crystalline systems and constants A, B, C (where $A = \lambda^2/4a^2$, $B = \lambda^2/4b^2$ and $C = \lambda^2/4c^2$) were found out from which the lattice constants a, b and c and hence the volume were obtained. The

complexes were made into pellets by applying the 7 ton pressure and density was calculated. The number of molecules per unit cell was also found out by using the equation (7) explained in Chapter I.

RESULTS AND DISCUSSION

The X ray diffraction pattern of Fe(II) complex of *o*-VALH exhibited 15 peaks between 5-23° 2θ values. $[NiL^{V}(H_2O)_3]$ recorded 16 peaks upto 28° of 2θ while $[CuL^{V}(H_2O)_3]$ exhibited the same number of peaks when charted upto 27°. All the reflections have been indexed for h, k, l values using methods reported in literature[196]. The X ray crystallographic patterns have been shown in Fig. III.3.1 to Fig.III.3.3. All the three complexes have been found to be orthogonal (orthorhombic). The values of $\sin^2\theta$ for each peak have been calculated with the help of the cell parameters and the corresponding h, k, l in all cases are in good agreement with observed $\sin^2\theta$ values as shown in Table III.3.1 to Table III.3.3. The lattice constants a, b and c for each unit cell have been found out and are given in Tables, along with the density and number of molecules per unit cell.

TABLE II.3.1 **X ray data of** $[FeL^{V}(H_2O)_3]$

Crystal system : orthorhombic.
A = 0.002971; B = 0.001980; C = 0.000990;
a = 14.1335A°; b = 17.3245 A°; c = 24.5006A°;
Cell volume V = 5999.1145A^{o3}
Density D = 1.7398 gm/cm^3; n = 16

Peak No.	d spacing (A°)	Relative Intensity ($I/I_o \times 100$)	$Sin^2\theta$		h k l
			Observed	Calculated	
1	14.1450	31	0.00297	0.00297	100
2	11.0444	69	0.00486	0.00495	110
3	10.2787	28	0.00562	0.00594	012
4	8.2273	52	0.00877	0.00890	021
5	7.6936	21	0.01003	0.01080	013
6	7.0780	29	0.01185	0.01188	200
7	6.8101	35	0.01281	0.01287	201
8	6.6802	25	0.01331	0.01386	210
9	6.3256	18	0.01485	0.01485	211
10	5.1404	38	0.02249	0.02178	131
11	4.9008	28	0.02474	0.02475	132
12	4.4846	24	0.02955	0.02970	311
13	4.2709	28	0.03258	0.03260	041
14	4.0404	35	0.03640	0.03564	141
15	3.9513	32	0.03806	0.03861	142

TABLE II.3.2 **X ray data of $[NiL^{V}(H_2O)_3]$**

Crystal system : orthorhombic.
A = 0.00885; B = 0.00177; C = 0.000885;
a = 8.1945A°; b = 18.3234 A°; c = 25.9133A°;
Cell volume V = 3890.9105A^{o3}
Density D = 1.7401 gm/cm^3; n = 10

Peak No.	d spacing (A°)	Relative Intensity ($I/I_o \times 100$)	$Sin^2\theta$		h k l
			Observed	Calculated	
1	8.1923	53	0.00885	0.00885	100
2	7.5283	39	0.01048	0.01062	110
3	6.5110	31	0.01401	0.01416	112
4	5.9073	82	0.01703	0.01680	121
5	5.0124	62	0.02366	0.02301	104
6	4.8729	33	0.02501	0.02560	131
7	4.5534	34	0.02867	0.02830	040
8	4.0767	26	0.03575	0.03540	200
9	3.9352	28	0.03839	0.03805	211
10	3.8182	32	0.04077	0.04070	202
11	3.7532	28	0.04216	0.04240	212
12	3.6622	25	0.04429	0.04425	050
13	3.5073	26	0.04833	0.04690	135
14	3.4141	31	0.05098	0.05130	204
15	3.2902	28	0.05489	0.05398	151
16	3.2041	43	0.05791	0.05750	205

TABLE II.3.3 **X ray data of $[CuL^{V}(H_2O)_3]$**

Crystal system : orthorhombic.
A = 0.007596; B = 0.001519; C = 0.000844;
a = 8.8427A°; b = 19.7795 A°; c = 26.5352A°;
Cell volume V = 4641.1175A^{o3}
Density D = 1.7508 gm/cm^3; n = 12

Peak No.	d spacing (A°)	Relative Intensity ($I/I_o \times 100$)	$Sin^2\theta$		h k l
			Observed	Calculated	
1	8.8406	100	0.00759	0.00759	100
2	7.6936	20	0.01003	0.00995	111
3	7.3140	26	0.01110	0.01360	030
4	6.1086	40	0.01592	0.01500	014
5	5.6106	51	0.01889	0.01704	032
6	5.2158	52	0.02184	0.02120	130
7	5.1565	17	0.02314	0.02430	040
8	4.9290	28	0.02447	0.02457	132
9	4.6217	38	0.02781	0.02767	0.42
10	4.4407	67	0.03015	0.03030	200
11	4.0767	27	0.03575	0.03526	142
12	3.9513	32	0.03806	0.03798	106
13	3.7080	28	0.04322	0.04390	036
14	3.6040	52	0.04574	0.04557	150
15	3.3634	32	0.05253	0.05310	153
16	3.3029	32	0.05449	0.05460	060

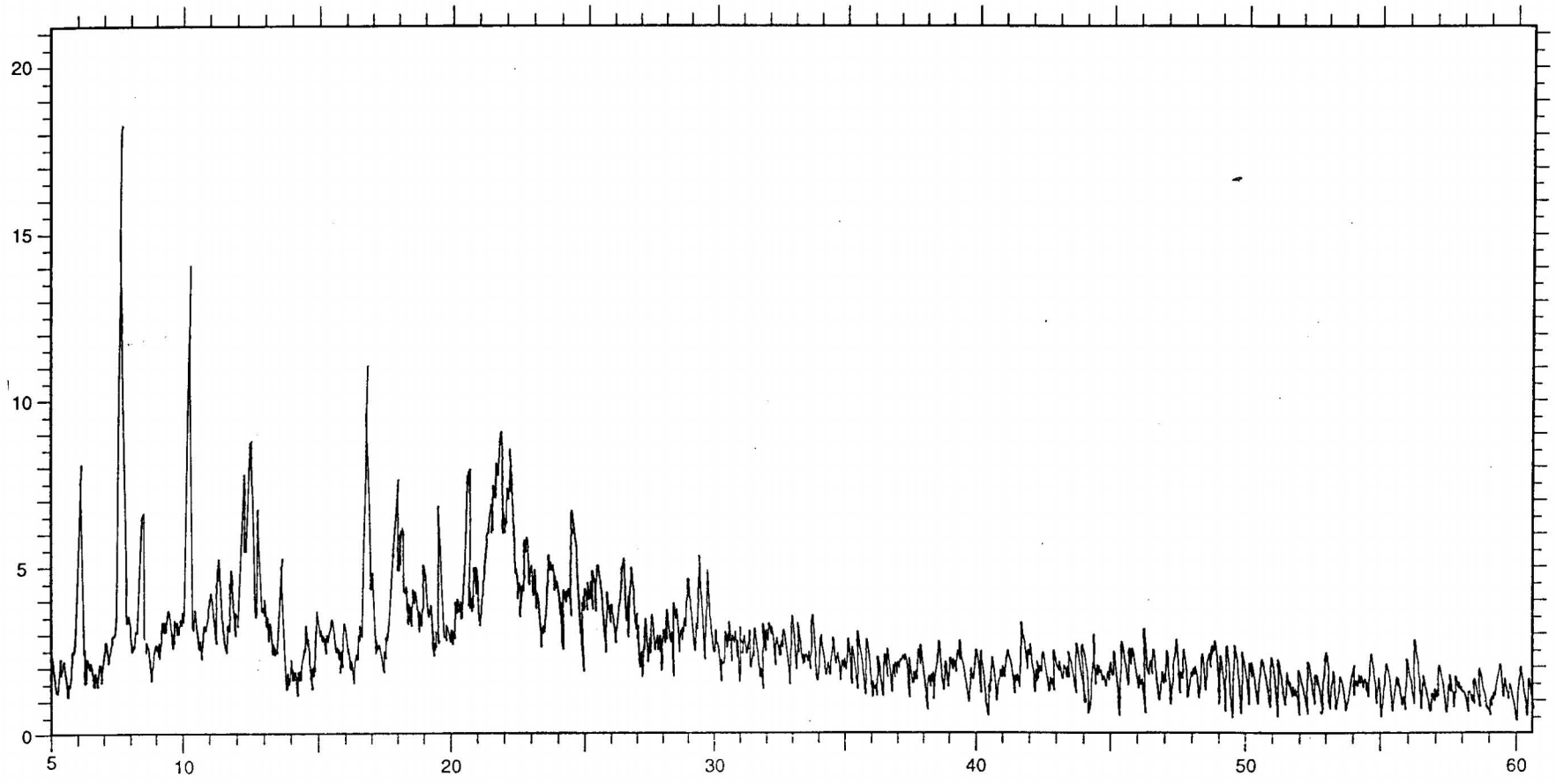

Figure III. 3.1 **X-ray crystallographic pattern of [$FeL^{V}(H_2O)_3$]**

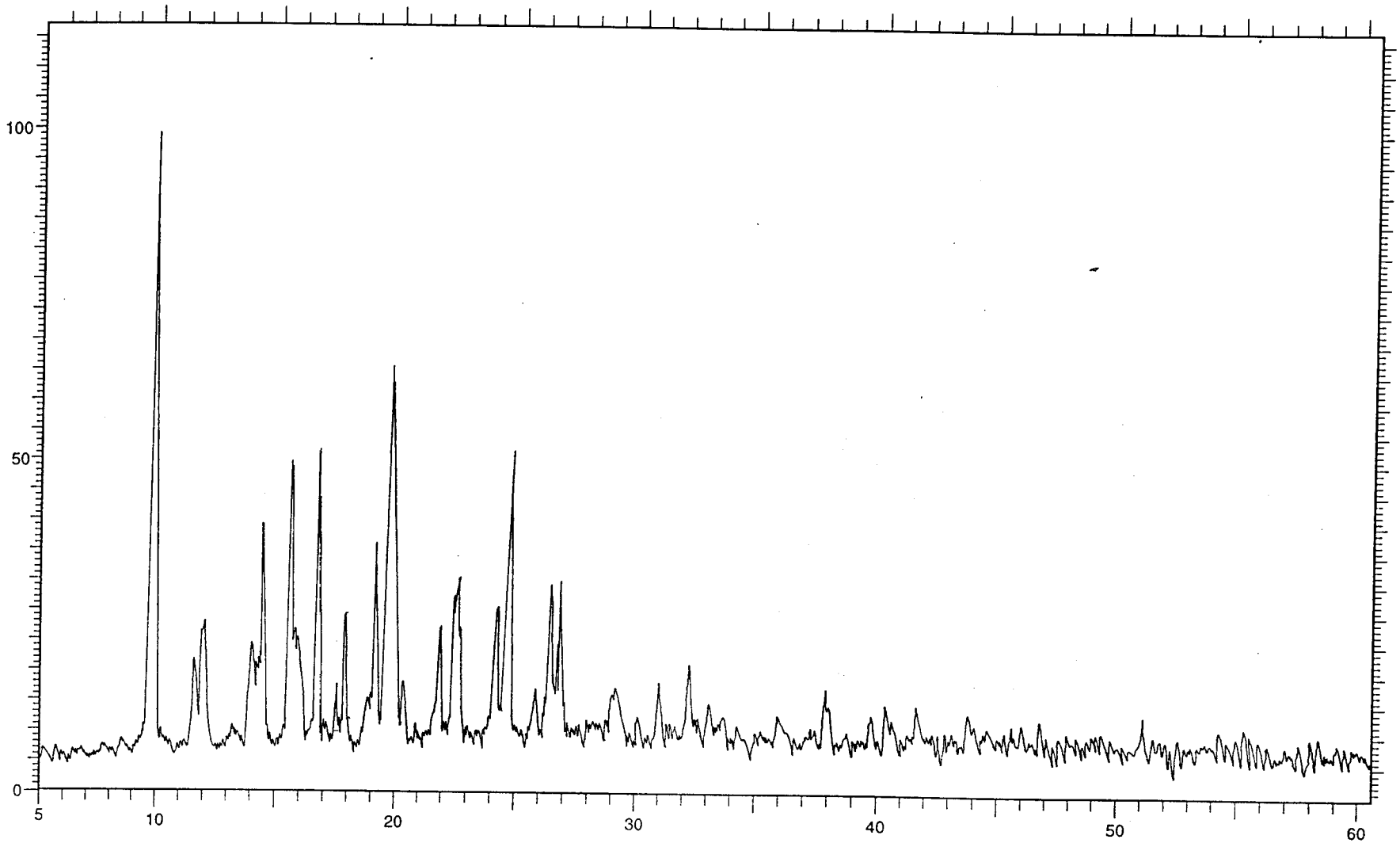

Figure III. 3.3 **X-ray crystallographic pattern of** $[CuL^{V}(H_2O)_3]$

PART IV

ANTIBACTERIAL STUDIES

CHAPTER I

INTRODUCTION

Natural antimicrobial systems are set to become an increasingly important component in food preservation methodology. One reason for this is that the consumers are rejecting the use of chemical preservatives but still demand foods with an acceptable shelf-life. The current trend is towards less heavily preserved foods (less chemical preservatives, salt, sugar) that are not severely damaged by heat processing or freezing and do not contain artificial additives.

There are many natural antimicrobial compounds that could be used in food preservation systems but only a few have been exploited. This is mainly because more research needs to be done on their practical applications in food, particularly their use in combined preservation system. In many cases the mechanism of antimicrobial action is unknown and the effectiveness in a food system has not been studied. In natural eco-systems many of these compounds operate in combination and might therefore be more effective in a combined system with another biopreservative or with a reduced amount of an established preservative system.

Antagonistic cultures, particularly lactic acid bacteria, have been traditionally used to preserve fermented foods in the tropics. In the USA and other developed countries, such fermented foods as yoghurt, buttermilk, fermented sausages, kefir, kumiss and tofu are increasing in popularity as they are considered natural and healthy.

Although the discovery and continued development of new antibiotics and chemotherapeutic agents have provided the tools for the most spectacular control of infectious diseases caused by bacteria and certain protozoa, there is still a need for immunization procedures for some of these diseases and a need for a continuing search for new antibiotics and drugs to meet the challenge of emerging resistant strains and of other special problems.

The appearance of tubercle bacilli with increasing resistance to isoniazid, even in previously untreated patients, emphasizes the continuing race between the development of new drugs and the emergence of resistant microorganisms. For this reason, competent workers in this field believe that there is a great need for the development of a better method of vaccination than by the currently used BCG vaccine.

Recent experiences of American Forces in Vietnam have emphasized the fact that we still do not have a good preventive for bacterial dysentery, and a continued effort is indicated for the development of an effective vaccine against this disease. Cholera is another bacterial disease for which an improved method of vaccination is highly desirable.

Despite the great successes that have been achieved by the use of residual insecticides and of highly effective drugs in the control of malaria, this disease continues to present challenges which call both for the development of new drugs for the emerging resistant parasites and for those basic studies on the immunology and cultivation of the parasites that might lead to the ultimate prevention of malaria by immunization.

Antibacterial drugs exert their action by interfering with either the structure or the metabolic pathways of bacteria. Important methods of antibiotic action include interfering with metabolic pathways, binding to the cytoplasmic membrane, inhibiting protein biosynthesis, inhibiting nucleic acid biosynthesis and disrupting cellwall biosynthesis.

Growth of Bacteria

Growth and viability of bacteria are influenced by various external factors like nutrients in growth media, the gaseous atmosphere, temperature, water, acidity, pH, light and many inhibitory substances.

An adequate supply of suitable food materials in the growth medium is necessary for bacterial growth. The specific nutrient requirements vary for different species of bacteria. The general nutrient requirements of bacteria are:

1. a source of energy
2. a source of carbon
3. a source of nitrogen
4. a source of inorganic salts
5. a source of accessory growth factors.

A suitable culture medium for bacterial growth should provide all the above requirements. Water is absolutely necessary for existence of living cells.

Bacteria require energy for synthetic reactions of growth and repair, maintenance of membrane equilibria in cell, motility etc. carbon and

nitrogen are required mainly for synthesis of proteins and nucleic acids. The inorganic elements required by bacteria are phosphorus, sulphur, potassium, sodium, magnesium, calcium, iron, manganese and cobalt. Accessory growth factors, also called bacterial vitamins, are required in very small amounts for synthesis of essential metabolites. Only certain bacteria require accessory growth factors in the culture medium, others synthesise themselves.

The majority of bacteria including all the parasitic species require organic nutrients such as carbohydrates, aminoacids or peptides, and lipids to serve as source of carbon and energy. They are unable to synthesise their requirements from simple inorganic salts. Such bacteria are called heterotrophic bacteria. The great majority of bacteria show characteristics intermediate between autotrophs and heterotrophs, i.e., they are able to utilise both inorganic and organic compounds.

Effect of environment on bacterial growth

Bacterial growth is markedly influenced by many factors such as temperature, pH of the growth medium and the nature of the gaseous environment.

Each bacterial species has a range of temperature in which it has optimum growth. Also, there is a minimum temperature below which bacterial growth does not take place and a maximum temperature above which bacteria cannot grow. The optimum growth temperature is the most favourable temperature for growth.

The hydrogen ion concentration of the growth medium plays a very important role in bacterial growth. Most of the bacteria prefer to grow in neutral or near neutral pH (i.e., pH 6.5 to 7.5). Highly acidic and alkaline pHs are not suitable for bacterial growth.

The gaseous environment of the growth medium will affect bacterial growth. The important gases which influence bacterial growth are oxygen and carbondioxide. Based on their requirements for oxygen, bacteria are generally classified into three groups.

1. Aerobic bacteria: Growing in the presence of free oxygen or air
2. Anaerobic bacteria: Growing in the absence of free oxygen or air
3. Facultative anaerobic bacteria: They are really aerobic but also have the capacity to grow in the absence of air or oxygen. The majority of bacteria belong to this group

Antibacterial activity of metal complexes of Schiff bases and related ligands

Dwyes and Albert[206, 207] have shown that some metal complexes are very effective against certain microbial infections. It has been suggested by various authors that metal chelates are more potent than the metals and the chelating agents themselves[208,211].

Antibacterial activities of the ligands and a few representative complexes were determined by Bipin, Behera and Promod[212]. A series of copper complexes of some aminoacid displayed antimicrobial activity against gram positive bacteria[213]. Co(II), Cu(II) and Ni(II) complexes of chloramphenicol were evaluated for their antibacterial activity against

bacterial species *E. coli, S. pneumoniae* and *S. typh*[214]. The screening studies showed the metal complexes to be more antibacterial than the simple uncomplexed chloramphenicol.

Ten new thiosemicarbazone derivatives and nine of their transition metal coordination compounds have been tested for bacteriostatic activity against bacteria[215]. Hussain and Humayun synthesized the biologically active complexes of cobalt and nickel with pyrimidine derived Schiff bases having the same metal atom but different anions, such as chloride, sulphate, nitrate, oxalate and acetate. Inorder to evaluate the effect of anions on their bioability, they were screened against *Escherichia coli, Pseudomonas aeruginosa* and *Klebsiella pneumoniae*[216].

Stabilities of some bivalent metal ion chelates of Schiff bases of 3-ethoxy-2-hydroxy benzaldehyde were determined and the antibacterial and anticoagulant activities of these reagents were evaluated[217]. Synthesis, characterization and antibacterial activity of N-salicylideneamino acid with 3d metal complexes were carried out by few authors[218, 219, 220]. In all cases antibacterial activity of the complexes is superior to that of the ligands.

The antibacterial activity of acetylbiphenyl thiosemicarbazone and its Cu(II) complex against *S. aureus, S. flexneri* 26, *B. subtilis, B. proteus* and *A. aerogenes* were examined[221]. Platinum group metal complexes of o-vanillin thiosemicarbazone were characterized by chemical and spectral methods and studied for their antibacterial, antifungal and amoebicidal activity *in vitro*[222]. The platinum group metal chelates exhibited significant activity against a wide spectrum of microorganisms at different concentrations.

The Pt(II) and Ru(II) chelotes derived from o-vanillin-(4-phenylthiosemicarbazone) seem to be the most efficient inhibitors.

The results of the antibacterial activity studies of isothiphendyl complexes of Mn(II), Cr(II), UO_2(II), Zn(II) and Cd(II) show that the complexes strongly inhibit *Escherichia coli, Pseudomonas aeruginosa, Staphylococcus aureus* and *Klebsiella*[223]. Antibacterial activity of Zn(II) complex with salicylidene-2-aminothiazole was studied by Fangzlen, Jingchen and Ruqui[224].

Biologically active aminoacid (alanine, glycine and tyrosine) derived Schiff base ligands and their Co(II), Cu(II) and Ni(II) metal chelates having the same metal atom but different anions (e.g. nitrate, sulphate, oxalate or acetate) were synthesized and characterized by their physical, spectral and analytical data[225]. The role of anions in these biologically active metal chelates against the bacterial species *Staphylococcus aureus, Escherichia coli, Klebsiella pneumonae, Proteus vulgarus* and *Pseudomonas aeruginosa* was studied and reported. Zahid and Syed also screened their metal complexes with various anions against different bacterial species[226] to understand the possible role of anions on the antibacterial properties. The thiosemicarbazone and its copper(II) complexes showed growth inhibitory activity against human pathogenic bacteria *Salmonella typhi, Shigella dysenteriae, Noncoagulace staphyloccocus, Photobacterium* species and *Staphylococcus aureus*[227].

CHAPTER II

MATERIALS, METHODS AND INSTRUMENTS

Materials

All the complexes used in this study were synthesized and characterised as discussed in Part I. Analar grade chemicals and commercially available media purchased from BDH, Oxoid, Glaxo, Sisco and E. Merck were used. Prawn samples for the present study were collected from the market and the soil samples from an agriculture land.

Methods

1. Preparation of media

a) Tryptone Glucose Agar (TGA)

Tryptone	5 g
Beefextract	3 g
Glucose	1 g
Sodiumchloride	5 g
Agar	15 g
Distilled water	1000 ml

The ingredients were dissolved in distilled water, pH adjusted to 7.1 $\pm$ 1 and sterilised at 121°C for 15 minutes in autoclave.

b) H. & L glucose O/F medium (Hugh & Leifson's oxidative verses fermantative medium)

Peptone	:	10 g
Sodium chloride	:	5 g
Dipotassium hydrogen phosphate	:	4 g
Dextrose	:	10 g
Agar	:	3 g
Distilled water	:	1000 ml
pH	:	7.1

Dissolved, pH adjusted to 7.1 and added 1 ml of 0.1% solution of phenol red indicator. Dispersed in 8 ml quantities in 15 cm x 12 mm tubes and sterilized at 10 lbs for 20 minutes.

c) Glucose fermentation broth

Peptone	:	10 g
Sodium chloride	:	5 g
Glucose	:	10 g
Distilled water	:	1000 ml

Dissolved, adjusted pH to 7.2. Added 1 ml of Andrade's indicator. Dispersed in 4 ml quantities in small test tubes with inverted Durham's tube, sterilized at 10 lbs/20 minutes.

d) Nutrient Broth

Beef extract	:	3 g
Peptone	:	10 g

Sodium chloride	:	5 g
Distilled water	:	1000 ml

Dissolved by heating, pH adjusted to 7 ± 0.1. Distributed in 225 ml quantities in 500 ml conical flasks, plug with non-absorbant cotton. Autoclaved at 121°C for 15 minutes.

e) Tryptone broth

Tryptone	:	10 g
Sodium chloride	:	5 g
Distilled water	:	1000 ml
pH	:	7.1 ± 0.1

5 ml quantities in 10 cm x 12 mm tubes.

sterilised at 15 lbs for 15 minutes.

f) P_1N_0 medium (Peptone medium without NaCl)

Peptone	:	10 g
Distilled water	:	1000 ml
pH	:	7.2 ± 0.2

Dissolved; adjusted the pH and dispensed 5 ml quantities in test tubes. Sterilised at 121°C for 15 minutes.

g) Antibiotic agar

Peptone	:	10 g
Sodium chloride	:	10 g
Agar	:	15 g

Distilled water : 1000 ml

pH : 7.2

Sterilized at 15 lbs for 15 minutes.

2. Sampling

Generally the procedure adopted for estimation of bacterial count is as reported[228].

Sampling of prawn for isolation of bacteria

Asceptically cut 10 g prawn neat was mascerated with 90 ml normal saline (0.85% w/v NaCl) in a stomacher and serially diluted to 10^{-3}, 10^{-4} and 10^{-5} dilutions with the same diluent.

Sampling of garden soil for isolation of bacteria

10 g of garden soil was aseptically weighed in a sample dish, macerated with 90 ml diluent (NS) in a sterile mortar and serially diluted to 10^{-3}, 10^{-4}, 10^{-5} dilutions with the same diluent.

One ml. and 0.5 ml. each of the 10^{-3}, 10^{-4} and 10^{-5} dilutions are innoculated by pour plate and spread plate methods respectively using Tryptone Glucose Agar (TGA) plates were incubated at 37°C for 48 h.

Pour plating

Arranged 6 petri dishes in rows in duplicates. Labelled them appropriately. Pipetted 1 ml each of 10^{-3}, 10^{-4} and 10^{-5} dilutions to the respectively marked petri dishes. Cooled the flask of TGA to 45°C, poured about 15-18 ml medium to each of the above dishes, mixed well with the innoculum and allowed to set.

Spread plating

Arranged the pre-set TGA plates in 3 rows in duplicate. Labelled appropriately. Inoculated 0.5 ml each of the 10^{-3}, 10^{-4} and 10^{-5} dilutions on the surface of the respective plates. Using a sterile bend glass rod, spread the innoculum uniformly well on the surface of each plate.

3. Enumeration of bacteria

The colonies of bacteria in the above plates after 48 h of incubation were counted using a Qubec colony counters. The colony counts falling between 30 and 300 were selected. From the average, the total bacterial count (TPC) was calculated, using the formula TPC/g = Average count x dilution factor.

4. Isolation of bacterial cultures from TPC plates

From a suitable TPC plate, on which the colonies were well apart and the counts fall preferably between 30 and 60, colonies were picked into a suitable liquid medium (NO_3 medium or Tryptone broth). Different colonies were picked in the same proportion of their relative occurrence in the plate. Labelled the tubes and incubated at 37°C.

5. Purification of bacterial isolates

Eventhough, a bacterial colony is assumed to have arisen from a single cell in the inoculum, occasionaly mixed growth is possible.

Hence, the culture was purified. In the present study streak dilution method was used to purify the culture.

2. Motility

A drop of borth culture on a clean slide, coveredwith a cover slip was observed under high power lens. Observed the movement of cells. Cells showing movement of their own were motile.

3. Catalase test

Placed a speck of young culture on a clean glass slide and flooded with 2 drops of 30% H_2O_2. Evolution of gas from the culture indicates positive test for catalase.

4. Cytochrome oxidase test

Smeared a little of the young culture on the test paper which was already impregnated with kovac's cytochrome oxidase reagent (N, N, N', N' - Tetramethyl paraphenylinediamine hydrochloride). Development of a blue colour in 30 seconds indicated a positive test.

5. Penicillin sensitivity

Prepared pre-set antibiotic agar plates and dried the surface at 56°C for 45 minutes,cooled to room temperature. Divided each plate into four quarters by drawing lines on the bottom so that we can use one plate for four cultures. A little of the culture was smeared over about $4cm^2$ area in each quarter. A filter paper disc impregnated with penicillin (each disc contains 2.5 IU penicillin) was placed on the surface of each smear. Plates were incubated without inverting for 18-24 h. Examined for clear zones of inhibition around the discs. Cultures showing clear zones of inhibition are sensitive to 2.5 IU penicillin.

6. H & L glucose O/F reaction test

Using a platinum wire (needle), a little of the culture was stabinoculated into the H & L glucose O/F medium, in such a way that at least 2 cm long column of the medium at the bottom of the tube remains uninoculated. The culture incubated for 18-24 h and the changes were observed. A colour change into yellow indicates acid production from glucose. A deepening of red colour of the medium indicates an increase in pH to alkaline level.

Growth of bacteria along the line of inoculation and an yellow colour throughout the medium indicated fermentative reaction (Fermentative with acid but no gas; FANG). In few cases a deep pink colour developed near the top surface, indicating change of pH to alkaline side (Alkaline top).

7. Fermentation of glucose (Durham tube method)

Inoculated the culture into glucose fermentation broth and incubated. Noted acid and gas production after 24-48 h. A deep pink colour showed acid production.

8. Pigmentation

Noted the colour of the bacterial culture on TGA slants after72-96 h. Some bacterial cultures were pigmented yellow, pink, brown or red.

9. Growth at zero NaCl level

Inoculated the culture to P_1N_0 medium and incubated. Noted the growth after 48h. Turbidity indicated bacterial growth.

10. Identification of bacterial cultures upto genus level

The purified cultures were identified upto genus level using the key proposed by Surendran and Gopalkumar[229].

Apparatus and equipments used

1. Petridishes
2. Sample dishes
3. Pipette-1 ml, 10 ml cap
4. Test tubes - 10 ml, 25 ml, 50 ml, cap.
5. Durham's tubes
6. Flasks - 150 ml, 250 ml, 500 ml, 1 litre
7. Microscopic slides, cover slips
8. Qubec colony counter
9. Microscope (Olympus Model K.H) Olympus India Pvt Ltd. New Delhi.
10. Incubator 37°C (Tempo)
11. Stomacher seward (Stomacher 400, U.K)
12. Electronic balance (Afcoset)
13. Serological waterbath
14. Air oven
15. Pestle and Mortar
16. Auto clave
17. Platinum loop

CHAPTER III

ANTIBACTERIAL STUDIES OF SOME TRANSITION METAL COMPLEXES

Antibacterial activity of Fe(II), Co(II), Ni(II) and Cu(II) chelates were studied and results evaluated. The present investigation is divided into two catagories. First one includes the study of the activity of five different complexes of Ni(II) ion and the second one includes the study of the screening antibacterial effect of complexes of different metal ions on bacterial isolates. VAAP, VAAT, *o*-VAAP *o*-VAAT and *o*-VALH are the five different ligands used for complexation with the above metal ions.

Preparation and characterization of the ligands and complexes

The detailed methods of preparation and characterization of the above mentioned ligands and complexes are presented in Part I.

Determination of antibacterial activity

The analysis of the antibacterial activity of the present complexes were done by paper disc method. Filterpaper discs were cut from Whatman No.1 filter paper sheet, using a standard paper punch (hole diameter = 5 mm). Sterilised the disc in a sample dish at 140°C for 2 hr.

Ni(II) chelates of the five ligands and Co(II) chelate of *o*-VAAT and Fe(II), and Cu(II) chelates of *o*-VALH were carefully and aseptically weighed and transfered in different sterile 150 ml conical flasks. 1% solution of the complexes were prepared by dissolving them in suitable

solvents. Sterile alcohol and sterile distilled water were used as solvents. From 1% solution three different dilutions (0.25%, 0.2% and 0.1%) were made by adding required solvent.

Prepared pre-set antibiotic agar plates were prepared, dried the surface at 56°C for 45 minutes and cooled to room temperature. Each plate was divided into four quarters by drawing lines on the bottom so as to get one plate for three different concentrations and one for blank. The sterile filterpaper discs were dipped in different concentrations of the complex solution taken in a sample dish, drained by pressing against the inside wall of the dish and placed on the surface of the respective quarters of the agar plate. Each sterile filterpaper disc dipped in 0.25%, 0.2% and 0.1% solution of the complexes contain 12.5 μg, 10 μg and 5 μg. of the metallic complex respectively. The plates were then incubated without inverting for 24 h and examined for clear zones of inhibition around the discs using hand lens.

After 24 h of the inhibition at 37°C, the zones of inhibition formed around each disc were measured in mm and the results of the growth inhibition of different bacterial cultures were recorded.

RESULTS AND DISCUSSION

The growth inhibition of the known bacterial genera by theCo(II), Cu(II), Fe(II) and five Ni(II) chelates were determined and presented in Table IV.3.1 - IV.3.16.

Thirty two bacterial cultures were isolated from prawn and soil, sixteen from prawn and sixteen from soil. All the purified cultures are identified upto the genus level[229]. The cultures isolated from prawn

includes *Alcalgenes, Bacillus, Lactobacillus, Maraxella, Micrococcaceae, Pseudomonas* and *Vibrio* and those isolated from soil includes *Arthrobacter, Bacillus, Micrococcaceae* and *Pseudomonas Alcalgenes, Maraxella, Pseudomonas* and *Vibrio* are found to be gram negative and the remaining bacteria listed above are gram positive.

All the five Ni(II) chelates showed moderate to good antibacterial activity. Of these $[NiL^{III}(OAc)(H_2O)_3]$ is more active towards prawn bacteria than the others whereas $[NiL^{V}(H_2O)_3]$ is more active towards soil bacteria.

Antimicrobial evaluation of the different metal complexes (Fe(II), Co(II), Ni(II) and Cu(II) was also carried out by standard methods against gram positive and gram negative bacteria. Fe(II) chelate showed remarkable activity when compared to the others.

Generally the activity is more in isolates from prawn than soil. Three cultures namely *Bacillus, Pseudomonas* and *Micrococcaceae* were isolated from two sources viz., prawn and garden soil and were common. The antibacterial activity of the chelates were more in isolates of biological origin namely prawn than from the soil.

Chelates are more sensitive towards gram negative bacteria. For example, *Pseudomonas* is more sensitive than gram positive in all cases.

Table IV.3.1. **Effect of $[NiL'H(OAc)_2(H_2O)_3]$ on bacteria isolated from Prawn**

Bacteria (Genus)	No. of cultures tested	Average diameter of inhibited area at different concentrations of the complex (mm)		
		0.25%	0.2%	0.1%
Alcalgenes	3	13	12	9
Bacillus	2	12	11	8
Lactobacillus	2	7	6	5
Maraxella	2	16	15	11
Micrococcaceae	2	11	10	7
Pseudomonas	2	14	12	8
Vibrio	3	15	14	10

Table IV.3.2. **Effect of $[NiL'H(OAc)_2(H_2O)_3]$ on bacteria isolated from soil**

Bacteria (Genus)	No. of cultures tested	Average diameter of inhibited area at different concentrations of the complex (mm)		
		0.25%	0.2%	0.1%
Arthrobacter	3	10	9	8
Bacillus	4	7	6	5
Micrococcaceae	5	6	5	5
Pseudomonas	4	12	11	8

L'H – Vanillin-2-aminopyridine

Table IV.3.3. **Effect of [NiL"H(OAc)$_2$(H$_2$O)$_3$] on bacteria isolated from Prawn**

Bacteria (Genus)	No. of cultures tested	Average diameter of inhibited area at different concentrations of the complex (mm)		
		0.25%	0.2%	0.1%
Alcalgenes	3	12	11	9
Bacillus	2	9	8	7
Lactobacillus	2	7	6	5
Maraxella	2	10	9	6
Micrococcaceae	2	7	6	5
Pseudomonas	2	12	11	10
Vibrio	3	14	13	11

Table IV.3.4. **Effect of [NiL"H(OAc)$_2$(H$_2$O)$_3$] on bacteria isolated from soil**

Bacteria (Genus)	No. of cultures tested	Average diameter of inhibited area at different concentrations of the complex (mm)		
		0.25%	0.2%	0.1%
Arthrobacter	3	9	8	6
Bacillus	4	8	7	6
Micrococcaceae	5	7	6	5
Pseudomonas	4	9	8	6

L"H – Vanillin-2-aminothiazole

Table IV.3.5. **Effect of [NiL'''(OAc)$(H_2O)_3$] on bacteria isolated from Prawn**

Bacteria (Genus)	No. of cultures tested	Average diameter of inhibited area at different concentrations of the complex (mm)		
		0.25%	0.2%	0.1%
Alcalgenes	3	12	10	8
Bacillus	2	10	9	7
Lactobacillus	2	9	7	6
Maraxella	2	13	11	9
Micrococcaceae	2	11	9	8
Pseudomonas	2	15	13	11
Vibrio	3	15	14	10

Table IV.3.6. **Effect of [NiL'''(OAc)$(H_2O)_3$] on bacteria isolated from soil**

Bacteria (Genus)	No. of cultures tested	Average diameter of inhibited area at different concentrations of the complex (mm)		
		0.25%	0.2%	0.1%
Arthrobacter	3	7	6	5
Bacillus	4	8	7	6
Micrococcaceae	5	7	6	5
Pseudomonas	4	8	7	6

L'''H – *o*-Vanillin-2-aminopyridine

Table IV.3.7. **Effect of [NiL^{IV}(OAc) $(H_2O)_3$] on bacteria isolated from Prawn**

Bacteria (Genus)	No. of cultures tested	Average diameter of inhibited area at different concentrations of the complex (mm)		
		0.25%	0.2%	0.1%
Alcalgenes	3	10	9	7
Bacillus	2	9	8	6
Lactobacillus	2	8	7	5
Maraxella	2	13	12	8
Micrococcaceae	2	11	10	8
Pseudomonas	2	14	12	10
Vibrio	3	9	8	7

Table IV.3.8. **Effect of [NiL^{IV}(OAc)$(H_2O)_3$] on bacteria isolated from soil**

Bacteria (Genus)	No. of cultures tested	Average diameter of inhibited area at different concentrations of the complex (mm)		
		0.25%	0.2%	0.1%
Arthrobacter	3	10	7	6
Bacillus	4	9	7	6
Micrococcaceae	5	8	7	5
Pseudomonas	4	11	9	8

L^{IV}H – o-Vanillin-2-aminothiazole

Table IV.3.9. **Effect of [NiL^{v}(H$_2$O)$_3$] on bacteria isolated from Prawn**

Bacteria (Genus)	No. of cultures tested	Average diameter of inhibited area at different concentrations of the complex (mm)		
		0.25%	0.2%	0.1%
Alcalgenes	3	10	9	7
Bacillus	2	8	6	5
Lactobacillus	2	12	10	9
Maraxella	2	9	8	6
Micrococcaceae	2	12	11	9
Pseudomonas	2	15	14	12
Vibrio	3	13	11	9

Table IV.3.10. **Effect of [NiL^{v} (H$_2$O)$_3$] on bacteria isolated from soil**

Bacteria (Genus)	No. of cultures tested	Average diameter of inhibited area at different concentrations of the complex (mm)		
		0.25%	0.2%	0.1%
Arthrobacter	3	13	12	10
Bacillus	4	7	6	5
Micrococcaceae	5	12	11	9
Pseudomonas	4	14	13	11

L^{V} — *o*-Vanillin-L-histidine

Table IV.3.11. **Effect of $[CoL^{IV}OAc(H_2O)_3]$ on bacteria isolated from Prawn**

Bacteria (Genus)	No. of cultures tested	Average diameter of inhibited area at different concentrations of the complex (mm)		
		0.25%	0.2%	0.1%
Alcalgenes	3	12	10	7
Bacillus	2	11	10	8
Lactobacillus	2	10	9	7
Maraxella	2	12	10	7
Micrococcaceae	2	11	10	7
Pseudomonas	2	14	13	10
Vibrio	3	12	9	7

Table IV.3.12. **Effect of $[CoL^{IV}OAc(H_2O)_3]$ on bacteria isolated from soil**

Bacteria (Genus)	No. of cultures tested	Average diameter of inhibited area at different concentrations of the complex (mm)		
		0.25%	0.2%	0.1%
Arthrobacter	3	11	10	7
Bacillus	4	9	8	6
Micrococcaceae	5	10	9	7
Pseudomonas	4	12	10	7

L^{IV} — *o*-Vanillin-2-aminothiazole

Table IV.3.13. **Effect of $[FeL^{V}(H_2O)_3]$ on bacteria isolated from Prawn**

Bacteria (Genus)	No. of cultures tested	Average diameter of inhibited area at different concentrations of the complex (mm)		
		0.25%	0.2%	0.1%
Alcalgenes	3	15	13	11
Bacillus	2	9	8	6
Lactobacillus	2	15	13	11
Maraxella	2	20	18	10
Micrococcaceae	2	12	11	10
Pseudomonas	2	21	19	14
Vibrio	3	17	15	12

Table IV.3.14. **Effect of $[FeL^{V}(H_2O)_3]$ on bacteria isolated from soil**

Bacteria (Genus)	No. of cultures tested	Average diameter of inhibited area at different concentrations of the complex (mm)		
		0.25%	0.2%	0.1%
Arthrobacter	3	14	13	11
Bacillus	4	9	8	6
Micrococcaceae	5	16	15	12
Pseudomonas	4	17	16	14

L^{V} — *o*-Vanillin-L-histidine

Table IV.3.15. **Effect of $[CuL^{V}(H_2O)_3]$ on bacteria isolated from Prawn**

Bacteria (Genus)	No. of cultures tested	Average diameter of inhibited area at different concentrations of the complex (mm)		
		0.25%	0.2%	0.1%
Alcalgenes	3	9	8	6
Bacillus	2	13	11	8
Lactobacillus	2	11	9	7
Maraxella	2	10	9	7
Micrococcaceae	2	11	7	6
Pseudomonas	2	14	12	9
Vibrio	3	11	8	6

Table IV.3.16. **Effect of $[CuL^{V}(H_2O)_3]$ on bacteria isolated from soil**

Bacteria (Genus)	No. of cultures tested	Average diameter of inhibited area at different concentrations of the complex (mm)		
		0.25%	0.2%	0.1%
Arthrobacter	3	9	7	6
Bacillus	4	8	7	6
Micrococcaceae	5	9	7	6
Pseudomonas	4	12	10	7

L^{V} — *o*-Vanillin-L-histidine

SUMMARY

This thesis consists of four parts. Part I of this thesis gives a detailed description about the synthesis and characterization of 50 complexes of five Schiff base ligands - vanillin-2-aminopyridine (VAAP), vanillin-2-amino-thiazole (VAAT), *o*-vanillin-2-aminopyridine (*o*-VAAP), *o*-vanillin-2-amino-thiazole (*o*-VAAT) and *o*-vanillin-L-histidine (*o*-VALH). Metals used for the complexation are manganese, iron, cobalt, nickel, copper, zinc, cadmium, mercury, zirconium and uranium. Structural elucidation was carried out on the basis of elemental analysis, magnetic measurements, conductance experiments, spectral and thermal studies.

Elemental and spectral study revealed that the ligands VAAP and VAAT are neutral and monodentate, *o*-VAAP and *o*-VAAT are monovalent and bidentate and *o*-VALH is divalent tridentate. 1:1 Metal ligand ratio is found in most of the complexes. A few metals form 1:2 complexes with ligands. As expected Zn(II), Cd(II), Hg(II), ZrO(II) and UO_2(II) complexes are found to be diamangetic while the other chelates showed paramagnetic behaviour. Except a few almost all complexes behave as nonelectrolytes in water and common organic solvents. TG studies of the transition metal chelates proved that the residue was the corresponding metal oxide. All the five ligands form octahedral complexes with Mn(II), Fe(II), Co(II), Ni(II), Cu(II), Zn(II) and UO_2(II) ions and tetrahedral complexes with Hg(II) ions. ZrO(II) complexes are found to possess a square pyramidal geometry around the central metal atom. Cd(II) complexes of VAAP, VAAT, *o*-VAAP

and *o*-VAAT are found to be tetrahedral while that of *o*-VALH is octahedral.

Part I is divided into seven chapters. Chapter I consists of an introduction and a critical review of published work on the topic. In chapter II, materials, methods and instruments utilised for the various studies are described.

Chapter III deals with the preparation and characterisation of the metal complexes of VAAP. Microanalytical data reveal that there exists a 1:1 stoichometry between the metal and the ligand in all these complexes. Mn(II), Fe(II) and UO_2(II) chelates are found to be 1:1 electrolyte. The remaining complexes were found to be non-electrolytic in nature.

Chapter IV covers the preprative as well as physicochemical investigation of the metal complexes of the Schiff base VAAT. Mn(II) and Co(II) ions were found to be forming 1:2 complexes with the ligand. The remaining metals form 1:1 metal ligand ratio. Conductance data explain the non-electrolytic character of the complexes except Fe(II) chelate which acts as an 1:1 electrolyte.

Synthesis and characterisation of the ligand *o*-VAAP and its complexes with Mn(II), Fe(II), Co(II), Ni(II), Cu(II), Zn(II), Cd(II), Hg(II), ZrO(II) and UO_2(II) are described in chapter V. All these complexes possess 1:1 stoichiometry except Cu(II) complex which possesses 1:2 stoichiometry. Mn(II) and UO_2(II) complexes possess a molar conductance

value which is in agreement with the 1:1 electrolyte while all others are four to be non-electrolyte in ethanol.

Chapter VI deals with the preparation and characterisation of t metal complexes of *o*-VAAT. All these complexes possess 1:1 stoichiometr and are found to be non-electrolyte in methanol.

Chapter VII describes the physicochemical investigation on the met chelates of *o*-VALH. There exists a 1:2 stoichiometry between the metal ar the ligand in all these complexes. Conductance data explains the no electrolytic character of the complexes in distilled water.

Part II deals with thermal studies of 28 complexes of the above Sch bases. This part consists of 7 chapters. Chapter I gives an introductic about the thermal studies and the various approaches used to determine t kinetic parameters. Chapter II gives a description of the materials, metho and instruments used for thermogravimetric studies.

Kinetic methods, both mechanistic and nonmechanistic have be utilised in order to analyse the decomposition curves. All the TG trac were subjected to kinetic analysis and the kinetic parameters name energy of activation, Arrhenius frequency factor and entropy of activati of different decomposition stages have been calculated. Attempts were al made to suggest the mechanism and order of decomposition reactio followed during the thermal decay of these complexes. On the basis of t temperatures of inflection and initial decomposition, the relative thern stabilities of the chelates were tentatively assigned.

Thermal decomposition studies on Mn(II), Co(II), Ni(II), Cu(II) and Zn(II) chelates of VAAP are discussed in chapter III. Co(II) chelate shows a four stage decomposition pattern while Mn(II), Ni(II), Cu(II) and Zn(II) show a three stage decomposition pattern. The thermal decomposition data as well as the kinetic parameters calculated are presented in the Tables II.3.1-II.3.8.

Chapter IV includes the kinetics and mechanism of thermal decomposition of complexes of the Schiff base VAAT with Mn(II), Co(II), Ni(II), Cu(II) and Zn(II). Mn(II) and Co(II) undergo a two stage decomposition, Ni(II) and Cu(II) a three stage decomposition and Zn(II) a four stage decomposition. Results of these studies are summarised in the Tables II.4.1-II.4.8.

The thermal behaviour of *o*-VAAP complexes of Mn(II), Co(II), Ni(II), Cu(II), Zn(II) and UO_2(II) were studied by TG and the results are presented in chapter V. Mn(II) and Co(II) complexes are decomposed in two stages while the remaining four complexes decomposed in three stages. Thermal and kinetic data of these complexes are given in Tables II.5.1 - II.5.8.

Chapter VI describes the thermal behaviour of the five complexes of *o*-VAAT. Mn(II), Co(II), Ni(II), Cu(II) and Zn(II) complexes are selected for the above study. All these complexes except those of Ni(II) exhibited a two stage decomposition pattern. Ni(II) chelate gives a three stage decomposition pattern in its TG curve. Results are summarised in Tables II.6.1 - II.6.7.

Chapter VII explains the thermal decomposition studies of Mn(II), Co(II), Ni(II), Cu(II), Zn(II), Cd(II) and ZrO(II) chelates of *o*-VALH. Cd(II) undergoes a three stage decomposition and the other six complexes undergo a two stage decomposition. Tables II.7.1 - II.7.8 give the detailed information regarding the kinetic parameters of decomposition of these chelates.

Part III deals with the unit cell determination of selected few complexes using X ray powder diffraction technology. This part consists of three chapters. Chapter I and II gives the introduction and materials, methods and instruments employed respectively.

In Chapter III the X ray crystallographic pattern of Fe(II), Ni(II) and Cu(II) complexes of *o*-VALH have been investigated. The indexing of peaks uncovers the fact that all the above complexes are orthorhombic.

Part IV deals with the studies on antibacterial activity of selected Schiff base complexes derived from all the five ligands. This part also consists of three chapters.

Chapter I gives emphasis to the need of antimicrobial compounds in food preservation and for the development of new drugs. It also describes kabout the bacterial growth and the action of metal chelates against many human pathogenic bacteria. Chapter II deals with the materials, methods and instruments utilised for the studies.

Chapter III discuss the activity of metal complexes against different bacteria isolated from soil and prawn. Antibacterial activities of Ni(II)

complexes of the five ligands are studied and the results are given in Tables IV.3.1-IV.3.10. Complexes of different metal ions namely Fe(II), Co(II) and Cu(II) are also employed for the study. Of these Fe(II) complex exhibits remarkable inhibition. Details of inhibition of Fe(II), Co(II) and Cu(II) chelates on various bacteria are given in Tables IV.3.11 - IV.3.16.

References are given in serial order at the end of the Thesis.

REFERENCES

PART I

1. H. Schiff, Ann., 150 (1869) 193.
2. M. Delepine, Bull. Soc. Chim., France, 21 (1899) 943.
3. R.H. Holm, G.W. Everett Jr. and A. Chakravorthy, 'Progress in Inorganic Chemistry', Interscience, New York, 7 (1964) 83.
4. N.H. Cromwell, Chem. Rev., 38 (1946) 83.
5. L. Sacconi, Coord. Chem. Rev., 1 (1966) 192.
6. B.O. West, 'New Pathways in Inorganic Chemistry', Cambridge University Press, London, (1968) 303.
7. D.J. Hodgson, 'Progress in Inorganic Chemistry', Interscience, New York, 19 (1975) 173.
8. L. Sacconi, Coord. Chem. Rev., 7(1972) 385.
9. R.H. Holm, 'Inorganic Biochemistry,' Elsvier Scientific Publishing Company, 2(1973) 1137.
10. A. Syamal, Coord. Chem. Rev., 16 (1975) 309.
11. H. Connor, C.A. Mc Auliffe and J. Tames, Rev. Inorg. Chem., 3(1981) 199.
12. D.N. Dhar and C.L. Taploo, J. Sci. Ind. Res., 41 (1982) 501.
13. M. Calvin and K.W. Wilson, J. Am. Chem. Soc., 97 (1945) 2003.
14. A.K. Mukherjee and P. Ray, J. Ind. Chem. Soc., 32 (1955) 633.
15. R.K. Mehta., S.P. Rao and R.C. Kapoor, Indian J. Chem., 7 (1969) 933.
16. G.F. Desa, E. Giesbrecht and L.C. Thompson, J. Inorg. Nucl. Chem., 37 (1975) 109.

17. S.L. Pania, K.N. Kaul and R.K. Mehta, J. Ind. Chem. Soc., 51 (1974) 972.

18. S.L. Pania, K.N. Kaul and R.K. Mehta, Indian. J. Chem., 13 (1975) 295.

19. L. Muslim, W. Roth and H. Erkumeyer, Helv. Chim. Acta, 36 (1953) 886.

20. T. Takahashi and S. Nishigaki, Japan Patent 3, 681 (1955), Chem. Abst., 52(1958) 10206 b.

21. W.M. Farrow, H. Calvin and F.W. Suhneler, J. Am. Pharm., 43(1954) 370.

22. N.B. Singh, H. Singh and S. Singh, J. Indian Chem. Soc., 52 (1973) 1200.

23. M.N. Rotminstrov, G.V. Kulik, O.S. Newkipila and V.O. Kovtum, Z.h. Microbiol., 29 (1967) 150.

24. M.N. Rotminstrov, G.V. Kulik, T.V. Gorbonos and A.N. Bredikhina, Zh. Microbiol., 32 (1970) 510.

25. S.K. Chakraborti and B.K. Dey, J. Indian Chem. Soc. 50 (1973) 137.

26. J. Sengupta, Indian J. Appl. Chem., 29 (1966) 33.

27. E.Bayer, Angw. Chem., 73(1961) 659.

28. J. Aggett, A.W. Khoo and R.A. Richardson, J. Inorg. Nucl. Chem., 43 (1981) 1867.

29. S. Krishner (Ed.), 'Coordination Chemistry', Plenum Press, New York (1969).

30. M.D. Aptekar, T.N. Matskevich, E.P. Trailina and J.A. Sevich, Zh. Obsch. Khim., 41(1971) 652.

31. H.A. Cyba and R.H. Rosenwald, U.S. Patent 3, 361 (1968) 711, Chem. Abst., 68 (1968) 5027.

32. J. Chacko and G. Parameswaran, J. Ind. Chem. Soc., 57 (1980) 95.

33. J. Chacko and G. Parameswaran, Indian J. Chem., 24A (1985) 977.

34. G.Parameswaran and J. Chacko, J. Ind. Chem. Soc., 63 (1986) 774.

35. B. Purushotham Chakraworthi, Khanna and Pramila, J. Indian Chem. Soc., 62(1) (1985) 23.

36. R.L Dutta and R.K. Ray, J. Inorg. Nucl. Chem., 39(1977) 1848.

37. P.K. Sharma, A.K. Sen, S.N. Dubey, Ind. J. Chem., 33A (1994) 1031.

38. A. Angoso et al. J. Inorg. Chim. Acta., 195(1992) 45.

39. V.V. Dixit, B.H. Mehta and D.N. Patkar, Proc. Natl. Acad. Sci. India, Sect. A, (60) 1 (1990) 121.

40. R.N. Mohanty, V. Chakravorthy and K.C. Dash, Indian J. Chem., Sect. A., Inorg. Bioinorg. Phys. Theor. Anal. Chem., 30A (5) (1991) 454.

41. K.P. Rema, S. Laly and Parameswaran Geetha, Asian J. Chem., 4(1) (1992) 71.

42. B. Sleema and Geetha Parameswaran, Proc. of the Eighth Kerala Sci. Cong., (1996) 416.

43. B. Sleema, M.Phil thesis, Calicut University 1992.

44. L.J. Theriot, G.O. Carlisle and H. J. Hu, J. Inorg. Nucl. Chem., 31(1969)2841.

45. R.L. Dutta and G.P. Sengupta, J. Ind. Chem. Soc., 49(1972) 919.

46. A. Syamal and L.J. Theriot, J. Coord. chem., 2(1973) 193.

47. N. Thimmiah Kuntebommanahalli and W. Lloyd, Transition Met. Che., 10 (1985) 94.

48. B.Purushotham Chakraworthi , J. Ind. Chem. Soc., 62(1985) 20.

49. N. Thimmaiah Kuntebommanahalli, Transition Met. Chem., 10(1985) 299.

50. N. Thimmiah Kuntebommanahalli and V.C Sekhar, Acta. chim. Hung. , 124(1987) 491.

51. T.R.Goudar and S.M.Shindagi, J.Ind. Chem. Soc., 64 (1987) 361.

52. B. Konunova and S.A. Kundritskaya, Zh. Neorg. Khim. 32(1987) 1587.

53. Jessy Chacko and Geetha Parameswaran, Ind. J. Chem., 27A(1988) 174.

54. B.Purushotham Chakraworthi, Maini and Ashok, Vijnana Parishad Anusandhan Patrika, 32(1989) 85.

55. Chatterjee Papia, Duggal and Harjit Kaur, J. Ind. Chem. Soc., 66(1989) 550.

56. B.V. Agarwala and S.Hingorani, Inorg. Chim. Acta., 176(1990) 149.

57. Chatterjee, Papia and B.V. Agarwala, Bull Chem. soc. Ethiop., 4(1990) 39.

58. Liu, Guofa, Na, Chongwu, Jilin Dauxue Ziran Kexue Xuebao, 1(1991) 109.

59. M. Kumar, Asian J. Chem., 6(1994) 572.

60. M.L. Dhar, Singh and V.K. Omkar Gupta, J. Iraqui, Chem.Soc., 11(1986) 41.

61. Roy, Rita, Saha and C. Manik, Inorg. Chem. Acta., 129(1987) 265.

62. T.R. Goudar and S.M. Shindagi, J. Ind. chem.Soc., 64(1987) 636.

63. T.R. Goudar, G.S. Nadagoud and S.M. Shindagi, J. Ind. Chem Soc. 65(1988) 509.

64. M.L.Dhar and V.K. Gupta, Ind. J. Chem., 27A(1988) 739.

65. Roy, Rita, Saha, C. Manik, Roy and S. Parag, Transition Met. Chem 15(1990) 51.

66. K.H. Reddy, Ind. J. Chem., 29A (1990) 497.

67. Sunita Hingorani, and B.V.Agarwala, Spectrose. Lett., 23 (1990) 1097.

68. Liu, Guofa, Na, Chongwu, Synth. React. Inorg. Met. Org. Chem. 20(1990) 1387.

69. Liu, Guofa, Na, Chongwu, Polyhedron, 9(1990) 2019.

70. Li, Bin, Zhao, Guioliang, Yingyoong Huaxue, (1990) 70.

71. Li, Bin, Na, Huaxue xurbao, 49(1991) 365.

72. M.L. Dhar and O.P. Singh, J. Termal Anal., 37(1991) 499.

73. Sunita Hingorani, Kavitha Singh and B.V. Agarwala, J. Ind. che. soc. 71(1994) 183.

74. Wang, Guangbin, Chang, C. James, Synthesis, React, inorg, Met. Org Chem., 24(1994) 623.

75. Li, Shu Lan, WangHong Liu, De-xin, Cui, Xue-Gui, Li, Xiasyan, yang Zhao-He, Huaxue., 53(1995) 455.

76. Panchanan Subrata, Hamalainon Reizio Prag, J. Chem Soc., DAltoı Trans 16(1994) 2381.

77. P.K. Sharma, A.K. Sen, S.N. Dubey, Indian J. Chem Sect A, Inorg, Bio inorg Physical, theoretical, Analy Chem., 33A(1994) 1031.

78. MP Mc Curdie,LA Belfiore, Jounal of Polymer Science Part B-Polymer Physics., 37(1999) 301.

79. Rosamma Thomas, N.L. Mary and Geetha Parameswaran, Proc. o the Third Kerala Sci. cong., (1991) 319.

80. Costamagna J, Vargaus J, Lattore R, Alvarado A and Meena G, Coord. Chem. Rev., 119(1992) 67.

81. Chirayath Alice J. and Chantrakudam Prabhakaran P., Transition Met. Chem., 15(6) (1990) 449.

82. M.I. Ayad, S.A. Sallam and H.E. Mabrauk, Thermo-Chim. Acta, 189(1) (1991) 65.

83. C. Alvarino, J. Romero and A. Souza, Z. Anorg. Allg. Chem., 556(1988) 223.

84. Contreras J. Guillermo, Seguel Gloria C. and Gnecco Juan A., Spectochim. Acta, Part A, 48A(4) (1992) 525.

85. Atria ana M, Blasquez Ines, Spodine and J. Evgenia, Bot. Soc. Chil. Quim., 27(1982) 82.

86. C.K. Bhaskara and P.G. More, J. Indian Chem. Soc., 54(11) (1987) 687.

87. B.K. Dwivedi, H.N. Mehrotra, Bhatnagar and Kiran, Proc. Natl. Acad. Sci. India, Sect. A, 58(2) (1988) 341.

88. J. Utamchandani and R.N. Kapoor, Indian J. Chem., 24A (1985) 242.

89. M.T. El Haty and F..A. Adam, Bull. Soc. Chim. Fr., (9-10, pt.1) (1984) 284.

90. N. Kumar; Pandita, Veena and Namarta, J. Indian Chem. Soc. 69(1992) 706.

91. Bala, Manju, Dube, Sangeeta; A.I. P. Sinha, Asian J. Chem. Rev 4 (1993) 85.

92. P.G. More; T.N. Powar, J. Indian Chem. Soc. 70 (1993) 154.

93. Ahmad, Jameel, Mohammad, Ali, Spectrochim Acta, Part A 50A(1994) 1807.

94. Yang, Rui Na, Jin, Dou Man, Chin. Chem. lett 5(1994) 1063.

95. M. Aarif, R.H. Tariq; M.A. Shad, Sci Int. (Lahore) 7(1005) 105.

96. Wang, Dong-Mei; Hou, Yi-Min; Yang, Rui-Na; Hu, xiao-yuan; xuo, Bao-yu; Jin, Dou-Man; Chen, Liao-Rong; Luo, Bao-Sheng, Jiegou Huaxue 14(1995) 300.

97. B. Singh; Singh K. Praveen, Spectrochim., Acta, Part A 52A(1996) 705.

98. Al-Allaf, Talal A.K. Sheet, Z.M. Abeer, Asian J. Chem., 8(1996) 305.

99. Thomas, Rosamma; K. Joby, Thomas; Parameswaran, Geetha, J. Indian Chem. Soc., 73(1996) 529.

100. Knupp, Vagner Fernan des; Nicesio, Isa Carla; Queiroz, Fernanda de Megathaes; Matos, Robson Mendes; Trigo Passos, Bernadettede F, Quim Novo 20(1997) 382.

101. MGA El Washed, SM Metwally, MM El Gamel and SMA ElHaleem ; Gazz. Chim. Ital. 127(1997) 425.

102. M. Arnaudov, S Dinkov, L. Shishkova, L Pindeva, C. Petrov, E Dobereva, Spectrosc. Lett., 30(1997) 1595.

103. S. Dinkov, M Arnaudov, Spectrosc. Lett., 31(1998) 529.

104. S. Dinkov, M. Arnaudov, Spectrosc. Lett., 32(1999) 165.

105. A. Weissberger. D.S. Proskauer, J.A.Riddick and E. Troops, 'Organic Solvents' , Interscience, New York, 2(1956).

106. A.I. Vogel, "A text book of Quantitative Inorganic Analysis," ELBS and Longman (1968).

107. N.H. Furman, "Standard Methods of Chemical Analysis". D Van Nostrand Company Ltd. (1962).

108. J. Lewis and R.G. Wilkins, 'Modern Coordination Chemistry', Intrscience, New York (1963).

109. B.N. Figgis and J.Lewis ' Progress in Inorganic Chemistry', Vol.6, Intescience, New York (1964).

110. A. Earnshaw, E.A. King and L.K. Larkworthy, J.Chem. Soc., Sect.A(1968) 1048.

111. B.N. Figgis and R.S. Nyholm, J. Chem. Soc. (1959) 388.

112. Luigi Casella, Alessandro. Pasini, Renato Ugo and Mario Visco, J. Chem . Soc. (D), (1980) 1665.

113. M.Fathy Ashmowy, Charles A. McAuliffe, R.V. Parish and Joseph Tames, J. Chem. Soc., (D) (1985) 1391.

114. B. Dash, M. Patra and P.K. Mohapatra, J. Indian Chem. Soc., 62(1985) 460.

115. R.C. Speck Jr., P.T. Rowley, T. Cheng and B.L. Horeckes, Biochem. Biophys. Reo. Commum, 9 (1962) 30.

116. Vogel's Text book of Practical Organic Chemistry, Ed. B.S. Furniss, A.J. Hannaford, P.W.G. Smith and A.R. Tatchell, Longman Group, U.K. (1989).

117. J. Lewis and R.G. Wilkins, "The Magneto Chemistry of complex compunds in Modern Coordination Chemistry". Interscience Publishers. (1969)

118. A. Earnshaw, "Introduction to Magnetic Chemistry", Academic Press, London and New York (1968).

119. R.K. Mahapatra, B.K. Mahapatra and S. Guru, J. Inorg. Nucl. Chem., 39(1977) 2281.

120. N.B. Colthup, L.H. Daly and S.E. Wiberley, Introduction to 'Infrared and Raman Spectroscopy', Academic Press, New York, 2nd Ed. (1975)

121. K. Nakamoto, 'Infrared Specta of inorganic and Cordination Compounds', John Wiley, New York (1966).

122. Y.R. Sharma Elementary Organic Spectroscopy S. Chand & Co. New Delhi (1989).

123. E.P. Hertzenberg and J.C. Bailer Inorg. Chem. 10, 2371(1971).

124. C.C. Addison and W.B. Simpson, J. Chem. Soc. 598(1965).

125. ABP Lever, Inorg. Chem. 4(1042) 1965.

126. V.K. Manchanda and M. Subramanian, Acta. Chim . Acad. Sci. Hug., (1982) 11169.

127. A.E. Comyns, B. M. Gatehouse and E. Wait, J. Chem. Soc., (1958) 4655.

128. Mc. Glymn, S.P. Smith, J.K. and Neely, W.C., J. Chem. Phys., 35(1961) 105.

129. J. Selbin, J. Chem. Educ., 41(1964) 86.

130. L.J. Theriot, G.O. Carlislie and H.J. Hu, J. Inorg. Nucl. Chem., 31(1969) 2847.

131. J.R. Ferrare, 'Low Frequency Vibrations of Inorganic and Coordination Compounds'. Plenum Press, New York (1971).

132. N.N. Greenwood and K. Wade, J. Chem. Soc., (1960) 1130.

133. ABP Lever, "Inorganic Electronic Spectroscopy", Elsevier, London (1968).

134. Manju Bala, Sangeetjh Dube and A.I.P. Sinha, Asian J. Chem. Rev., 4(1993) 85.

135. R.L. Dutta and G.P. Sengupta, J. Chem. Soc., 48(1971) 33.

136. C.G. Barrachlough, J. Leuis and R. Nyholm, J. Chem. Soc., (1959) 3552.

137. S.M. Silverstein and G.C. Bassler, 'Spectro Photometric Determination of Organic Compounds', John Wiley, New York (1967).

138. S.B. Hendricks, C.K. Wulf, G.E. Hilbert and U, Lidle, J. Am. Chem. Soc., 58(1955) 1991.

139. J.C.D. Brand and T.M. Cawthon, J. Am. Chem. Soc., 77(1955) 314.

140. S.A. Cotton, Coord. Chem. Rev., 8(1972).

141. Russel S. Drago, "Physical methods in Inorganic Chemistry." an east-west edition (1965).

142. S.P. Mc Glyn and J.K. Smith, J. Mol. Spectroscopy 6(1961) 164.

143. G.C. Walrand and L.G. Vanquickenborne, J.Chem. Phys. 54(1971) 4178.

144. J.R. Wasson and C. Trapp, J. Phys. Chem., 73(1969).

145. William Kemp, "Organic Spectroscopy", Second edition, Mac Millan (1987).

146. D.H. Williams and I. Fleming, "Spectroscopic methods in Organic Chemistry." Tata Mc Graw Hill (1986).

147. A.E. Derome, "Modern NMR techniques for Chemistry research". Maxwell Mac Millan International Editions (1989).

148. D. Kivelson and R. Neiman, J. Chem. Phys., 35(1961) 149.

149. H.J. Stoklosa, G.L. Seebach and J.R. Wasson, J. Phys. Chem., 35(1973) 2584.

150. D.K. Johnson, H.J. Stoklosa, J.R. Wasson and G.L. Seebach, J. Inorg. Nucl. Chem., 37((1975) 1397.

PART II

151. R.C. Mackenzic, 'Differential Thermal Analysis', Academic Press, London , Vol. I (1970) 17.

138. S.B. Hendricks, C.K. Wulf, G.E. Hilbert and U, Lidle, J. Am. Chem. Soc., 58(1955) 1991.

139. J.C.D. Brand and T.M. Cawthon, J. Am. Chem. Soc., 77(1955) 314.

140. S.A. Cotton, Coord. Chem. Rev., 8(1972).

141. Russel S. Drago, "Physical methods in Inorganic Chemistry." an east-west edition (1965).

142. S.P. Mc Glyn and J.K. Smith, J. Mol. Spectroscopy 6(1961) 164.

143. G.C. Walrand and L.G. Vanquickenborne, J.Chem. Phys. 54(1971) 4178.

144. J.R. Wasson and C. Trapp, J. Phys. Chem., 73(1969).

145. William Kemp, "Organic Spectroscopy", Second edition, Mac Millan (1987).

146. D.H. Williams and I. Fleming, "Spectroscopic methods in Organic Chemistry." Tata Mc Graw Hill (1986).

147. A.E. Derome, "Modern NMR techniques for Chemistry research". Maxwell Mac Millan International Editions (1989).

148. D. Kivelson and R. Neiman, J. Chem. Phys., 35(1961) 149.

149. H.J. Stoklosa, G.L. Seebach and J.R. Wasson, J. Phys. Chem., 35(1973) 2584.

150. D.K. Johnson, H.J. Stoklosa, J.R. Wasson and G.L. Seebach, J. Inorg. Nucl. Chem., 37((1975) 1397.

PART II

151. R.C. Mackenzic, 'Differential Thermal Analysis', Academic Press, London , Vol. I (1970) 17.

152. C. Duval, 'Inorganic Thermogravimetric Analysis, Elsevier, New York, 2nd Ed. (1963).

153. W.J. Smothers and M.S. Yaochiang, 'Hand Book of Differential Thermal Analysis', Chemical Publishing Co., New York (1966).

154. P.D. Garn, Thermoanalytical Methods of Investigation ', Academic Press, New York.(1964)

155. D. Schulze, 'Differential Thermoanalyser', VEB Verlangder Wissenchiften, Berlin (1969).

156. K. Honda, Sci.Repts.Tohoku Imp. Univ. (2) 4, (1915) 97-103. CA IX 1915 No 19 p 2610

157. F.W. Wilburn and J.F. Herford, Sci. Instr., 40(1963) 91.

158. F. Paulik, J. Paulik and L.Z. Erdey, Anal Chem., 160(1968) 241.

159. F.W. Wilburn and C.V. Thomson, J. Soc. Glass. Tech., 42(1958) 158.

160. W.W. Wendlandt, 'Thermal Methods of Analysis', John Wiley, New York, 2nd Ed. (1974).

161. E.P. Manche and B. Carrol. 'Physical Methods in Macromolecular Chemistry', Marcel Dekker, New York, 2(1972) 239.

162. A.W. Coats and J.P. Redfern, Analyst 88(1963) 2938.

163. G.M. Luckssżewski. and J.P. Redfern Lab. Pract., 10(1961) 721.

164. J. Sestak, V. Satava and W.W. Wendlandt., Thermochim . Acta, 7(1973) 333.

165. J. Sestak, Talanta, 13(1966) 567.

166. J. Sestak, Silikaty, 11(1967) 153.

167. C.D. Doyle, J. Appl. Polym. Sci., 5(1961) 285.

168. B. Carrol and E.P. Manche, Thermochim. Acta, 2(1972) 449.

169. A.W. Coats and J.P. Redfern, Nature, London, 68(1965) 201.

170. D. Rainville, 'Special Functions', Mac Millan, New York 44(1960).

171. J. Sestak and G. Berggren, Thermochim. Acta, 3(1971) 1.

172. V. Satava, Thermochim. Acta, 2(1971) 423.

173. M.D. Juddo and M.T. Pope, J. Therm. Anal., 4(1972) 31.

174. V.M. Gorbachev; J. Therm Anal., 8(1975) 349.

175. G.D. Ascenzo and W.W. Wendlandt, Anal. Chim. Acta, 50(1970) 75.

176. F.C. Chang and W.W. Wendlandt, Thermochim. Acta, 2(1971) 293.

177. D.L. Perry, C. Vaz and W.W. Wendlandt, Thermochim. Acta, 9(1974) 76.

178. C,.G. Scency, J.O. Hill and R.J. Magee, Thermochim. Acta, 11(1975) 301.

179. C.G. Scency, J.F. Smith, J.O. Hill and R.J. Magee, J. Therm. Anal., 9(1976) 415.

180. M. Lehtinen and K. Maire, Acta Pharm. Fenn., 90(1981) 187.

181. L. Pardeshi and R.A. Bhobe, Acta Cienc. Indica., 8(1982) 178.

182. K.N. Johri and B.S. Arora,Thermochim.Acta, 54(1982) 237.

183. L. Pardeshi and R.A. Bhobe, Acta Cienc Indica., 9(1983) 18.

184. W.W. Wendlandt, J. Inorg. Nucl. Chem., 25(1963) 545.

185. A.V. Nikolaev, V.A. Logvinenko and L.I. Myachina, 'Thermal Analysis', Academic Press, New York (1969) 779.

186. S. Vatsala and G. Parameswaran, J. Therm. Anal., 31(1986) 883.

187. R. Sheshadri Naidu and R. Raghava Naidu, Indian J. Chem., 15A(1977) 652.

188. R.S. Naidu, E.N. Rao, R.Ruby and K. Mallikarjun, Thermochim. Acta, 131(1988) 299; 140(1989) 97.

PART III

189. A.W. Hull, W.P. Davey, Phys. Rev., 17(1921) 549.

190. T. Bjurstrom, Phys. Z., 69(1931) 346.

191. C.W. Bunn, "Chemical Crystallography" Oxford University Press (1945) 133.

192. C. Runge, Phys. Z., 18(1917) 509.

193. A. Johnsen, O. Toeplitz, Phys. Z., 19(1918)47.

194. R. Hesse, Acta Crystallogr., 1(1948) 200.

195. H. Lipson, Acta Crystollogr., 2(1949) 43.

196. N.F.M. Henry, H. Lipson, W.A. Wooster, "Interpretation of Xray Diffraction Photographs", (1951) 81.

197. S. Bhagavantam, Proc. Ind. Acad. Sci., 4b(1955) 72.

198. R.F.S. Hearmon, Phil. Mag., 5(1956) 323.

199. R.S. Krishnan, Progress in Crystal Physics., (1958).

200. M. Krishnamurthi, M. Suryanarayana, "Physics of the Solid State", Accademic Press (1969) 487.

201. K.K. Mahesh, R.K. Gautam, Asian J. Chem., Vol. 3,4 (1991) 417.

202. P. Chouraia, K.K. Suryesh, A.P. Mishra, Proc. Indian Acad. Sci., Vol. 105, 3(1993) 173.

203. R. Singh, R.K. Gautam, J. Ind. Chem. Soc., 14(1987) 631.

204. J.A. Cherayath, C.P. Prabhakaran, Trans. Met. Chem., 15(1990) 449.

205. S. Caric,D. Petrovic, D. Lazar and V.M. Leovaz, Z. Kristllogr., 148(1978) 153.

PART IV

206. F.P. Dwyer and D.P. Meller, 'Chelating Agents and Metal Chelates' (Academic Press, London) 1964.

207. A. Albert, 'Selective Toxicity' (Methuen, London).

208. D.R. Williams,Chem. Rev., 72 (1972) 203.

209. A. Furst and R.T. Haro, Progr. Exp. Tumor. Res., 12 (1969) 102.

210. Y. Okada, Jap. Pat., 7, 017, 189 (1970); Chem. Abstr., 73, 77252y (1970).

211. R.S. Srivastava, J. Inorg. Nucl. Chem., 42 (1960) 1526.

212. B. Bipin Mahapatra, A.K. Behera and K. Promod Bhoi, Asian J.Chem., 4 (1992) 873.

213. M. Tarek Ibrahim, A. Ahmed Shabana and A. Hamdy Hammad, Arch. Pharmacol. Res., 15 (1992) 130.

214. Zahid Hussain Chohan and Humayun Pervez, J. Res. (Sci.), 4 (1992) 49.

215. Liu, Pieman, Li, Zhong; Li Yingchun; Wang, Xingbo and Xu, Lijun Shandeng Yike Daxue Xuebao 30 (1992) 340.

216. Zahid Hussain Chohan and Humayun Pervez, Pak. J. Pharmacol, 10 (1993) 17.

217. R. Vijaya Shastry and M.S. Mayadeo, Acta.Cienc. Indica, Chem., 18 (1992) 149.

218. Bi, Siwei, Gao, Enqing, Tian, Junlian, Li, Yantuan; Tiam Laijin, Liu, Shuxiang and L. Guizhi, Ying Yong Huaxue, 12 (1995) 13.

219. Tian Laijin; Tian Junliam; Li,Tantuan; Li, Guizh; Bi,Siwei; Gao Enqing and Liu, Shuxiang, Huaxua Shiji 18 (1996) 114.

220. Bi, Siwei and Liu Shuxiang, Wuji Huaxwe Xuebao 12 (1996) 423.

221. Bi, Siwei, Liu, Shuxiang; Liu, Yongjum; Sun, Haitao and Tian, Junlian, Ying Yong Huaxue 13 (1996) 15.

222. Offiong, Offiong E Fanga, Etok, Comfort and Martelli, Sante Fasmaco 51 (1996) 801.

223. S. Shanmukappa and P.G. Ramappa, Synth.React. Inorg. Met.-Org. Chem., 27 (1997) 967.

224. Liang, Fangzleni, Hao, Jing Cheng and Hueeng, Ruqi, Huaxue Tongbao 10 (1997) 42.

225. H. Zahid Chohan, Marapaka Praveen and A. Ghaffar, Synth. React. Inorg. Met.-Orgl. Chem., 28 (1998) 1673.

226. H. Zahid Chohan and K.A. Syed Sherazi, Synth. React. Inorg. Met.-Org. Chem., 29 (1999) 105.

227. Bindu, Panampilly; R. Pratrapachandra Kurup, Maliyeckal and R. Satyakeerty, Thonduparambil, Polyhedron 18 (1999) 321.

228. U.S. Food and Drug Administration, Bacteriological Analytical Manual, 6th Edition (1984), Association of official Analytical Chemists, Arlington, USA.

229. P.K. Surendran and K. Gopakumar, Fishery Technology, 18 (1981) 133.